UNIVERSITY OF SOUTHAMPTON

FACULTY OF THE ENGINEERING AND THE ENVIRONMENT

School of Engineering Sciences

Bioengineering Group

Dynamic Modelling of Glycaemic Prediction in People with Type 1 Diabetes based on Genetic Algorithm Optimisation

by

Ahmad Uzair Mazlan

Thesis for the degree of Doctor of Philosophy

June 2017

UNIVERSITY OF SOUTHAMPTON

ABSTRACT

FACULTY OF ENGINEERING AND THE ENVIRONMENT

Bioengineering Research Group

Thesis for the degree of Doctor of Philosophy

DYNAMIC MODELLING OF GLYCAEMIC PREDICTION IN PEOPLE WITH TYPE 1 DIABETES BASED ON GENETIC ALGORITHM OPTIMISATION

Ahmad Uzair Mazlan

Type 1 diabetes is caused by the destruction of insulin-producing mechanisms in the pancreas, resulting in uncontrolled blood glucose concentration (BGC). Previous modelling techniques have generally been marginally successful in producing accurate predictions, in part due to the lack of real physiological data from patients. This research considers a Diabetes UK study, which collected free-living data from individuals with Type 1 diabetes using a continuous glucose monitor, activity armband and food and insulin diaries to investigate methods to predict BGC over several hours. A further aim was to improve understanding of the role of physical activity in BGC variations.

Initial tests were performed to directly find invisible patterns within the raw meal, insulin, sleep and activity data but no significant correlations that could be beneficial to help develop better predictive models was found. A number of methods of modelling BGC in Type 1 diabetes are investigated and it was found out that every diabetic subject has his/her own parameter variations, different to the one-size-fits-all reference parameters, hindering improved predictions. As a resolution, an optimization-driven technique is developed for the linear time-invariant ARX class of models, aiming to refine reference constant parameters in glucose and insulin sub-models to suit the very distinct features of each set of Type 1 BGC data. The outcome of this work showed that optimising these values for parameters of digestion in the gut and insulin diffusion in subcutaneous tissue could improve the predictive properties of the ARX models. However, although the prediction was improved over previous research, it was still far from satisfactory due to the non-linearities existing in the BG data. Thus, non-stationary Gaussian Processes was investigated to address the BGC's non-stationarity and autocorrelation with variations present both intra and inter-patient. This approach was not only able to better describe local blood glucose dynamics in response to carbohydrate and insulin intake, but also permitted the inclusion of physical activity energy expenditure data, an advantage over the previous linear time-invariant ARX.

Physiological based-models were then investigated for parameter learning, especially the physical activity data for BGC prediction over several hours. These models showed some predicting capability, highlighting periods of low and high BGC. However, physiological variables analysed were found to differ from estimates in the literature derived from healthy individuals. Therefore, a new semi-empirical compartmental model was developed to better represent the underlying physiology, however resulted in only minimal improvement. Finally, a multi-objective optimization-based approach, constrained by published upper and lower bounds for the variables, was employed to refine these parameter estimates. This cohort-driven technique was shown to perform the best, exceeding those of the previous physiological-based modelling methods and while it is not limited to only short-term predictions, it achieved better prediction on most of the volunteers' studied.

Table of Contents

List of Tables

List of Figures

DECLARATION OF AUTHORSHIP

I, **Ahmad Uzair Mazlan**, declare that this thesis and the work presented in it are my own and has been generated by me as the result of my own original research.

Dynamic Modelling of Glycaemic Control in People with Type 1 Diabetes based on Genetic Algorithm Optimisation

I confirm that:

1. This work was done wholly or mainly while in candidature for a research degree at this University;
2. Where any part of this thesis has previously been submitted for a degree or any other qualification at this University or any other institution, this has been clearly stated;
3. Where I have consulted the published work of others, this is always clearly attributed;
4. Where I have quoted from the work of others, the source is always given. With the exception of such quotations, this thesis is entirely my own work;
5. I have acknowledged all main sources of help;
6. Where the thesis is based on work done by myself jointly with others, I have made clear exactly what was done by others and what I have contributed myself;
7. None of this work has been published before submission.

Signed: .....

Date: .....

Acknowledgements

In the name of Allah the Most Gracious Most Merciful.

First and foremost, I am deeply grateful to Allah for the countless blessings He has showered me with, especially in keeping me sane and steadfast during the completion of this research. It would never be possible without the knowledge and wisdom, the will and determination that indeed all come from Him.

It is a great pleasure to acknowledge my deepest thanks and most sincere gratitude to my supervisor and mentor, Dr. Andrew Chipperfield, for his continuous support and guidance, meticulous advice, witty words and patience, never giving up on me and being a great coach and a good friend at the same time throughout. It was definitely a great privilege to work and study under his guidance.

My appreciation also extends to my family especially my parents, Dr. Mazlan Ismail and Fadhilah Abdullah, and my parents-in-law, Tuan Azmi Tuan Amat and Jalita Haji Ali, for being understanding and ever helpful, and whose love and support have never been unwavering particularly in the final stage of my work.

I am extremely thankful to my beloved wife, Auni Tuan Azmi, for the love, patience and acceptance. She was with me at my lowest, still loved me when I was not very lovable and stood by like a pillar in times of needs. Your constant love is in indeed a great blessing. And not forgetting, the two cheeky little boys, Ubaid Affan and Umair Yaseer, whom we have been blessed with during my PhD journey; in a foreign but much loved land, Southampton. Thanks for being by my side through the thick and thin of it all!

Also, thank you to all friends in Southampton for making us feel like home. Your camaraderie will always be treasured and last but not least, to all the people who have contributed to the work described in the thesis.

May Allah bless all of you who have helped me directly or indirectly throughout this PhD journey.

This is for you.

Definitions and Abbreviations

ACF	Autocorrelation Function
AIDA	A Diabetes Educational Simulator
AP	Artificial Pancreas
AR	Autoregressive
ARD	Automatic Relevance Detection
ARMAX	Autoregressive Moving Average Model with Exogenous Inputs
ARX	Autoregressive Model With Exogenous Inputs
BG	Blood Glucose
BGC	Blood Glucose Concentration
BMI	Body Mass Index
CCF	Cross-correlation Function
CGM	Continuous Glucose Monitoring
CGMS	Continuous Glucose Monitoring System
CH	Control Horizon
CHO	Carbohydrates
CM	Control Move
CSII	Continuous Subcutaneous Insulin Infusion
DE	Differential Equations
DEXA	Dual X-ray Absorptionmetry
DP	Dawn Phenomenon
DUK	Diabetes UK
EGP	Endogenous Glucose Production
FIT	Goodness of Fit Metric
GA	Genetic Algorithm
GA-ARX	ARX Model with Genetic Algorithm
GI	Glycaemic Index
GO	Global Optima
GP	Gaussian Processes
GSR	Galvanic Skin Response
HbA_{1c}	Glycosylated Haemoglobin
Hf	Heat Flux
I	Insulin
Ins	Insulin
LTI	Linear Time Invariant
LO	Local Optima
MA	Moving Average
MDI	Multiple Dose Injection
METs	Metabolic Equivalent
MK	Mueen-Keogh
MOGA-NSPM	Multi-Objective Genetic Algorithm with Non-Stationary Physiological-Based Model
MPC	Model Predictive Controller

MPO	Model Predicted Output
NHS	National Health Service
NSGP	Non-Stationary Gaussian Processes
NSPM	Non-Stationary Physiological Based Model
ODE	Ordinary Differential Equation
OGTT	Oral Glucose Tolerance Test
PA	Physical Activity
PC	Personal Computer
PAEE	Physical Activity Energy Expenditure
PAMM	Percentage of Active Muscle Mass
PH	Prediction Horizon
R&P	Roy and Parker
REM	Rapid Eye Movement
RMR	Resting Metabolic Rate
RMSE	Root Mean Square Error
SG	Sensor glucose
SISO	Single In-Single Out
SMBG	Self-Monitoring Blood Glucose
SPGP	Sparse Gaussian Processes
SD	Standard deviation
SVM	Support Vector Regression
T1	Type 1
TAA	Transverse acceleration average (TAA)
TAM	Transverse acceleration mean absolute deviation
TAP	Transverse acceleration peaks
TEE	Total Energy Expenditure
UI	User Interface
UK	United Kingdom
USA	Unites States of America
WHO	World Health Organisation

Chapter 1: Introduction

Diabetes is characterised by both elevated and wider excursions of blood glucose (BG) levels. People with high blood glucose need to maintain their blood sugar levels within certain bounds. Nevertheless, this can be problematic for some especially those with not-well-regulated blood sugar levels as untreated diabetes will cause cardiovascular diseases such as high blood pressure and heart attack, other complications like kidneys failure, nerve damage, eye problems, skin issues, foot damage, possible amputations, ketoacidosis, and in the worst case, coma and subsequent death.

The trend of an increasing diabetic population is global. In 2013, there were 3.2 million people in the UK diagnosed with diabetes [1]. That has not even included the undiagnosed ones which is estimated to be around 630,000 people. The number is more than the population of any county in the UK except Greater London [2]. This has increased from 2.9 million in 2011 and is predicted to climb to more than 5 million by 2025, which is equivalent to an increase of 400 people a day or over 17 people per hour over that period. This constitutes a huge burden to the UK government as the National Health Service (NHS) currently spends approximately £10 billion a year on diabetes care, amounting to 10% of the total annual cost on UK health care, the equivalent to £1 million an hour [1].

In the past, there have been many attempts to understand the relationships between BG level, diet, exercise and insulin, but most of them have been hampered by lack of continuous measurement data from patients or were taken under unnatural conditions, e.g. in a clinic. Also, the physiology is not completely understood as often the focus was only on one important aspect contributing to BG level, insulin, while other critical aspects were neglected. Data collection and measurements which were taken at intervals of many hours have resulted in much previous data being unreliable as most of the variations in BG levels were missed because of infrequent sampling [3] and thus, no strong conclusions could be made.

In this work, the initial aim was to use feature extraction techniques to identify recurring patterns in time series data which can be readily recorded from individuals. It was hoped that these patterns would elucidate areas such as HbA_{1c} (a clinical measure of blood glucose sugar levels over a 60-90 day period), problems in dietary intake of individuals, or lifestyle factors that affect glycaemic control. As an example, one's sleep quality can be examined and the patterns then compared between all diabetics to see if there are characteristic clusters of people who have similar time series attributes in the recorded data. This motivated the investigation of time-series models for use with the artificial pancreas, self-management decision support and therapeutic prediction. In themselves, better modelling is hoped to better understanding of the disease pathology and biology and possibly clinical understanding. Because of the complexity within the data in finding the patterns and models, it is expected that an optimisation technique, e.g. particle swarm [4] or genetic algorithms [5], could help refining the clustering and parameter identification.

This chapter will introduce the main features of diabetes, guidelines in diabetes management and practices in treating diabetes. The motivations and hypothesis of the proposed research are presented along with the objectives which this study sought to achieve. Contributions arising from the research are described and an overview of the thesis is given.

1.1 Diabetes Mellitus

Diabetes Mellitus, or in short, diabetes, is a chronic medical condition caused by high levels of glucose in the bloodstream due to the body's inability to adequately produce or properly use insulin, or both. The hormone insulin is the main regulator which controls the blood glucose concentration. There are two main forms of diabetes: Type 1 and Type 2. However, it is important to note that this research will only consider Type 1 diabetes although it is expected that the methods and results should also be applicable to data from people with the latter.

1.1.1 Type 1 Diabetes

Type 1 diabetes, often referred to as insulin-dependent diabetes mellitus, develops when the cells in the pancreas that make insulin, β-cells, are destroyed by the body's immune system. As the pancreas fails to secrete insulin and the body's cells are unable to uptake glucose from the blood, blood glucose will rise and ketones then start to develop, leading to unconsciousness and even death as the blood becomes acidic. Other common symptoms of Type 1 diabetes include abnormal urination repetition (polyuria), excessive thirst (polydipsia) and hunger (polyphagia), extreme tiredness, blurred vision, unexplained weight loss, itching and prickling and tingling skin sensations.

Despite active research, Type 1 diabetes has no cure, although it can be managed by supplying exogenous insulin daily. Insulin was first identified and used exogenously in 1921 by Frederick Banting and Charles Best at the University of Toronto. People with Type 1 diabetes today still rely on this stimulus, making it one of the major breakthroughs in medicine of the 20th century [6]. Prior to this there was no treatment possible and people often died within a few weeks of discovery of diabetes.

Currently, there are four different types of insulin delivery in use:

a) Insulin syringe
   This form of insulin delivery is an injection of insulin into the subcutaneous tissue with a fine needle. This method is the most popular and cost-saving. Patients with regular schedules and consistent meal patterns usually opt for this method.

b) Insulin pen
   The pen comes with a predefined load and the patient dials the correct dose and presses a plunger to inject the insulin. It is used in the same manner as the syringe.

c) Insulin jet injector
   Insulin jet injectors are designed to send a fine spray of insulin through the skin using a high-pressure air mechanism. While this is often a good solution for patients who find insulin injections uncomfortable, its use is not widespread.

d) Insulin pump
   This form of insulin delivery system operates on the belt or in a pocket and delivers an appropriate stream of insulin to the body through a needle that can stay in place for a number of days. This background, or basal rate, is augmented by the user with an additional bolus at meal times or when the BG levels are above the normoglycaemic range. In this

way, the pump aims to mimic the action of the pancreas to help achieve better BG regulation.

In order to supply the required insulin, Type 1 diabetes patients have to repeatedly check their BG levels throughout the day. But at night as they sleep, levels can go unmonitored and may fluctuate dangerously. The artificial pancreas (AP) [7][8] is a recent model that automatically measures the patients' BG levels and supplies insulin even when they are asleep. The AP, known as closed-loop control of blood glucose in diabetes, is a system combining a glucose sensor, a control algorithm, and an insulin infusion device. This model tries to imitate the original pancreas by secreting sufficient insulin exogenously, replacing a malfunctioned pancreas.

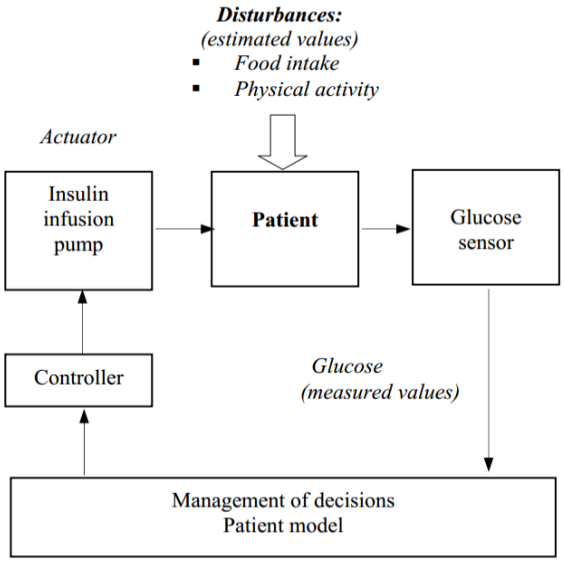

Figure 1.1: The structure of the predictive system for blood glucose control [9].

An outline of the AP is shown in Figure 1.1. Here, the insulin is delivered by an infusion pump to the patient who experiences disturbances from food intake and physical activities. Using a glucose sensor, these disturbances are detected and the management and control algorithm is used to determine the delivery of insulin to the individual. The problem with this model is that the rate of insulin uptake is not taken into account. As different patients would require a different rate of insulin uptake, it would be very useful to refer to the time series data of BG levels in predicting future insulin requirements. In addition, this model does not cater other parameters causing BG levels to go up and down, aside from insulin. There is also a time delay in insulin action and BG levels, dependent on the site it is measured at.

Although insulin is an important factor in controlling the BG levels, newer research has shown that variables affecting the BG levels also include diet and physical activity or lifestyle [10][11]. Therefore, consideration of all parameters rather than just insulin is crucial for better diabetes management. The three main factors which ought to be considered simultaneously when deciding on the insulin dosage and timing are illustrated in Figure 1.2.

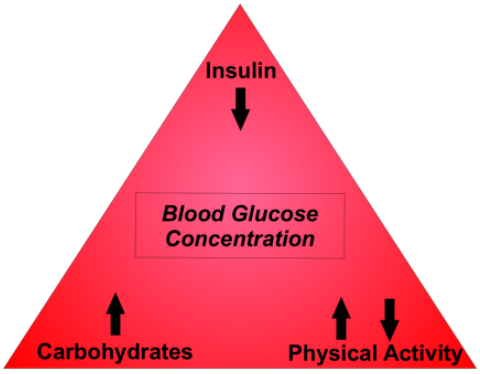

Figure 1.2: Factors controlling the blood glucose levels [9].

Insulin is the main parameter that can be used to lower BG concentration likewise carbohydrates (CHO) will always raise it. Physical activity which is variable throughout a day can work either way as glucose is released from the liver to cater for greater activity levels or stored when the body's glucose requirements are low when at rest.

1.2 Motivation for Research

The goal of this research is to extract features appearing in data from Type 1 diabetes patients recorded for BG, dietary intake, insulin and physical activity. Having features extracted, it is hoped that the clinicians could do a better job in refining the current diabetic treatment model management by treating patients according to their individual characteristics or by membership of groups with given features.

As stated previously, most of the diabetic managements attempt to model the processes that regulate or predict BG levels keeping them within certain bounds rather than focussing on the factors affecting the BG levels in patients. Bergman's minimal pharmacokinetics model of glucose and insulin [12] is arguably the most widely used model due to its simplicity, and has been used as the basis for a number of new model developments. Other studies have also proposed further models describing the appearance of glucose in the bloodstream from foods [13][14]. With current glucose-insulin models, comprehensive models for glucose metabolism were proposed as a means to predict the time profile effect of glucose concentration, given digested food and insulin dosage as parameters.

There has been little work on the modelling of physical activity as a variable that influences BG level, mostly due to of the difficulty in measuring it. The dietary effects of patients are also seldom considered in diabetic model management. This has resulted in physical activity and dietary effects mostly being disregarded as causes of BG variation.

In summary, current diabetic management models are often ignorant of important variables that contribute to the variations of BG level, especially in the effects of patients' dietary and physical activity. Therefore, this study will focus on finding the associations between diet, physical activity and BG levels by feature extraction and characterisation of patients' health data. This objective is novel because we will be utilizing data from devices that monitor and store patients physiological parameters continuously with short sampling intervals ensuring that the data are reliable, real and faithfully correspond to patients' health conditions and not just synthetic data interpolation.

Previous studies were short of accurate, reliable and continuous monitoring devices that continuously measured physical activity energy expenditure (PAEE) and glucose level in the bloodstream.

With various data constituting physical activity, such as sitting down, cycling, sleeping and data of dietary intake, we can extract features appearing in patients' data and attempt to characterise them according to their lifestyle, fitness, dietary intake, body composition, and find the physical manifestation or effects of those variables to patients' BG regulation and consequently, the indicators of long-term health or therapeutic efficacy.

1.3 **Applicability of Research**

This research aims to extend the current research of diabetic model management by extracting features of diabetes patients using time-series pattern recognition. By obtaining continuous time series data of dietary, physical activity and BG level, we hope to understand more about physiological process that occur in people with diabetes. One way to do this is by being able to recognise the main parameters within the glucose-insulin dynamics that have the most significant impact whether they could be adjusted for individuals specifically for a better prediction of BG regulation.

Better prediction would help determine better prescribed treatment by clinicians. It is hoped that if these main parameters can be identified, we would be able to group individuals along with the treatment accordingly, or determine personal treatment plans.

Apart from this, various reviewed linear, non-linear modelling and even physiological-based models are reviewed and modified to better reflect metabolical responses within T1 diabetes patients. The decision for this objective is mainly attributed to poor nature of data collection from patients in the past, resulting in inaccurate parameters estimated, despite the rational physiologically based prediction.

Data have been previously collected from a number of individuals in an earlier Diabetes UK (DUK) supported study [15]. The study group of 22 volunteers was heterogeneous, covering a wide age range, levels of PAEE, current BG control and sexes. Data obtained will be analysed in terms of its recurring patterns in and across the individual parameters and volunteers. The physiological parameters obtained from various devices are statistically correlated in terms of bodily composition, daily activities and fitness. Underlying features are also extracted to obtain any recurring patterns of dietary, insulin utilisation and BG levels and their possible effects to one another. If necessary, parameters within the glucose-insulin dynamics might be adjusted for better prediction using optimisation methods, for intra and inter-patient purposes.

Utilizing all the key parameters regulating BG level, i.e. insulin and dietary intake and PAEE, this research hopes to identify new approaches of characterising individuals into specific clusters, much possibly according to the wellbeing and lifestyle, for a better devised treatment and diabetic management. Thus, the main objectives of this research are:

- to identify recurring patterns and effects in BG and physical activity data together with dietary, insulin intake from multiple subjects,
- to investigate variables that have the most impact within existing insulin-glucose models in predicting BG variation,
- to use optimisation techniques to improve the predictive capability of these models, and
- to classifying patients according to respective methods of treatment.

1.4 Contribution of Research

This chapter introduces diabetes and its current available treatments. Following chapters are structured as follows:

- Chapter 2: Presents relevant literature in the field of glucoregulatory system modelling, especially on the glucose control, insulin behaviour and the effects of physical activity. A linear system identification model was presented with its justification. A preliminary problem of prediction in Type 1 diabetes is discussed, with the relevant mathematical models used for interpreting data.
- Chapter 3: Describes physiological measurements performed on each volunteer and the methods used for continuous monitoring of blood glucose and physical activity in a free-living environment. Preliminary analysis on the correlations between data from various devices are also discussed.
- Chapter 4: Discusses features extraction technique for time series glycaemic data collected from Type 1 diabetic volunteers. The prospect of using the technique to discover more repetitive patterns within diabetes data are weighed accordingly to elucidate any underlying effects or phenomenon that might have been caused by them.
- Chapter 5: Tests linear system identification models as a tool to predict BG levels in diabetes patients. Optimisation technique to address respecting individual variations (intra-patient) is also utilised. Main parameters existing in the meal and insulin models are adjusted continuously using recursive system identification model with GA.
- Chapter 6: Explores non-parametric Gaussian Processes (GP) techniques to capture the non-linear dynamics within glycaemic data. A GP variant to address the non-stationary behaviour especially present in the physical activity data is also investigated. The role of physical activity which triggers various metabolic pathways with its regular stochasticity is regularly highlighted.
- Chapter 7: Assesses the physiological-based model to see if the underlying literature of diabetes modelling truly reflects actual physiology of diabetes patients. This is due to the past studies that are of rational parametric modelling, but having synthetic data and parameters derived from healthy individuals in a controlled environment, creating a gap in better prediction of BG, hence the limited understanding of T1 Diabetes, possibly leading to substandard treatment.
- Chapter 8: Attempts to revise diabetes physiological-based model with taking into account realistic diabetes considerations. Shortcomings of the previously proposed model are addressed and tested using collected free-living data. A modified physical activity minimal model was also presented.
- Chapter 9: Investigates multi-optimisation technique to further adjust the physiological model, finally targeting at improving the generic parameters of the glucoregulatory modelling. It is therefore a cohort-driven optimisation where every volunteer's data are included in refining process, thereby producing the most suitable parameters for the general Type 1 diabetes patients.

1.5 Main Contributions

- Presenting a technique to discover recurring patterns within the time series glycaemic data. The technique could be used in future studies to find recurring patterns occurring in intra or inter-patient health data and help researchers find more correlations in them.
- Applying linear-time invariant ARX models fused with an optimisation technique, GA, to further optimise parameters within glucose-insulin dynamics. Local BG was properly detected in response to carbohydrate intake and insulin administration using linear ARX. The case is different to the global glucose dynamics. Free-living data were proven to not help improve the quality of the models because sporadic nature of physical activities occupied only a small portion of the datasets, thus not properly accounted by the model. Models were not able to estimate parameters related to response caused solely by physical activity, however have been improved by the use of genetic algorithm. GA was able to allow parameters to adapt to intra-patient variabilities, a positive find.
- Testing a non-stationary Gaussian processes model to capture the non-stationary dynamics of glycaemic data and produce better glycaemic prediction. The method was shown to predict better even with the presence of physical activity data, compared to other techniques studied.
- Using community-driven multi-optimisation technique to fine-tune original parameters estimated from healthy people towards the cohort's own estimates where all volunteers' data were used. The optimised parameters were shown to predict better BG response among Type 1 diabetics, shown to be an effective solution. This method could be used to other targeted groups as well, such as Type 2 patients, or even Type 1 patients with narrower specifics such as lifestyle, wellbeing, gender or age.

Chapter 2: Literature Review

Understanding variations in BG levels in people with Type 1 diabetes involves recognising the physiology, measurement techniques and therapeutic regime, and interpreting them by meaningful analysis. In this chapter, an overview of the physiological problem and mathematical models used for interpreting these data are presented. Linear system identification model ARX, physiology-based modelling and genetic algorithm as an optimisation technique are also introduced. They are important to assess and model patients' habitual behaviour in their diet, physical activity and lifestyle.

2.1 Glucoregulatory System

This section will explain the basic concepts of how lifestyle and other physiological factors affecting glycaemic variations, starting from food ingested where the nutrients are obtained. The food that we digest comes from these two nutrient groups [16]:

1. Micronutrients:
   They are essential for metabolic process and the synthesis of new tissues and organs, and are divided into two categories:
   - Vitamins
   - Minerals

2. Macronutrients:
   They provide fuel needed by the body to sustain life and perform mechanical work, and are essential in building new tissues and organs. Macronutrients consist of three types:
   - Carbohydrates
   - Lipids (Fats)
   - Proteins (Amino Acids)

Among all these nutrients, carbohydrates (CHO) are the most essential since they provide immediate energy supply to the body. As shown in Figure 2.1, after nutrients are extracted from food, excessive glucose from the glucose pool will be dumped into urine if BG is not properly regulated and the renal threshold is exceeded. Glucose, which is the simplest form of carbohydrate, can be digested and metabolised easily by the body before being used directly by the central nervous system and red blood cells.

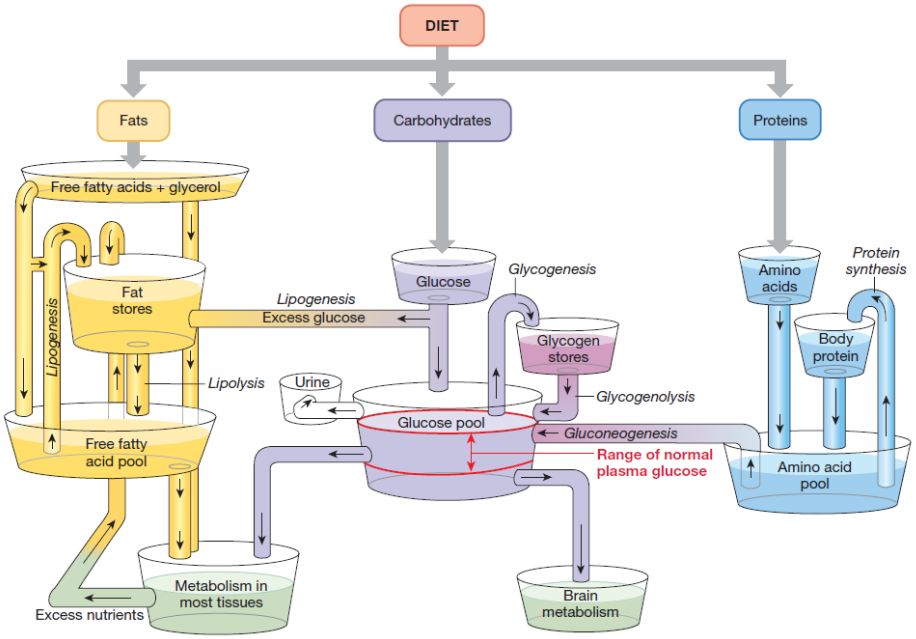

Figure 2.1: Visual representation of the metabolic processes inside the body [17].

The glucose pathways shown in Figure 2.1 are:

1. Anabolic Pathways:
    1. Glycogenesis (glucose → glycogen): Glucose is stored as glycogen in the liver and muscle.
    2. Gluconeogenesis (fat, protein → glucose): The synthesis of glucose from non-carbohydrate precursor. Proteins are mainly used in this pathway; however, glycerol from fats can be used as well.
    3. Lipogenesis (glucose → fat): Excess glucose (that cannot be stored in the liver or muscle) is stored as fat (triglycerides).

2. Catabolic Pathways:

1. Glycolysis (glucose → pyruvate, lactic acid): Considered to be the reverse process of gluconeogenesis. It creates pyruvate and a small amount of ATP from glucose.
2. Glycogenolysis (glycogen → glucose): The breakdown of glycogen stores in the liver and muscle into glucose.

As shown in Figure 2.2, the body regulates BG within a certain range by relying on two hormones produced in the pancreas which have opposite actions: insulin and glucagon. When BG is elevated, the body stores the excessive BG in the liver and muscles with the help of insulin as glycogen. This storage process is important to preserve constant glucose concentration in blood throughout the day; otherwise critical cells, e.g. in the brain and heart, that need constant energy will have an oversupply of glucose after a meal and starve in between meals. Nevertheless, whenever the glucose is in short supply, glycogen is converted into glucose by the hormone glucagon and stimulates us to eat. But during fasting, additional glucose supplies may be needed where amino acids, lactic acids and glycerol are converted into glucose.

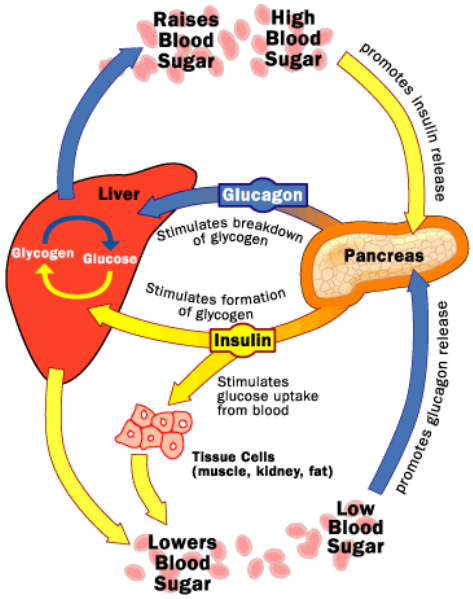

Figure 2.2: Insulin and glucagon that have opposite effects for BG regulation [18].

A chronological process of glucose uptake and utilisation in a non-diabetic person is depicted in Figure 2.3. In Figure 2.3 (a), a high blood sugar level raises the electrical potential at channels (KATP) of the β-cells causing insulin to be released into the blood. This allows glucose to be transported from the blood to muscles and other tissues. Excess glucose, beyond the tissue's immediate requirements, may be converted to glycogen and stored in the liver (which has approximate capacity of 2400 calories per an adult male). In contrast, Figure 2.3 (b) shows the response to low BG levels. Here, the lack of glucose in the blood stimulates the release of glucagon from the pancreas enabling the liver to convert glycogen to glucose raising BG level.

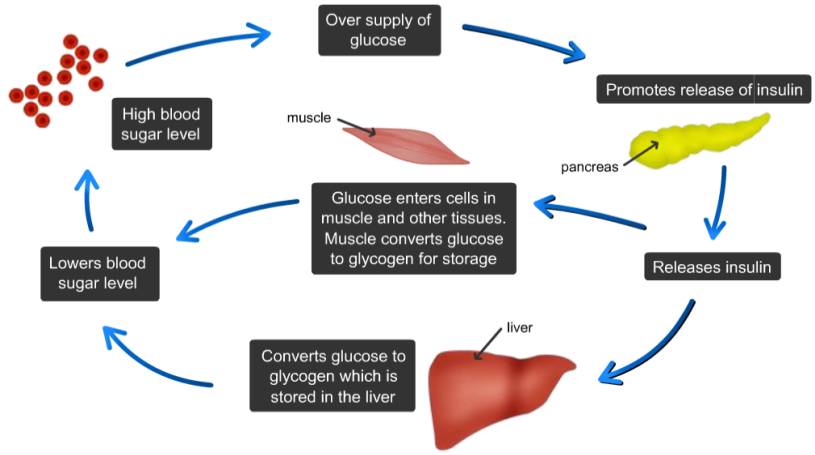

(a) High BG response.

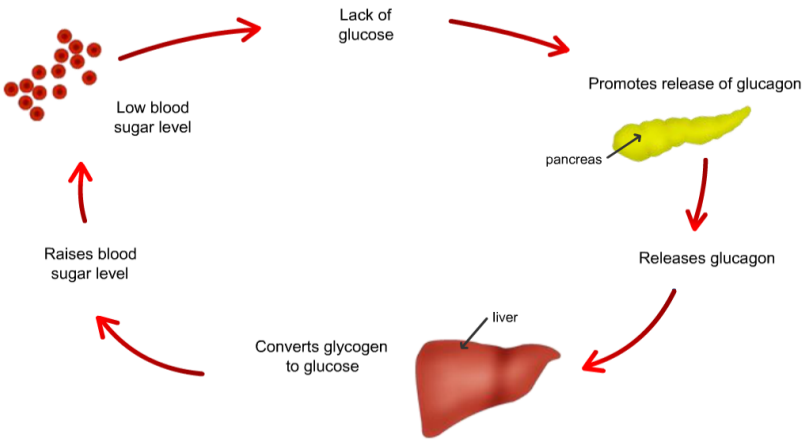

(b) Low BG response.

Figure 2.3: Body response to glucose intake and release in a non-diabetic person [5].

As outlined in Section 1.1, diabetes is a disease where the body cannot properly absorb glucose received from food ingested due to the lack of insulin, and BG concentration goes high exceeding the normal range, usually defined to be between 4 to 9 $mmol\ l^{-1}$ [19]. This situation, known as hyperglycaemia, happens when the body develops insulin resistance or the pancreas does not produce enough insulin or both (Type 2 diabetes). As a result, vital organs and tissues that need energy prompt the liver to convert glucagon into glucose, resulting in a higher glucose concentration in the bloodstream. If this situation is prolonged, the body then breaks down fats and proteins as a source of energy and ketones are produced. Ketoacidosis occurs when too many ketones appear in the bloodstream and can lead to diabetic coma and death as the blood becomes acidic.

In response to the elevated glucose level in blood, the kidneys cannot filter out all glucose and expel it in the urine, making it the major reason why preliminary identification of diabetes in clinics would be by the detection of excessive glucose in patient's urine.

Another critical condition in Type 1 diabetes is hypoglycaemia, in which there is too much insulin in circulation normally from excessive medication. The body cells take too much glucose in response to excessive insulin, resulting in insufficient glucose in the bloodstream. Critical organs, such as the brain, which need a constant energy supply are starved from glucose and start to malfunction, causing nervousness, shakiness and confusion. A prolonged condition may lead to diabetic coma [20].

Therefore, the amount of glucose uptake or release must be in the correct proportion to maintain a normal blood glucose concentration (known as euglycaemic or normoglycaemic levels). An Oral Glucose Tolerance Test (OGTT) can be used to diagnose instances of diabetes or insulin resistance. This involves taking a BG reading before and a short time after consumption of a concentrated sugary drink typically containing between 50g and 75g of sugar. An example of the difference in glucose concentration between a healthy subject and diabetic one is shown in Figure 2.4. The OGTT result shows the difference between a healthy subject and a diabetic one, where the former will have a lowered BG levels after a given period of time, signifying insulin uptake whereas the latter will have an elevated BG levels above the normal range. Glycated Haemoglobin (HbA_{1c}) is another test, usually performed in a clinic, which determines the average plasma glucose concentration or, simply, an average blood glucose level over a long period of time (60-90 days) that mirrors how well one's diabetes is controlled. A diabetic patient who has a well-controlled BG over time will have a lower HbA_{1c} compared to the one poorly controlled. The former may typically have more steady BG levels rather than a fluctuating one in the latter.

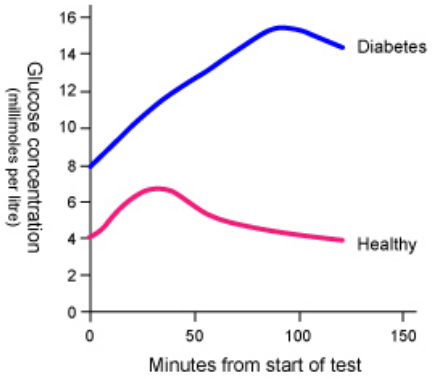

Figure 2.4: Blood glucose levels in a healthy person and in a diabetic person after an OGTT test [164].

The results of the above tests demonstrate the importance of people with diabetes continuously having knowledge of their current and recent BG levels in a time-series manner, and understanding any possible risks posed by their BG levels. This raises patients' awareness to regularly check, maintain and improve their BG levels on an everyday basis. Also, it would be more helpful if the BG data can be examined and analysed and the results are included in the diabetes healthcare model as a way to improve treatment.

2.1.1 Carbohydrates Effect on The Blood Glucose Levels

Elevation of BG concentration is primarily an effect of food digestion. This process is managed by the 'glucose sensors' within the β-cells which releases insulin directly into the bloodstream from the pancreas. BG levels are differently affected depending on the food taken-whether they contain

carbohydrates, proteins, fats, or a combination of these. Even food containing same amount of carbohydrate can produce different impact towards BG levels, albeit each one will definitely increase it. The glycaemic index (GI) level plays the biggest role, where the highest one produces the most impact on BG levels while also the fastest. An effect of different levels of GI in food intake towards BG can be seen in Figure 2.5 [21].

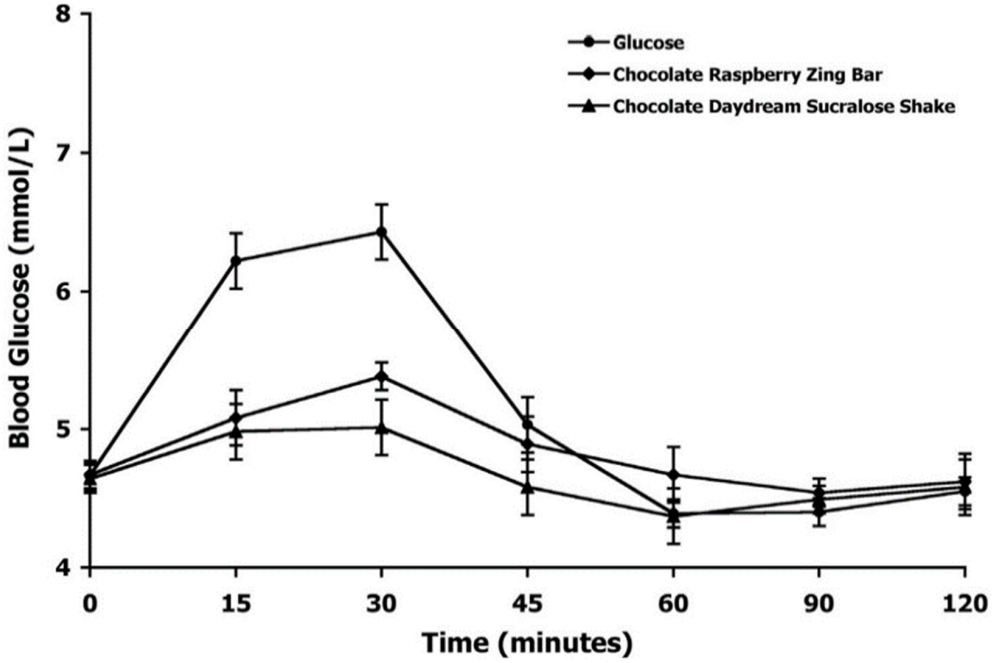

Figure 2.5: Glucose response curve of different level of carbohydrate foods [21].

Glucose (liquid), chocolate bar and sucralose shake (both solid with low GI) are consumed separately on different days and each having the BG response curve measured after a specific time. All are shown to increase BG levels, but with varying response. Chocolate bar and shake containing low GI have smaller impact on BG variation compared with high GI food despite each having the same portion of carbohydrate (10 g). Glucose produced the largest rise in BG during the first 30 minutes as well having the biggest area under the curve, meaning greater overall glycaemic response that the other two test foods. Therefore, different diets mean different glucose responses.

Since the data in the Figure 2.5 are expressed in BG levels from the fasting baseline concentration, it is not too difficult to understand the response curve. However, it would be a different case in someone who has had previous meals and insulin effecting the current glucose response from more recent meals. Powers *et al.* [11] conducted research to find whether the same meal would cause the same glucose concentration response after a certain time. It was revealed that consuming double the carbohydrate content did not double the glycaemic response variables and that there is a significantly different response in glucose values or time for each individual. The differences also applied to the peak glucose, change from baseline glucose to peak, time to return to pre-prandial glucose, 4-hour glucose area under the curve and 4-hour mean glucose.

Furthermore, different people would have a different metabolic rate and this too includes the rate of insulin uptake and release. Overweight people tend to have a slower metabolic rate while those who exercise would have better insulin sensitivity and faster metabolism. Even so, it is useful to examine our health pattern in the time domain to acquire a robust description of our glycaemic response and measure of how well-controlled it is.

2.1.2 Role of Physical Activity in Glucose-Insulin Dynamics

This section provides a short review on the modelling of diabetes. The modelling of diabetes which includes insulin therapy (see Section 2.4), digestive system (see Section 2.2) and exercise (see Section 2.3) that make up the glucose-insulin dynamics is illustrated in Figure 2.6.

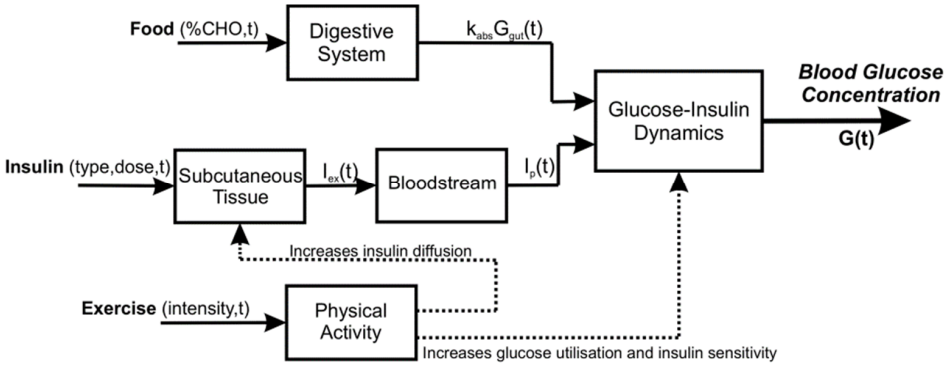

Figure 2.6: Block diagram of diabetes modelling [9].

From Figure 2.6, food consumed causes glucose in the bloodstream to rise. When insulin is injected into subcutaneous tissues, it dissolves and arrives in the bloodstream transporting glucose from the bloodstream to tissue or cells. The glucose level in the bloodstream gets lowered and BG levels are maintained according to the glucose-insulin dynamics.

From the model, it can be seen that increased physical activity can excite glucose utilisation, subsequently increasing insulin diffusion and insulin sensitivity. However, these processes are not well understood and exercise is typically characterised by time-varying intensity.

People with Type 2 diabetes are highly encouraged to participate themselves in regular physical activity as part of daily treatment. It can help them regain the insulin sensitivity as that in healthy people while preventing cardiovascular risks. The case is however different to Type 1 diabetes where only physical activity along with extra attention, care and very careful planning can be devised, otherwise events of hypo or hyper are inevitable.

Exercise facilitates the diffusion of insulin from the subcutaneous tissue to the bloodstream and also increases glucose uptake for the muscle contractions. Glucose uptake is increased even further by the exercise induced glucose-transporter (GLUT4). Depending on the amount of circulating insulin and activity, glucagon may or may not counter-react this effect. In the event of the latter, a rapid decrease in blood glucose occurs, causing hypoglycaemic episode. On the opposite, as more and more glucose is synthesised through glycogenolysis and gluconeogenesis, both stimulated by glucagon hormone, glucose becomes more concentrated, resulting in another extreme situation, hyperglycamia.

All these factors are fundamental in controlling BG levels and it can be very helpful if patients' glycaemic data are carefully analysed, taking into consideration their diet, physical activity, their wellbeing and physical condition, HbA_{1c} and others. The results can be used to improve current diabetes healthcare models, subsequently addressing people with diabetes according to their wellbeing and lifestyle. Individual variations mean that such a model will not have unique and constant parameters, each individual has different physiological and metabolic parameters and they vary with time and other external parameters (e.g. temperature, humidity and mood).

2.2 Modelling the Digestive System

Carbohydrate-based meals increase the blood glucose levels quickly when consumed as seen in Figure 2.5. Therefore, modelling of the digestive system is important to predict the rate of glucose presence in the bloodstream following consumption of meals. The gastrointestinal tract is responsible for the absorption of nutrients into the cells, having organs from mouth, pharynx, oesophagus, stomach, small intestine, large intestine, rectum and anus [17] (see Figure 2.7). The organs are where the food is broken down, bit by bit until the molecules are small enough to be absorbed and waste products are then eliminated. The process involves cutting the food (mechanically) and chewing the food providing enzymatic reactions (chemically). In the case of carbohydrates, monosaccharides such as glucose, galactose and fructose can be absorbed directly by the digestive system while disaccharides (e.g. sucrose) and polysaccharides (e.g. starch) need to be broken down into simple sugar first. After that, the small intestine works to absorb them via its mucous membrane.

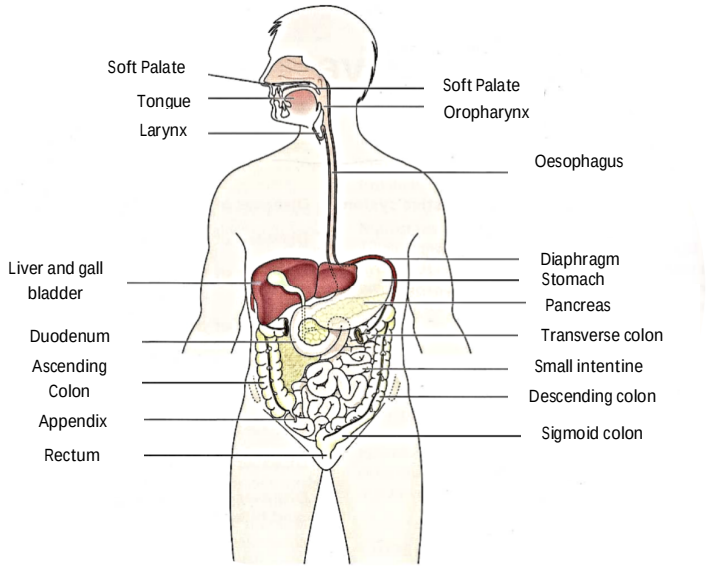

Figure 2.7: Overview of the digestive system [22].

Only a relatively few models have been proposed in the literature to describe the physiological process of food ingestion [14][23][24]. A reasonably good one was used in the AIDA v4 simulator, the widely used model developed by Lehmann and Deutsch [25]. It is also the particular model utilised by Valletta [9] who collected data in the DUK study. The model described is the approximation results for the rate of glucose appearance from foods which is based on the assumption that food ingestion in the stomach is a single stage process.

The amount of glucose entering the guts is modelled as:

$$G_{gut}(t) = G_{empt}(t) - k_{abs}G_{gut}(t) \quad (2.1)$$

$$G_{in}(t) = k_{abs}G_{gut}(t) \quad (2.2)$$

Where

G_{gut} (t) is the amount of glucose in the gut [$mmol$]

G_{empt} (t) is the rate of gastric emptying [$mmol$ min^{-1}]

k_{abs} is the rate constant for gut absorption of glucose [min^{-1}]

G_{in} (t) is the rate of glucose appearance in the bloodstream [$mmol$ min^{-1}]

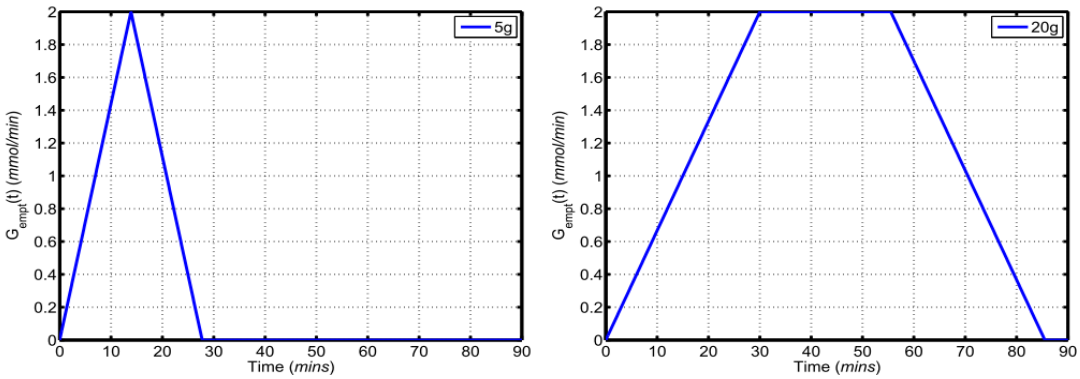

Figure 2.8: Trapezoidal function of rate of gastric emptying for 5 g and 20 g.

The authors assume that the rate of gastric emptying is equal to that of the amount of carbohydrates in the guts until it saturates to the maximum rate (Vmax) of 2 $mmol$ min^{-1}. The association is modelled as a trapezoidal function as in Figure 2.8, showing two cases (5g and 20g of carbs). The governing equation is presented below.

$$G_{empt}(t) = \begin{cases} \frac{T_{up}}{V_{max}}(t) \text{ for } t < T_{up} \\ V_{max} \text{ for } T_{up} \leq t < (T_{up} + T_{max}) \\ V_{max} - \frac{V_{max}}{T_{down}}(t - T_{up} - T_{max}) \text{ for } (T_{up} + T_{max}) \leq t < (T_{up} + T_{max} + T_{down}) \end{cases} \quad (2.3)$$

$$T_{max} = \frac{Ch - \frac{1}{2}V_{max} - (T_{up} + T_{down})}{V_{max}}$$

Where

T_{up} is the duration of increasing gastric emptying rate (min)

T_{down} is the duration of decrfeasing gastric emptying raet (min)

T_{max} is the duration of maximum gastric emptying rate (min)

V_{max} is the maximum gastric emptying rate (2 $mmol$ min^{-1})

Ch is the amount of ingested carbohydrates ($mmol$)

T_{up} and T_{down} will be set to 30 minutes or $\frac{1}{2}$ hour. Note that whenever the amount of ingested food is below the threshold of Ch_{crit} in (2.1),the gastric emptying does not saturate.

$$Ch_{crit} = \frac{1}{2}V_{max}(T_{up} + T_{down}) \quad (2.4)$$

Therefore, the gastric emptying rate was modelled by a triangular function such as

$$T_{up} = T_{down} = \frac{Ch}{V_{max}} \quad (2.5)$$

2.3 Modelling of Physical Activity

Despite many publications on physiological modelling of diabetes, very few of them consider physical activity as an important parameter affecting blood glucose levels [26][27][28][29]. Also, currently available diabetes software packages do not take exercise into consideration [30][31]. The main reason is the lack of a quantitative measure of physical activity. E. Salzsieder *et al.* [28] tried to model exercise as equivalent to insulin action but as discussed earlier in Section 2.4, exercise can affect BG in terms of increasing it depending on the concentration of circulating insulin as well as to decrease BG.

Hence, a modified model of Bergman's was proposed by Derouich and Boutayeb [26] which accounts for physical activity considering three parameters defining the model which are: q_1, a rate constant for increasing glucose utilisation during exercise; q_2, constant representing the effect of exercise on increasing insulin sensitivity; and q_3, the constant representing the effect of exercise on increasing insulin sensitivity. However, the model was only validated with artificial data where no experimental data were involved and there are also no direct relationships between the parameters.

On the other hand, another approach was taken by Lenart *et al.* [29] by quantifying physical activity as a percentage of the maximal oxygen uptake ($PV0_2$ max) and percentage of active muscle mass (PAMM). This is a more convincing measure that uses the exercise intensity directly. Finally, Hernandez *et al*. [27] extended the work done by modelling glycogen depletion during exercise, which so far is the most comprehensive literature on modelling the effect of physical activity on BG concentration in people with Type 1 diabetes. Another measure for physical activity is the Metabolic Equivalent Tasks (METs) by having non-invasive sensors such as in [32]. Further discussion on the approximation of METs can be seen in Section 3.3.2 (page 37).

2.4 Modelling the Exogenous Insulin Flow

Figure 2.6 shows a block diagram of the Type 1 diabetes identification problem. Both food intake and insulin absorption generally occur simultaneously, and typically guidance is given to inject insulin to match the carbohydrate intake being consumed. The inputs are transformed to give the rate of exogenous insulin flow ($I_{ex}(t)$) and the rate of exogenous glucose appearance in the bloodstream ($G_{in}(t)$). In the case of people with Type 1 diabetes where they have a complete insulin deficiency, the insulin concentration will entirely dependent on the injected dose and its diffusion from the subcutaneous depot to the capillaries.

Some authors have proposed a description of time-evolution of insulin appearing in the bloodstream following subcutaneous insulin administration. Cobelli *et al.* [33] reviewed insulin flow models; most are two compartmental models consisting of a subcutaneous depot and blood plasma. However, none are able to describe a wide spectrum of insulin preparations. A more recent generic insulin model proposed by Tarin *et al.* [34] was employed in this study due to its ability to describe this whole range of insulin preparations, from rapid-acting to long-acting, in current use.

The novelty with this model is the introduction of the bound state, an artificial insulin state that enables the modelling of long-acting preparations such as Glargine [35]. The model assumes the insulin injected first resides in the bound subcutaneous depot and is then gradually converted into a hexamer and then dimer, before being absorbed into the bloodstream. However, the case is

different with all other types of insulin like short, rapid or intermediate acting preparations in which are already considered to be in a hexameric state upon injection. The administered insulin is assumed to be a sphere whose volume is equal to the injected dose, diffusing symmetrically over time, outwardly. Therefore, the distance and concentration varies over time during the diffusion. The coupled partial differential equations governing this model are given below.

$$\frac{\partial c_d(t,r)}{\partial t} = P(c_h(t,r) - Qc_d(t,r)^3) - B_d c_d(t,r) + D\nabla^2 c_d(t,r) \tag{2.6}$$

$$\frac{\partial c_h(t,r)}{\partial t} = -P(c_h(t,r) - Qc_d(t,r)^3) + \kappa c_b(t,r)(c_{h,max} - c_h(t,r)) + D\nabla^2 c_d(t,r)$$

$$\frac{\partial c_b(t,r)}{\partial t} = -\kappa c_b(t,r)\left(c_{h,max} - c_h(t,r)\right) + d_b D\nabla^2 c_d(t,r)$$

$$I_{ex}(t) = B_d \int_{V_{sc}} c_d(t,r)\,dV$$

Where

r distance from injection site (cm)

$c_d(t,r)$ dimeric insulin concentration ($U\ ml^{-1}$)

$c_h(t,r)$ hexameric insulin concentration ($U\ ml^{-1}$)

$c_b(t,r)$ bound insulin concentration ($U\ ml^{-1}$)

$I_{ex}(t)$ exogenous insulin flow into the bloodstream ($U\ min^{-1}$)

P = 0.5 dimeric production rate (min^{-1})

Q hexameric-dimeric equilibrium constant (ml^2U^{-2})

B_d absorption rate constant for dimeric insulin (min^{-1})

D diffusion constant (cm^2min^{-1})

κ bound-hexameric conversion factor ($ml\ U\ min^{-1}$)

$c_{h,max}$ bound-hexameric saturation constant ($U\ ml^{-1}$)

d_b reduction factor of the diffusion constant for the bound state

V_{sc}subcutaneous volume (ml)

2.4.1 Hovorka Model

The Hovorka model simulates the physiology of a person with Type 1 diabetes consisting three subsystem of CHO absorption, insulin absorption from subcutaneous insulin injections, and glucose-insulin kinetics. It simulates the response of glucose and insulin concentration in response of the mentioned inputs.

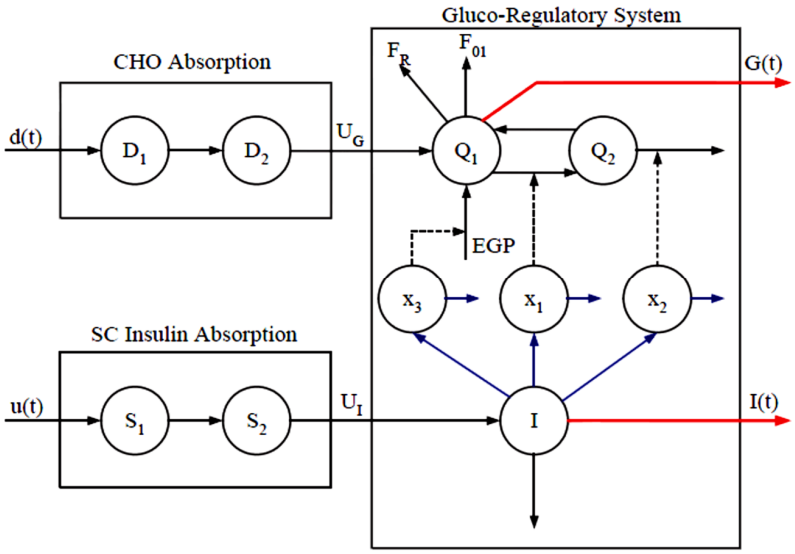

Figure 2.9: Flow of compartments in Hovorka model. Each subsystem contains two or more compartments. The largest compartment, 'Gluco-Regulatory System' simulates the action of pancreas and glucose-insulin kinetics.

Figure 2.9 shows the flow of the compartments in the Hovorka model. The input to the subsystem 'CHO Absoprtion' is the amount of ingested CHO, d(t) being the first external input to the model. The output comes as the glucose absorption from the gut U_G(t). The second external input is u(t), subcutaneous insulin injection. The absorption of the injected short-acting insulin is modelled by two compartments, S1 and S2 described by:

$$\frac{dS_1(t)}{dt} = u(t) - \frac{1}{\tau_S} S_1(t) \tag{2.7}$$

$$\frac{dS_2(t)}{dt} = \frac{1}{\tau_S} S_1(t) - \frac{1}{\tau_S} S_1(t)$$

$$U_I(t) = \frac{1}{\tau_S} S_2(t)$$

where τ_S is the time for the rate of insulin absorption to reach its maximum. The output, insulin absorption rate, U_I(t) comes from the subsystem into the gluco-regulatory compartment, biologically insulin now to appear in the plasma.

On the other hand, the gluco-regulatory system that is to receive both U_G and U_I inputs, has two compartments denoted by Q_1 and Q_2 with output BG levels denoted by G(t). Q_1 and Q_2 represent

the mass in $mmol$ of glucose in accessible and inaccessible glucose compartments, respectively. They are defined by:

$$\frac{dQ_1(t)}{d(t)} = U_G(\mathrm{t}) - F_{01,c}(t) - F_R(t) - x_1(t)Q_1(t) + k_{12}Q_2(t) + k_{12}Q_2(t) + EGP_0(1 - x_3(t)) \quad 2.8$$

$$\frac{dQ_1(t)}{d(t)} = x_1(t) - Q_1(t) - k_{12}Q_2(t) + x_2(t)Q_2(t)$$

$$G(t) = \frac{Q_1(t)}{V_G}$$

where k_{12} is the transfer rate constant between inaccessible and accessible compartments, V_G is the distribution volume of the accessible compartments, and finally, EGP_0 denotes the body's estimated glucose production at zero insulin concentration found by extrapolation. The term $EGP_0(1 - x_3(t))$ represents the time-varying endogenous glucose production (EGP). Whilst the main equations are presented above, further literature can be found in [36]. Main estimated parameters for the Hovorka models are listed in the Table 2.1 below.

Specification	Value	Unit
Transport insulin sensitivity (SI1)	0.03	*L=mU*
Disposal insulin sensitivity (SI2)	0.138	*L=mU*
EGP insulin sensitivity (SI3)	0.12	*L=mU*

Table 2.1: Main Hovorka parameters.

The three main parameters listed in Table 2.1 are insulin sensitivities dictating the major response in the whole model, as can also be seen in Figure 2.9. They will also be revised in Chapter 5 along with the system identification model.

2.5 A Review on the Modelling of the Insulin and CHO Model

Hemmingsen and Johnsen [36] and Valletta [9] investigated the possibility of predicting glucose levels in Type 1 diabetes patients using simple black box models, particularly ARX and ARMAX. The former model was implemented as an internal model of the Model Predictive Controller (MPC) to help predict better glucose levels, by updating the ARX over the time, hence the presence of Prediction Horizon (PH) and Control Horizon (CH) terms. In order to improve the prediction of glucose levels, the authors manipulated the parameters in the insulin model by considering it as the main factor affecting BG levels.

One of the most significant applications of the research presented in Hemmingsen *et al.* [36] study is in the insulin rate control capability present in the popular device known as Artificial Pancreas (AP). One approach to the AP consists of continuous glucose monitor (CGM), a MPC, and a Continuous Subcutaneous Insulin Infusion (CSII) pump. The device works by computing the optimal insulin infusion rate from the CGM measurements, using available knowledge of prior insulin infusions and possible information regarding meals. This setup works as a feedback control for better predictions in the future and is illustrated in Figure 2.10. Here, y, r, d, u, $\bar{y}$, z are the output, set-point or desired reference value, disturbance, actuator, desired BG, plant output, and noise

respectively. The noise is actually an output disturbance, arising from the variation by the prediction and the measured meal. The MPC block components depicted in Figure 2.12 is based on an ARX model of a SISO (single-input-single-output) system having the insulin as the sole input, discarding the other main input to the system, carbohydrate.

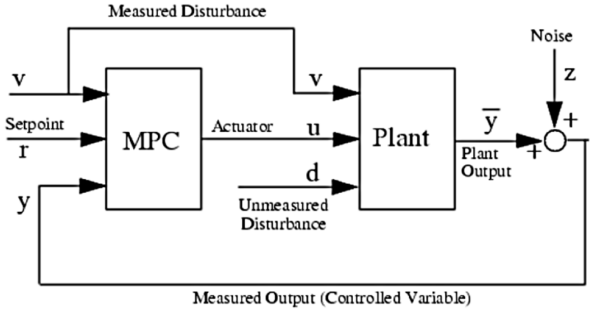

Figure 2.10: Block Diagram of an MPC scenario in the AP setup. The CHO intake would be regarded as unmeasured disturbance (later assumed to be constant), insulin being the control move and the controlled variable is the BG concentration [36].

The main purpose of the MPC is to hold an output at reference value and adjusting the optimum control moves (CM) on the manipulated variable, by minimizing a cost function. The optimisation cost function which is based on knowledge of past control insulin infusion and future predictions provided by the internal model is minimised. Further parameters include prediction and control horizon, and model order. The optimal control strategy is calculated by the minimizing the objective function given by [36]

$$\phi = \frac{1}{2}\sum_{j=0}^{N-1} \left|\left|\hat{y}_{k+1+j|k} - r_{k+1+j|k}\right|\right|_2^2 + \kappa \left|\left|\omega_{k+1+j|k}\right|\right|_2^2 + \eta \left|\left|\upsilon_{k+j|k}\right|\right|_2^2 + \lambda \left|\left|\Delta u_{k+j|k}\right|\right|_2^2, \quad (2.11)$$

where r_k is the reference value, at time k, and λ is a penalty term, penalising large fluctuations in u. ω_k and $\upsilon_k$is the minimum and maximum BG concentrations. κ is a weight parameter penalising below ω_k (hypoglycaemic event) and higher than υ_k (hyperglycaemia event). Note the asymmetric function, where lower constraint violation (hyperglycaemia) results in higher penalty than the upper constraint (hyperglycaemia).

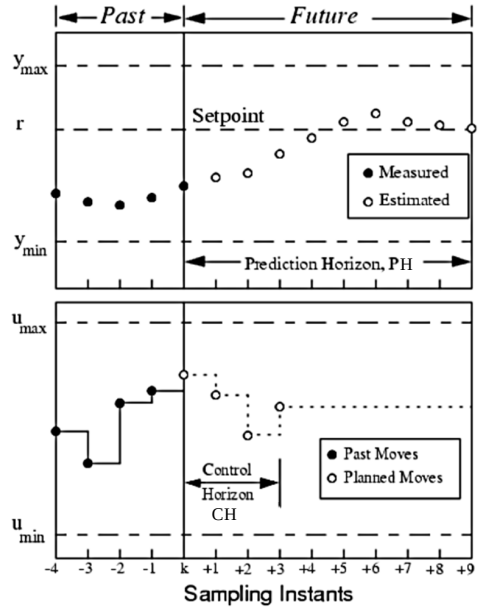

Figure 2.11: Prediction and control horizons of a SISO MPC system. Prediction Horizon (PH) determines how far ahead the model should be predicting, while Control Horizon (CH) determines how far ahead the controller should plan the optimal control moves. y_{min} and y_{max} are constraints placed on BG levels and r is the desired concentration [36].

Figure 2.11 illustrates the role of input and output variables in the MPC model. r is the reference value or desired BG level, PH being the prediction horizon of the output from the output data (y) and CH determines the control prediction from the input data (u). For each sample, the MPC uses BG predictions from the model to generate a control strategy, for example the insulin infusions.

Hovorka's [31] insulin model was then employed to describe active insulin. The authors incorporated the digestion model into its insulin model and included a number of tests involving CHO inputs alongside insulin. However, due to the uncertainty arising from inability to properly estimate the value of CHO (patient themselves need to estimate the amount and time of ingested CHO), they decided that it was best to leave the meal information out from the equation. In the tests done, models that involve CHO the most were only limited to the meal announcement given 15 minutes in advance to the model.

Despite the arrangements, one can easily guess that at best performance, reducing the meal information to only meal announcements would result in unreliable predictions, as seen with predicted hypoglycaemic events in many cases, which were inaccurate. The model was also limited to predicting BG with a strict adherence to daily meals, as the model regards the size of every meal being very similar every day, due to the only meal announcement arrangement, one that is not relative to an actual lifestyle. If the model were to be tested on a free-living data such as of those collected in this study, one would expect a worse prediction.

However, one constructive arrangement in Hemmingsen and Johnsen's work was that of the manipulation of the insulin physiological parameters within the Hovorka model (see Section 2.4.1)), namely:

1. Transport insulin sensitivity, SI1
2. Disposal insulin sensitivity,SI2
3. EGP insulin sensitivity, SI3

Figure 2.12 illustrates the general outline of the components inside the MPC. U_{ID} and D_{ID} are the insulin and meal information respectively. It can be observed that D_{ID} was not included in the parameters manipulated. Rather, in a number of cases, the meal information was of assistance to the MPC for the manipulation of SI1, SI2 and the SI3 parameters.

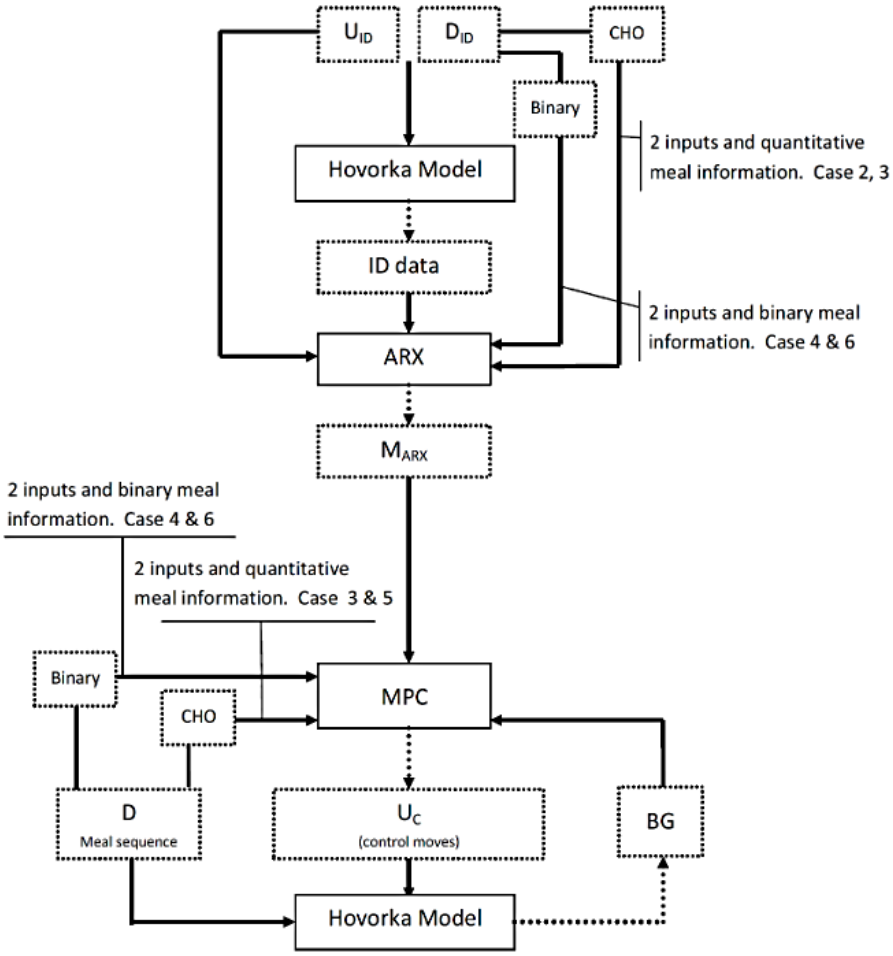

Figure 2.12: General outline of the components involved in the MPC [36].

The result shows that manipulated parameters were however found to have significant effects on the insulin-dynamics being modelled as they control the glucose distribution or transport, removal and endogenous production. Therefore, despite the minimal performance, a better understanding of their roles is attained even with the neglect on any manipulation on meal model. The study shows that a model geared towards a patient-specific nature will somehow improve BG prediction. Nevertheless, as meal information was not directly accounted but rather considered as a

disturbance (i.e., its presence was not inside the MPC structure), the MPC was unable to manipulate it and at many times prevented the MPC from reaching the target value in simulations.

In summary, the authors actually demonstrated that although the data being used is already synthetic in nature, the prediction had already shown to be minimal. One can imagine how the performance would be if an actual free-living data such as from Diabetes UK is employed. On the other hand, another relevant contribution of their work is that they introduced the method of varying the insulin parameters within the Hovorka model, and this can be emulated in other models. The method may address the limitations of the various modelling estimated from synthetic data.

Their result showed that the ARX model employed performed better for the predictions due to its much superior robustness to errors in meal information and variation in insulin sensitivity levels compared to ARMAX. While firm conclusions was unable to be drawn due to the weak result obtained, most probably because of insufficient clinical data used, the ARX model demonstrated the best prediction with better consistencies than ARMAX models, as also agreed by Jabali [37].

Chapter 4 will discuss further on the patient-specific model, using ARX to take into account the affecting variables such as the insulin and meal consumption, and propose the improvement that can be possibly done. The various following chapters will also present the hypothesis that not only meal input can be directly or exogenously modelled with insulin, but as well as having physical activity incorporated.

Further information on the use of ARX model using training and validation datasets for prediction purposes can be found in [38], [39].

2.6 Simulation and Prediction

A simulation is the computing of output(s) based on the inputs as well as the model response without prior knowledge at all about past outputs. On the other hand, prediction means producing a qualified guess of future output based on not only the model response, but together with the past observations of system's inputs and outputs. These distinct identification methods serve different purposes. For practical use of treatment in patients for healthcare, predictions are more commonly used because it is less prone to error due to its characteristics, where the future outputs are guided by past observations. Hence, it is safer for use on patients. However, in terms of model study which is not life-threatening to patients, simulation is better to ensure the accuracy of tested models, minimizing any interference from external parameters such as past outputs.

2.7 **Multiple Step-Ahead Prediction**

Multiple-step ahead prediction is a task of predicting the consecutive values in a time series. The sequence is predicted step-by-step, where current predicted time step is used to determine the next sequence in the following time step. By iteratively feeding back the output, any desired step ahead predictions can be tested such as 30 minutes, 60 minutes or 90 minutes. There is also the model-predicted output (MPO) that is the infinite-step prediction, where the output(s) is based purely on inputs with no feedback involved and can be considered as the simulation of the process.

2.8 **Performance Metrics**

Two widely used terms of performance metric, FIT and RMSE are used to evaluate the quality of prediction models made. FIT metric refers to the variation in the output explained by the model [40], [41] and RMSE tells the difference between the predicted and original output.

$$\text{FIT} = \left(1 - \frac{\sqrt{\sum_{k=1}^{N}\left(G(k)-\hat{G}(k)\right)^2}}{\sqrt{\sum_{k=1}^{N}(G(k)-\bar{G})^2}}\right) * 100\% \tag{2.12}$$

$$\text{RMSE} = \sqrt{\frac{1}{N}\sum_{k=1}^{N}\left(G(k)-\hat{G}(k)\right)^2} \tag{2.13}$$

where G is the vector of measured glucose values, $\hat{G}$ is the vector of model predictions, $\bar{G}$ is a vector whose elements are the mean of the measured glucose values, and the norms are Euclidean. Thus, FIT = 100% means a perfect prediction, FIT = 0 is obtained by predicting the mean of the measured glucose at every sample, and FIT < 0 is established from very poor model predictions. FIT value is the opposite of RMSE value. RMSE or square root of the mean squared prediction error is the absolute metric used, referring to a quantification of the magnitudes of the prediction errors and is given in physical units (i.e., mg/dl). In simple terms, higher FITs means that less variations exist between two compared plots, and vice-versa. Note that throughout this thesis, negative FIT values will frequently be encountered, and are only evaluated in terms of the magnitude value. They do not in any way represent negative output levels nor negative correlation.

2.9 Genetic Algorithm as an Optimisation Technique

The Genetic algorithm (GA) is one of the many optimisation techniques based on the process of natural selection emulating natural biological evolution. By repeatedly generating populations of individual solutions through exchanging partial information and random mutation of that information contained in the individuals, the solution improves with respect to the objective the individuals are attempting to satisfy. In the GA, crossover and mutation of the individuals are essential in that each iteration aims to improve the current best solution from the previous one, reaching an 'optimal' one at some point [42]. In this study, GA will be used a number of times to improve glycaemic prediction by finding the best solution referring to the parameters within the glucose-insulin models, to better predict predictions of BG values in patient. It is hoped that produced solutions could better fit inter-patient and intra-patient characteristics.

A set of solutions constituting the individuals represented by binary strings, or chromosomes, are called the population. From all the solutions, some will be selected to form a new population, with the hope that the new population will contain better individuals than the former. However, the newly selected population are not randomly chosen. Fitness is calculated for each individual, with fitter ones having better chances of replicating and forming the next generation. This is very much different to classical optimisation algorithms because they generate only a single point in each iteration while the GA generates a population of potential solutions. Another difference to note is that the next population is computed using random crossover of information from the individuals and mutation; not deterministic computation that usually relies on gradients.

The diagram in Figure 2.13 explains the three types of offspring generated [43]:

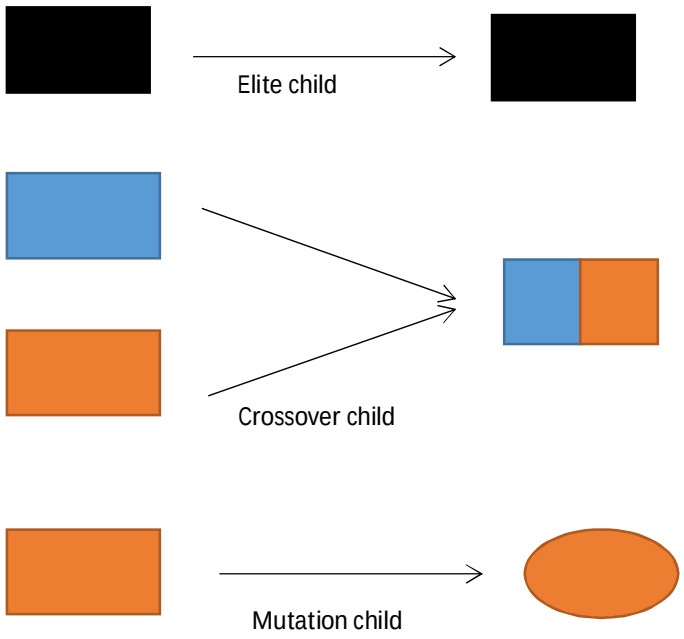

Figure 2.13: Types of offspring created.

The elite child is where an exact replica of the individual from previous population is chosen due to its fitness value - it has a relatively very good objective function value. The selection of both the parents' genes and entries be assigned to the offspring is called crossover. In the case of linear

constraints, the default crossover function picks the random weighted average of the two parents for the creation of the new child. An entirely changed offspring is called mutation child. A mutation child can arise from both a crossover and elite child. All of these processes are determined probabilistically by the fitness calculated.

There are conditions and bounds that can be set to improve the GA operation. Given the approximate solutions or points of where the relatively good objective functions can be identified, an initial population could be seeded to contain some of these good known solutions. Potential solution can be constrained to be within certain bounds, equivalent to inequality constraints on the free variables in classical optimisation. For example, the initial population shown in Figure 2.14 is seeded with individuals with parameters [x_1, x_2] corresponding to known good solutions (or initial estimates) while the parameters are bounded within the ranges $-5 \leq x_1 \leq 15$ and $-1 \leq x_2 \leq 1$.

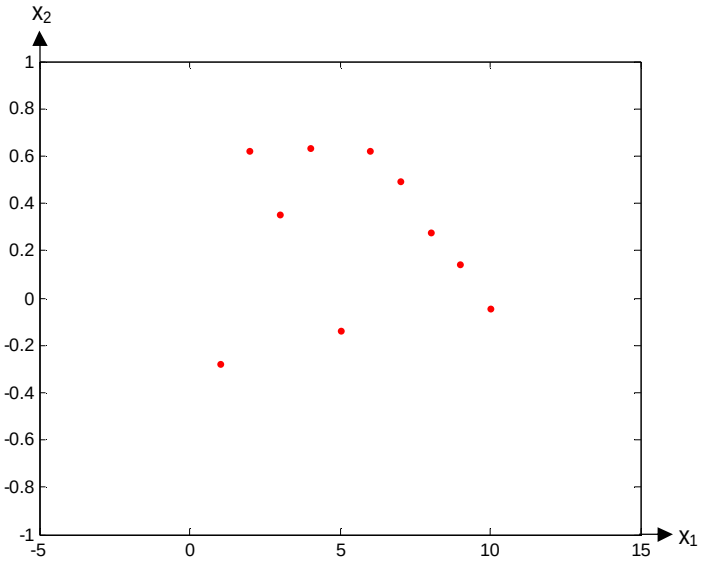

Figure 2.14: Example of initial populations within the bounds set.

The objective function is the function that we intend to optimise by finding the set of parameters that produce the largest (maximisation) or smallest (minimisation) cost value. A fitness value is calculated for each of the individuals in each generation and generally used to determine how often, if at all, each individual will be selected for reproduction into the next generation. Individuals with better objective values are proportionally more likely to be selected for reproduction than those that yield poor solutions. Through repeated generations, fitter individuals are more likely to reproduce and lead to better and better solutions.

In this study, GA will be used a number of times to improve glycaemic prediction by finding the best parameters to fit inter and intra-patient characteristics. In Chapter 5, the optimisation technique is used to tune and adjust parameters within the gut and insulin model of a respective subject. Measured BG levels was set as the prediction target in the single objective optimisation. With a linear system identification model having GA as the optimisers, the original parameters are initially considered and adjusted by the GA, allowing adaptation to volunteer's own bodily parameters. On the other hand, Chapter 8 discusses the use of GA in a multi-objective manner, to provide

improvised parameters, catered for the diabetes Type 1 cohort as a whole, an inter-patient investigation. This time, GA is used to modify parameters in the physical activity model, previously presented for Type 1 diabetics but its parameter estimates derived from healthy people. The case now differs to the linear identification model used in Chapter 5 as GA is used with an ordinary-differential-equation (ODE) model.

2.10 Missing Evidence and the Gap in Type 1 Diabetes Literature

None of the models described earlier was developed, tested or validated on free-living physical activity data. Most of the experimental data available in the literature was obtained in a controlled environment, such as hospitals and clinics, where many of the variables could be set independently. This is substantially different to the varying conditions experienced by Type 1 diabetics. Perry and Gallen [44] also stated that the evidence available to clinicians to develop guidelines is limited, and most of the current evidence comes from small cohorts that mostly are fit young adults, with old insulin preparations.

Kavookjian *et al.* [45] questioned the reliability of the research evidence, where most data of which collected in a controlled environment under strict protocols that do not reflect free-living conditions, can actually be translated into practical guidelines. Riddell and Iscoe [39] identify a lack of BG prediction models based on insulin dose, carbohydrate intake and type of physical activity. All of these have rendered unreliable prediction not properly addressing Type 1 diabetes. With all of these in mind, one can never be sure of any modelling that can actually efficiently reflect the nature of Type 1 Diabetes and its following treatments.

A number of modelling approaches have been discussed in the literature despite the fact that ambulatory data were used. To name a significant few, Hovorka *et al.* proposed [23] a Bayesian technique to estimate parameters for patients physiological model derived in a clinical environment. Sparacino *et al.* [46] estimated parameters for first order polynomial using autoregressive models for Type 1 diabetes patients, and the data were filtered for its noise removal. Oruklu [47], [48] however estimated for Type 2 diabetes patients with both clinical and ambulatory data. Finan *et al.* [49] did tests for Type 1 diabetics with unfiltered data represented in normal conditions and in reduced insulin sensitivity through medicinal administration, aiming to create changes in modelling dynamics for the model to adapt to.

In a sense, an interesting area of research would be the individualisation of glucoregulatory models, especially when this type of data is available in hand, which will be thoroughly discussed in Chapter 5. The holy grail of glucoregulatory system modelling is the identification of a stable generic model that can be tuned to each subject via knowledge of easily accessible clinical parameters such as body mass index (BMI), insulin sensitivity and body composition. In addition, from optimisation of parameters within the insulin, meal or physical activity models, parameters drawn to certain bounds may reveal similar associations or characteristics of diabetes patients, and clinicians can then classify them accordingly together with specific treatment types. In this sense, Patek *et al.* [50] worked around this classification by individualising the cost function of their model predictive controller rather than the model itself.

Therefore, the main study presented in this thesis attempts to address the shortcomings identified, mainly by the use of free-living data in a cohort of Type 1 diabetics, investigating correlations using data collected from the devices, and identifying the possible classifications of patients using optimisation in various diabetes gluco-regulatory models.

2.11 **Summary**

A thorough review of glucose metabolism in healthy individuals and diabetics were presented. A brief review of glucose metabolism, insulin absorption, and the complicated role of physical activity was presented. It highlights the day-to-day challenges faced by individuals with diabetes to maintain normoglycaemic levels. The different sub-systems making up the glucose-insulin dynamics and also several models proposed in the literature were discussed. A linear time-invariant system identification model was also presented, discussing previous models employed in the modelling of glucoregulatory-system. With system identification model, assessment can be made on the quality of metabolic models in predicting or simulating an individual's BG response, given specified inputs. However, there were inherent limitations to the model where not only the physical activity parameter was ignored, but the meal consumed was not appropriately quantified as well. Following chapters will further discuss ways on improving the limitations from previously presented studies. The rest of the chapter presents genetic algorithm as an optimisation technique to be utilised in this study. Using optimisation, it is hoped to refine current insulin-glucose model and accounts for physical activity, as will be discussed in the chapters ahead. The next chapter present in detail the research methodology employed in the study in detail, where physiological measurements of volunteers in a free-living condition were made.

Chapter 3: Data Collection and Research Methodology

This chapter discusses the methods of data collection and the nature of free-living data collected as part of a previous DUK Study [4],[46]. Subject recruitment and the research facility are described initially. Important features of the physical activity, food and insulin data collected are then described, followed by a number of correlations analysed from collected data such as BG with physical activity metric and fitness. The correlation analysis is important to investigate preliminary significant associations between the inputs. The tests can be valuable in the end when together with strong statistical power, firm conclusions can then be made. Finally, an explanation on the cross-validation method using k-fold validation is explained.

3.1 Diabetes UK Study

A DUK funded study (2007-2011) [9] investigated the effects of physical activity energy expenditure on BG control in people with Type 1 diabetes. Volunteers with Type 1 diabetes were recruited through Southampton Diabetes Clinics and their baseline characteristics were recorded at the Welcome Trust Clinical Research Facility based in Southampton General Hospital. Health variables such as HbA_{1c}, fat distribution, relative quantity to lean tissue and others were measured among the participants. Further details can be found in [9]. Free-living-data, those of particular interest to the study are discussed in the following sections: BGC measurements from the MiniMed Guardian real-time continuous monitor, metabolic equivalent task of unit measurements from BodyMedia SenseWear® armband, and the food and insulin diaries.

3.2 Subject Selection

Individuals recruited to this study aged between twenties to fifties, having HbA_{1c} levels from 5.5% to 11.7%. The study aimed to contain a wide range of diabetic patients and produce non-biased results. The data were collected among the individuals continuously over a two, two-week periods, six months apart. The study observed various patients with different physical activity levels, from sedentary to more active ones. In order to monitor their physical activity energy expenditure, they were required to wear devices that continuously measured their BG levels and metabolic equivalent tasks (MET) which are units of physical activity.

Table 3.1 shows the baseline characteristics of the 25 volunteers for which free-living data were collected. It is obvious from the table that there are quite variations of HbA_{1c}, age (20 to 51 years old), diabetes duration (1 to 34 years), wellbeing and others. These characteristics reflect the broad-ranging groups of T1 diabetic patients that are of interest, and it is desirable that the results to be concluded are formed from a neutral perspective. The volunteers' selection based on sex were also fairly distributed due to the fact that females have more hormonal changes that affect glucoregulatory systems as compared to men. Volunteers mostly used 3- 4 CGMS sensors during the each set of data collection, with each spanning around 72 hours of sensor reading. While there is a time gap (around 1 to 3 days as depicted in Figure 3.1) exists between the consecutive datasets from the sensors, the datasets are still considered contiguous for the purpose of this study.

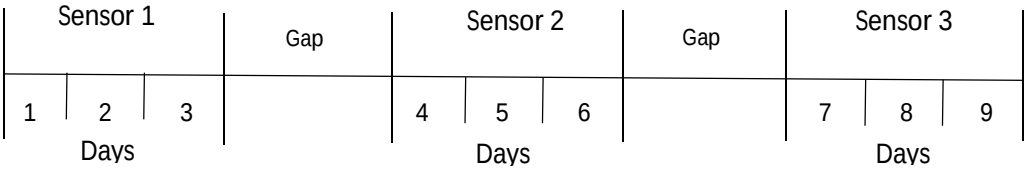

Figure 3.1: Timeline of duration of sensors worn by volunteers.

Subject	**Sex**	**Age** (*years*)	**Diabetes Duration** (*years*)	**Height** (*m*)	**Weight** (*kg*)	**BMI** (kg/m^2)	**Total Fat (%)**	**HbA_{1c} (%)**	**Sensors Used**	**Total CGMS Data** (*hours*)	**Total PAEE Data** (*hours*)
01	Male	23	5	1.65	63.8	23.6	17.6	5.5	6	407	362
02	Female	33	17	1.59	73.1	29.1	31.2	7.3	3	206	210
03	Male	44	24	1.72	63.6	21.5	17.7	9.1	4	331	270
05	Male	28	7	1.82	112.	33.8	28.5	6.7	4	184	271
06	Female	51	30	1.64	69.4	25.8	33.3	8.2	3	192	239
07	Female	39	27	1.64	97.1	36.1	40.4	7.7	3	196	111
08	Female	43	30	1.60	93.8	36.6	44.7	8.8	2	139	143
09	Female	45	27	1.66	61.4	22.3	30.8	6.3	4	235	275
10	Male	31	1	1.78	74.3	23.5	26.2	8.0	4	286	281
11	Female	47	23	1.62	77.4	29.5	35.6	8.4	3	208	215
12	Male	47	34	1.70	74.5	25.8	16.3	7.1	4	233	146
13	Male	24	22	1.91	72.2	19.8	16.6	9.1	5	315	321
14	Male	21	3	1.80	66.2	20.4	13.8	7.7	4	283	290
15	Female	41	3	1.68	62.6	22.2	31.1	11.7	3	202	215
16	Female	27	19	1.63	69.9	26.3	26.8	7.9	2	136	140
18	Male	45	12	1.66	56.1	20.4	17.7	7.6	6	292	320
19	Female	20	4	1.64	59.8	22.2	33.7	7.7	4	287	252
20	Female	43	20	1.63	80.7	30.4	37.7	7.4	4	284	296
21	Male	26	1	1.74	104.	34.7	24.6	8.8	4	270	172
22	Male	60	20	1.73	75.3	25.2	15.9	7.3	5	271	263
23	Female	35	1	1.70	73.4	25.4	32.8	6.1	4	231	156
24	Female	25	17	1.60	73.3	28.6	42.1	5.6	4	283	288
25	Male	45	24	1.81	87.3	26.6	26.4	7.3	2	194	238
Mean±SD		37±1	16±11	1.69±	75.7±1	26.5±5.	27.9	7.7±1.3	4±1	246±64	238±67

Table 3.1: Baseline Characteristics of the 18 study volunteers of whom their free-living data were collected.

Ahmad Uzair Mazlan, 2017. PhD Thesis Chapter 3: Data Collection and Research Methodology

3.3 Baseline Clinical Tests

The volunteers undertook a number of baseline clinical tests so that a number of physiological parameters can be established for future statistics and analysis in the study.

The variables that were collected in the DUK Study included VO_2^{max}, fat distribution, relative quantity to lean tissue, and standard diabetes screens such as HbA_{1c}. Key parameters of variables measured providing significant attributes of the volunteers suffering from diabetes Type 1 are explained in the following section.

3.3.1 DEXA Scan

The Dual X-ray Absorptionmetry (DEXA) scan is considered to be the gold standard for assessing body composition. Apart from fat and lean mass, it returns as well the body mass. DEXA uses two X-rays of different energy levels to scan the whole body and depending on the different levels of X-ray's absorption, body composition can be estimated. The scan involved volunteers lying down for approximately 10 minutes while the scanner measures the body fat with a small amount of radiation equivalent to walking around Southampton over three days in summer. Therefore, the exposure is widely assumed negligible.

3.3.2 Fitness Test

The maximal oxygen consumption is a measure of fitness, representing the maximum amount of oxygen that the body can combust for aerobic energy production per minute per kilogram of body weight. Volunteers were asked to wear a mask having a gas sensor attached to it. Then, the oxygen and carbon dioxide exhaled was measured using a Metalyxer 3B. The participants were then asked to run on a treadmill under the well-known Bruce protocol [16] which both speed and gradient increased every three minutes (see Table 3.2) and participants were encouraged to keep on going until exhaustion. VO_2^{max} is reached when the rate of oxygen consumption reaches a steady-state. The heart rate was also monitored during this time using a Polar Electro T61 chest heart rate monitor. To estimate respective VO_2^{max} values, for men, the Foster equation [52] was used and for women, the Pollock equations [53]. They are the function of the time spent on the treadmill under the Bruce protocol.

Time (min)	Speed (mi hr^{-1})	Slope (%)
0	1.7	10
3	2.5	12
6	3.4	14
9	4.2	16
12	5.0	18
15	5.5	20
18	6.0	22
21	6.5	24
24	7.0	26
27	7.5	28

Table 3.2: The Bruce Protocol.

Other than the baseline clinical tests measured, other free-living data collected that are of particular interests are BGC measurements from the MiniMed Guardian real-time continuous glucose monitor (Section 3.4.1), metabolic equivalent task (METs) of unit measurements from the BodyMedia SenseWear® Pro_2 armband (Section 3.4.2), and the food and insulin diaries (sections 3.4 and 3.5, respectively).

3.4 Data Acquisition

3.4.1 Blood Glucose Concentration

The Guardian Real-Time Continuous Glucose Monitoring System (CGMS) [54] was used for regular monitoring of BG levels. A depicted use of the CGMS can be seen in Figure 3.2.

Figure 3.2: The Guardian Real-Time Continuous Glucose Monitoring System (CGMS). The system consists of a glucose sensor and a transmitter.

The device works by having the glucose sensor to sample the interstitium and measure an electrical current proportional to interstitial glucose concentration. The glucose sensor data is then transferred to the monitor at a rate of 0.1Hz by the transmitter, while the display module displays the latest BG concentration updated every 5 minutes. The IF surrounds the cells throughout body tissues and a sensor is placed in the IF (usually in the lower torso or leg) to measure the current generated by glucose oxidation, which will be proportional to the glucose concentration at the site of measurement. Then, BG levels are estimated from a regression equation from the sensor readings, and is calibrated using finger-prick readings, using standard BG meters. Calibrations must be performed at least every 12 hours due to the sensor drifts. The sensor is connected to the monitoring device via a wireless link and must be within the range of a few metres to the sensor. An example of the CGMS output of one day of measurements is shown in Figure 3.3. Collected data yield physiological occurrences of activities done throughout a day which are reflected in BG levels. This CGMS output describes a reliable estimate of BG levels that can be further analysed and interpreted with the help of other data.

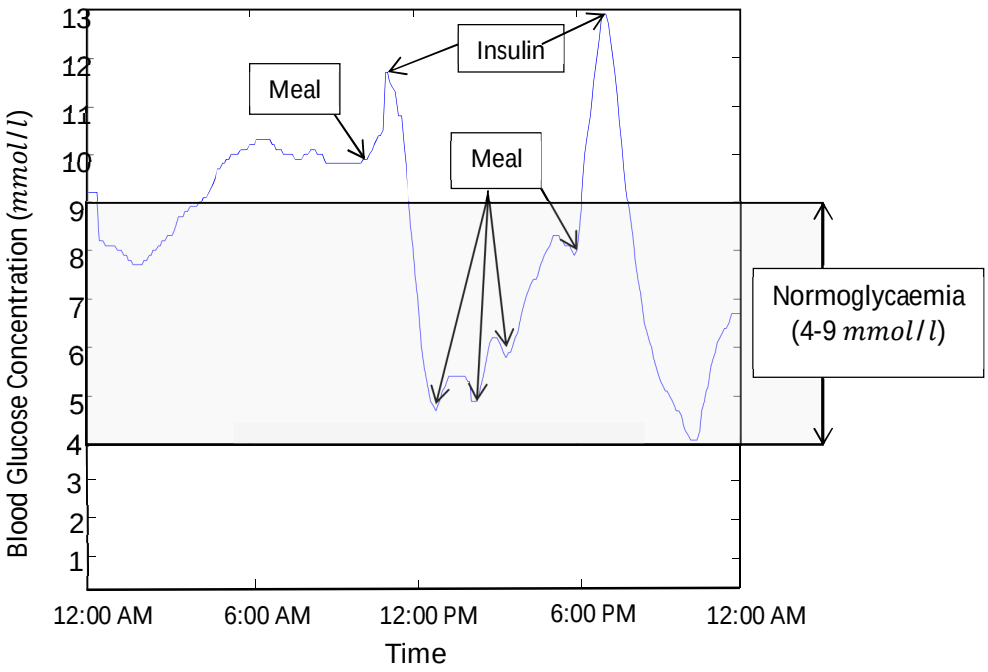

Figure 3.3: BG concentration over a 24-hour period.

As recorded in Figure 3.3, it is evident that this subject has experienced the dawn phenomenon, which is a normal early-morning rise in BG, followed with a rapid rise in BG levels at around 10 A.M. due to the consumption of morning breakfast, and then a steep fall with the taking of fast-acting insulin. Subsequently, a number of peaks varying within the normoglycaemic range (4 - 9 $mmol$/l) occurred, which are reasonably expected. This is followed by a swift rise due to evening meal and a sharp drop of BG levels from insulin administration possibly combined with intense physical activities.

The BG levels measured correspond to a number of parameters that raise and lower them – insulin and dietary uptake. With the help of data from SenseWear® armband that measures physical activity, it is also possible to identify any relationship between physical activities done and BG levels resulting from the activity levels and duration monitored. The armband operation will be presented in the following section.

3.4.2 Physical Activity Data

The SenseWear® Pro_2 armband was used to collect physiological variables as listed in Table 3.3 [51] and with these data, an estimation of metabolic equivalent of task (METs, $kcal/kg^{-1}\ hr^{-2}$) is calculated by first evaluating calorific utilisation. Figure 3.4 depicts the armband with the respective sensors to measure bodily data.

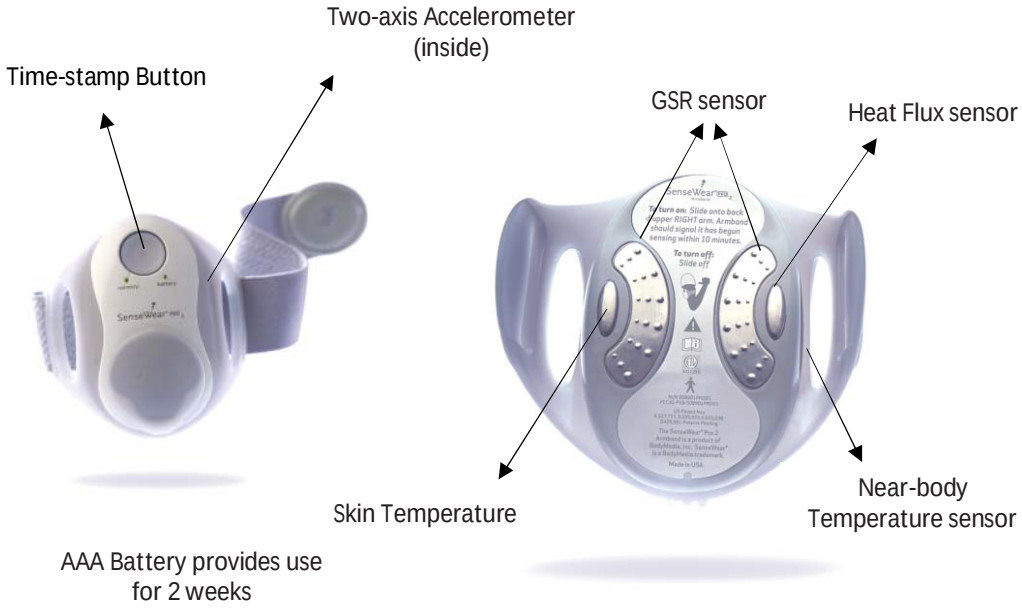

Figure 3.4: The SenseWear® Pro_2 armband. Reproduced from [55].

METs indicates a specific measure of energy expenditure as a multiple of resting metabolic rate (RMR). RMR is the energy expenditure at rest (at room temperature and in a post-absorptive state), demonstrating the amount of energy required for normal vital organ activities. The methods of calculating calorific utilisation and METs are described and validated against the gold-standard doubly labelled water method in [55].

Variable	Description	Unit
Transverse acceleration average (TAA)	Using two-axis accelerometer providing information on body position and movement (average over time interval)	*counts*
Transverse acceleration mean absolute deviation (TAM)	As above but records mean absolute deviation	g
Transverse acceleration peaks (TAP)	As above but records peak during time interval	*counts*
Longitudinal acceleration average	Measurement perpendicular to TAA	*counts*
Longitudinal acceleration mean absolute deviation	As above but for TAM	g
Longitudinal acceleration peaks	As above but for TAP	*counts*
Near body temperature	Average ambient temperature	℃
Skin temperature	Average temperature of the skin	℃
Heat flux	Measures of heat dissipated by the body along a conducted path between skin and armband's vent	W/m^2
Galvanic skin resistance	Measures conductivity of the skin using two sensors (relates to physical and emotional stimulus)	μ*Siemens*

Table 3.3: Variables recorded by the Sensewear® Armband [51].

Activity	METs Equivalent
Sleeping	0.9
Lying Down	1
Walking (2mp)	2
Bicycling (general)	4
Jogging	6

Table 3.4: Examples of METs approximations to designated activities taken from [56].

Components and functions of the Sensewear® Armband device are discussed in [15][57]. Its reliability and repeatability are also explained, as well as the advantages of the device compared to other methods for calculating energy expenditure. Furthermore, the design of the devices permits continuous wearing throughout daily activities (except in wet condition) with minimal impediment to the mobility of the individual. As a result, free-living data are readily obtainable and recorded every minute. In this study, it was important to measure the activities done without any intrusion on user's daily life. Different levels of METs and measured parameters are associated with different physical activities and these can then be associated with typical activities as shown by the examples in Table 3.4. It is an approximation from the data in Table 3.3 taken by the SenseWear® armband.

Figure 3.5(a) shows an example of the skin temperature, Figure 3.5(b), the longitudinal acceleration and Figure 3.5(c), the energy expended recorded from a single subject over a 24-hour period. From Figure 3.5(c), the subject appears to be relatively inactive until around 11:00 AM, then variably active for a period of a few hours, and then reducing in his/her activity level until the subject sleeps at night. This is reflected in the longitudinal accelerations recorded in Figure 3.5(b) capturing a component of the body movement. Similarly, we can observe in Figure 3.5(a) that after the relatively high body temperature occurring during sleep, skin temperature reduces during heavier level of physical activity due to the skin's thermoregulatory function producing sweat to cool the body. Such patterns are typical in the activity data in the DUK study with highly varying METs during waking hours. However, different individuals will show markedly different BG responses.

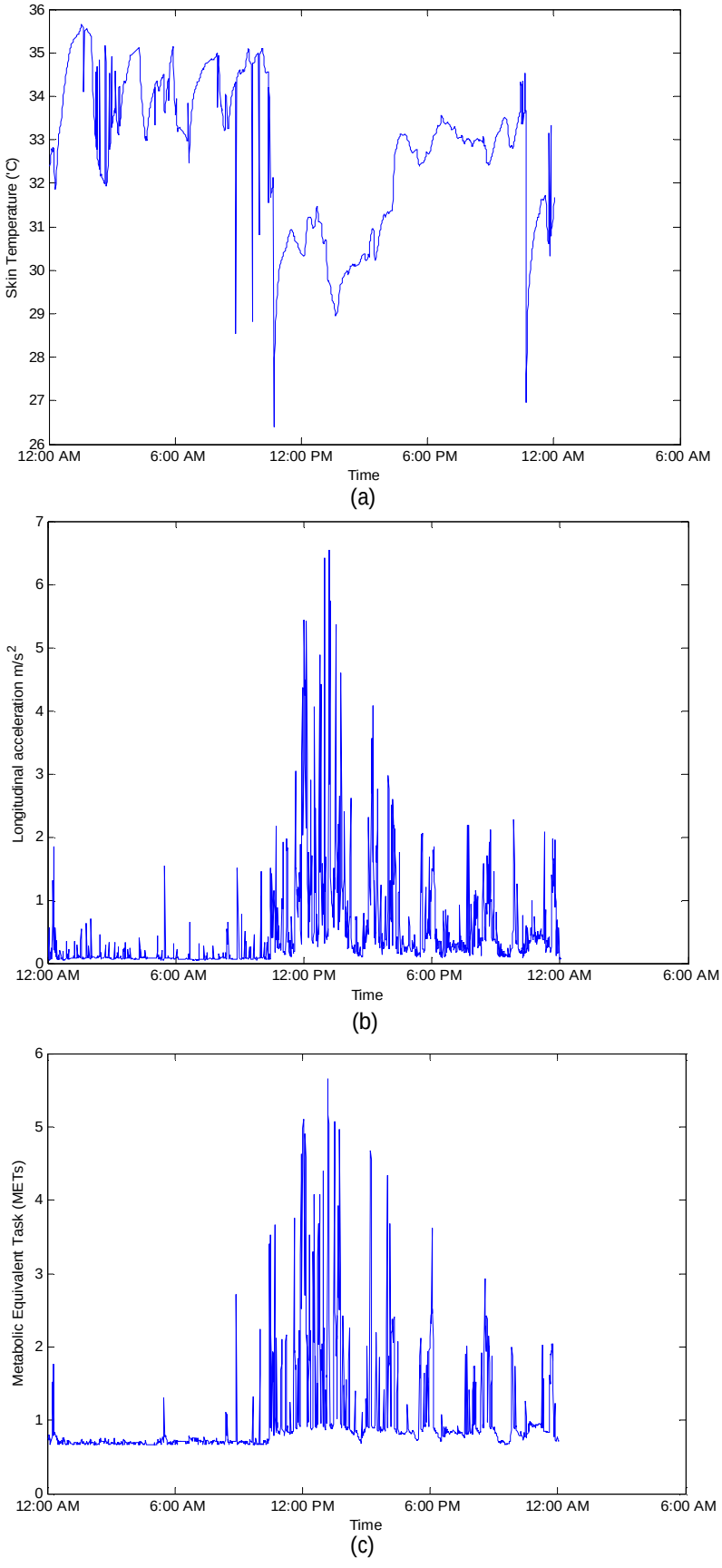

Figure 3.5: (a) refer to skin temperature over a 24-hour period collected from armband. (b) refers to longitudinal acceleration over a 24-hour period collected from armband. (c) Metabolic Equivalent Tasks approximated from SenseWear® armband data.

3.4.3 Heat Flux

Heat Flux is an important parameter measured also by the Senswear armband, representing the net convective heat lost by the body. Thermal equilibrium states that heat produced by the body is equal to the heat released. Heat released by the body is a by-product of the ATP generation in the mitochondria where glucose exists as the main substrates. Despite only convective heat flux is being measured by the armband (thereby disregarding heat released via conduction, radiation or evaporation), it is still reasonable to assume that changes in heat flux are related to changes in glucose concentrations. Researchers also showed the concept of estimating BG levels from the amount of heat dissipated by the body, albeit having limitations in the technology. This study will also test the hypothesis that heat flux is indeed associated with BG concentrations.

Valletta showed that there is a significant inverse association between area under the curve for BG and heat flux, but relative association between standard deviation of BG and standard deviation of heat flux. This thereby suggests that increasing levels of heat flux is related to the increase usage of glucose by the mitochondria to generate ATP, and hence a decrease of glucose in the bloodstream. Heat flux data were also found to vary between active and inactive diabetic volunteers, as well as between people having HbA_{1c}< 7.5% and HbA_{1c}> 7.5%. Mean heat flux in the afternoon and evening were also observed to be significantly different between inactive and active groups, but not the case for morning and night. This is reasonable since many high physical activities are done during afternoon and evening, and augmented contractions in the muscle induce more heat dissipation in the active group than in sedentary one.

Figure 3.6 depicts the typical free-living data of variables modelling diabetes with also physical activity data as an additional important parameter as discussed in Section 2.1.1. The physical activity data was quantified using metabolic equivalent (METs), which is the multiple of the resting metabolic rate, and heat flux, as it could be a marker of ATP generation in the mitochondria.

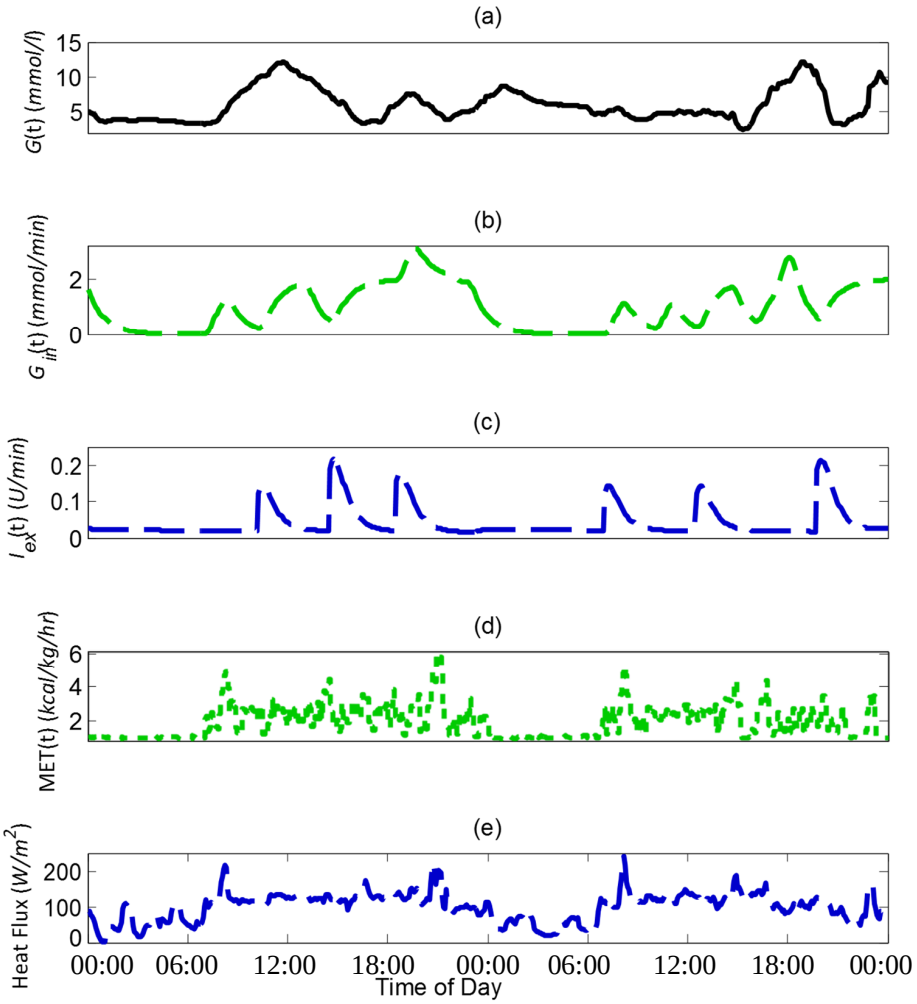

Figure 3.6: Typical free-living data in Type 1 diabetes patients used for modelling. (a) BG (b) rate of exogenous glucose appearance in the bloodstream G_{in}. (c) rate of exogenous insulin flow I_{ex} (d) METs and (e) heat flux Hf(t).

3.5 Food Diary

Every participant in the DUK study recorded their food intake in a diary. Type and amount of food were recorded, along with the time of consumption, and the nutritional content estimated from the nutritional information or food databases. Food consumed were converted into grams of carbohydrate intake by using food databases, or for specific branded foods, having them as stated by the producers. However, the process is susceptible to various sources of error such as lack of a detailed description of food, the inter-patient subjectivity in the estimation of portion sizes, the under-reporting of foods consumed as well as the variations in translating food description into grams of carbohydrates.

Note that the difficulties in estimating calorific intake have always been a pressing issue among nutritionists and to circumvent this, various techniques have been established. For example, Beasly *et al.* [58] used PDAs having built-in food libraries and Martin *et al.* [59] made their participants to undergo food training on how to describe their food and estimate the portion sizes properly, albeit

none has actually shown significant improvements. Currently, image processing technique has as well taken the lead in this field where individuals can take a photo of the meal and have its calorific intake displayed on their devices. Despite its limitation in the database capacity and individual technical know-how, satisfactory improvements are shown. In this study, the self-reported diary was the method chosen. It was deemed sensible since many Type 1 diabetes patients are able to properly recognise consumed food as they are experienced and well-trained for carbohydrate counting, compared to the general population. Hence, a better description of their portions' estimates is highly likely expected from them in the latter.

In general, the method of data collection is appropriate enough in terms of the applicability of the study's outcomes to the bigger Type 1 diabetes population, who generally uses carbohydrate counting as part of the Multiple Dose Injection (MDI) regime. Finally, the food diaries do not present any dynamical description of the effect of carbohydrate towards BG response. However, a model of the digestive process (as presented in Section 2.2) will be used to better represent how food intake affect BG levels in the volunteers.

3.6 Insulin Diary

On the other hand, the volunteers also recorded information of every insulin injection, such as the time of injection, dose and the insulin type. Due to the nature of Type 1 diabetics having a completely malfunctioned pancreas and being fully insulin-deficient, circulating insulin concentrations depend on the injected dose and the diffusion from the subcutaneous depot to the capillaries. Therefore, one can expect a more precise and accurate estimation of insulin injected into the body with the details in hand, in contrast to Type 2 diabetics where the flowing insulin estimation could be confused with ones coming from the pancreas together with the injected. Similar to the food diaries, the records do not offer dynamical description of the effect of the insulin on BG level. To properly understand the behaviour of blood insulin concentration, it requires a frequent blood sampling and specialised equipment, and hence is not feasible in free-living conditions. Due to this, models describing the process of insulin absorption (as shown in Section 2.4) can provide the alternative to the invasive blood samples, offering important information on the appearance of insulin in the blood.

3.7 Free-Living Data Properties

Figure 3.7(a) shows typical free-living data, in this case collected from subject #13, for BG, insulin type and intake and CHO intake. Figure 3.7(b) and (c) show the insulin activity calculated using Tarin's model (presented in Section 2.4) and CHO response from dietary intake proposed by Lehman *et al.* (discussed in Section 2.2). The plots are actually quantitative values computed from impulses seen in Figure 3.7(a), labelled as green, red and black bars. In Figure 3.7(a), the plot shows measured CGMS values along with impulses of insulin injection (Rapid-Acting and Long Acting) and carbohydrate consumed (normalised to the same scale). The insulin and carbohydrate can be seen being impulses in nature, and as explained earlier, were self-reported by volunteers, and therefore needed modelling to become quantitative and of continuous nature as seen in Figure 3.7(b) and (c).

It is clear that consumption of carbohydrate raises BG levels while injection of insulin does the opposite. The 'Insulin Flow' and 'Carbohydrate Intake' however show the quantitative or modelled version of the impulses from respective models – i.e. insulin and food are considered instantaneous

uptakes resulting in a continuous release. Observationally, a relationship can be seen between BG, insulin and CHO data in Figure 3.7(a) and the modelled insulin and CHO availability in Figure 3.7(b) and (c) respectively. In Figure 3.7(c), the different characteristics of rapid and long-acting insulin and their combined role in maintaining a suitable basal rate using bolus injection to address rises in BG from the appearance of CHO can be observed. It should be noted that this subject was unusual in the use of long-acting insulin in this particular subset of data. The relationship between the two stimuli and BG will be explored in detail using various dynamic modelling approaches in Chapters 4, 5 and 6.

Despite the fact that humans tend to have fairly regular daily routines and activities including physical activity, eating patterns and insulin injections, it is worth noting on the spontaneity of events that may occur at times. An example of this could be the consumption of snacks, missed injections and a counter-reacting manner to this, and a somewhat intense but short physical activity like running for a bus.

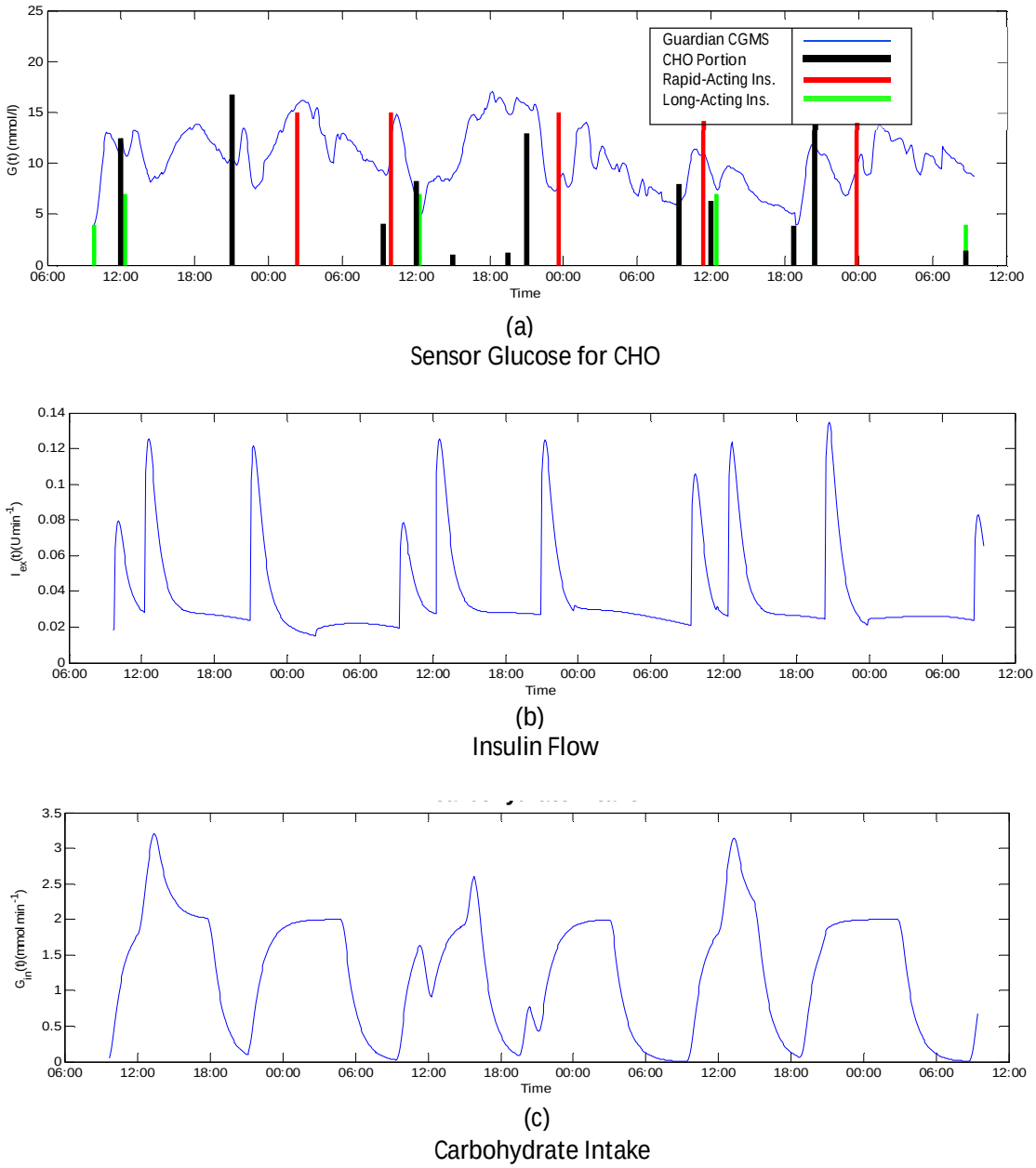

Figure 3.7: Typical free-living Type 1 diabetes data used for system identification from subject #13. (a) refers to the BG levels measured. (b) refers to the insulin flow into the bloodstream. (c) depicts the carbohydrate intake.

3.8 **Stationarity**

Many linear modelling techniques such as ARX requires the data to be covariance stationary. However, in real life examples, blood glucose levels vary over time due to various physiological and external reasons, evident by the HbA_{1c} assay. In the case of ARX prediction for diabetes data, the signals need to be stationary within the prediction horizon. After all, a short-term prediction is what is desirable by clinicians.

In order to assess the stationarity of free living sensor glucose (SG) data, an auto-correlation function (ACF) was calculated along different portions of the same dataset in an individual's data. Figure 3.8 yields the computed ACF in three different portions across patient's #12 dataset from hours 0 - 72, 24 to 72 and 48 to 72. Subject #12 is selected for the ACF computation example due to its more illustrative behaviour than the rest. It is prevalent that variations can even occur within the same individual's sensor glucose data. While (a) depicts diverging curves at just 50 minutes of lag, (b) shows the three ACF having similar curve until lag of 200 minutes. However, the fact remains true that ACF is similar at low lags despite the discrepancies that exist due to inter-patient and intra-patient variability.

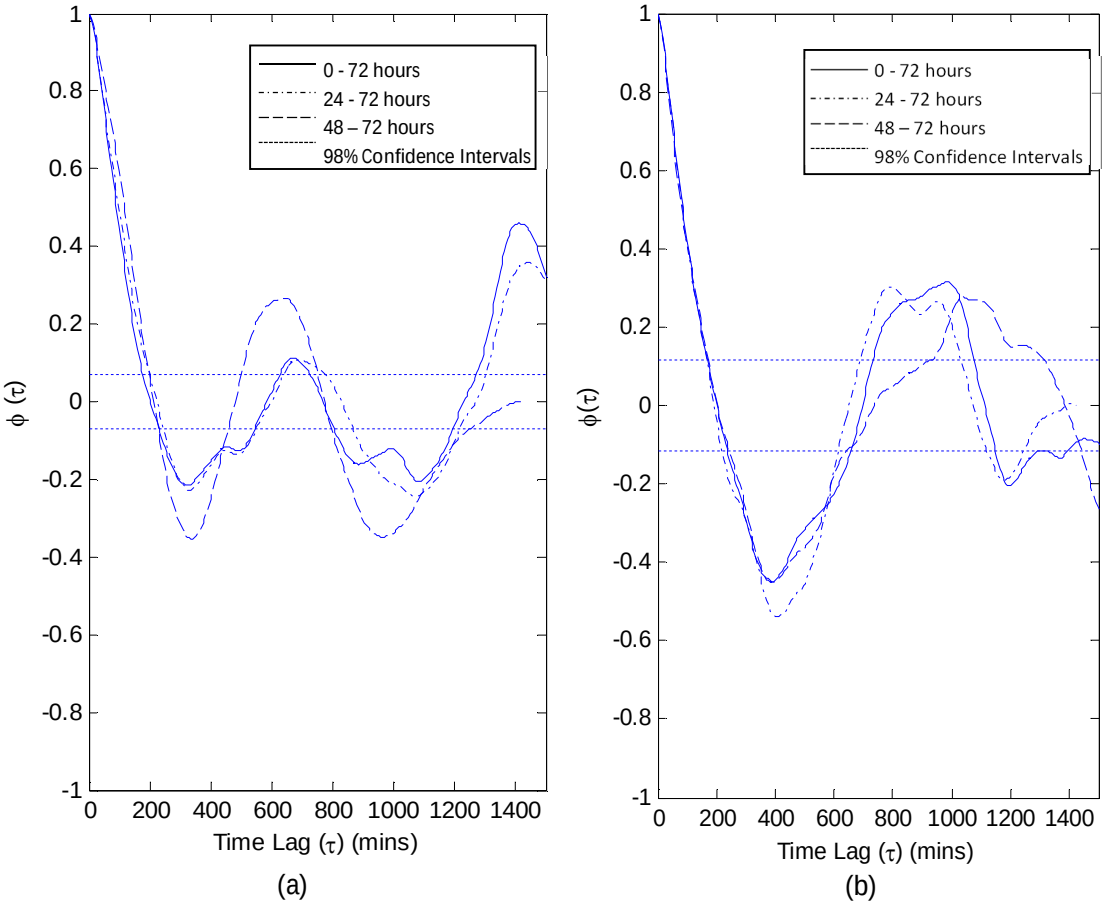

Figure 3.8 Auto-correlation function of sensor glucose for contiguous datasets of subject #12.

3.9 Data Correlation between Inputs and Physiological Parameters

The various physiological parameters obtained from the Diabetes UK data collection are correlated to investigate any significant associates. The initial correlation test considered carbohydrates ($G_{in}(t)$) input and insulin flow ($I_{ex}(t)$), as shown in Figure 3.9, with data taken from subject #4. A solid positive cross-correlation found at low lags proves the administering of insulin at a similar time following the main meal. However, a negative correlation was found in larger lags, possibly due to the quasi-periodicity of inputs that resulted both being in "anti-phase" to each other.

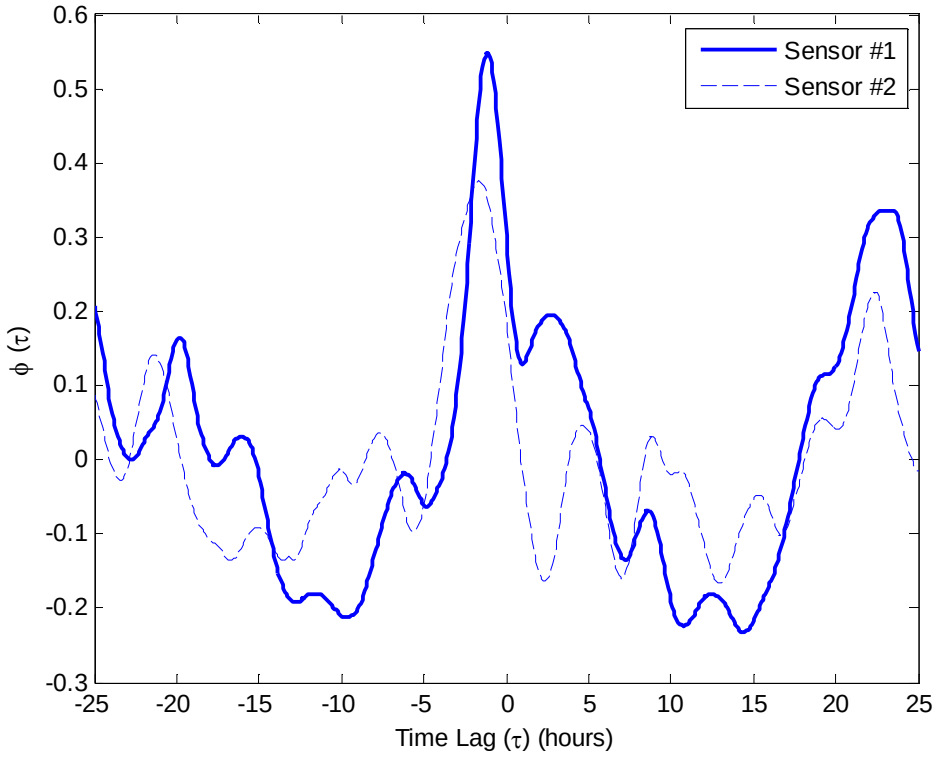

Figure 3.9: Cross correlation function (CCF) between inputs, being insulin flow ($I_{ex}(t)$) and carbohydrate intake ($G_{in}(t)$) for subject #12.

3.9.1 Correlation between Physical Activity and Blood Glucose

Physical activity and blood glucose is then correlated to investigate any significant associations, using Pearson product-moment correlation coefficient. A p-value for the null hypothesis that there is no correlation between two variables, was computed using a Student's t-distribution and a p-value smaller than 0.05 was considered as being statistically significant.

The possible associations between physical activity and blood glucose are then analysed using the two main metrics, the daily average physical activity energy expenditure (PAEE) and the daily average METs (Metabolic Equivalent). The former is calculated from the difference between the average total energy expenditure (EE) and the resting metabolic rate (RMR) while the latter was taken directly from the Sensewear® armband. Glucose is calculated using four metrics, being the daily average area under the curve (AUC), the daily mean, the daily variance (big variance may show

signs of poor glycaemic regulation) and HbA_{1c}, as depicted in Table 3.5. Note how the variance in many parameters between the subjects is high, as well as METs data being very wide, reflecting a wide range of people from sedentary to active, although limited to the number of people within the cohort.

The Pearson correlation coefficient and the corresponding p-value between physical activity and blood glucose metrics are shown in Figure 3.10. A negative correlation was seen in the area under the curve, mean BG and HbA_{1c} with the increase levels of physical activity, due to the increase glucose uptake and utilisation. This observation reckons the general assumption that increased activities reduces the mean BG and HbA_{1c}. Though a positive correlation is seen for the blood glucose variance, it is a little weak and therefore, cannot be confidently summarised. A general expectation would be much less excursions of BG from the mean due to the same reason - physical activity. However, the odd occurrence can be attributed to the weak management of the meal and insulin combination, whereby the two extremes of hypos and hypers can occur despite the physical activity performed.

The correlation between average METs and blood glucose metrics are shown in Figure 3.11. Being similar to the previous observation, the associations are much stronger with correlation between AUC and mean glucose being nearly significant. Note that for the glucose variance it matches with what being anticipated - positive associations. In other words, higher average METs do correspond to better glycaemic control.

Subject	Sex	Age (*years*)	Diabetes Duration (*years*)	Height (*m*)	Weight (*kg*)	BMI (kg/m^2)	Total Fat (%)	HbA_{1c} (%)	Sensors Used
	Ages (years)	Total Energy Expenditure (kcal/24hr)	Resting Metabolic Rate (kcal/24hr)	Physical Activity Energy Expenditure (kcal/24hr)	Metabolic Equivalent (kcal/kg/hr)	Area Under Curve (mmol/l) * 24hr	Mean (mmol/l)	Variance (mmol/l)2	HbA_{1c} (%)
01	23	2968	1738	1230	2.19	1513	5.25	0.78	5.5
03	33	2263	1455	808	1.33	2127	7.39	2.93	7.3
03	44	2459	1655	804	1.56	1763	6.12	6.02	9.1
05	28	3704	2361	1343	1.46	1710	5.94	4.84	6.7
06	51	2469	1369	1100	1.51	1999	6.94	9.89	8.2
07	39	2233	1762	471	1.03	2355	8.19	5.76	7.7
08	43	2477	1562	915	1.15	3947	13.71	15.58	8.8
09	45	2039	1202	837	1.41	2503	8.69	4.79	6.3
10	31	2519	1690	829	1.48	3100	10.77	8.69	8
11	47	2626	1466	1160	1.43	2783	9.66	12.74	8.4
16	27	2851	1653	1198	1.71	2273	7.89	12.75	7.9

Table 3.6: Physical activity and blood glucose results for the study cohort

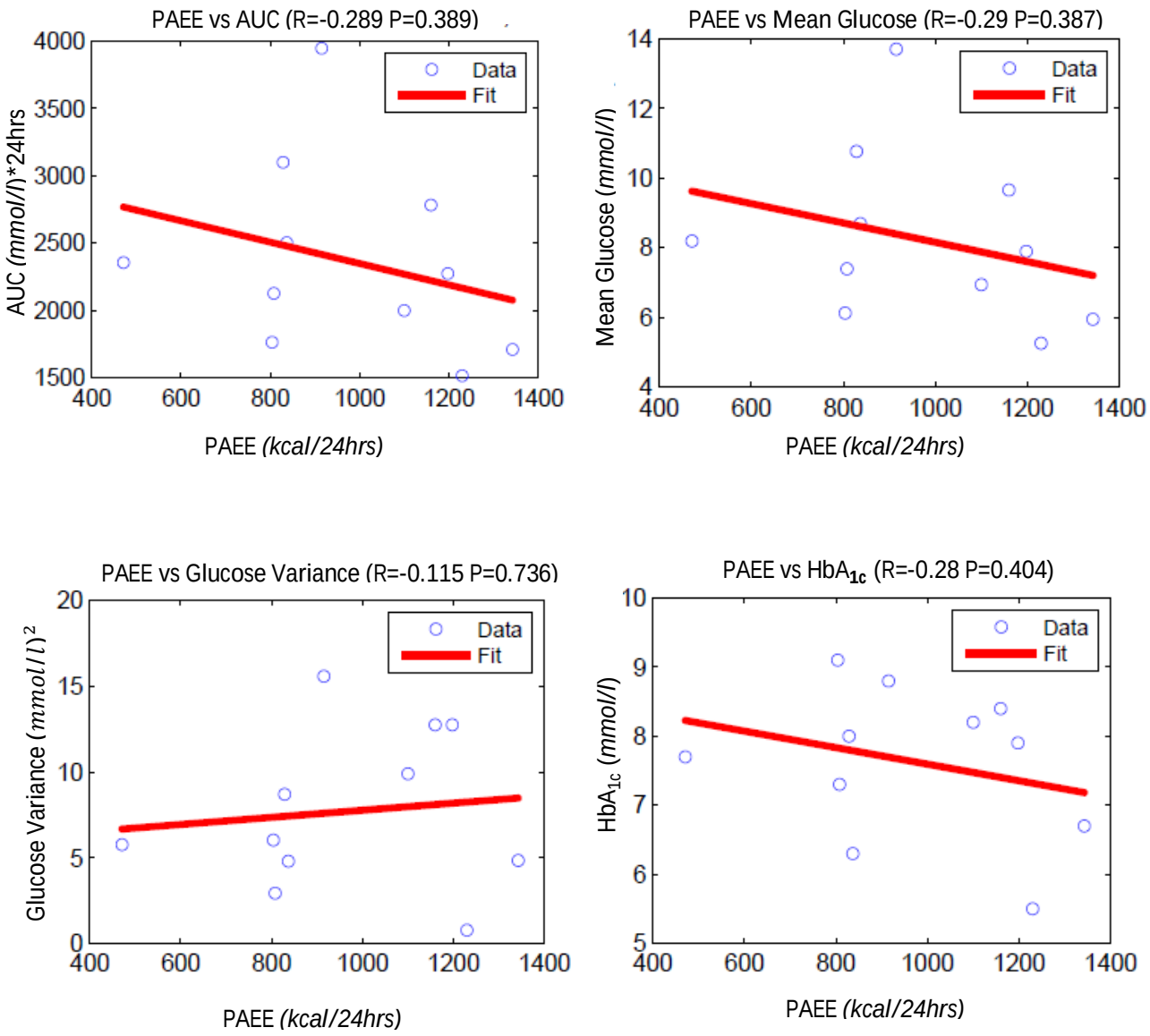

Figure 3.10: Correlation between physical activity energy expenditure and blood glucose.

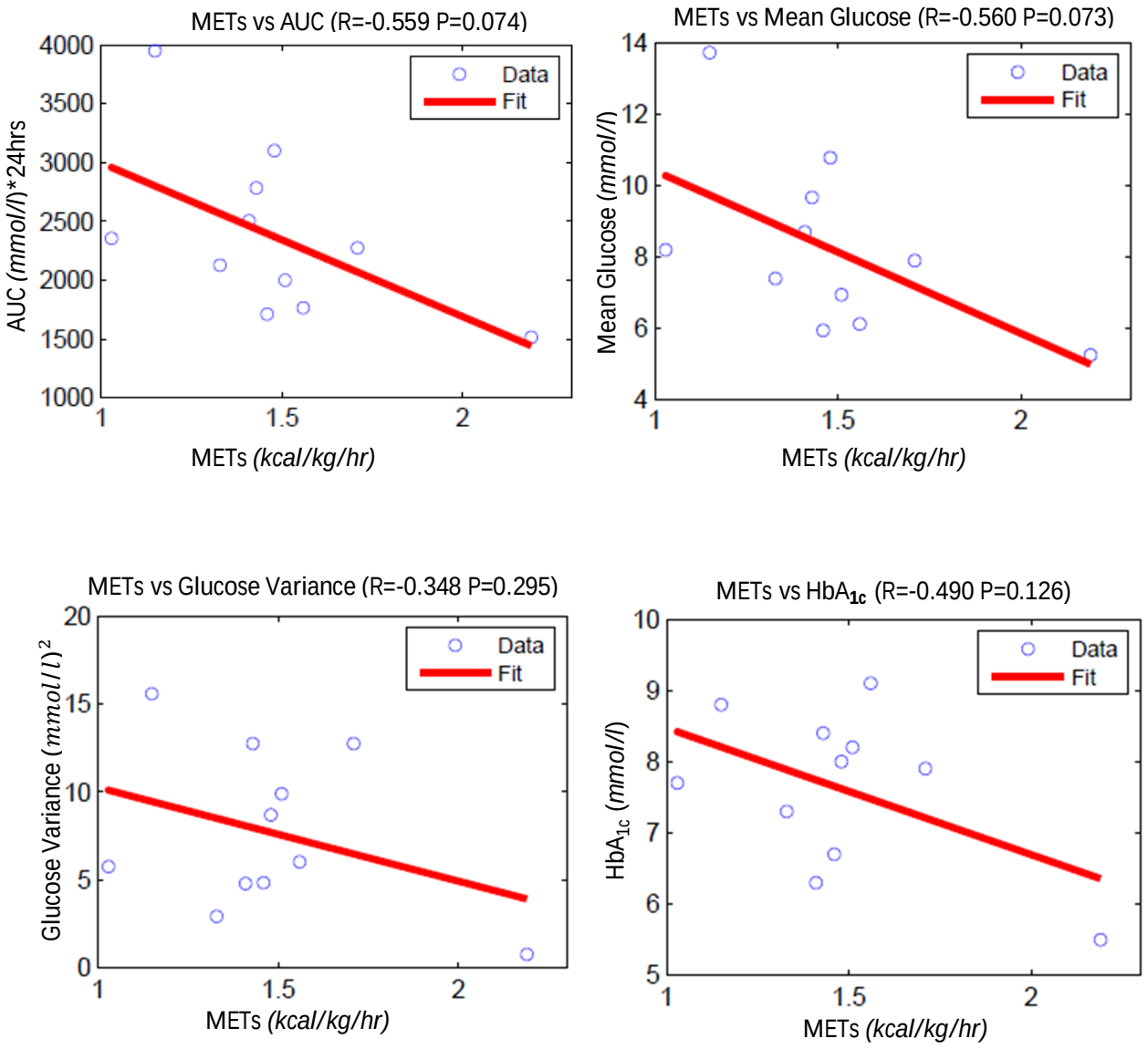

Figure 3.11: Correlation between average METs and blood glucose metrics.

3.9.2 Correlation with Body Composition

To associate correlation with body composition, four metrics for body composition were considered, the body mass index (BMI), the % body fat, the % truncal fat and the % lean mass. All of the data (apart from BMI), was acquired from a full-body DEXA scan and the % lean mass was obtained after subtracting the % bone mass [9]. The results obtained are shown in Table 3.7. The Pearson correlation coefficient, its corresponding p-value between the physical activity and glucose metrics, and body composition are given in Table 3.8, with significant correlations shaded in grey.

Subject	Body-Mass Index (BMI) (kg/m^2)	Body Fat (%)	Truncal Fat (%)	Lean Mass (%)
01	23.58	17.6	17	78.3
02	29.10	31.2	28.9	65.4
03	21.27	17.7	15.3	79.4
05	33.88	28.5	31.6	68.7
06	25.71	33.3	33.1	63.4
07	36.23	40.4	40	57.5
08	36.64	44.7	45.1	52.8
09	22.42	30.8	32.1	66
10	23.40	26.2	30.3	70.5
11	29.46	35.6	30.2	60.6
16	26.31	26.8	26.2	69.9

Table 3.7: Body composition data.

As expected, there is a correlation between METs and BMI, body fat, truncal fat and lean mass, confirming the supposition that people more physically active tend to have lower BMI, less body and truncal fat, and therefore higher lean mass. As a note, fat is basically an efficient way of storing excess glucose which cannot be stored in the liver or the muscle. Active people constantly have increased glucose uptake and utilization in the peripheral tissues, producing less excess of fat to be stored in the adipose tissue. On the other hand, less active people will have excess glucose being stored in the liver or the muscle. All of these much possibly relate to the insulin-regulated and exercise-dependent GLUT4 glucose transporter facilitating the diffusion of glucose.

In addition, a significant correlation is seen in the area under the curve (AUC) and mean glucose with body fat, truncal fat and lean mass. This confirms the fact less excess glucose in active people will translate into lower BG levels within their data.

	BMI (kg/m^2))	Body Fat (%)	Truncal Fat (%)	Lean Mass (%)
PAEE	r=-0.114 (p=0.7384)	r=-0.315 (p=0.3452)	r=-0.305 (p=0.3624)	r=0.286 (p=0.3932)
METs	r=-0.640 (p=0.0338)	r=-0.812 (p=0.0024)	r=-0.796 (p=0.0034)	r=0.787 (p=0.0041)
AUC	r=0.379 (p=0.2504)	r=0.689 (p=0.0191)	r=0.703 (p=0.0157)	r=-0.692 (p=0.0182)
Mean	r=0.380 (p=0.2490)	r=0.689 (p=0.0189)	r=0.704 (p=0.0156)	r=-0.693 (p=0.0181)
Variance	r=0.304 (p=0.3637)	r=0.554 (p=0.0767)	r=0.497 (p=0.1202)	r=-0.561 (p=0.0728)
HbA_{1c}	r=0.157 (p=0.6457)	r=0.330 (p=0.3224)	r=0.228 (p=0.4997)	r=-0.314 (p=0.3463)

Table 3.8: Correlation between physical activity, blood glucose and body composition.

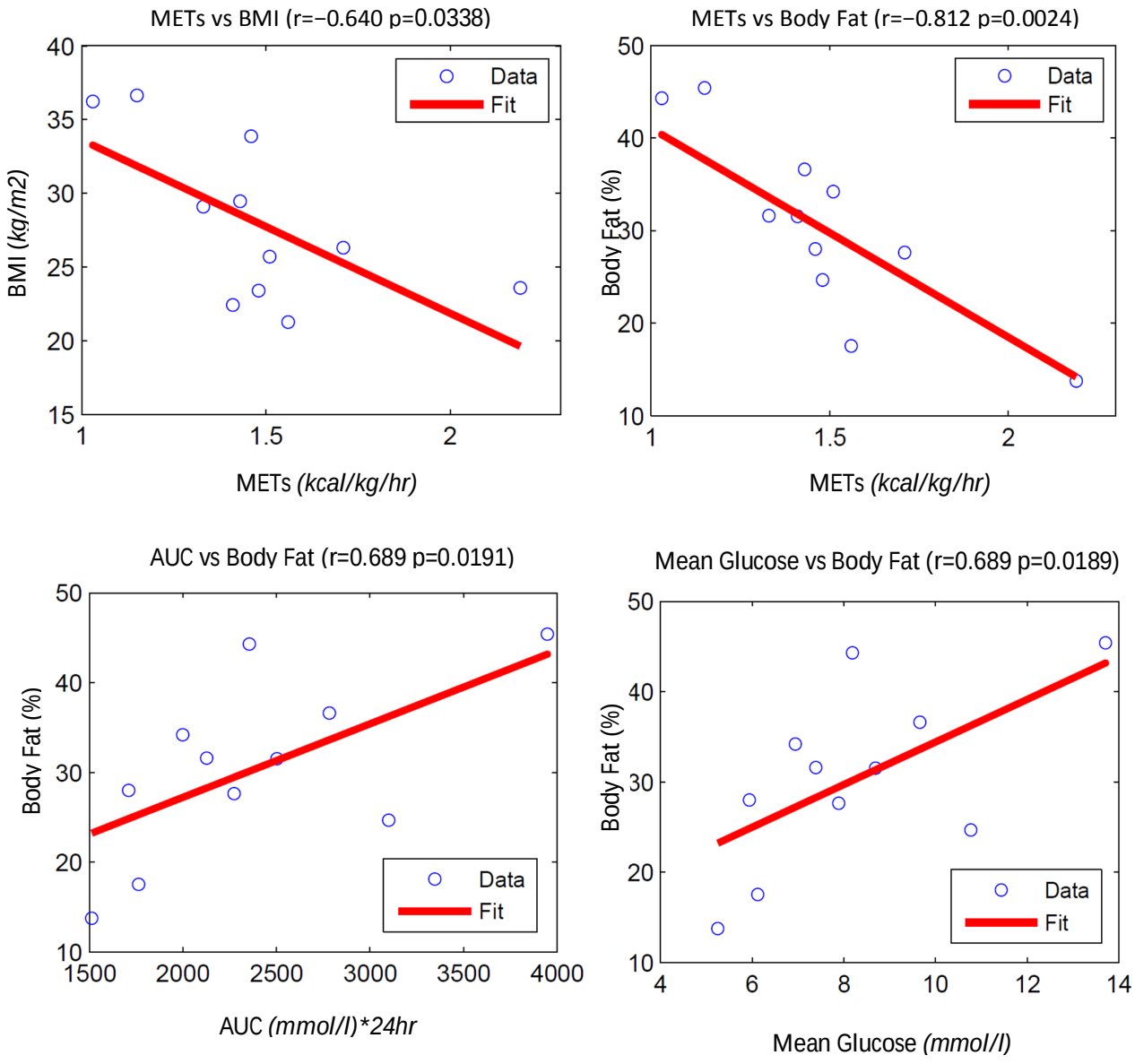

Figure 3.12: The significant correlations with body composition.

3.9.3 Correlation with Fitness

Using the term maximal rate of oxygen consumption (VO_2^{max} in ml/min/kg), fitness of a person can be reasonably derived. As stated earlier, the VO_2^{max} was estimated from the time spent on the treadmill (under the Bruce Protocol), using the Foster and Pollock equation for male and female, respectively. Table 3.10 depicts the results. The Pearson correlation coefficient and the p-value between physical activity, glucose and fitness are shown in Table 3.9.

Subject	VO_2^{max}
01	50.12
02	39.97
03	33.64
05	38.86
06	36.98
07	23.48
08	Unavailable
09	42.6
10	36.5
11	29.53
16	47.64

Table 3.10: VO_2^{max} results

	VO_2^{max}
PAEE	r=0.580 (p=0.0787)
METs	r=0.792 (p=0.0063)
AUC	r=-0.372 (p=0.2906)
Mean	r=-0.373 (p=0.2885)
Variance	r=-0.250 (p=0.4853)
HbA	r=-0.596 (p=0.0692)

Table 3.9: Correlation between physical activity, blood glucose and fitness

From the results, a significant positive correlation between METs and fitness was observed. People who are active in daily exercises have shown improvements in their fitness levels. Fitness, in a sense, is the ability to increase the perfusion of blood through the working muscle, the capillary-to-muscle fibre ratio and the ability to hyperventilate or allowing more oxygen available to the bloodstream for aerobic energy production. During the fitness test, the cardiovascular and respiratory systems are put under tremendous stress and therefore, the measured VO_2^{max} translates the quality of the physiological systems in an overall metric. It can also be observed that fitness has a positive correlation with physical activity energy expenditure too. However, a negative association with HbA_{1c} was seen, showing an improved glycaemic regulation as a result of high fitness. Nevertheless, it was observed as well that no significant association was found with glucose AUC, mean or variance. From this analysis, it is fair to assume that similar to HbA_{1c}, fitness can be presumed as a 'long-term' health metric, while others can be deemed as short-term metrics. It is also true that VO_2^{max} can only be improved after sustained periods of regular training over time.

3.10 **Cross Validation in Data Testing**

Cross-validation techniques is a way to validate any training or estimation made earlier using part of a dataset without leaving any unaccounted for. This is to reduce any variance especially when the dataset is small and a resampling may be required so that a single data instance can be used many times.

In the context of our study where human care (devising of treatment) and lives (prevention from extreme cases of hyper/hypo) are involved, it is paramount that the prediction of the phenomenon such as events of hyperglycaemia or hypoglycaemia is done in the most accurate way possible. This could be achieved with the maximisation of the learning process, in our case during the training and testing of dataset, for example, BG data. One would prefer that ideally, each and every point is taken into account so that the whole underlying processes are learned as the envelope of the relationships is acquired in the training phase. Psychologically, this means that an efficient treatment could then be devised to counter-react events of highs and lows in BG levels. It also reduces the chance of false positives and consequently, saves lives, whereby a corresponding insulin injection may be given due to an expected highs or lows, leading to unintended hypoglycaemia.

A good prediction requires a good training and testing of the dataset in question. A common practice is done by splitting the time series data into two datasets for training and testing purposes. However, whilst an even separation of data is guaranteed, the dataset would have been lost partly to the training set and partly for the testing set, reducing the learning processes. This is as depicted in Figure 3.13, using BG dataset as an example with its data points split for testing and training.

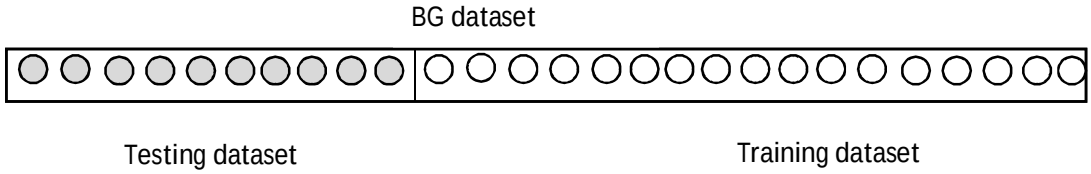

Figure 3.13: Testing and training dataset from blood glucose dataset.

Cross validation comes handy to address this matter. Using k-fold cross validation, the dataset is partitioned into k separate subsamples. For example, a dataset containing 200 data points are divided into k=10 subsamples, therefore each subsample will contain 20 datasets, as depicted in Figure 3.14.

20	20	20	20	20
20	20	20	20	20

k=10

Figure 3.14: Samples divided into *k* dataset, for k-fold validation tests.

Of the 10 subsamples, a single subsample (*i*=1) is retained as the validation data for testing the model, and the remaining k-1 are used as training dataset. The process is then repeated k times with every other subsample will be tested once for data testing. In the end, the k results from the repetition will be averaged to produce a single estimation, without leaving any of the dataset unaccounted for.

While the choice of the value k depends on the number of instances, number of variables and the types, k value is usually set to 10 with various studies stating high k results in lower bias and higher variance estimator, and with low k results in higher bias with lower variance estimator[60]–[62]. Our tests with various k values for multiple subjects, as depicted in Figure 3.15, yields more bias at lower folds, especially for two and four, while the estimates are reasonably good from 10 folds onwards.

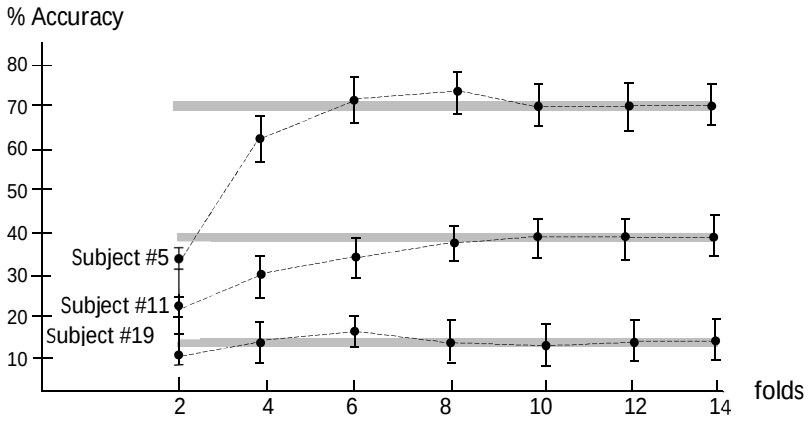

Figure 3.15: The bias of cross-validation with varying folds. Grey regions indicate the 95 % confidence intervals.

Once the training process is completed and the underlying processes learned, the model can be rest assured to predict better output from an unseen input data set, given that all of the relationship have been acquired in the training phase.

In our test, there are 22 diabetes patients as the subjects, with each and every one having 3 to 4 CGMS sensors during each of data collection, and each sensor spans up to 72 hours of sensor reading (see Section 3.2) or 360 instances of data points. According to the cross-validation method, the dataset is split into k=10 (36 instances), and then k-1 (324) instances are used for training while the former for testing. These arrangements are continuously used for training and testing throughout the models presented in this study.

3.11 **Summary**

Initially, the two main measurement devices have been introduced and described in terms of their use to measure and collect data of BG levels and PAEE. With the CGMS data, accurate and continuous measurements of BG levels can be obtained. From the Sensewear® armband, we are able to quantify the METs data into approximations of physical activities and its occurrence. This chapter has also introduced the idea of converting a discrete stimuli, such as an insulin injection, into a longer-term stimuli representing the appearance of usable insulin in the blood flow.

Next, the correlations between physical activity, blood glucose and other physiological parameters were considered. Significant associations found from the analysis are physically active people have less fat deposits and it can be safely associated with better glycaemic regulation. Regular physical activity also improves fitness level within a diabetes patient.

The observed associations highlight the benefits of routine physical activity and its effects on glycaemic regulation. Note also that the subjects were in no way intervened in terms of their daily lifestyle. On the other hand, they are encouraged to perform the same activities that they would do normally. It is hoped that further analysis on these parameters help predict BG levels better, and hence, better devised treatment.

The final section deals with the dilemma in maximising the best learning results whereby the dataset would be partly lost for the training set and some for the testing set, reducing the learning result. Therefore, a k-fold cross validation method was used for training and testing purposes to address this matter. With k validation method, the whole instances within the dataset was considered for testing without leaving any unaccounted for. This is especially important for human healthcare purposes, where the risks of underfitting or overfitting of data can be potentially reduced, and false positives in predicting BG levels decreased.

Chapter 4: Type 1 Diabetes Features Extraction

This chapter explains the investigation using particular tools effort to discover and investigate BG and other data for repeating patterns or motif. With the discovery of repeating pattern in BG data, it could potentially help elucidate time constants in the processes underlying BG regulation, effects that might be caused from repeating routines in the subjects such type of meals, insulin injection routine such as its time and amount, physical activity intensity and frequency, or simply the efficacy of the particular therapeutic regimen that one an individual has adopted.

4.1 Introduction

Understanding variations in BG levels in individuals with Type 1 diabetes involves recognising the physiology, measurement techniques and therapeutic regime, and interpreting them by meaningful analysis. In this chapter, an overview of a recent feature detection technique is introduced as it is important to consider patients' habitual, and possibly cyclical, behaviour in their diet, physical activity, lifestyle and corresponding glycaemic regulation.

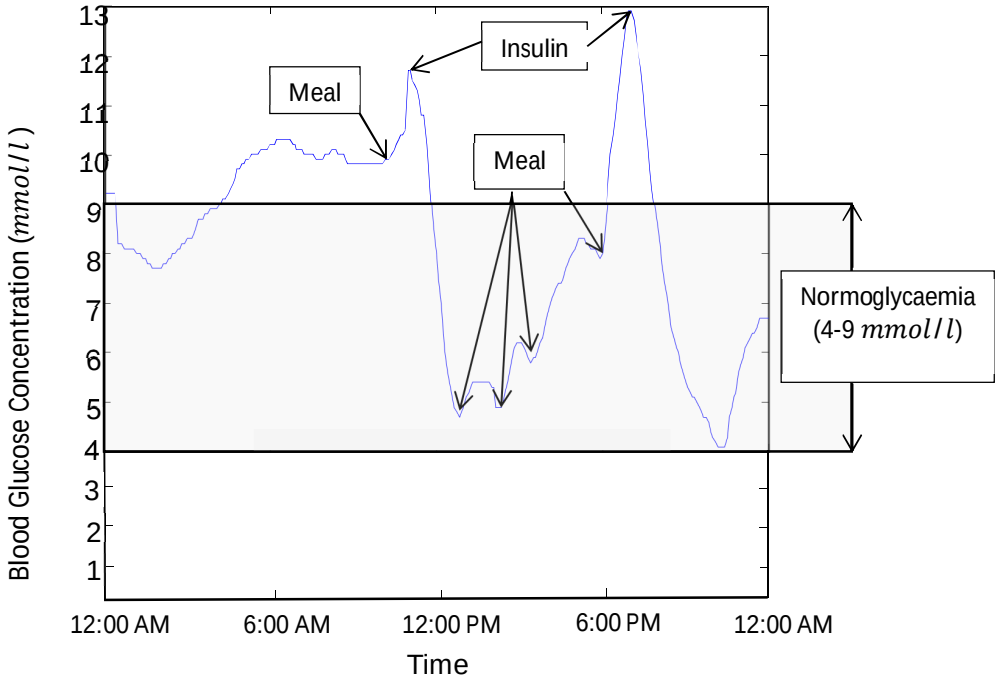

Figure 4.1: Example of BG concentration over a 24-hour period.

Figure 4.1 shows an example of a BG concentration over a 24-hour period obtained from a typical Type 1 diabetic volunteer. In this example, as no long-acting insulin was taken during the 24-hour period, the effect of CHO and fast-acting insulin intake can be seen more clearly. During the night, BG drops then gradually increases with a higher rate of increase after a meal. Following insulin around 11:00 A.M. and 7:00 P.M., BG drops rapidly. Several items of food are then consumed which can be seen to raise the BG level. The meal at 6:00 P.M. is followed by a raise in BG as the fast-acting insulin at 11:00 A.M. has dissipated and is followed by a rapid drop following the insulin at 7:00 P.M. It is a difficult job for people with diabetes to keep and maintain their glucose concentration within the indicated normoglycaemic bounds by regulating between these two main inputs accordingly.

In this chapter, the recently developed MK algorithm [63][64] will be introduced and used to assess BG and other data to try and find repeating patterns.

4.2 **Mueen-Keogh (MK) Algorithm**

The MK motif discovery technique was originally proposed to find recurring patterns or motifs (used interchangeably throughout) within a sequence of data. Time series motifs are pairs of individual time series, or subsequences of a longer time series which are very similar to each other. The method was proposed to find recurring patterns and the developers demonstrated the ability of the technique to find repeating insect behaviours, construct EEG dictionaries, data compression [63] and also, patterns in music data and eruptive volcano activities [65]. The MK algorithm utilises a Euclidean distance measure to compute comparisons between time series subsequences with the objective of finding the closest-pairs subsequence of given length *m* in the time series *T* [66].

The underlying characteristic of the MK algorithm is the assumption that initially a *best-so-far*-distance is presumed to be infinity. Figure 4.2(a) shows a dataset in the form of two-dimensional time series objects, represented by Object 1 to Object 8 (*O1-O8*). Object *O1* is chosen at random as the reference point in the example in Figure 4.2(b), and the rest of the other objects are arranged according to their distance to it. In this example, the distance between *O1* and *O8* as its nearest neighbour, now updates the *best-so-far* distance to be 23.0. The distance between adjacent pairs, as shown in Figure 4.2(c), can then be calculated while sorting the objects on distance. Note that in the original space, these distances are not true distances, but rather the lower bounds of them. This linear ordering of data provides heuristic information for the motif search. It can be observed that two objects can actually be arbitrarily close in the linear ordering but wide apart in the original space.

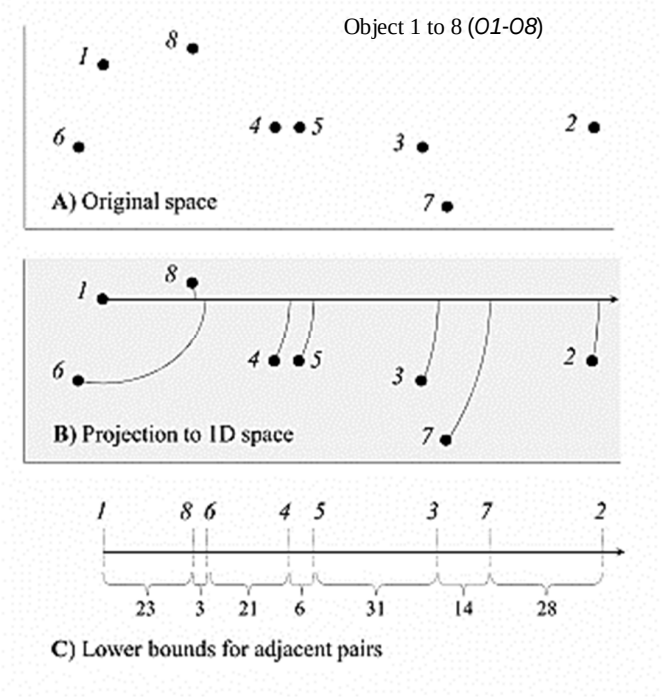

Figure 4.2:(a) Two dimensional time series object. (b) The object arranged in one-dimensional representation by measuring distance to a reference point (*O1*). (c) Distances between adjacent pair along the linear projection is a lower bound to the true distance between them. Reproduced from [66].

Next, the linear ordering is scanned and the true distances are measured between the adjacent pairs. Whenever a pair having distance less than the current *best-so-far* is encountered, the *best-so-far* value is updated, as shown in Figure 4.3. Sliding from left to right would update the estimated distance between *O8* and *O6* and be corrected to 42.0. The next update yields the true distance between *O4* and *O5* to be 7.0. Since it is less than the current *best-so-far*, it is updated and further sliding through the data objects shows it having the lowest value, and the desired motifs have been found.

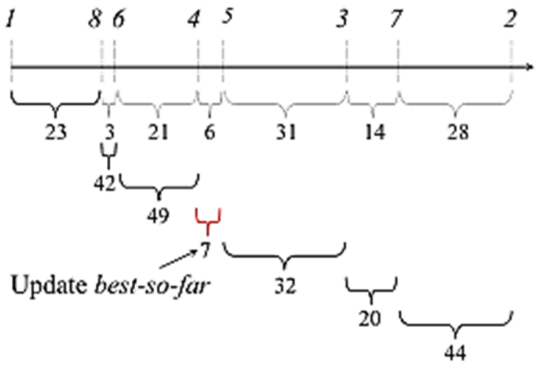

Figure 4.3: Objects are scanned from left to right to measure the true distances between them. Note that only the first pair *O1* and *O8* have the linear distance as the true distance while for others, they are only lower bounds.

Further pruning of the search space can be achieved by combining the linear representation with the *best-so-far* value. Looking at the lower bound distance between the pair *O8* and *O3* (60.0), and comparing it to our *best-so-far* (7), the pair can clearly be eliminated as a motif candidate. This is done without having to measure the true distance between the pair *O8* and *O3*. More generally, a sliding window of exactly width 7 (*best-so-far*) can be tested on the linear order for possible pairs while also eliminating incorrect candidates, as shown in Figure 4.4.

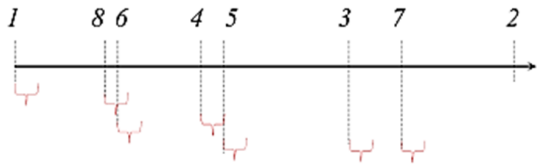

Figure 4.4: A required condition for two objects to become the motif is that both of them intersect the sliding window at the same time. Only the two pairs *O8*, *O6* and *O4*, *O5* matches it becoming candidates while others are eliminated.

The above is an intuitive explanation of the approach of the MK algorithm. However, in reality, not all objects are as equally good for a reference point. Thus, there is a need for multiple rounds of pruning steps with multiple reference points in contrast to the single-step approach presented.

A more formal statement of the MK algorithm is depicted in Figure 4.5. As mentioned earlier, the requirement of it are the time series (*T*), the number of reference objects (*R*) and subsequence length (*m*), while the outcome would be the locations L_1 and L_2 (location of motif). Following the arrangement of objects from the initial reference point, the distances of all subsequences are calculated and stored in a table called *Dist*, which is also sorted [65]. Objects that are worse than

the *best-so-far* are disregarded for computing of the actual distance of the two motif candidates (reflected in lines 20-21). After the arrangements, the linear ordering is scanned and true distances between adjacent pairs are measured, followed by an update to the *best-so-far*. All data points not pruned in the initial ordering step are stored in *I* (line 13). During actual distance computation, a variable *offset* is introduced, an integer between 1 and *m*-1, to refer to the j^{th} and j^{th}+*offset* item in the ordered list *I*, which are both candidate pairs for testing. The algorithm starts with an initial *offset* of 1 and searches pairs that are *offset* apart in the *I* order. Until all pairs have been identified, the *offset* is increased, meaning that the current round of search is completed. This continues until all the pairs have been evaluated revealing the motif locations L_1 and L_2 [65]. Further explanation on how MK code works can be found in [63][64].

Algorithm. L_1, L_2 =*MK-Motif(T, R, M)*

in: T is a time series, R is the number of reference objects, m is the subsequence length

out: L_1, L_2 are the locations for a Motif

1: *best-so-far* = INF
2: **for** $i = 1 \rightarrow R$ **do**
3: ref_i = a randomly chosen subsequence T_r from T
4: **for** $j = 1 \rightarrow m$ **do**
5: $Dist_{i,j} = d(ref_i, T_j)$
6: **if** $Dist_{i,j} <$ *best-so-far* **then**
7: *best-so-far* $= Dist_{i,j}, L_1 = r, L_2 = j$
8: **end if**
9: $S_i = standardDeviation(Dist_i)$
10: **end for**
11: **end for**
12: find an ordering Z of the indices to the reference objects in ref such that $S_{Z(i)} \geq S_{Z(i+1)}$
13: find an ordering I of the indices to the subsequences in T such that $Dist_{Z(I),I(j)} \leq Dist_{Z(I),I(j+1)}$
14: $offset = 0, abandon =$ **false**
15: **while** $abandon =$ **false do**
16: $offset = offset + 1, abandon =$ **true**
17: **for** $j = 1 \rightarrow m$ **do**
18: $reject =$ **false**
19: **for** $i = 1 \rightarrow R$ **do**
20: $lowerBound = |Dist_{Z(i),I(j)} - Dist_{Z(i),I(j+offset)}|$
21: **if** $lowerBound >$ *best-so-far* **then**
22: $reject =$ **true, break**
23: **else if** $i = 1$ **then**
24: $abandon =$ **false**
25: **end if**
26: **end for**
27: **if** $reject =$ **false then**
28: **if** $d(D_{I(j)}, D_{I(j+offset)}) <$ *best-so-far* **then**
29: *best-so-far* $= d(D_{I(j)}, D_{I(j+offset)})$
30: $L_1 = I(j), L_2 = I(j + offset)$
31: **end if**
32: **end if**
33: **end for**
34: **end while**

Figure 4.5: MK algorithm step by step representation. Reproduced from [65].

4.3 **Pattern Discovery in Blood Glucose data**

Two fairly common phenomena occurring in people with Type 1 diabetes that are considered for initial reference motifs are discussed here: the dawn phenomenon (DP) and the Somogyi effect. The two are hyperglycaemia occurrences experienced by Type 1 diabetics during sleep-wake cycles, with high BGs prior to waking.

Dawn phenomenon usually occurs when any insulin taken late in the evening causes BG levels to drop sharply around midnight to 3:00 A.M, the time where our body generally sleep most soundly and has little need for insulin. Subsequently, between 3:00 A.M. and 8:00 A.M., the body starts releasing stored sugar to prepare for the coming day, while also producing hormones, e.g. insulin-like growth factors IGF-1 and IGF-2, that reduce the body's sensitivity to insulin. These occur just as the night-time insulin where it is also wearing off. These events, when taken collectively, cause the body's blood sugar to rise in the morning (depicted in Figure 4.6(a)), hence the term 'dawn phenomenon'.

A second cause of high blood sugar levels in the morning might be due to the Somogyi effect or reactive hyperglycaemia, shown in Figure 4.6(b). Although the end result is the same as the DP, the cause is not as natural, and is more 'man-made' (diabetes management). A probable cause would be due to too much insulin intake earlier or insufficient bedtime snack, leading to a large drop in BG during the night, followed by a counter-reaction response from the body: the release of glucose from the liver signalled by glucagon when low BG is detected to raise it back to safe levels [67]. The hypoglycaemic events at night are not recognised by the patient as they are sound asleep and the liver response leads to high BG upon waking. Somogyi, the person who first investigated this phenomenon, speculated that excessive insulin uptake made diabetes unstable [68]. As a result of these events, the insulin dose would be further increased by the patient, promoting the likelihood of further hypoglycaemic events and instability in diabetic control.

These two events are often described as the morning effect where high BG in the morning was preceded by low BG the night before. Indeed, these two were among the first observations found using MK Algorithm in CGMS data, and examples from the volunteer cohort are shown in Figure 4.7.

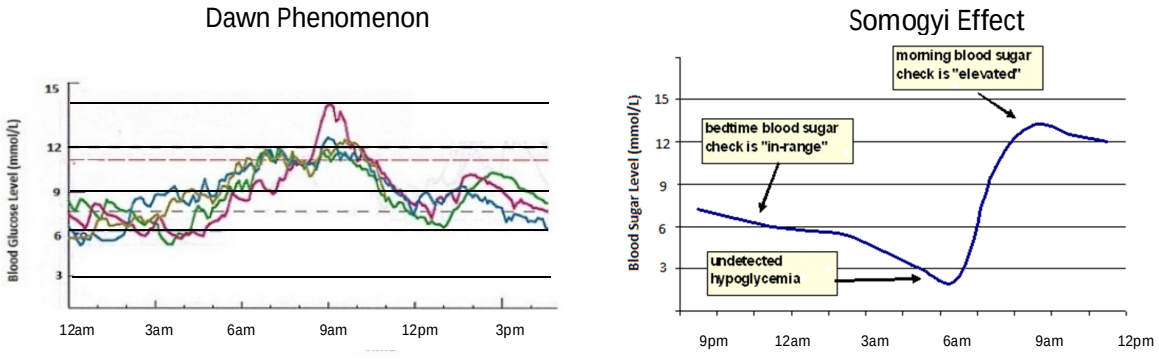

(a) (b)

Figure 4.6: (a) the dawn phenomenon [69], and (b) the Somogyi effect [70].

In order to help understand the associations within volunteer data and these events, the MK technique is investigated to detect such repeated events in the BG. Although not what the MK

algorithm was originally intended for, it provides a suitable basis for finding approximately similar patterns in time series which is hoped to be useful, as well as to the finding of parameters that could be affecting the cyclical events such as food, exercise, insulin injections or sleep cycles. Analysis of the other recorded data (physical activity data, CHO and insulin intake) might then help to understand the parameters that correlate with these phenomena in general, and these type of morning effects specifically. It could be used potentially for developing broader time-series models for use in Type 1 diabetes. Despite the fact that DP and Somogyi effect are similar in pattern in the time series, the former was found to be much easily detectable with CGMS and hence selected for initial investigation.

4.4 DP Detection in Volunteer Health Data

Having represented the desired data as time series, the motif discovery algorithm was used to find the closest-pair subsequence or motif. Running the algorithm requires five main input values:

- *m*, the full length of the time series;

- *R*, the number of reference points (significant changes to execution time only in high-dimensional data);

- *n*, the length of the searched motif;

- *X*, the coefficient used for motif range *r* (default $X = 2$), in this case *r* corresponds to the *best-so-far* (the larger the value more likely motifs appearing with lesser similarities in them); and

- *K*, the number of types of motifs. The *k*'th group corresponds to the *k*'th subsequence motif , combined with all subsequences distant from it at most *Xr*.

Since the MK algorithm is originally intended for motif discovery, or in other words discovering of motifs that are most prominent in the dataset with regards to the input parameters above, it does not take any reference motif as one of the search terms. The reference time series is initially selected randomly in the MK algorithm as the original intent of the developers was to discover motifs in the data. However, since we intend to use the method to find a well-known phenomenon, we need to modify it to allow a predefined pattern be searched in the whole time series data.

Here, we modified the MK algorithm by forcing the reference points to be only one, and the reference motif only to search for patterns of a user-defined one. A DP pattern is chosen manually from within one volunteer's data experiencing the phenomenon shown in Figure 4.7. Data of BG measured by the CGMS from 12 volunteers' spanning 3 to 4 periods of up to 3 days each are used to test this approach. Because the technique can only search across one single dataset, it was necessary to combine individual volunteer BG datasets into a single time series, as seen in the long stream of data in Figure 4.8. This way, occurrences of the same pattern can be detected across different volunteers' data although they are not observable within Figure 4.8. With concatenation, the time information in the BG data are lost and is no longer sequential, however can be traced manually. The number of data points belonging to each volunteer, the sorting arrangement and the equivalent number of concatenated data are shown in Table 4.1. Total number of data points yield 29734, which will be useful during the time-locating process.

Volunteer	Number of data points
1	2694
2	2585
3	2487
4	3424
5	1721
6	3440
7	3314
8	2470
9	2232
10	1698
11	1708
12	1961
Total data	29734

Table 4.1: Patients and their size of respective time series

In this experiment, DP which usually occurs between 3:00 to 10:00 A.M. (7 hours) takes about 84 samples of CGMS data collection (CGMS measures at every 5 minutes intervals thereby 84 data points are equivalent to 7 hours). Therefore, the dataset representing the DP motif were made reference by inserting the start and end point of an already discovered motif (searched manually) into the search parameter, *U*. The number of data points in the whole time series was set to *m*. The default value of *R* and *X* remain as suggested by Mueen. *K* was set to 1 since it is irrelevant in this experiment (The parameter $K>1$ is set to find multiple motifs recurring in the dataset. We are interested in only one motif, hence *K* set to 1). The algorithm was then set to scan the whole dataset for any recurrence of the search term.

From the results obtained, a separate look into other information about the subject in other data collected was conducted. With the help of other measuring devices (e.g. the activity armband), it was hoped that more information regarding the subject's physiology such as amount of sleep time, meal and insulin data, and the amount of physical activity energy expenditure would elucidate the findings so that they can be better explained. It was also hoped that further investigation could be done into other volunteers to see whether there are shared characteristics or lifestyle properties of individuals having these recurrences of DP.

4.5 **Results**

Figure 4.7 depicts multiple DP patterns that were found recurring within the patients' CGMS data. The blue plot refers to the user-predefined pattern of DP, the red line shows the closest pattern found within the dataset while the rest are discovered patterns also in the same dataset. Because MK algorithm looks for only the motif and less attention on its magnitude, only the pattern and shape of the motif recurring in the data was discovered, and automatically normalised, as seen in Figure 4.7. The motif's time information, to whom it belongs to, and its actual magnitude needs to be examined manually. Figure 4.8 shows the instances and locations of the recurring pattern (red lines) seen in Figure 4.7 within the concatenated time series data. The appearances of the red lines establish 11 motif recurrences of DP pattern discovered.

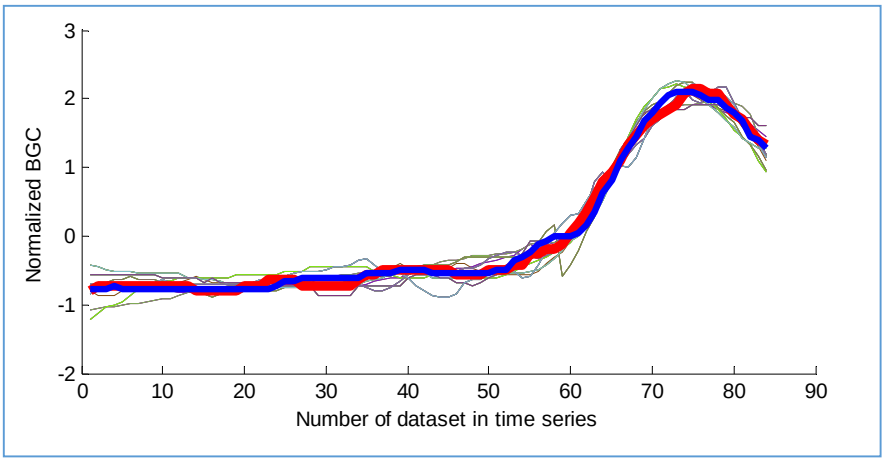

Figure 4.7: Detected DP patterns in the time series data. Blue line represents the user-predefined pattern of DP. The red line shows the closest pattern found within the dataset while the rest are discovered patterns also in the same dataset.

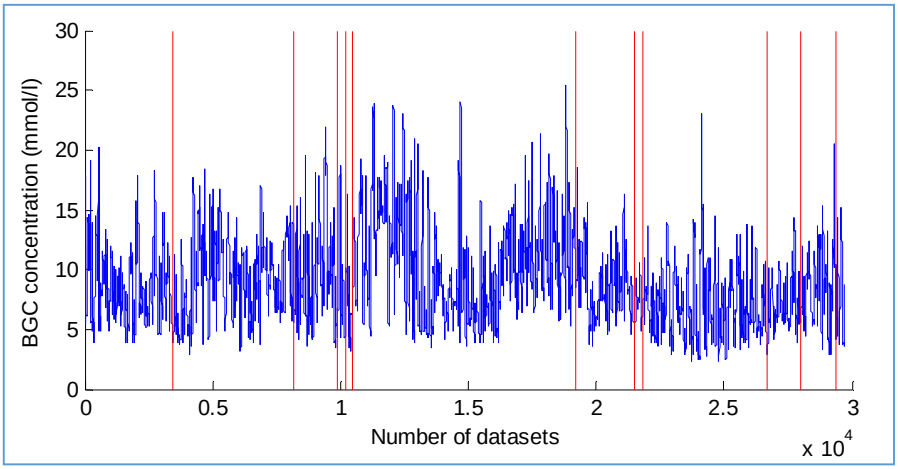

Figure 4.8: Concatenated volunteers' BG data and occurrences of the pattern in the single time series data.

As earlier stated, this phenomenon commonly occurs in Type 1 diabetics at around midnight until morning, and therefore the pattern is expected to be found within this period of time in the dataset. The number of occurrences and their instances in the volunteers' dataset are depicted in Table 4.2. Result shows that Subject #4 and #12 both have more than one occurrences of the motif, possibly indicating poor therapeutic control.

Subject	Number of occurrences	Location in the dataset
1	0	
2	1	3428
3	0	
4	4	8204, 9908, 10194, 10486
5	0	
6	0	
7	0	
8	1	19192
9	0	
10	1	24482
11	1	26664
12	3	25670, 27972, 29377

Table 4.2: Volunteers, their respective number of occurrences and pattern instances in the dataset.

From these locations in the concatenated dataset, the actual time information of the occurrences can then be traced to reveal the actual time information from specific volunteers, as depicted in Figure 4.9. The phenomenon can be seen to match the literature, whereby it occurs between 3:00 and 10:00 A.M.. Despite having the same shape of DP, they differ by the magnitudes of BG levels, hence plotted separately. This was also the feature, but a disadvantage of the MK algorithm that searches for a pattern while disregarding its magnitude. However, it can be established that the time of occurrences still demonstrate that the found patterns are the well-known DP.

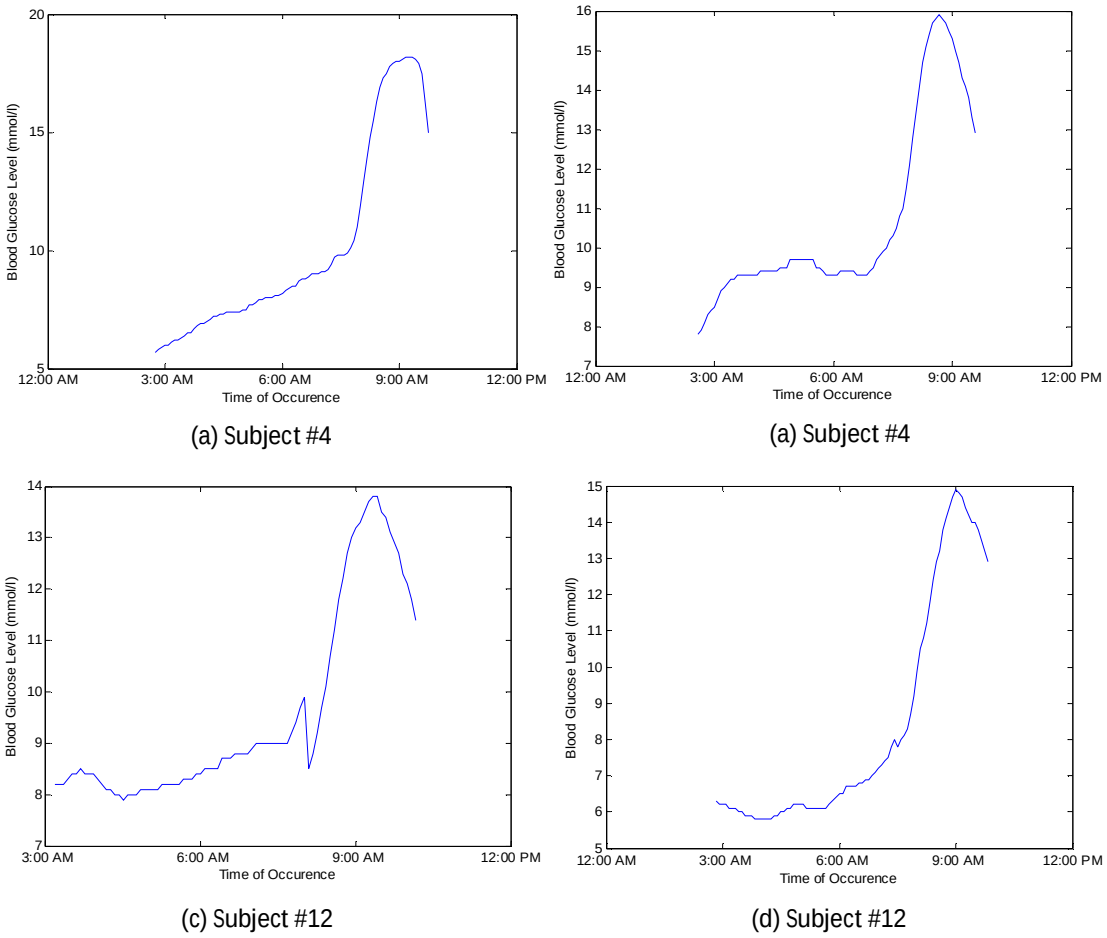

(a) Subject #4

(a) Subject #4

(c) Subject #12

(d) Subject #12

Figure 4.9: DP motifs traced with their time of occurrences across subject #4 and #12.

Another phenomenon, the Somogyi effect, was also examined by replacing the reference motif to that of the Somogyi pattern, from a location of known occurrence. The same procedure was followed and occurrences of the motif are recorded in Figure 4.10. As pointed out previously in Section 4.3, Somogyi effect is different to DP because of its characteristic that starts with a hypoglycaemia during the night and then ends with an upward drift of BG levels into hyperglycaemia in the morning. Note the time of occurrences of the phenomenon in Figure 4.6 (b) that starts around 3:00 A.M. and ends at about 10:00 A.M. in the morning, having similar time occurrence with DP. In Figure 4.10, it can be seen that initially BG levels were high and then reduced sharply until reaching dangerously low levels of BG before rapidly increasing.

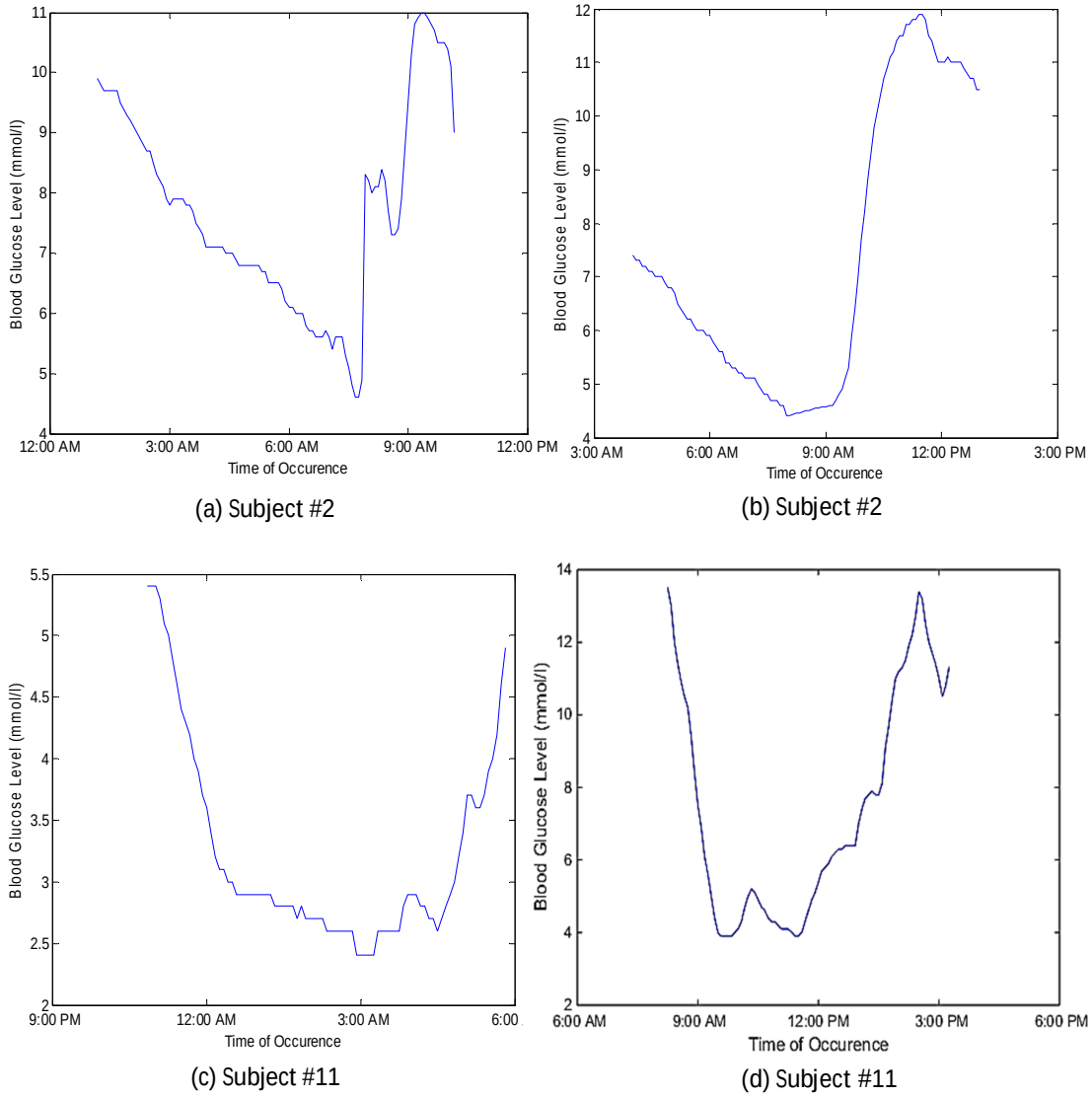

Figure 4.10: Somogyi effect motifs with their time of occurrences across the subjects.

Despite the apparent success in using the algorithm to identify known features, further investigation reveals that because the algorithm works to find the known features, there were a number of instances where it detected false positive of the Somogyi effect. It also failed to detect actual occurrences that did not form a pattern close enough to the reference. Further, other events occurring during the daytime were identified as Somogyi (As an example, in Figure 4.10 (a), (b) and (d), while showing patterns that look like a Somogyi effect, they did not show the prior hypoglycaemic events while the BG pattern in Figure 4.10 (b) did not end with a hyperglycaemic event during the late morning hours, hence rendering them as non-occurrences). In terms of DP detection shown in Figure 4.9, because the pattern comprises of a simple shape, having being indistinct and quite common, producing further false positives, as 5 out of the 11 detections occurred during the day - thus they are not DP. This means that the method may not be used solely to find these features and without an intervention by the researcher.

Further examination into meal data occurring around the same time as of the dawn phenomena, revealed further insights. In subject #4, it appears that two of the DP patterns found were not

actually DP occurrences but rather responses to CHO consumption events, activities done by the volunteer. Figure 4.11 shows a contiguous plot of 3 days in subject #4's meal data, generated from CHO intake data and a gut model. It can be seen in the enlarged plot, Figure 4.11(c), that the increased BG was due to a meal taken at around 7:00 A.M. corroborating the previous result of a rise in BG levels. On the other hand, there were no meal intake until 9:30 A.M. in the other two enlarged meal data, Figure 4.11(a) and (b). The reason why the other two were not in response to any meal consumption, remains a question. Probable causes could be that the patient reported inaccurate ingestion of food, or assumed that the meal consumed were trivial in quantity and did not report, or the digestion modelling was lacking and hence, ingested food was not sufficiently represented. But these assumptions can be true only if they are not at all occurrences of DP. To examine this further, investigation of CHO uptake is necessary, since reported meals consist of impulses which are transformed by a standard model of the gut into glucose appearance in the blood (see Section 3.7).

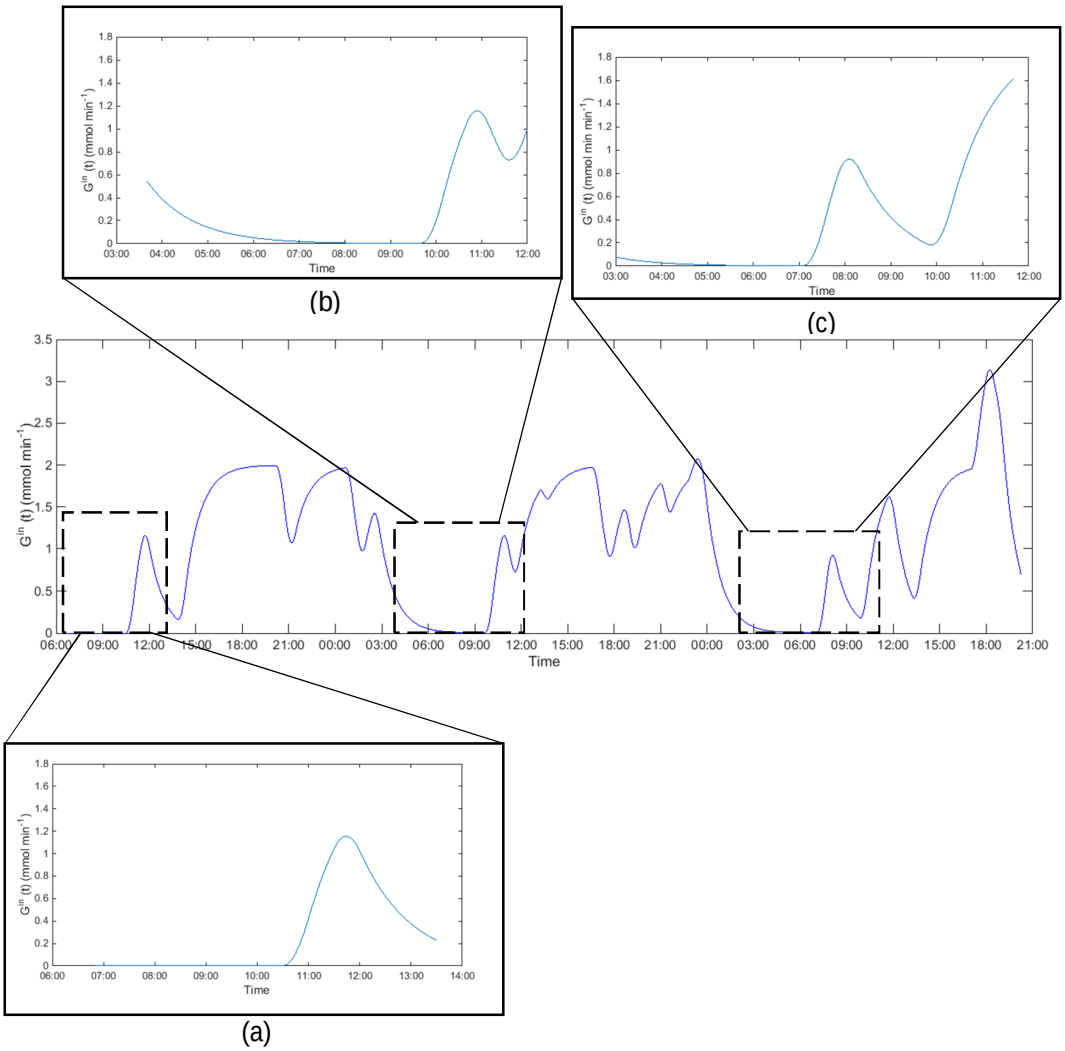

Figure 4.11: Close-up look into meal data belonging to subject #4.

Other data collected in the DUK study that could be relevant to this feature detection are the sleep and physical activity data obtained from the SenseWear armband. Sleep data could possibly help elucidate occurrences of DP because both of them should practically occur at the same time.

Examples of sleep data from 2 volunteers are shown in Figure 4.12. The advantage of using the SenseWear® armband is that it was to be able to produce and display sleep activity from the user's measured activity data with a very high success rate [57]. Outputs are given in discrete steps, according to the 4 sleep stages and rapid eye movement (REM) for the 5th stage. It was hoped that the use of MK algorithm would reveal a significant pattern related to the DP detected previously. In addition, it is also expected that characteristics and lifestyle led by individuals having these recurrences of DP could be revealed.

In contrast to DP where the pattern is already distinguishable, it is anonymous to us on how any related patterns in sleep would appear in volunteers' sleep data. Therefore, rather than replacing the reference motif to a predefined one, the original MK algorithm was tested on volunteers' sleep data for automatic discovery. Because sleep data and the investigated patterns occur only at night, it enables us to narrow down the search. As observed in Figure 4.12, sleep events start to occur from 10:00 P.M.

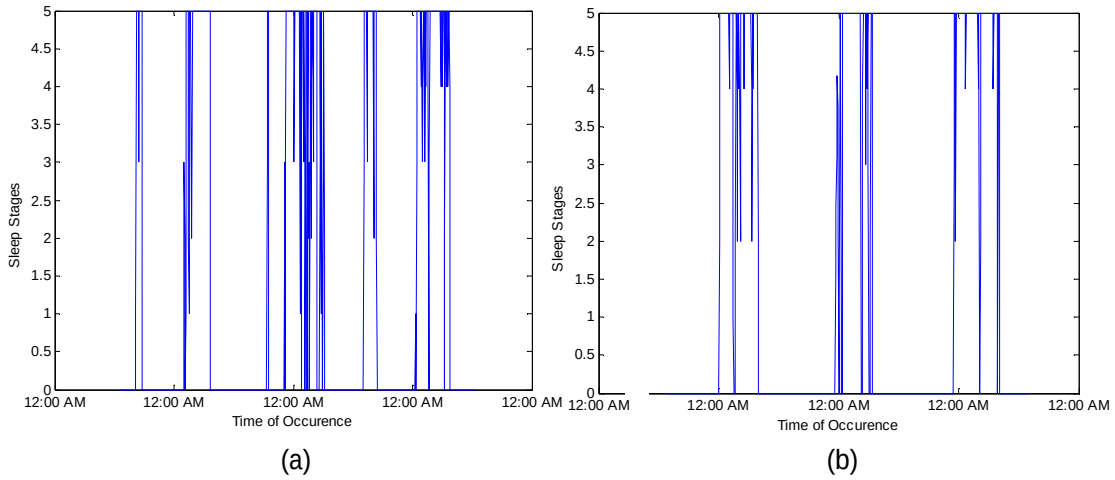

Figure 4.12: Sleep data from volunteers. (a) sleep data from comes from subject #2. (b) sleep data from comes from subject #4.

A more descriptive view of the sleep data can be observed in Figure 4.13 provided by the armband developer [57]. It was found that when sleep data were directly tested with the MK algorithm, the detected motifs were only those of the horizontal lines of long duration of sleep stages illustrated in the red circles in Figure 4.13. This yields irrelevant and therefore the method appears to work poorly with discrete values.

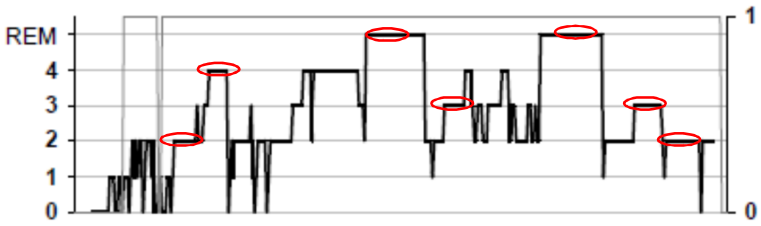

Figure 4.13: Sleep stages detected by the SenseWear® armband. Red circles refer to the pattern detected by MK algorithm which is an error. Reproduced from [57].

A potential solution to this was to perform a non-parametric fitting to the data to transform the highly discrete values to be continuous. A non-parametric fitting means that a fit is made to the data without assuming any parametric relationship between the variables. Smoothing was achieved using localised regression fitting multiple curves to local subsets of data and then combining them into a single larger curve. To avoid underfitting or overfitting the data, and preserve the original curve while still allowing realistic detection by the MK algorithm, a suitable smoothing parameter value was necessary. A sensitivity analysis was undertaken by running multiple trial-and-error tests with different values of smoothing parameter, and the retrieved dataset was then tested with MK algorithm for motif discovery. The number of motif detected is reasonably expected to match the number of DP occurrences found earlier, which is 11.

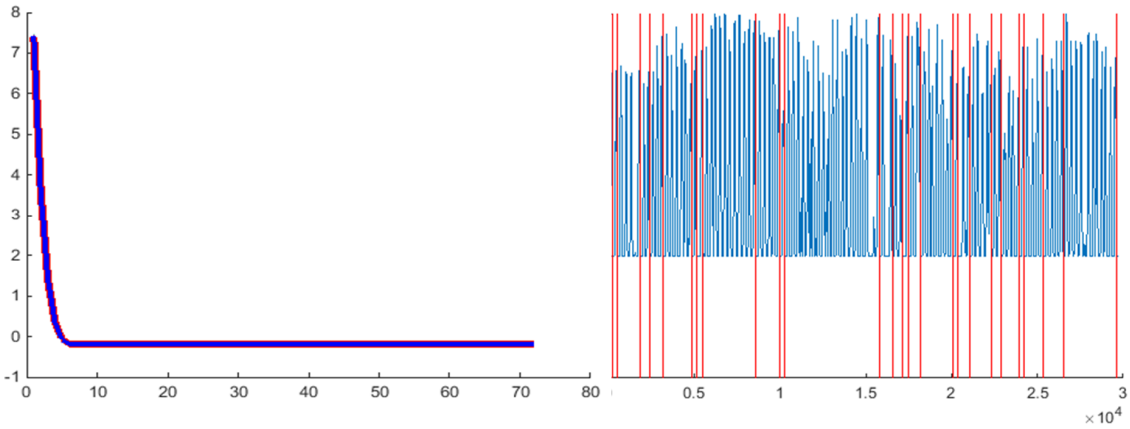

Figure 4.14: Discovered motif and their occurrences in the dataset. (a) shows the motif shape found in the data and (b) refer to the locations of discovered motif.

25 occurrences of one distinct pattern were found being close in terms of their shape and time to the DP occurrences, as shown in Figure 4.14(a). They occurred within the time series dataset as shown in Figure 4.14(b), and further examination reveal the recurrences correspond to various volunteers as shown in Table 4.3.

Volunteer	Number of occurrences	Number of DP occurrences detected earlier
1	4	0
2	2	1
3	1	0
4	0	4
5	2	0
6	1	0
7	4	0
8	3	1
9	4	0
10	2	1
11	1	1
12	1	3

Table 4.3: Motif in sleep pattern across the 12 volunteers.

It is apparent that the motif discovered was not distinct or unique but rather a straightforward one. Hence, we were unable to produce any possible correlation between the sleep patterns and DP detected earlier. Surprisingly, the highest number of pattern recurrences discovered in the sleep data did not correspond to volunteers who experienced DP in the previous test. Four of the same sleep pattern were found in subjects #1, #7 and #9 datasets but none of the volunteers were found with DP occurrences from the earlier test. This possibly indicates that these volunteers had regular sleep patterns but would require further work to verify this. These results show that the MK Algorithm performs poorly with discrete data, despite it already being filtered and smoothed. It is further limited by the inability to prescribe any predefined pattern as a reference for the MK algorithm, due to the unknown sleep pattern of interest.

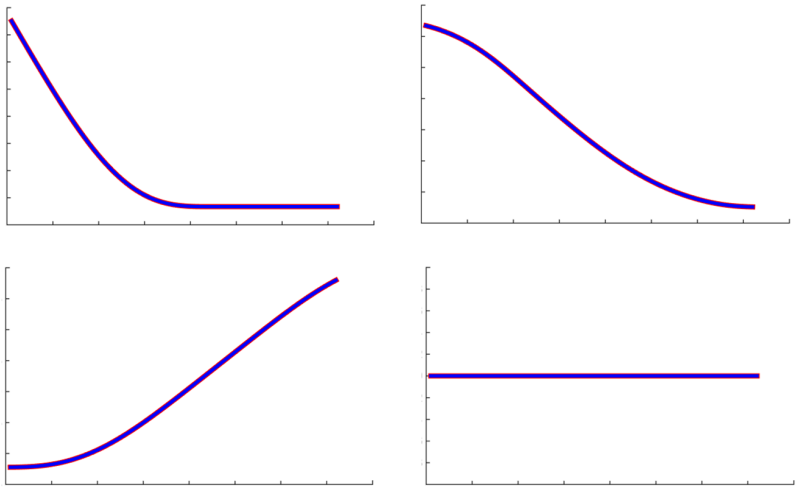

Figure 4.15: Various motifs discovered in sleep data.

Following the failure to search for the most prominent motif in the dataset, the MK algorithm was tested again by increasing the number of cluster *K* and also the factor of radius, widening the sensitivity of search, with more motifs discovered, depicted in Figure 4.15. However, no improvement was obtained as no unique motif was detected in the sleep data, just as it performed with the unsmoothed ones. The incident can again be attributed to the discrete steps of sleep data that even with smoothed ones, the step changes from one stage of sleep to another was only converted to a continuous curve with many still taking up a similar shape, leading to the same outcome. A depiction of this event is recorded in Figure 4.16, with smoothed sleep data shown in red. Note that the data were filtered using local regression with weighted linear least squares and a second-degree polynomial model. Despite the use of high ratio that causes significant losses of trend in data, the same non-fruitful results were produced, demonstrating the inability of MK Algorithm to scan sleep data directly for this purpose.

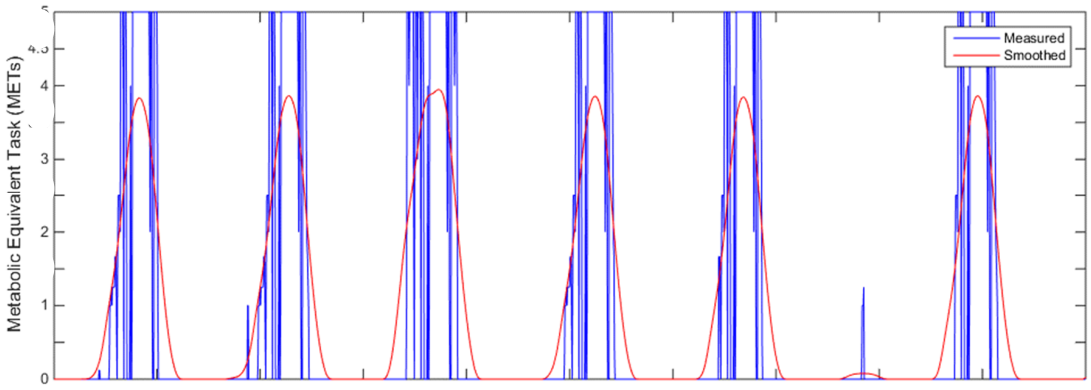

Figure 4.16: Difference between original measured and smoothed sleep data.

Finally, the physical activity data, also collected using the SenseWear® armband was investigated. Collected physical activity data were in form of METs, being continuous and also highly variable as depicted in Figure 4.17. Physical activity data contains important information for diabetes research and can help identify lifestyle parameters and fitness measures. Physical activity is responsible for both raising and decreasing BG levels and is the least understood parameter in insulin-glucose dynamics. Exercise is highly recommended for Type 2 diabetics, but rigorous monitoring by a patient's healthcare team is required for people with Type 1 diabetes to help avoid excessive glycaemic excursions.

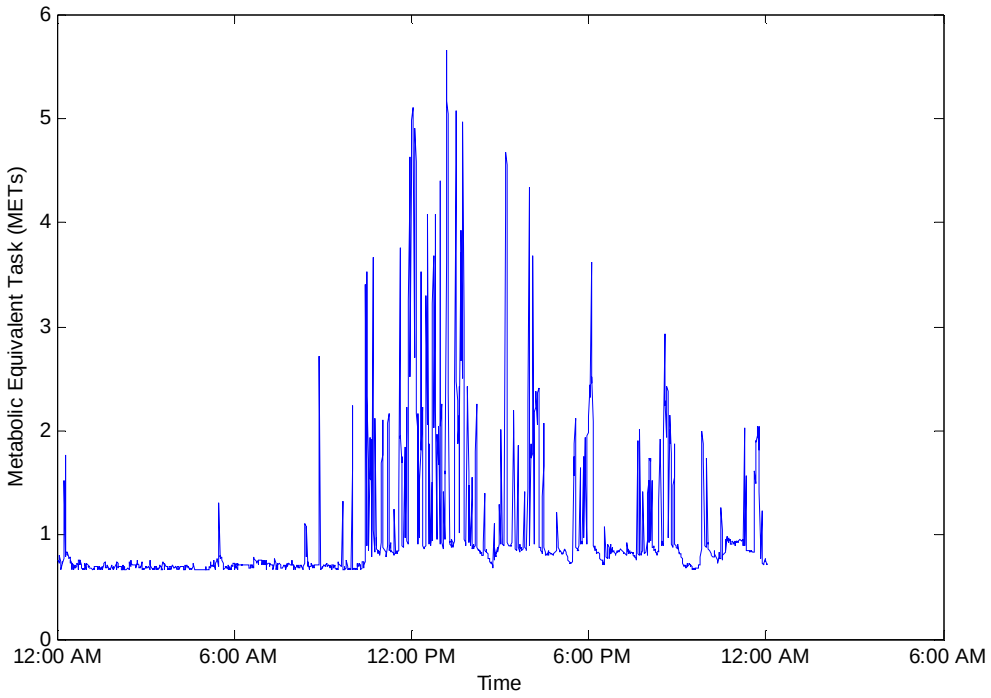

Figure 4.17: METs over a 24-hour period collected from armband.

Data from volunteers were smoothed separately to avoid data in one subject overfitting others, and then combined for MK Algorithm tests as before. The previous test used probabilistic interpolations due to the discrete nature of the sleep data. The continuous and highly variable METs data simply require a simple moving average (MA) to reveal hidden trends without significant loss

of the data [9]. This was done by averaging the past observations and consecutive data, producing a smoothed version of offset between the two. Figure 4.18 depicts the new plot of subject #23's METs data with various hours of MA value. A lower value of MA yields much more variable and erratic behavior, while higher ones remove many oscillations at the expense of the trend, e.g. when someone runs for a bus or climbs a series of stairs in a tall building. A 24 hour MA (red colour) produces the most flattened curve. Note the highly variable nature of the data even within one volunteer's data.

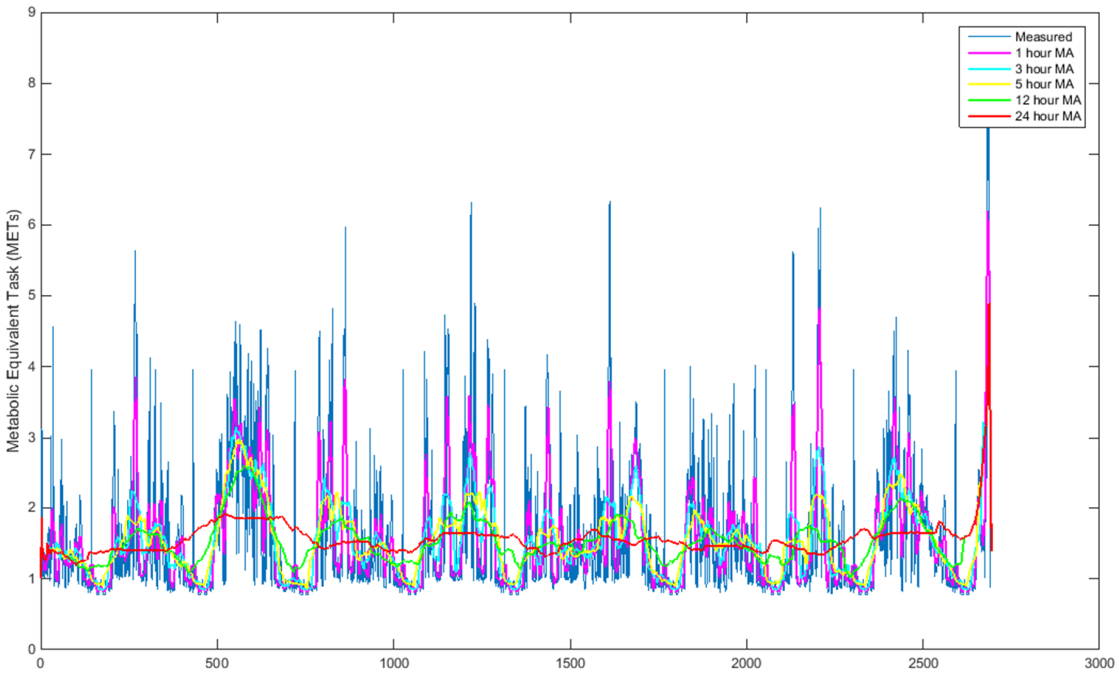

Figure 4.18: BG levels in subject #23's data with various MA values.

Figure 4.19 shows the various motifs discovered using MK Algorithm. They are quite distinct in the shapes appearing in various parts of the METs time series data, as compared to those in sleep data. The blue plots refer to the most prominent motif, appearing the most frequent in the dataset, while the red plots refer to the second most prominent motif. The absence of magnitude and time reference are due to the nature of the MK algorithm that disregards it. The occurrences appear to be inconsistent throughout the day or appearing randomly at various times. Note that motif in Figure 4.19(a) and (d) have more recurrences than the others (shown by the lines of various colours), showing repetitive events of a similar physical activity. A reference to the time information reveals that each pattern in Figure 4.19(a) mainly appears in evening times while the one in Figure 4.19(a) occurs in morning times, probably showing the start of activities in the former and the resting periods at night.

Nevertheless, we were still unable to correlate them to the morning events detected earlier. The result could mean that there was no connection at all or there is still a phenomenon that we have yet to understand. In particular, the time-lags associated with physiological processes governing BG dynamics are difficult to capture in terms of how these patterns affect future BG profiles. However, the MK algorithm, to a certain extent, can be used to detect distinguishable motifs given the appropriate type of data and user assistance addressing the false-positives detection.

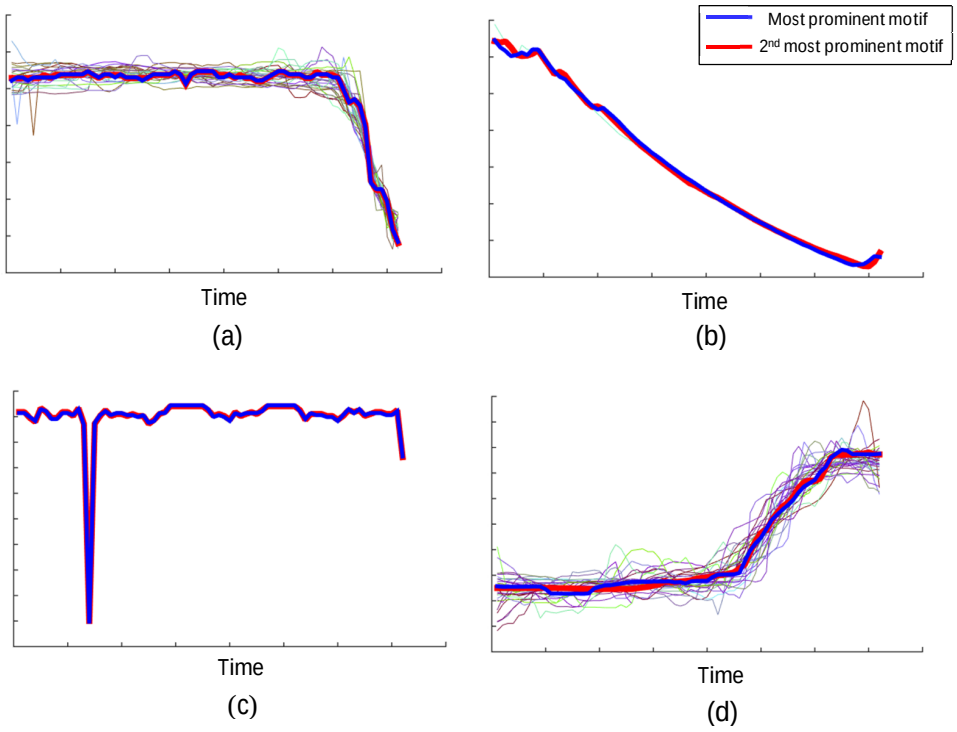

Figure 4.19: Various motifs found in the METs data.

4.6 **Summary**

Multiple data from sensors worn by the volunteers were used to find hidden distinct patterns using the MK Algorithm. Apart from BG data, meal, sleep and physical activity data were scanned and analysed for repeating motifs that can be hidden from general discovery techniques. However, there was little correlation to this data that could be linked to the motifs found to our phenomena of interest, DP and Somogyi effect.

In terms of the performance of the MK Algorithm, its deficiency lies in the inability to search for a predefined pattern, addressed by our modifications to allow such a feature. Another issue is that the code does not take into account the magnitude of the motif, allowing only the shape of pattern to be searched. In terms of physiological measurements, this is undesirable as it is the magnitude that set aside normal BG levels to dangerous ones, and also differentiates DP from Somogyi effect – two very different events in diabetes management. The MK algorithm also detects poorly in discrete time series data, where only flat and horizontal curves were detected as a motif. A smoothing method did not help to cope with the issue. The user needs to be aware that the MK algorithm needs further assistance for better detection and cannot practically work with just raw data. It would be of great help if only the motif search could be done on multiple data sets simultaneously, so that occurrences, for example of motifs in BG data, physical activity data and in sleep data can be readily comparable.

Also, there were possible inaccurate reports of meals consumed by the volunteers, leading to missing impulses in meal data. Recurrences of motif found in them also did not show any relation to volunteers experiencing DP. The MK algorithm failed to detect any pattern in the sleep data while performed minimally with METs data. Therefore, MK technique appears to be less useful in using this knowledge to develop improved dynamic models for BG prediction without considerable further study beyond the scope of this research.

However, among bodily parameters in the DUK study, there are those that can be further investigated because they actually consist of impulses that are later modelled into quantitative values, such as meal data, insulin and METs data. It is also desirable that the impulses be parameterised to see the corresponding effects on BG levels. A study into the data could reveal reasons why there were missing impulses in the meal data; whether it was an error from modelling or human error.

It is also established that a motif search alone is inadequate to describe the metabolic processes exist in Type 1 diabetes patients due to their complexity. The causes are definitely wide-ranging as one may lead different lifestyle (active or sedentary), or have a different metabolism (genetics) or meal types, various insulin injection positions throughout the body, or even different volumes of injection and insulin formulation. A thorough examination into the causes varying BG levels is palpable if the glucose-insulin models are better understood. The general models of digestion and insulin dynamics are rather inadequate to explain the metabolic processes of every person with Type 1 diabetes.

This chapter concludes that although it is possible to detect features in the data or patterns in BG control that recur across volunteers, they cannot be associated with the insulin, diet or physical activity using MK method due to the fact that none of the features detected in them were significant. This motivates investigating the models that allow us to parameterise the insulin and dietary intake and/or the PAEE which is the subject of the following chapters.

4.7 Contribution to the Body of Knowledge

Based on the results obtained from the experiments, it is shown that the MK algorithm is able to identify patterns of the same shape that appear across individual datasets (people). They are found having parametrically similar shape and contour. Albeit having its shortcomings, the method can be vastly improved to allow detection in multiple datasets or predefined patterns as illustrated here. The method also allowed only specific length of time series data to search for, when realistically a pattern could be of the same shape but have different lengths, hence the later studies by other researchers addressing this [71]–[76].

This initial study focused on finding recurrence of patterns by manipulating the datasets. Concatenating multiple patients' data into one single stream of data can be helpful in terms of pattern finding, but the time of pattern occurrences can become a problem since the time information in the datasets are then not in chronological order. Nevertheless, the examples show a detection of well-known phenomena in diabetes is possible and this technique has potential to be a useful tool in obtaining correlation of wellbeing and lifestyle.

In summary, the patterns or motifs that exist within the data collected are not random and are actually produced as a result of exogenous inputs. Time series motif discovery is one of the techniques to trace and discover factors influencing the BG levels in an individual. The initial study shows that a well-known pattern or motif such as DP is discovered within the patients' health data. However, as applied to other health data, either non-related motifs or poor detection in certain dataset were revealed. Inaccurate or unreported impulses of meal impulses could very well be the reason of missing impulses in meal data, hence the prospect of further examining the glucose-insulin-dynamics as the major factors varying glucose concentrations in human body.

Chapter 5: Type 1 Diabetes System Identification

The aim of this chapter is to use a system identification technique to produce better BG prediction typically in the short-term horizon. Initially, a number of literatures studying the use of CGMS data with linear time-invariant models such as ARX and ARMAX are presented and reviewed. Then, the chapter discusses the need for a model that fine-tunes its parameters to adapt to the constantly evolving physiology exists within a diabetes patient. Therefore, an optimisation method, genetic algorithm is used to adjust the diabetes sub-model parameters fed as inputs to the ARX model. With optimisation, the estimation parameters could be continually updated following changes in the bodily response in an individual. The chapter also discusses the probable causes of these intra-patient variability and finally suggests possible classifications of patients for a more responsive and efficient treatment.

5.1 Introduction

Short term BG prediction is desirable mainly to assess the variability of glucose levels to anticipate glucose excursions away from the desired bounds and adjust the therapy accordingly. A number of researchers have previously proposed ways to better predict the variability of BG levels. The use of CGMS has contributed a lot to this prediction as the quasi-continuous nature of data collection, which means more accurate input-output data can be used to derive modelling equations in any model training process. Once the training process is completed and the underlying processes learnt, the model can better predict an output from an unseen input data set, given that it is within the envelope of the relationships acquired in the training phase.

Ideally, a best BG prediction requires the time series data from CGMS to be stationary and by definition this means that the mean and variance of the signal are time-invariant. Real life conditions however differ as physiological aspects of the body do change over time and as Valetta [9] demonstrated from CGMS data collected from a range of individuals, the data are not stationary although they may have periodicity over time. The simplest measure of stationarity in BG concentration is the HbA_{1c} used by clinicians [77]–[80]. Broadly speaking, it represents the equilibrium point in the patients' glucose-insulin system.

Some researchers in the past disregarded this by investigating time-invariant or non-recursive models [81]–[84]. More recently, researchers have taken into account the variation in glucose-insulin dynamics over time [85]–[87]. Furthermore, there is a need for this kind of prediction to suit the person-specific BG variation due to insulin preparations and injection site, medication side-effects and lifestyle changes which will all affect the glucose-insulin dynamics differently in each individual. In closed-loop BG control, such as the artificial pancreas [7], [8], [87], this gives rise to the need for a model-based control in which the model parameters can be updated continuously. It is actually reasonable to presume stationarity if the prediction horizon is relatively short, such as a two or four-hour period. Therefore, by training a simple model with the most recent CGMS data collected, the prediction model will employ the most up-to-date parameters suitable for the current 'operating' conditions of the patient.

This chapter will focus on the use of autoregressive with exogenous input (ARX) models such as those used in previous studies of Finan *et al.* [49] and Gani *et al.* [88]. A compelling feature of the ARX model is its ability to quickly estimate parameters from a set of training data. There exists a least-square solution that minimises the sum of squares of the one-step ahead prediction errors for

training data [49]. The solution is to keep the parameters acquired from training dataset and use them to predict BG concentration and if the glucose-insulin dynamics have changed, the estimation parameters could be updated allowing adaptation to the changing bodily response.

5.1 Autoregressive with Exogenous Inputs (ARX) Modelling

An ARX model contains a least-square solution that minimises the sum of squares of the one-step ahead prediction errors. Third-order ARX models prediction have been proposed by Valetta [9] which preformed fairly similar to those of Finan's [49]. ARX modelling is still attractive in system identification model particularly with regards to insulin-glucose dynamics, and here, we investigate the possibility of improving current ARX modelling with sub-system optimisation. The structure of $ARX(n_a, n_b, n_k)$ model has been discussed in Section 2.4.

5.1.1 ARX Modelling and Optimisation to Improve Prediction

The aim here is to investigate any improvements that can be made over previous studies such as those of Hemmingsen and Johnsen [36]. In their thesis, they presented a prediction technique using the ARX model with MPC to adjust to insulin dynamics parameters. Figure 5.1 shows the process within a typical ARX-Insulin-CHO. Both carbohydrates (CHO) and insulin (I) inputs first arrive at their respective models. The Insulin Model and CHO Model then converts the discrete inputs into outputs of I_U and G_U, later be directed to the ARX model, producing BG. In Hemmingsen and Johnsen's case, adjustment was made in the Insulin model.

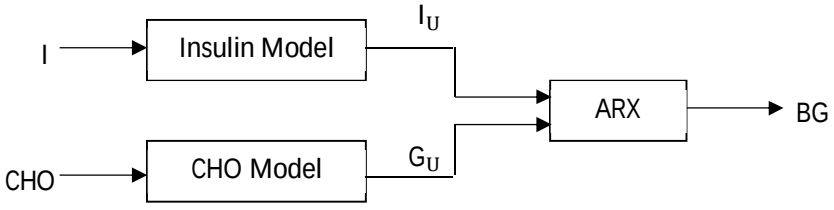

Figure 5.1: Diagram on ARX Insulin-CHO sub-models.

Both insulin input and carbohydrate intake from meals were recorded in diaries of volunteers. These are just records of the amount of insulin or CHO consumed such as impulse inputs, which need converting to the appearance of insulin and glucose in the blood. Figure 5.2 shows the stated impulses with their respective quantitative meal and insulin appearances. The black, green and red bars refer to the reported impulses while blue plots in Figure 5.2(b) and (c) are the modelled quantitative information of insulin and CHO, using reference parameters. The appearance varies when converted using other models.

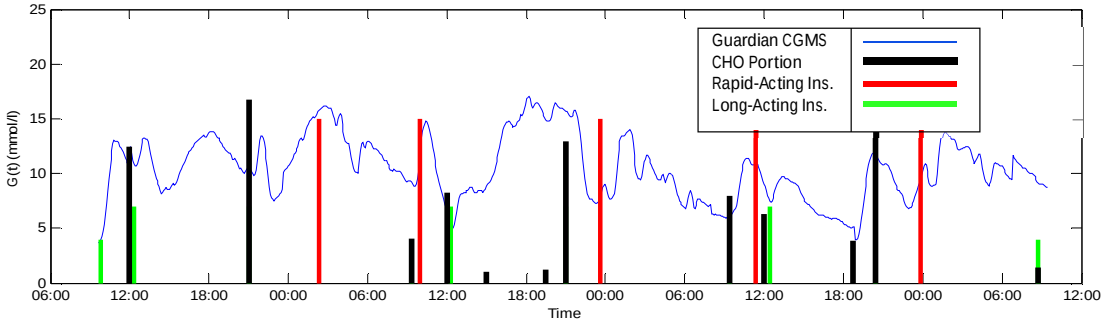

(a)
Sensor Glucose

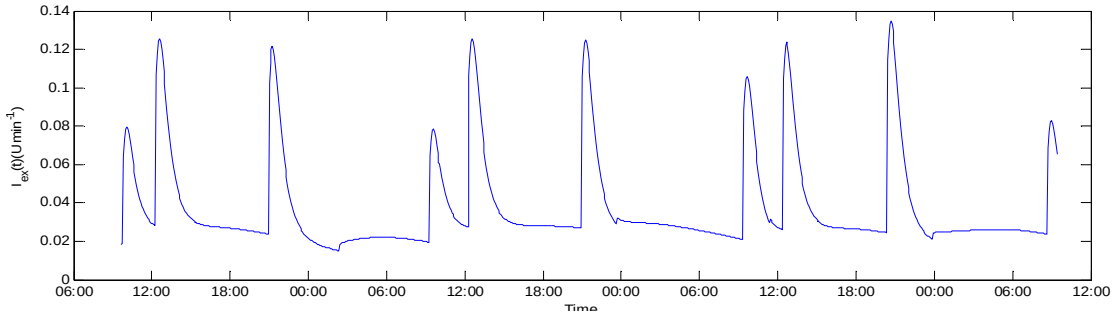

(b)
Insulin Flow

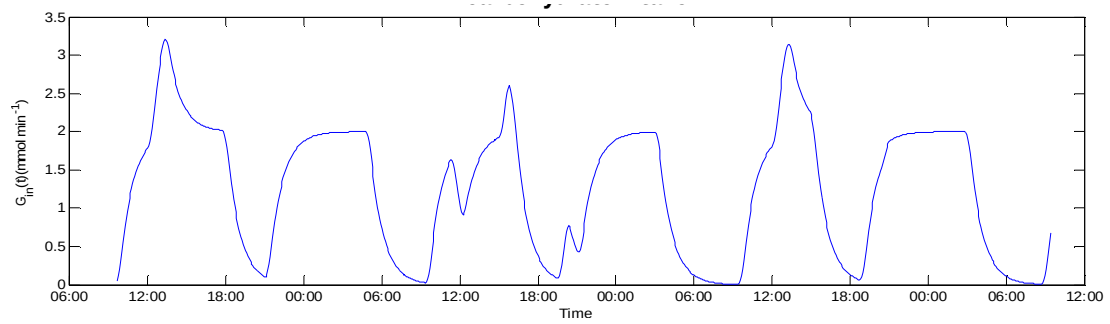

(c)
Carbohydrate Intake

Figure 5.2: Typical free-living Type 1 diabetes data used for system identification from subject #13. (a) refers to the BG levels measured. (b) refers to the insulin flow in the bloodstream. (c) depicts the carbohydrate intake.

In [36], the CHO parameter in digestion model was regarded as disturbance rather than an actual input due to the poor predictions obtained when the converted meal information is fed into the ARX model. The result was even poorer than using only binary meal information, and thus was perceived as coming from the poor modelling of the meal impulses, hence, the adoption of only binary-type meals inputs. The binary meal information however just acts like an announcement to the ARX model that a substantial CHO is to be consumed (taken 15 minutes before insulin injection) and the assumption taken is that the model should respond accordingly. The meal announcement was actually based on a set of means estimated from a strict daily CHO intake, with respective CHO

amount for breakfast, lunch and dinner. The estimated mean meal sizes used are shown in Table 5.1.

	Breakfast	Lunch	Dinner	All
μMeal CHO [g]	48	51	55	52
(±σ) CHO [g]	(±22)	(±26)	(±23)	(±24)
μRatio [mU/g]	34	35	34	35
(±σ) Ratio[mU/g]	±(2.4)	(±2.8)	(±2.8)	(±2.7)

Table 5.1: Table describes the mean meal sizes, μMeal and the std for breakfast, lunch and dinner, σ [36].

On the other hand, the reason for the poor prediction using quantitative meal information as an input was due to the inaccuracy of patients' recording of amount and time of ingested CHO, thus the uncertainty. An essential contribution of Hemmingsen and Johnsen is that despite the model's inaccuracy in estimating ingested CHO within the ARX model, it has been demonstrated that the tuning and adjustment of parameters within the insulin dynamics can improve BG prediction.

In this section, we present another glucose prediction technique using coupled optimisation and an ARX model, which includes parameter adjustments in both insulin and digestion models. Hemmingsen *et al.* [36] stated that the MPC has no control over the manipulation of the meal input and it is true to a certain degree that the amount of carbohydrate consumed could not be changed. Nevertheless, the development of various digestive models (as presented in Chapter 2) predicting glucose appearance in response to carbohydrate uptake, gives us an idea that despite the constant amount of CHO consumed, the parameters within the digestive model translating them into quantitative stream of CHO could vary. This motivates the study of an ARX model with inputs that produces the same quantitative values, which in our case, the parameters in I_U and G_U (listed in Figure 5.1), continuously being adjusted. It is also in line with the general belief that individuals have a unique set of metabolisms for insulin and digestion model and therefore preferable to have absorption profiles uniquely suitable for each person.

To achieve this goal, a similar approach to MPC but a simpler one using a Genetic Algorithm is to be utilised. The Genetic Algorithm will be used to determine the quantitative inputs of CHO and insulin, by training their sub-model parameters with the most recent CGMS data collected before feeding them into the ARX, producing the corresponding BGC with the most suitable parameters matching the individual. In terms of physiological response, because data collection involved subjects receiving the least intervention within a non-clinical environment, a daily natural behaviour is expected to be present in the data and therefore the discrepancies such as in Gani's study [88] is avoided to some degree. To allow comparison with the previous studies, the same performance metric of FIT and RMSE will be used.

5.1.2 ARX Model Structure Selection

The ARX model's structure needs to be selected *a priori* in parametric modelling. Both Finan *et al.* [49] and Valetta [9] employed a third order ARX and ARMAX models respectively in their studies. The corresponding number of parameters to be estimated in the ARX polynomials A, B_1 and B_2 proposed are in the form (from Section 2.5):

$$A(z^{-1})G(k) = B_1(z^{-1})I_{ex}(k-n_k) + B_2(z^{-1})G_{in}(k-n_k) + \zeta(k) \quad (5.1)$$

Where $G(k)$ is BG concentration, $(mmol\ l^{-1})$, $I_{ex}(t)$ is exogenous insulin flow $(U\ min^{-1})$, $G_{in}(k)$ is exogenous glucose appearance in the bloodstream, and $(mmol\ min^{-1}$ and $\zeta(k)$ is assumed to be Gaussian white noise. In terms of the order model value, Valetta justified the selection of a third order model by evaluating the quality of fit for different ARMAX model structures as shown in Figure 5.3.

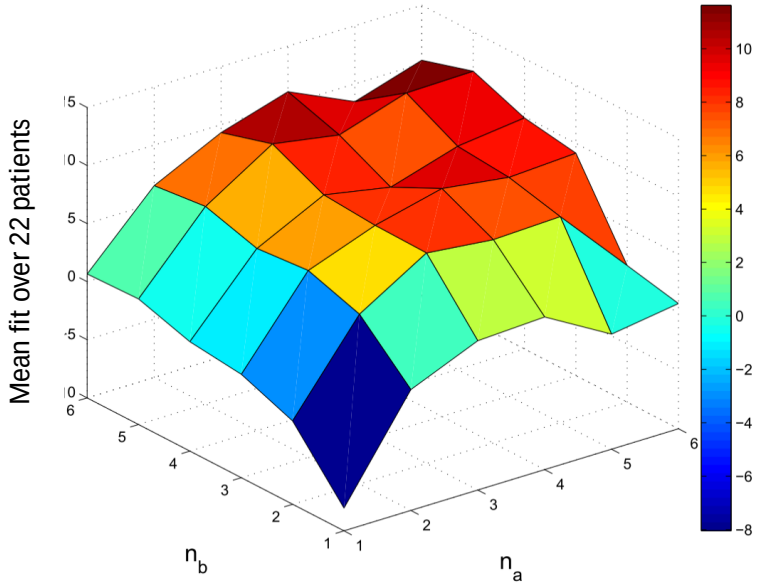

Figure 5.3: Mean simulation fits obtained from the training datasets for various orders of n_a and n_b.

The figure depicts the change in mean fit across the training sets for all 22 volunteers in order to determine the optimum model. This was achieved by simulating the ARMAX models with parameters of increasing orders of n_a and n_b from 1 to 6 while keeping n_c (noise model order) and n_k (delay) at 2 and 1 respectively. Note that the simulations were of MPO (infinite-step ahead prediction). The preliminary tests showed that the mean fit does improve with the increase of orders but only until n_a and n_b reach order 3, the fits stay relatively similar. No significant improvement was observed over increased model complexity that is larger than order 3 and variance across the volunteers increased. n_k was set to 1 since it did not have a significant impact on the model fit because the respective sub-models generating glucose appearance in the bloodstream and insulin flow (G_U and I_U in the ARX case) have already the delayed effect of inputs into the system. The ARMAX(3,3,2,1) was selected and fixed for every participants modelling. In our test, the same ARX model order is selected not just because the training and validation datasets are of the same, but a direct comparison can also be made between the study and those of Valletta's, Finan's and also Gani's who all employed the same fixed parameters.

The aim of determining an effective ARX model is to provide predictions of future BG trajectories given a previous time-history. The ARX model is sufficiently simple and transparent that it can be quickly found within the BG sampling period, 5 minutes. Prediction horizons of 30, 60 and 90 minutes have commonly been used in previous studies as this is generally considered sufficient for MPC type approaches in the artificial pancreas or for short-term clinical decision making. However, such predictions have often been poor and fail to accurately or consistently identify the direction of BG partly because they do not account for the person-specific insulin absorption or glucose production. Here, the aim is to investigate whether an optimisation-based approach tuning the gut and insulin models used with the ARX predictors can improve the quality of prediction of BG for individual diabetics.

5.2 GA-Based Optimisation Method (GA-ARX)

Hemmingsen *et al.* [36] proposed a relevant case of adjusting parameters within the insulin model coupled with ARX, but it was hampered by one missing vital contributor in the system identification model: the digestion model. Therefore, we wish to include this important parameter into the system by adjusting the existing models (presented in Section 2.32 and 2.3.3) to predict better and obtain a more suitable glucose-insulin dynamics representation for individual volunteers and across the cohort. An attempt using Genetic Algorithm would be used as a means for this objective.

The objective function in our case becomes the minimisation of the difference between the predicted BG from GA-generated-parameters and the original BG levels measured from volunteers. Datasets belonging to individuals consisting of inputs and outputs are divided into sections, for the purpose of training and validating using 10-fold validation technique. Each section spans around 3 days of data collection with short gaps where sensors are changed, but still considered contiguous. The model parameters were estimated from the training dataset. During optimisation, each GA iteration constitutes the generation of parameters for the governing equations (both insulin and digestion model) which later produces estimated BG levels, and later its FIT metric against measured BG values. Upon start-up, the original reference parameters were used first, and if need be, adjustments are then made.

The existence of validation data in addition to training data helps the GA operation to validate previously estimated model. Parameters generated are expected over time to fit measured BG levels better. Physiologically, if this succeeds, it means that the model will manage to track some of the patient's current bodily metabolism parameters in relative to the changes occurring in the glucose-insulin-dynamics. The block diagram of the process is as shown in Figure 5.4.

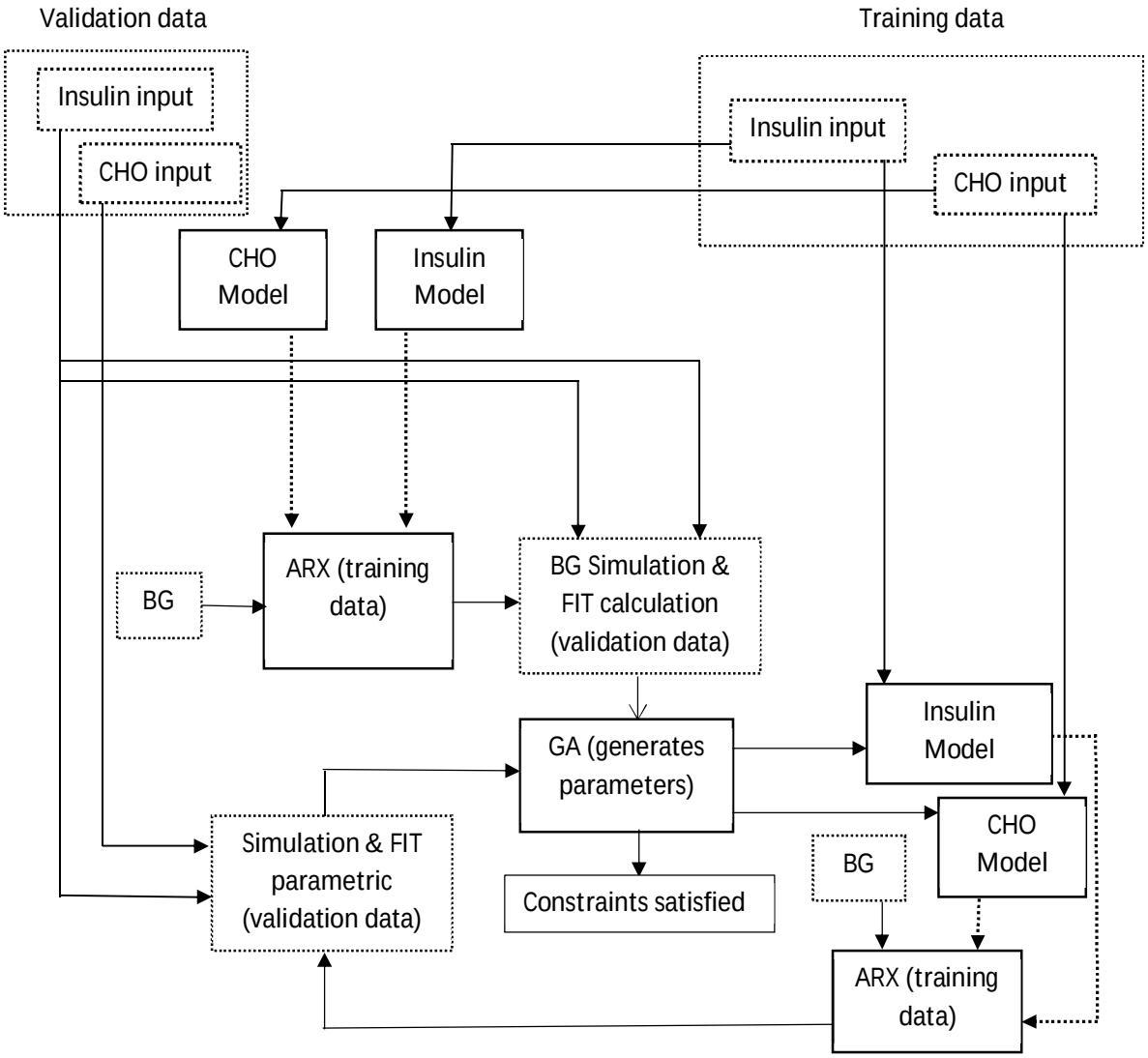

Figure 5.4: Outline of the components involved in the GA-ARX model. Dotted lines and boxes are output and data structures respectively. Solid lines and boxes are inputs and algorithms respectively.

In Figure 5.4 diagram, initially, the insulin and CHO impulse inputs reported by patients are fed into the respective models, before their corresponding insulin and CHO curves being computed using reference parameters. Afterwards, the relationship between the output and BG levels (output) is modelled by the ARX. The ARX model is then simulated with another unseen data (validation data) consisting of different Insulin and CHO inputs to be validated. The simulated output is then computed of its FIT value against the measured output of BG levels. The FIT value describes a comparison of simulated and actual output, where the simulated ARX model was derived from another input-output response dataset.

Separately, using the FIT value GAs works to achieve its objective function, thereby selecting individual solutions estimates that produces higher FIT. They are selected via crossover and mutation to produce solutions in next generation and with enough iterations, producing the most optimised parameters for the dataset.

In this experiment, 18 out of 22 individuals with Type 1 Diabetes with a broad range of age, HbA_{1c}, body mass index (BMI), duration of diabetes, and other physiological parameters were used in the GA-ARX tests, reflecting Type 1 diabetics with heterogeneous attributes. As glycaemic control in individuals naturally varies over time, and the gap between the wearing of glucose sensor to another occurs within a few days to each other, it is desirable in this test that the training and testing data originate from the same glucose sensor. This is to avoid the equilibrium point of the system differing too much over time. For this reason, 4 volunteers were excluded from the test as their dataset each spans only a short span of time.

Independent tests were conducted to optimise parameters within the sub-models of glucose-insulin dynamics, namely insulin, digestion, and then both of the models altogether. Four tests were carried out to assess the performance of the GA-ARX with selected parameters (shown in Table 5.2) namely:

a) ARX with reference parameters.
b) GA-ARX with optimised insulin parameters.
c) GA-ARX with optimised CHO parameters.
d) GA-ARX with optimised both insulin and CHO parameters.

The reason for the arrangement is that we are then able to contrast performance of each optimised model to another. It is also possible to evaluate which one of these models perform the most improvement in its optimised parameters, and if any other physiological parameters remain better with reference ones. The reference parameters to be adjusted are shown in Table 5.2, taken from the two models in Equation 2.1 to 2.6 presented in Chapter 2.

Model to be Optimised	Parameters	Default Parameter Values	Upper bounds	Lower bounds	Description
Insulin Model	P (min^{-1})	0.5	3	0.9	Dimeric production rate or velocity of transformation of insulin into other states.
	Q (rapid-acting) (ml^2U^2)	$4.75x10^{-4}$	0.09	0.05	Parameters representing the chemical equilibrium of the transformation of rapid-acting insulin into other states.
	Q (long-acting) (ml^2U^2)	3.04	5	2.0	Parameters representing the chemical equilibrium of the transformation of long-acting insulin into other states.
CHO/Digestion Model	V_{max} ($mmol$ min^{-1})	2	5	1	The maximum gastric emptying rate
	T_{up} (min)	30	60	10	Duration of increasing gastric emptying rate

Table 5.2: Parameters to be optimised by GA within the Insulin and CHO model.

As depicted in table 5.2, there are three parameters within the Insulin model and two from the CHO model.

5.2.1 Training and Validation

The datasets are partitioned into two subsets: training and validating, but following the 10-fold validation technique, earlier presented in Section 3.10. The training set is used to build the model. The main parameters affecting the absorption profile of insulin and digestion models will be inserted and continuously adjusted with values generated by GA.

ARX works by modelling the input(s)-output from available dataset, and then computing the respective BG concentration. This process continues in each iteration of GA until completion. An initial population corresponding to small perturbations from the original parameters are seeded to GA during the first iteration, thereby ensuring that the GA operation considers initially the reference parameters and improve from it. The FIT metric derived from producing BG using reference parameters therefore becomes the benchmark for GA. This will save computation, time and prevent the GA from getting stuck in local optima (LO). Furthermore, a GA ability allowing us to define designated bounds for parameters is proven to be useful to avoid GA from searching beyond tolerable range and ease the problem of optimisation.

In order to properly evaluate how well the model has been trained, which is dependent on the size of training data and prediction, the model obtained from the previous process is then validated against the validation data, using 10-fold validation method and its average is taken as the value.

The curve is generated by simulating the ARX model obtained from the training, and afterwards the FIT metric is calculated. Following the completion of GA operation, the results were later compared with the original model and previous studies using similar identification systems. There is also a concern over GA's stochastic behaviour and whether the results will differ in each run. This was addressed by taking the mean results after 10 runs.

5.3 **Results**

Table 5.3 summarises the results obtained. The total mean FIT summaries the overall FIT over the volunteers.

Subject	FIT with ARX (%) (reference parameters)	FIT with GA-ARX (%)		
		Insulin optimised	CHO optimised	Both optimised
1	-27.4	-3.3	-16.7	-3
2	-12.7	-5.34	-8	0.8
3	9.1	16.3	12.2	16.8
4	-22.2	-9.4	-3.8	2.8
5	-37.6	-5.6	-6.7	-1
6	-28.2	-17.4	-0.6	8.3
7	-28.2	-16.2	-2.6	4.8
8	-5.1	0.1	4.4	4.7
9	6	6.1	11.6	11.5
10	-2.7	-2.5	2.2	2.2
11	-4.4	-0.6	6.4	8.4
12	-4.5	-2.7	7	2.3
13	-2.0	-1.9	-1.7	-2
14	6.6	9.7	14.7	14.3
15	-43.9	-43.4	14.7	-17.7
16	-7.1	4.8	14.2	13.7
17	3.5	4.5	12.3	14.3
18	-0.7	2.6	0.9	5.7
Total mean	-11.2	-3.6	3.4	4.8
Percentage improvement (%)		9.34	12.78	15.51

Table 5.3: Simulation with MPO (infinite-step ahead prediction).

The first test was done by sliding the ARX fit across the original parameters. The mean FIT obtained was -11.2 % as in Table 5.3 (Note that the negative values are only evaluated in terms of the magnitude). Afterwards, the second and third tests were done with optimisation in each sub-model. The table shows the FIT obtained for each tested volunteer's data as well as the mean FIT for all of them. Comparatively, the CHO-optimised model shows more improvement over insulin-optimised model that are true in all cases except for only 6 which were otherwise. The percentage-improvement (%) for insulin-optimised and CHO-optimised to original FIT were 9.34 % and 12.78 % respectively. When both of the models were optimised, the result shows the highest improvement than all the other tests, although it was not the sum of both of the insulin and CHO-optimised tests. Nevertheless, improvements can be seen in all tests done. Even with the lowest performed model; the insulin-optimised test, a significant enhancement to original parameters is seen in all the volunteers.

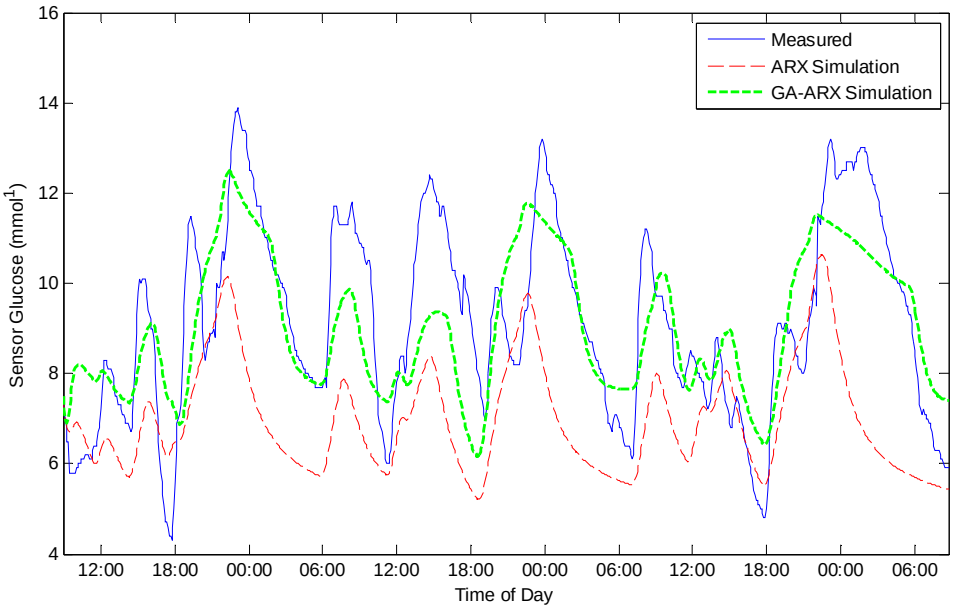

Figure 5.5: GA-ARX model simulation (MPO) (infinite-step ahead prediction) for subject #14 (RMSE= 2.23 $mmol\ l^{-1}$ and FIT = 14.27 %).

Figure 5.5 illustrates the comparison between 3 curves-measured BG, ARX simulation and GA-ARX simulation for subject #14. The FIT metric computed for ARX and GA-ARX simulation were 6.62 % and 14.27 % respectively. The ARX simulation used original parameters while GA-ARX used adjusted ones. The latter produced a much better simulation to the former, closer to measured BG. Even without the knowledge of past observations (simulation), still the main peaks were able to be simulated as in the figure. It was found that for prediction purpose, it is best to use a prediction horizon of 60 minutes, as were also done by Gani *et al.* and Finan *et al.* The following is a prediction with past observations (prediction) and ARX modelling with a 60 minutes prediction horizon.

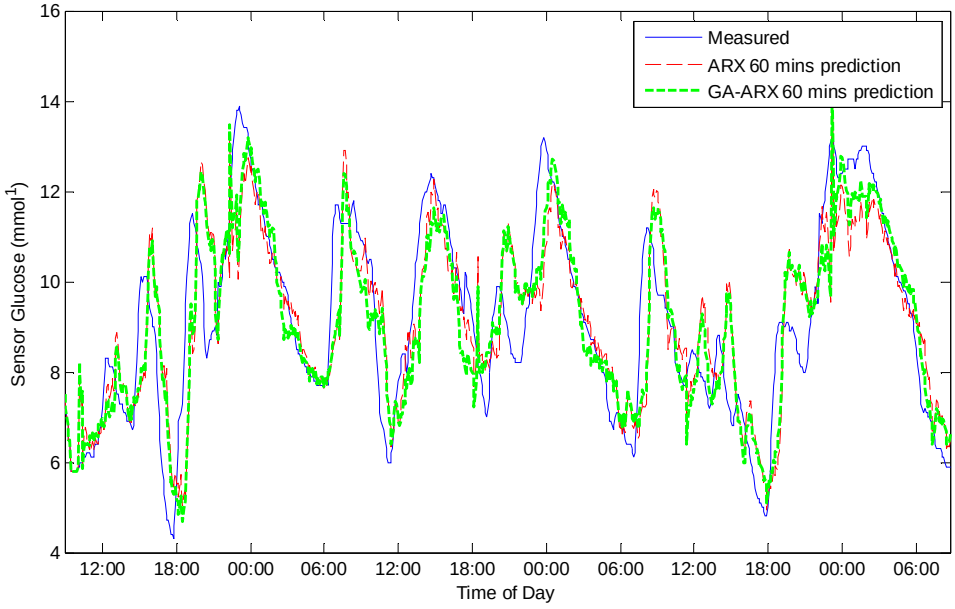

Figure 5.6: Comparing ARX 60 minutes prediction and GA-ARX 60 minutes prediction.

The outcome was much more positive, with 38.4 % FIT garnered in GA-ARX compared to just ARX at 36.2 % FIT. The improvement was also true in all other subjects. To test the performance of this method further, we investigated with longer horizons up to 150 minutes (2.5 hours) of prediction.

Model	Prediction Horizon							
	30 min		60 minutes		90 min		150 min	
	FIT (%)	RMSE ($mmol\ l^{-1}$)	FIT (%)	RMSE ($mmol\ l^{-1}$)	FIT (%)	RMSE ($mmol\ l^{-1}$)	FIT (%)	RMSE ($mmol\ l^{-1}$)
ARX	58.3	1.1	32	1.9	12.8	2.4	-5.5	3.2
GA-ARX	59.4	1.1	35.3	1.8	20.2	2.2	4.3	2.9

Table 5.4: ARX and GA-ARX model performance on the testing datasets for three prediction horizons.

From Table 5.4 above, over longer periods the prediction was still better with GA-ARX model, with improvements in both FIT and lowered RMSE. It is expected that longer horizons result in less predictive capability. In summary, over longer periods of time both ARX and GA-ARX prediction get considerably worse but the latter was always better than ARX.

Previous study done by Gani *et al.*, Finan *et al.* and Valletta was compared with our results from Test (a) and (d). The result, presented in Table 5.5 showed that with regards to the ARX test with reference parameters, our result yields fairly similar to Finan *et al.* but considerably worse than Gani *et al.* For GA-ARX with insulin and CHO optimised, except for the result of Gani's, the predictor surpassed all of them in terms of both the performance indicator FIT and RMSE.

Work	Model	FIT (%)	RMSE ($mmol\ l^{-1}$)	No. of Subjects
Gani *et al.* [49]	AR(6)	n/a	0.7	9
Finan *et al.* [88]	ARX(3,3,3)	35	2.2	9
Valletta [9]	ARMAX(3,3,3,1)	31	2.0	22
ARX with reference parameters (our study)	ARX(3,3,3)	32	1.86	18
GA-ARX (our study)	ARX(3,3,3)	35	1.77	18

Table 5.5: Results from various studies compared for 60 minutes prediction horizon.

However, one must note that Gani *et al.*'s result performing considerably well was probably due to the subjects were actually being hospitalised and confined to an investigational site, where meals and insulin were also well regulated and controlled, hence resulting in a more structured and predictable BG dynamics.

5.4 Discussion

The results, together with comparison from previous studies, confirm that it is feasible to employ the GA-ARX modelling technique to predict better glucose excursions within the short period of time. It is necessary to allow training and validation data to be close apart in the gap between, to ensure that the state of equilibrium of the physiological system does not differ very much over time. This can be due to manifold reasons such as changes in insulin preparations, use of other medications and lifestyle changes, evident by the HbA_{1c} assay widely used by clinicians.

The need for this kind of technique arises due to the absence of sensors that can measure insulin flow or glucose appearance in the bloodstream for free-living data collection. It is for this cause that the current artificial pancreas has been lacking in terms of better prediction. Even more, the only thing that can be accurately measured is CGMS. Although there is a significant improvement with the use of GA-ARX technique, it is still dependant highly on the ability of subjects to report accurately on the taken amount of insulin injections and consumed meals. Insufficient information on meals and insulin, uncertainty in the actual converted grams of carbohydrate from food consumed, and the timing of recorded food and insulin pose the risk of impeding in the data quality. Therefore, the insulin-to-glucose ratio may be flawed due to incorrect reports.

Another concern is that even if the inputs are well-known, the glucose-insulin dynamics modelling only approximates the general profiles for each insulin flow and glucose appearance with no regards to any group profile or specification, let alone individual. Furthermore, the physiological processes in the individuals are not at all accounted for. Some examples would be the insulin absorption rate that depends on the injection site and dose size and physical activities that affect insulin resistance by the change in blood flow or skin temperature. The proposed GA-ARX to some extent accounts for this matter by having patient-specific profiles BG prediction. Using optimisation, the varying dynamics were addressed to a certain extent if not partially improved with the GA-ARX method. This is a route towards a better glucoregulatory system modelling that is suited to each diabetic using clinical information such as body mass index (BMI), insulin sensitivity

and body composition. Future study could include these variables into the equation as was done by Patek *et al.* [50].

There are as well practical limitations in the ARX prediction. Short-term prediction is one of them. Despite various prediction horizons presented and the shortest time span being 30 minutes, insulin injection is known to take up to 20 minutes for absorption. The data collection also needs to be contiguous in the sense that the data for training and testing must not be far apart in its duration, or otherwise the physiological equilibrium may have changed. In this study, the minimum time span for two contiguous dataset is a few minutes and the maximum is 3 days, while the intended practice was actually immediate replacement of the wearable sensors.

The hypothesis is that shorter the time span yields more descriptive physiological states in the subject producing a much accurate prediction. The model will also need to be kept updated in its model parameters especially in the application of artificial pancreas, hence the desired practice is the continuous optimisation of parameters preferably embedded in the wearable system. The prospect of using a time varying ARX could also be explored for this objective given that the glucose-insulin parameters vary over time. Having known the varying parameters that were adjusted during optimisation, future work could be done in classifying patients so that treatment suggested would be done accordingly. Parameters that are drawn to certain bounds by the optimisation could mean that they were dictated by the lifestyle and wellbeing, and this may occur in other patients as well.

5.5 Contribution to the Body of Knowledge

In this chapter, we assessed the feasibility of using ARX and GA-ARX models to describe free-living observational Type 1 diabetes data and evaluate their performance. It was shown that an optimisation technique, GA, was able to improve the BG levels prediction by adjusting the governing parameters within the insulin and CHO subcutaneous models. The result is a much more reflective glucoregulatory process that is tuned and individualised accordingly. Personal adaptation of parameters in glucose and insulin models was found to be relevant to investigate. Substantial improvement can be made in the subcutaneous models by adjusting the most significant parameters within them. Adjusted parameters (GA-ARX) that fit individuals' particular physiological model were shown to be more effective than the ARX.

Prediction with short horizon can be demonstrated producing better identification model of BG levels with close fit to measured BG. However, over time the prediction FIT worsens regardless of the prediction horizon. Nevertheless, the feedback capability within GA-ARX will keep updating the parameters and prediction capability so long as this process is continued. Subjects also played a pivotal role in reporting the correct meal and insulin amount evident by the fact that a number of prediction for specific subjects received very good FIT (example: 48.92 % FIT in 60 minutes prediction horizon for subject #7 using GA-ARX) while the others did not (example: 5.84 % FIT in 60 minutes prediction horizon for subject #13 using GA-ARX).

The success of GA-ARX means that there is an inherent need to enhance and improve current knowledge on modelling the insulin-glucose-dynamics, especially within the models tested and found to be vastly improved with optimisation, in our case the CHO model. It is foreseeable that in the future a patient-oriented model will be of high interest and soon thoroughly explored. This study further stresses the importance of it. Since the result found that the proposed technique has managed to track major excursions in patients' BG in a timely manner, this would be helpful to clinicians that they can devise subsequent actions to counter-react any glucose drifting away from the normoglycaemic range.

In summary, ARX model was shown to be able to perform only short-term predictions. However, the prediction horizon is what is desirable by clinicians and patients themselves; being able to identify and treat drifting glycaemic excursions in the most critical time in order to prevent BG levels from worsening and being life-threatening. The need for individual-specific glucose-insulin modelling was shown to be promising. There are a lot more to the dynamics in the insulin-glucose models that were not yet dealt with such as physical activities but in the future, it is hoped that this can be investigated.

Chapter 6: Non-Stationary Gaussian Processes (NSGP)

This chapter presents the argument that regular linear time invariant models cannot fully capture the dynamics existing within the BG data. Physical activity data, though having its own periodicities like carbohydrate and insulin, is very much non-linear, particularly when it comes to data in free-living nature such as that used in this study, as opposed to those collected in a regulated and controlled environment, e.g hospitals or clinics. It can be observed that no matter how passive an individual is, his/her physical activity still shows very much the presence of short and irregular bursts throughout the day, producing a significant impact on the BG response and subsequently creating difficulties in modelling it. Even with the use of the non-linear gaussian processes model employed by Valetta on the same DUK data, minimal result was found when the activity parameter was added, a matter reported in this chapter. Therefore, a non-stationary gaussian processes technique is then discussed to identify the operating points of the various BG dynamics, with the presence of the extra flexibility associated with using the proposed technique.

6.1 Introduction

Regular LTI systems cannot capture all of the dynamics contained within the blood glucose data. An example of available dynamics existing within the blood glucose data is the saturation exhibited by the glucoregulatory system. This nonlinear behaviour occurs when the kidneys can no longer absorb surplus glucose in the blood exceeding the renal threshold, hence the excretion of it in the urine [89]. Various techniques like neural networks, fuzzy models and swarm optimisers have been applied in the modelling of the glucoregulatory system [82], [90]–[101]. All have drawbacks, primarily due to the number of decisions to be taken *a priori* like the number of hidden layers and activation functions. Moreover, the issue of the curse of dimensionality also becomes a problem with an increase in the number of input dimensions. Hence, Gaussian Process (GP) models which are a simple, probabilistic, non-parametric modelling which was tested by Valetta in his thesis, is again investigated of its performance. GP, primarily developed by Rasmussen and William [102] and popularised within the machine learning community for static problems have recently been applied to problems in system dynamics and identification as well.

6.2 Gaussian Process Models

The rationale for GP lies within its ability to model the correlations between the input and output rather than an estimation of parameters for a fixed model structure. It is essentially an infinite dimension of multivariate Gaussian Distribution characterised by a mean function $m(x)$ and a covariance function $k(x,x')$. A function can be seen as an infinitely long vector with each point representing a random variable. In this case, the function would be the blood glucose data and each reading is considered a random variable, such that whichever finite number of them consists of a joint multivariate gaussian distribution. Due to the infinite number of random variables, the mean vector becomes a mean function and similarly, a covariance matrix turns into a covariance function. Let us take x as a set of inputs characterising the output, examples for our case could be insulin, food or physical activity. Utilizing this Bayesian framework to obtain the posterior distribution, the prior belief is tuned by the likelihood and observed data's conditional probability model such that:

$$\text{posterior}=\frac{(\text{likelihood})(\text{prior})}{\text{marginal likelihood}}$$

Therefore, the prior contains the initial belief of how the probabilistic model should look like before seeing any data. It is then tuned by the likelihood and conditional probability model of the observed data. An eccentric characteristic of the GP framework is the very fact that the prior is placed on the function class itself, whereas in other Bayesian techniques, the function class is specified beforehand. The prior is applied on the parameters estimated from the data. While the mean functions usually are taken to be zero, in our case, the HbA_{1c} values for each patient are selected as the mean function because this better informs the approximation.

The covariance function conveys vital information about the system such as the stationarity and smoothness, quantifying the detected similarity between training and testing input sets. The output is inferred as in Bayes' law, effectively modelling the correlations between the inputs sphere. Hyperparameters can be estimated from data using various covariance functions, with the most popular one being squared exponential [102]:

$$k_{se}(\mathrm{x}, \mathrm{x}') = \sigma_f^2 \exp\left(-\frac{1}{2}(\mathrm{x}, \mathrm{x}')^{\mathrm{T}} L(\mathrm{x}, \mathrm{x}')\right) \quad 6.1$$

Here,

σ_f^2 is the function variance, and

$L = \mathrm{diag}(l)^{-2}$ is the length-scale matrix.

The length-scale l dictates how 'far' apart each scalar input x needs to be for the function output to be deemed uncorrelated. Together with σ_f^2, they form the hyperparameters of a GP model and are generally estimated from the data by minimising the marginal log-likelihood. As discussed by Rasmussen *et al.* [102], the length-scale l can be used for Automatic Relevance Detection (ARD). An input with a very large l will have no effect on the inferred output, hence can be considered irrelevant. Using the technique, the most important regressors can then be selected.

It is now important to look at the mathematics behind the inference of the posterior model. Although a GP is of infinite dimensions, inevitably inference is still done on a finite number of data points. Let us consider the problem of using the probabilistic model given a set of test inputs, assuming the observations are in the form:

$$y = f(x) + \epsilon \quad 6.2$$

where

ϵ is assumed to be zero-mean gaussian noise with variance σ_{n}^2 and the prior covariance function is given by:

$$\text{cov}(y, y') = K(X, X) + \sigma \frac{2}{n} I \quad 6.3$$

where
K(*X*,*X*) is any valid covariance function and
X is a vector of measured data points.

The joint probabilistic model using the assumed prior (m(x)≡0 and covariance function given above is:

$$\begin{pmatrix} y \\ f^* \end{pmatrix} \sim N\left(0, \begin{bmatrix} K(X,X) + \sigma^2 I & K(X,X^*) \\ K(X,X) & K(X^*,X^*) \end{bmatrix}\right) \quad 6.4$$

where,

X* are the input points for which the outputs needs to be predicted
f* is the predicted output

The posterior probability model for f*, five the observed data X* is given by:

$$f^* | x*, x, y \sim N(\tilde{f}^*, \text{cov}(f^*)) \quad 6.5$$

$$\tilde{f}^* = k(x^*, x) - k(x, x) + \sigma_n^2 I^{-1} y$$

$$\text{cov}(f^*) = K(X^*, X^*) - K(X^*, X) K(X, X) + \sigma_n^2 I)^{-1} K(X, X^*)$$

In Valetta's work, he modelled carbohydrate G(t) and insulin dosage I(t) formulated as:

$$G(k) = f(G(k-1), \ldots, G(k-3), Gin(k-1), \ldots, Gin(k-3), Iex(k-1), \ldots, Iex(k-3)) + \zeta(k) \quad 6.6$$

Initially, Valletta only included carbohydrate and insulin in the GP model. Later, in order to investigate whether exercise could be used as a predictor for BG concentration, physical activity data in the form of METs were added. The exact same regressors were used so that his model could be compared to a linear time-invariant system identification model, ARMAX. He concluded that with the two former inputs, GP models actually performed worse than ARMAX modelling for both short and long-term prediction (mean fit = -3.0±26.8% and -57.0±50.6%, respectively). The case was the same with physical activity inputs represented by two dataset: the METs and Heat Flux data, hoped to better represent body responses. Improvements over predictions were only discovered with the training data but not on unseen data (validation data). Short and long-term prediction yield 87.94 % and 92.2 % worse FIT than ARMAX respectively. As seen in the Figure 6.1, although the models typically managed to track changes in BG, they did not however match the magnitude of excursions.

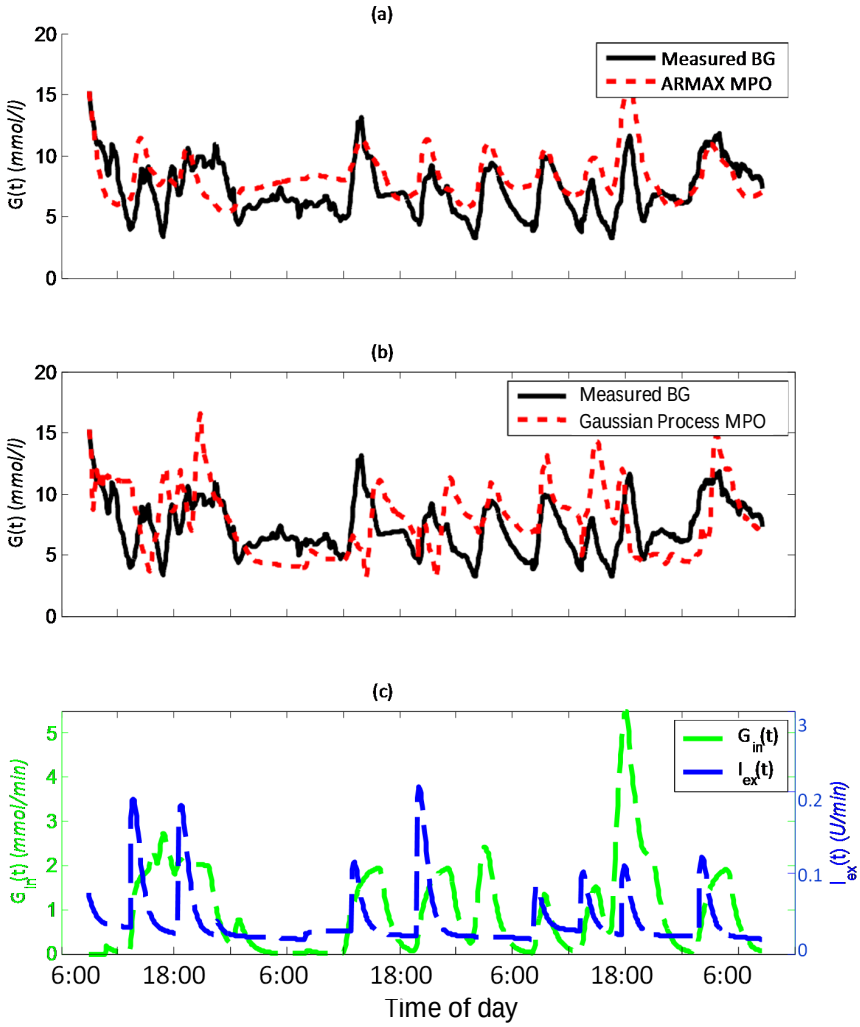

Figure 6.1: Reproduced from Valetta [9]. Model predicted output for subject #20 dataset 4 using (a) ARMAX model (FIT=-7.4% and RMSE=2.3 $mmol/l$) (b) GP model (FIT=-45.8% and RMSE=3.0 $mmol/l$), in response to inputs (c) $G_{in}(t)$and ($I_{ex}(t)$.

In contrary to the initial inference that more inputs would yield better results, multiple inputs produced worse prediction than that of the carbohydrate and insulin ones alone. This means that if better prediction is our primary objective, more inputs might then not be of help, like adding various additional measurement devices beyond CGMS. Therefore, Valletta noted that the method of system identification itself probably needs further modification with different models for different physiological operating regimes.

Valletta further observed that the poor results were probably due to the non-stationarity behaviour of BG dynamics present in free-living data from volunteers profiles which would be absent with simulated BG data as used in [103]. The stationarity analysis revealed that BG substantially varies over time, and in the longer period of time, HbA_{1c} does too. The author summarised that due to the BG dynamics time-varying nature, the model's accuracy could possibly be improved with recursive updates of covariance function parameters as new data become available.

Despite BG levels having daily periodicities just like carbohydrate ingestion, insulin dosage and physical activities, this is not always the case, stressing the stochastic nature of BG. Additionally,

cross-correlation analysis reveals a high dependency between the inputs as was the case with meal and insulin inputs. Physical activity however, generally takes place within short periods of time during the day but causes substantial impact on BG response for four hours or more after the activity ceases. It can rapidly change the system's operating region or state to another. These operating regimes are triggered while they also activate various metabolic pathways as depicted in Figure 6.2.

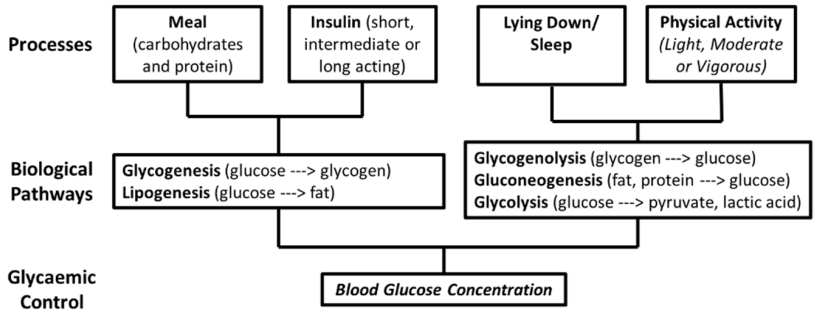

Figure 6.2: Various physiological operating regimes that affects blood glucose and their particular metabolic pathways.

Due to the nature of physical activity occupying a small proportion of the free-living datasets, the GP models of Valletta were unable to learn its dynamics which were also masked by the responses to carbohydrate ingestion and insulin administration. In summary, if the learning dataset was unable to capture sufficient system dynamics, the model could not learn correctly. Valletta then concluded that work should be focussed on identifying local models for the different operating regimes to better understand BG dynamics.

6.3 Non-Stationary Gaussian Process

Typical Gaussian Processes have limitations, notably computational difficulties for large datasets and restrictive modelling assumptions for complex ones [104]. Also, the curse of dimensionality still remains a problem (albeit reduced by computational advances in recent years), as the training cost for a GP has the complexity of O(N^3), where N is the number of training points. The non-parametric nature of a standard GP can also have high uncertainty about the interpolating function while assuming a uniform noise variance across modelled data.

To address some of these issues, Snelson [105] developed a new Bayesian non-parametric and non-linear regression method for their use in neuroscience. This modified version of GP utilises sparse approximations that selects a subset of the training points of size M to base for its training, thereby reducing the complexity to O(NM^2), where M has much lower value than N. The covariance value is parameterised by the location of M pseudo-input points, learnt by gradient based optimisation. The hyperparameters also originate from the same joint optimisation, hence the model can be viewed as a Bayesian regression model with a particular input-dependent noise. In other words, the modified sparse approximation or covariance function made the modelling of an input-dependent noise possible. Another extension from the standard GP is that the Gaussianity assumption of the process was relaxed by the learning of the nonlinear transformation of the outer space, therefore increasing the applicability of GP to model real complex datasets.

To demonstrate this, a data of {X,y} is given, where X is the training input and y the target pair. A new pseudo data set $\mathcal{D}$ of size M < N: pseudo inputs $\bar{\mathbf{X}} = \{\bar{\mathrm{x}}_m\}_{m=1}^{\mathrm{M}}$ and a pseudo target $\bar{\mathbf{f}} = \{\bar{\mathrm{f}}_m\}_{m=1}^{\mathrm{M}}$ are created. $\bar{\mathrm{f}}$ becomes the pseudo targets replacing y as they are not actually real observations but rather sparsely extracted data, having non-noisy data. The single data point likelihood is as follows:

$$p(y|\mathrm{x}, \bar{\mathbf{X}}, \bar{\mathbf{f}}) = \mathrm{N}\,(\mathrm{y}|\mathbf{k}_x^{\top}\mathbf{K}_M^{-1}\bar{\mathrm{f}}, \mathrm{K_{XX}} - \mathbf{k}_x^{\top}\mathbf{K}_M^{-1}\mathbf{k}_{\mathrm{X}} + \sigma^2), \quad 6.7$$

where $\mathbf{K}_{XM}$ is the covariance between the input x and the pseudo-inputs $\bar{\mathbf{X}}$, $\mathbf{K}_{\mathrm{X}}$ is the self-covariance of the pseudo-inputs. Note the parameterised mean function and input-dependent noise model, fixed within the standard regression GP model. The objective then is to find a suitable pseudo-data that represents real observed data well. Rather than maximising the likelihood with respect to X and f, the pseudo-outputs f are integrated out, placing the Gaussian prior on the pseudo-outputs:

$$p(\bar{\mathbf{f}}|\bar{\mathbf{X}}) = \mathcal{N}(\bar{\mathbf{f}}|\mathbf{0}, \mathrm{K_M}) \quad 6.8$$

By this, the pseudo-data are distributed evenly, closely similar to the real data, hence the term Sparse-Pseudo-input Gaussian Processes (SPGP) used by the developers. With the modifications made to the standard GP model, the SPGP can therefore be assumed to possess a form of non-stationary covariance modelling. In Figure 6.3 below, the comparison between predictive distributions on a synthetic data for standard GP and SPGP modelling is shown. During training, SPGP differs by being able to adjust its pseudo-inputs to the left due to the by-product of non-stationarity of the sparse covariance function [104]. Figure 6.3(b) shows that the noise was modelled much better than with standard GP. The outer lines refer to the upper and lower bounds that reduces the uncertainty with SPGP.

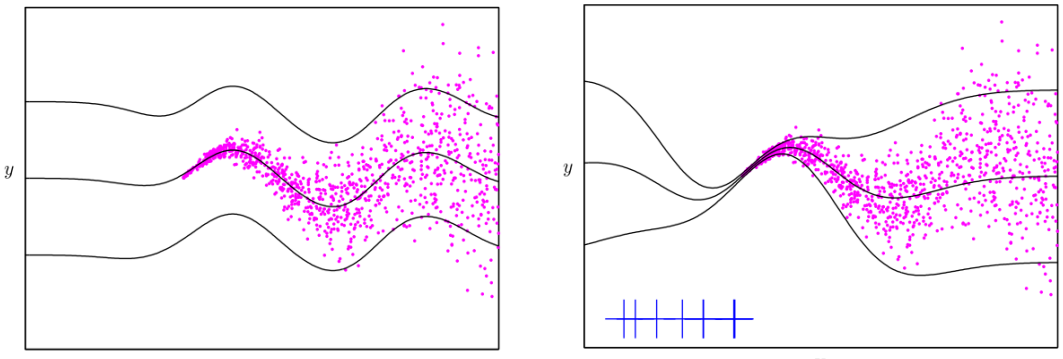

(a) GP (b) SPGP

Figure 6.3: The predictive distributions after training on a synthetic heteroscedastic data set are shown for the standard GP and SPGP [104]. The data points are the magenta points. The mean prediction and two standard deviation lines are plotted in black. x locations of pseudo-inputs are shown as blue crosses (crosses with larger crosses mean lower uncertainty).

Detailed description of SPGP can be found in [104]. However, in this study where we are particularly interested in incorporating the non-stationarity attribute of the model, the model will be referred to as Non-Stationary Gaussian Processes (NSGP) in the coming discussion.

With NSGP, similar to the previous experiments, a number of tests were conducted to assess the performance of NSGP, firstly with only the two parameters (CHO and insulin), and then with the addition of physical activity parameters discussed in Section 3.4.2 to 3.4.3, which are heat flux and METs. The four tests are:

i. 2 inputs NSGP (CHO and insulin).
ii. 3 inputs NSGP (CHO, insulin and heat flux).
iii. 3 inputs NSGP (CHO, insulin and METs).
iv. 4 inputs NSGP (CHO, insulin, METs and heat flux).

The two physical activity parameters were added to NSGP first separately and then together to reveal the respective roles of each parameter. The tests were done to all of the subjects' dataset, using 10-fold validation method presented in Section 3.1.1 and the average values taken and presented in the result.

6.4 **Results**

The prediction result will also be compared to the results and works of Valetta who utilised the standard Gaussian Processes model. Because this study investigates the model itself and is not too much constrained by the issue of volunteers' physiological status changing equilibrium over time, the issue of training and validation data that previously must be close in time does not arise. Therefore, all 22 volunteers' data including those having short duration of data collection and were excluded in the GA-ARX study before were tested. The dataset belonging to each subject was split for training and validation, to maintain the same physiological condition as in the GA-ARX study. In this study, each of the volunteer of whom at least two datasets were available, one dataset was used to train the NSGP model and the prediction tested on the remaining data sets, according to the k-fold validation protocol. Both 60 minute-prediction horizon (12-time points) and MPO (infinite-step ahead prediction) were evaluated for FIT and RSME values. The results of the NSGP modelling are shown in Table 6.1. Note that the nature of the model is different to GA-ARX modelling because while it will have one specific model tested throughout all patients, GA-ARX is a one-patient-optimisation and focused on optimising only the parameters for the respective test inputs. Therefore, due to the differences and constraints in the GA-ARX model, this model will not be compared to it, rather to the results from the standard Gaussian Processes employed by Valletta.

Subject ID	Dataset	Test (i)				Test (ii)				Test (iii)				Test (iv)			
		60 mins		MPO		60 mins		MPO		60 mins		MPO		60 mins		MPO	
		FIT	RMSE	FIT	RMSE	FIT	RMSE	FIT	RMSE	FIT	RMSE	FIT	RMSE	FIT	RMSE	FIT	RMSE
01	1	5.9	2.0	3.5	2.0	-4.1	2.2	-25.5	2.6	10.1	1.9	-13.4	2.4	3.5	2.0	2.0	2.4
	2	60.1	0.7	63.1	0.7	58.4	0.8	41.3	1.1	57.3	0.8	35.8	1.2	63.1	0.7	0.7	0.8
02	1	9.1	1.5	6.3	1.5	7.4	1.5	-90.3	3.1	12.0	1.4	-89.2	3.1	6.3	1.5	1.5	3.1
	2	-11.1	2.2	-5.7	2.1	-11.7	2.2	-51.2	3.0	-20.6	2.4	-78.9	3.6	-5.7	2.1	2.1	2.9
	3	59.4	0.7	72.4	0.5	72.1	0.5	51.2	0.8	64.5	0.6	48.2	0.9	72.4	0.5	0.5	0.6
03	1	5.0	2.3	14.8	2.0	6.8	2.2	-83.3	4.4	21.5	1.9	-123.0	5.4	14.8	2.0	2.0	4.7
	2	62.3	1.1	57.3	1.3	60.0	1.2	14.6	2.6	57.6	1.3	-23.2	3.7	57.3	1.3	1.3	3.5
	3	44.2	1.7	38.6	1.9	27.5	2.2	-32.6	4.1	18.5	2.5	-26.7	3.9	38.6	1.9	1.9	3.9
05	1	3.7	2.4	0.1	2.5	-6.4	2.6	-12.0	2.7	5.7	2.3	3.4	2.4	0.1	2.5	2.5	2.6
	2	54.6	1.1	53.5	1.1	63.6	0.9	-5.6	2.6	57.0	1.0	-2.3	2.5	53.5	1.1	1.1	2.6
06	1	-40.9	2.3	-58.0	2.6	-55.0	2.6	-219.2	5.3	-71.0	2.8	-258.0	5.9	-58.0	2.6	2.6	6.7
	2	11.6	2.5	22.1	2.2	19.6	2.3	-83.9	5.2	6.4	2.7	-216.4	9.0	22.1	2.2	2.2	5.0
	3	67.7	1.4	68.4	1.4	67.7	1.4	6.0	4.1	66.0	1.5	-17.5	5.1	68.4	1.4	1.4	5.4
07	1	53.5	1.1	60.4	0.9	56.3	1.0	-3.3	2.5	56.7	1.0	26.2	1.8	60.4	0.9	0.9	2.2
	2	21.0	2.1	18.3	2.2	23.1	2.1	-27.4	3.4	23.4	2.1	-11.9	3.0	18.3	2.2	2.2	3.2
08	1	62.8	1.3	66.3	1.1	66.3	1.1	31.2	2.3	64.7	1.2	24.6	2.5	66.3	1.1	1.1	2.3
	2	24.3	3.6	30.5	3.3	24.0	3.6	-17.0	5.5	20.2	3.8	-30.4	6.2	30.5	3.3	3.3	4.5
09	1	58.2	0.9	63.3	0.8	61.4	0.9	17.7	1.9	61.8	0.9	14.2	1.9	63.3	0.8	0.8	1.9
	2	13.3	1.9	19.9	1.7	13.9	1.9	-40.5	3.0	6.2	2.0	-50.7	3.2	19.9	1.7	1.7	3.2
10	1	45.8	1.2	58.5	0.9	57.1	0.9	5.1	2.1	50.0	1.1	-5.3	2.3	58.5	0.9	0.9	1.6
	2	0.1	3.1	9.6	2.8	16.9	2.6	5.7	3.0	16.8	2.6	8.2	2.9	9.6	2.8	2.8	3.1
	3	27.6	2.3	19.1	2.5	17.1	2.6	-0.1	3.1	26.4	2.3	1.9	3.0	19.1	2.5	2.5	3.1
	4	-5.6	3.7	1.1	3.4	0.0	3.5	-12.3	3.9	-4.1	3.6	-4.6	3.6	1.1	3.4	3.4	3.5
11	1	3.7	4.3	2.4	4.3	-0.1	4.4	-21.0	5.4	16.5	3.7	2.2	4.3	2.4	4.3	4.3	5.5
	2	62.4	1.1	62.3	1.2	67.9	1.0	29.5	2.2	64.7	1.1	20.1	2.4	62.3	1.2	1.2	2.6
	3	36.5	2.3	51.6	1.8	39.7	2.2	9.2	3.3	45.5	2.0	14.1	3.1	51.6	1.8	1.8	3.5
13	1	65.9	1.3	63.2	1.5	66.5	1.3	56.2	1.7	62.1	1.5	45.5	2.2	63.2	1.5	1.5	1.9
	2	21.9	2.9	21.7	2.9	14.6	3.2	4.0	3.6	15.3	3.2	2.4	3.7	21.7	2.9	2.9	3.4
	3	19.3	4.2	5.1	4.9	11.7	4.5	5.8	4.9	26.0	3.8	16.5	4.3	5.1	4.9	4.9	5.4
	4	3.2	2.8	-3.5	2.9	-3.9	3.0	-33.6	3.8	-6.5	3.0	-28.7	3.7	-3.5	2.9	2.9	4.1
14	1	-16.9	3.3	-4.9	2.9	-21.4	3.4	-151.5	7.0	-4.9	2.9	-61.1	4.5	-4.9	2.9	2.9	4.0
	2	60.4	1.7	61.9	1.6	57.4	1.8	6.0	4.0	60.1	1.7	2.5	4.1	61.9	1.6	1.6	3.6
	3	17.3	2.5	-8.1	3.3	-1.0	3.1	-57.4	4.8	-5.7	3.2	-29.3	3.9	-8.1	3.3	3.3	4.1
	4	12.9	3.4	30.0	2.8	18.9	3.2	7.7	3.6	27.6	2.9	7.8	3.6	30.0	2.8	2.8	3.6
15	1	27.7	2.2	20.0	2.4	27.4	2.2	3.9	2.9	1.7	2.9	-174.5	8.2	20.0	2.4	2.4	3.3
	2	46.3	1.4	51.0	1.3	49.8	1.3	25.9	2.0	41.8	1.6	3.6	2.6	51.0	1.3	1.3	2.2
	3	20.5	1.4	25.7	1.3	23.0	1.4	-37.6	2.4	26.7	1.3	-32.9	2.4	25.7	1.3	1.3	2.4
16	1	13.0	3.3	25.8	2.8	23.1	2.9	-20.2	4.6	26.4	2.8	-21.0	4.6	25.8	2.8	2.8	4.6
	2	65.9	1.2	71.1	1.0	70.2	1.0	56.5	1.5	68.3	1.1	47.5	1.8	71.1	1.0	1.0	1.8
18	1	15.0	2.5	29.2	2.1	22.4	2.3	-7.4	3.1	37.3	1.8	-1.7	3.0	29.2	2.1	2.1	2.8
	2	47.6	1.7	48.3	1.7	47.6	1.7	-33.2	4.4	43.9	1.9	-13.1	3.8	48.3	1.7	1.7	4.8
	3	17.9	1.7	13.1	1.8	14.3	1.7	-45.8	3.0	31.7	1.4	-17.3	2.4	13.1	1.8	1.8	3.4
	4	33.7	1.8	26.7	2.0	29.5	1.9	-14.7	3.1	26.9	2.0	-16.3	3.1	26.7	2.0	2.0	4.0
19	1	-7.2	3.3	3.3	3.0	-3.4	3.2	-35.0	4.2	2.3	3.0	-32.5	4.1	3.3	3.0	3.0	4.3
	2	-10.7	3.6	-16.3	3.8	-35.5	4.4	-44.2	4.7	-23.2	4.0	-50.2	4.9	-16.3	3.8	3.8	5.3
	3	59.6	1.3	63.2	1.2	63.2	1.2	21.4	2.5	59.4	1.3	36.2	2.1	63.2	1.2	1.2	2.7
20	1	64.2	1.3	67.4	1.2	67.3	1.2	31.6	2.5	65.7	1.3	25.1	2.7	67.4	1.2	1.2	3.0
	2	-117	3.3	-106	3.1	-131.5	3.5	-300.9	6.1	-130	3.5	-309.7	6.2	-105	3.1	3.1	4.8
	3	-8.8	3.1	4.0	2.8	-2.0	3.0	-36.2	3.9	-14.6	3.3	-63.3	4.7	4.0	2.8	2.8	3.6
	4	-53.1	3.2	-24.0	2.6	-48.2	3.1	-141.1	5.0	-52.5	3.2	-128.1	4.7	-24.0	2.6	2.6	4.5
21	1	47.8	1.4	56.5	1.1	55.6	1.2	2.5	2.6	48.9	1.3	9.4	2.4	56.5	1.1	1.1	2.0
	2	13.2	2.1	14.2	2.1	10.2	2.2	-81.7	4.4	18.2	2.0	-89.5	4.6	14.2	2.1	2.1	3.7
22	1	21.8	3.2	29.9	2.9	26.1	3.0	-5.8	4.3	26.7	3.0	-32.7	5.4	29.9	2.9	2.9	4.6
	2	77.1	1.0	76.9	1.0	76.3	1.1	5.8	4.3	79.9	0.9	46.9	2.4	76.9	1.0	1.0	2.2
	3	21.3	2.8	19.6	2.8	12.1	3.1	-40.4	4.9	17.0	2.9	-38.8	4.9	19.6	2.8	2.8	4.9
23	1	44.4	1.9	49.0	1.7	48.8	1.7	3.8	3.3	52.1	1.6	23.3	2.6	49.0	1.7	1.7	2.7
	2	-68.0	2.6	-63.6	2.6	-71.9	2.7	-192.5	4.6	-62.8	2.5	-196.3	4.6	-63.6	2.6	2.6	4.5
	3	25.0	2.6	31.6	2.3	27.0	2.5	-30.5	4.5	34.5	2.2	-13.6	3.9	31.6	2.3	2.3	4.8
	4	-68.8	2.4	-81.4	2.6	-84.6	2.6	-276.1	5.4	-73.9	2.5	-303.4	5.8	-81.4	2.6	2.6	4.1
24	1	-18.4	3.5	-38.5	4.1	-39.0	4.2	-36.0	4.1	-30.5	3.9	-22.3	3.7	-38.5	4.1	4.1	4.4
	2	18.9	1.3	43.7	0.9	45.8	0.9	-18.8	2.0	41.3	1.0	-13.8	1.9	43.7	0.9	0.9	1.7
	3	0.1	2.6	7.3	2.4	5.8	2.5	-6.3	2.8	10.6	2.4	-6.6	2.8	7.3	2.4	2.4	3.0
	4	-13.0	3.7	-17.0	3.9	-18.6	3.9	-21.8	4.0	-2.2	3.4	-24.7	4.1	-17.0	3.9	3.9	4.3
25	1	2.2	2.0	10.4	1.9	3.8	2.0	-30.5	2.7	14.7	1.8	-75.2	3.7	10.4	1.9	1.9	3.0
	2	5.1	2.6	7.1	2.6	6.8	2.6	-21.3	3.4	12.1	2.5	-49.4	4.2	7.1	2.6	2.6	3.7
	3	46.7	1.9	47.2	1.9	54.8	1.6	-50.8	5.3	47.4	1.9	-2.6	3.6	47.2	1.9	1.9	4.0

Table 6.1: NSGP prediction identified for each individual, with inputs being data of meals, insulin, METs data, heat flux. Training data is shaded in grey while other datasets were used for validation. Tests were done for 60 minutes ahead prediction and model predicted output (MPO). FIT is a metric used to evaluated fitness in comparison to measured BGC, at times showing negative percentage. Only magnitude is taken into account.

Result from Test (i) for subject #10 shows the predictor attained highest FIT with training data (45.8 %) and a lower FIT (27.6 %) for dataset 3, and an even lower FIT with dataset 2 (0.1 %). Based on the three recorded BG levels shown in Figure 6.4, it is observed that the result was due to BGC in dataset 3 sharing the most similar pattern to a dataset earlier used for training - Dataset 1, especially during the one day highlighted by the brown box. Glucose levels outside the box were not seen to be similar nevertheless. A similar pattern in BG levels in the datasets are a reflection of a rather repetitive and similar intake of food and insulin. This could be due to a firm adherence to the recommended daily intake by clinicians. Nevertheless, the result shows that only when a pattern is very similar reflecting a continuous daily lifestyle could a high FIT of modelling be attained. It also depicts the difficulty in modelling data of a free-living nature, with high spontaneity and variability, in comparison to ones in a regulated and controlled environment, where meal and insulin intake are thoroughly monitored and regulated.

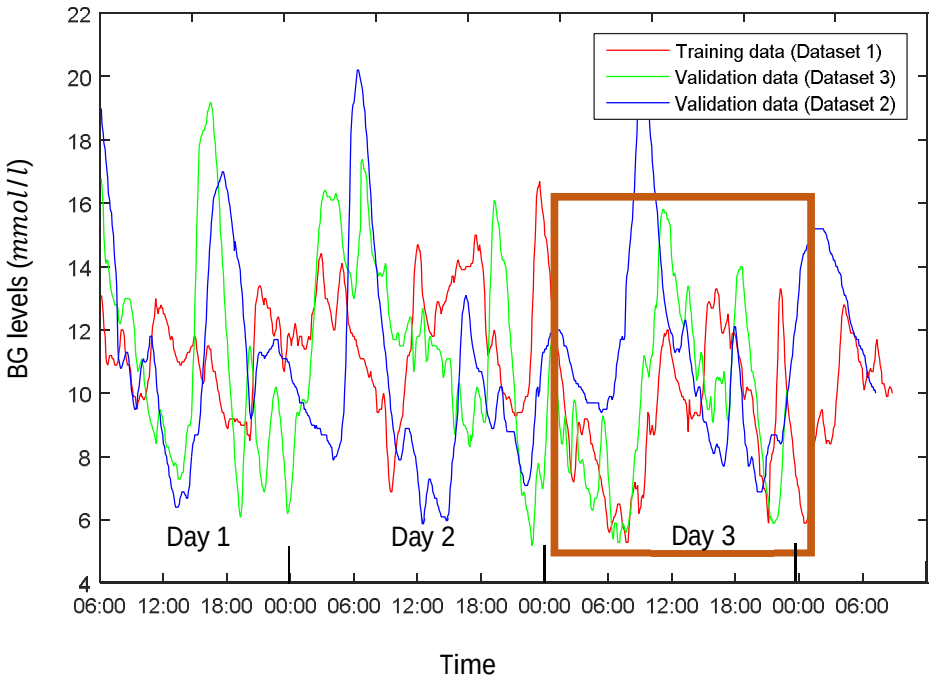

Figure 6.4: Recorded BG levels for 3 dataset from subject #10.

On the other hand, Figure 6.5 shows the prediction for subject #15, where it can be seen figuratively that the two validation datasets, although look a bit similar to each other (albeit of different magnitude) are much more different to the training dataset (highlighted by the brown box), as opposed to those in Figure 6.4. Hence, the lower difference of FITs obtained for the two validation datasets (FIT of 27.7 % for dataset 1 and 20.5 % for dataset 3).

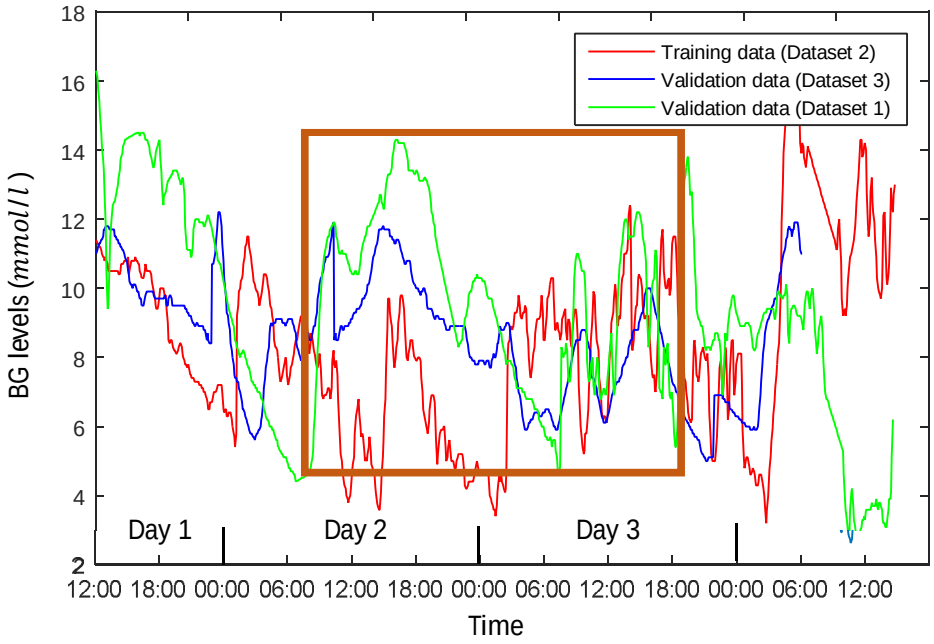

Figure 6.5: Recorded BG levels for 3 dataset from subject #15.

The overall summary for the mean FITs from the Table 6.1 above can be seen in Table 6.2.

Type of predicted data	60 minutes prediction				Model predicted output			
	Test				Test			
	(i)	(ii)	(iii)	(iv)	(i)	(ii)	(iii)	(iv)
Validation Data (%)	1.3	-1.49	1.88	3.1	-56.5	-53.38	-60.59	-49.2
Training Data (%)	56	60.65	57.78	60.2	9.9	13.39	15.05	17.4

Table 6.2: FITs summary of prediction for validation and training datasets.

While Table 6.3 shows the summary for the mean RMSE for the same result.

Type of predicted data	60 minutes prediction				Model predicted output			
	Test				Test			
	(i)	(ii)	(iii)	(iv)	(i)	(ii)	(iii)	(iv)
Validation Data (%)	2.7	2.77	2.66	2.6	4.2	4.02	4.19	3.9
Training Data (%)	1.3	1.17	1.25	1.2	2.7	2.64	2.57	2.5

Table 6.3: RMSEs summary of prediction for validation and training dataset.

The discussion will be mostly focusing on results from validation data since they are unseen by NSGP, unlike training data where they have been trained with NSGP previously. From Table 6.2, NSGP with only the insulin and CHO inputs received 1.3 % and -56.5 % in validation data respectively, thereby having better result than with the addition of either the heat flux or METs data, except when the two were added together. NSGP obtained the best result when the two physical activity parameters were added together than any other tests done, with 3.1% of FIT, attained as the highest value for validation data. Coincidentally, the model with added heat flux input performed better in the 60 minutes prediction (1.88 % FIT) but worse than when modelled with only METs added in infinite-step ahead prediction. Nevertheless, the overall result showed

that NSGP worked best with both the physical activity parameters added, but not with any single one.

A comparison of NSGP's performance to standard GP employed by Valletta with both models having the two physical activity inputs added (Test iv) were recorded in Table 6.4. Although Valletta's result was better in overall (higher FITs with training data), it was not the case with the unseen data where was no improvement at all on the validation data. The result suggests that standard GP modelling has predictive capability only with training dataset, however this is not surprising given that the dataset was already 'seen' earlier, and only with an unseen data that a model's performance can be evaluated truly.

In the case of NSGP modelling, both 60 minutes and MPO (infinite-step ahead prediction) prediction saw increase of FITs over both the training and validation dataset with the added physical activity inputs. Although standard GP's result exceeded NSGP's FITs for training dataset, it is inconsequential since predictions with unseen data are not anywhere comparable.

Type of Prediction	Type of Prediction Data		Standard GP (%)	NSGP (%)
60 minutes prediction	Training data	2 inputs	61	56
		4 inputs	69	60.2
	Validation data	2 inputs	-2.9	1.3
		4 inputs	-5.2	3.1
Model Predicted Output (infinite-step ahead prediction)	Training data	2 inputs	10	9.9
		4 inputs	29.2	17.4
	Validation data	2 inputs	-57	-56.5
		4 inputs	-57.1	-49.2

Table 6.4: Comparison between original GP and NSGP.

A direct comparison based on the number of predictions was also made. In order for a model to be recognised as better than the other, the former must obtain better FIT than the latter for at least half the number of predictions made, which is 22. Out of the 44 total number of prediction for validation data, with NSGP, 30 showed improvement (68 %) in a 2-input model (insulin and CHO), while 4-input modelling depicted an even better improvement of 36 (82% improvement). In terms of the 3-input model, the result obtained was similar to the one presented earlier. With only METs, the 60 minutes prediction improved in 30 datasets, but worsened to 19 out of the 44 in MPO. Models with added heat flux input however showed better result with MPO (25 improved) but lesser improvement in 60 minutes prediction (26 improved). Overall, with the use of NSGP, the two physical activity inputs do not appear to present better fit if added separately, and perform best only when both inputs are added together. Nevertheless, quantity-based-comparison depicts better effectiveness of the NSGP than percentage-FITs-based-comparison (as high FIT margin differences might alter our perception on the model's performance).

Our study is compared to the previous studies by Gani *et al.*, Finan *et al.* and Valletta, as compared earlier in Section 5.3. In addition, a comparison was also made to Cescon [83] where both ARX and ARMAX were tested for data from 9 patients in which the subjects were hospitalized for three days and brought the system home under normal living conditions, but without the METs data as additional input. All of this is depicted in Table 6.5. Another related study was by Pérez-Gandía *et al.* [106], where a connected three-layer Neural Network (with sigmoidal transfer functions in the first two layers and a linear for the output block) was used, with only the concurrent and previous CGM values up to 20 minutes back were taken as inputs, with no insulin nor meal information being used.

Work	Model	FIT (%)	RMSE ($mmol\ l^{-1}$)	No. of Subjects
Gani *et al.* [49]	AR	n/a	0.7	9
Finan *et al.* [88]	ARX	35	2.2	9
Valletta [9]	ARMAX	31	2.0	22
Cescon *et al.* [83]	ARX	n/a	1.9	9
Cescon *et al.* [83]	ARMAX	n/a	1.7	9
Pérez-Gandía *et al.* [106]	Neural Network	n/a	2.5	9
NSGP (our study)	Non-Stationary Gaussian Processes	17.4	1.6	22

Table 6.5: Comparison of NSGP to previous studies.

Due to the unavailability of FIT values from multiple researchers, the comparison was done for the RMSE values, and this means lower values reflecting better fits. From the results, it can be seen that while Gani's exceeded our result by a large margin (mainly due to the ambulatory data used), others were not except for with Cescon *et al.* study, with a slight improvement. On the other hand, despite Pérez-Gandía *et al.* employing neural network modelling, GA-ARX however performed better. However, as noted earlier, although Cescon *et al.* [83] study only did just better, it did not at all account the physical activity data parameter, and Pérez-Gandía's *et al.* [106] did not even include the insulin and meal data into the model. With these settings, the studies would be nowhere as comprehensive as the data from DUK, and any exercise-induced-effects would never be observed and accounted for, despite other sensors efficiently reporting on the normal living conditions of the subjects.

A figurative comparison between Valletta's prediction (standard AR, same DUK data) and ours to the actual measured BGC can be seen in Figure 6.6 below.

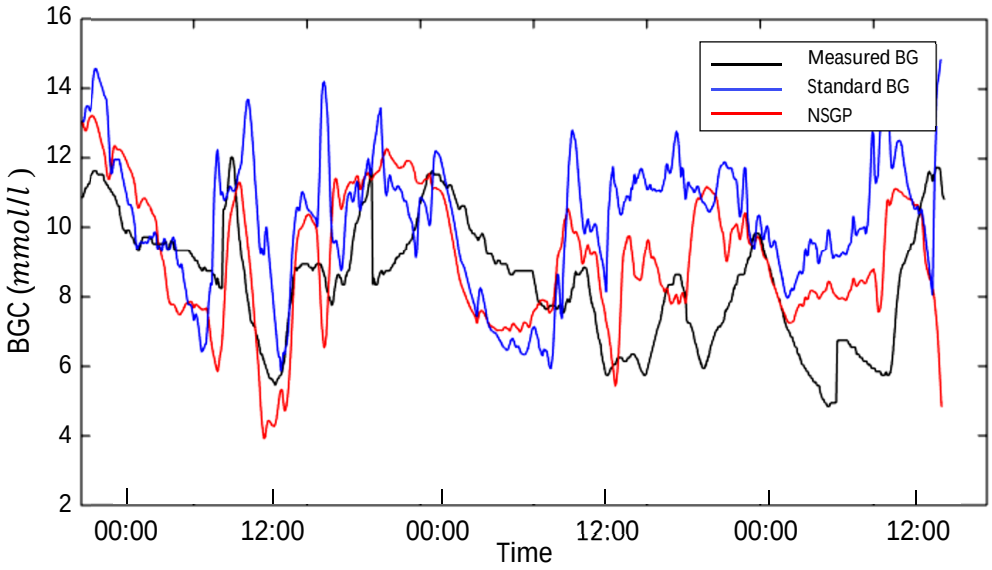

Figure 6.6: Plots comparison of NSGP (red), standard GP (blue line) and measured BG (black) for subject #15. The plots are of MPO prediction and have been normalised to account for subject's HbA_{1c} value.

Here, NSGP was shown to predict better than standard GP, which has tracked the trend of the actual BG better with lower magnitude excursions from it. This is an important improvement as any therapeutic adjustment or control made on the basis of a prediction should not have an adverse impact on the humans. Overly high predictions by the standard GP indicating the need for insulin could result in unwanted hypoglycaemia.

Example plots of 60-minute prediction and MPO (infinite-step ahead prediction) BG prediction from three subjects in Test iv are shown in Figure 6.7 and Figure 6.8 respectively. The figures show predictions from the validation (unseen) data, selected from among the best (subject #11, dataset 3), average (subject #18, dataset 1) and worst (subject #23, dataset 4) predictions. Predicted BG is normalised to subject's average glycaemic control (HbA_{1c}) by removing the mean of the output as all changes in the output occur with respect to this mean (representing subject's equilibrium [9]), produced by the following equation [107]:

$$\text{Average Glucose } (mmol\ l^{-1}) = 1.59 * HbA_{1c}(\%) - 2{:}59 \qquad 6.9$$

Note that arranged plots of prediction from the same volunteers will be continuously presented throughout this thesis for consistency. Predictions with horizon longer than one hour are presumed to possess prediction FITs varying between plots in Figure 6.7 (60 mins-prediction) and Figure 6.8 (MPO), with shorter horizons having better FIT, and vice-versa. Subject #23's prediction has BG obtained being the most deviated from the measured values, at times by a significantly high magnitude. Others however showed a slightly better fit. Nevertheless, the NSGP has been shown figuratively to adequately and also efficiently model various datasets.

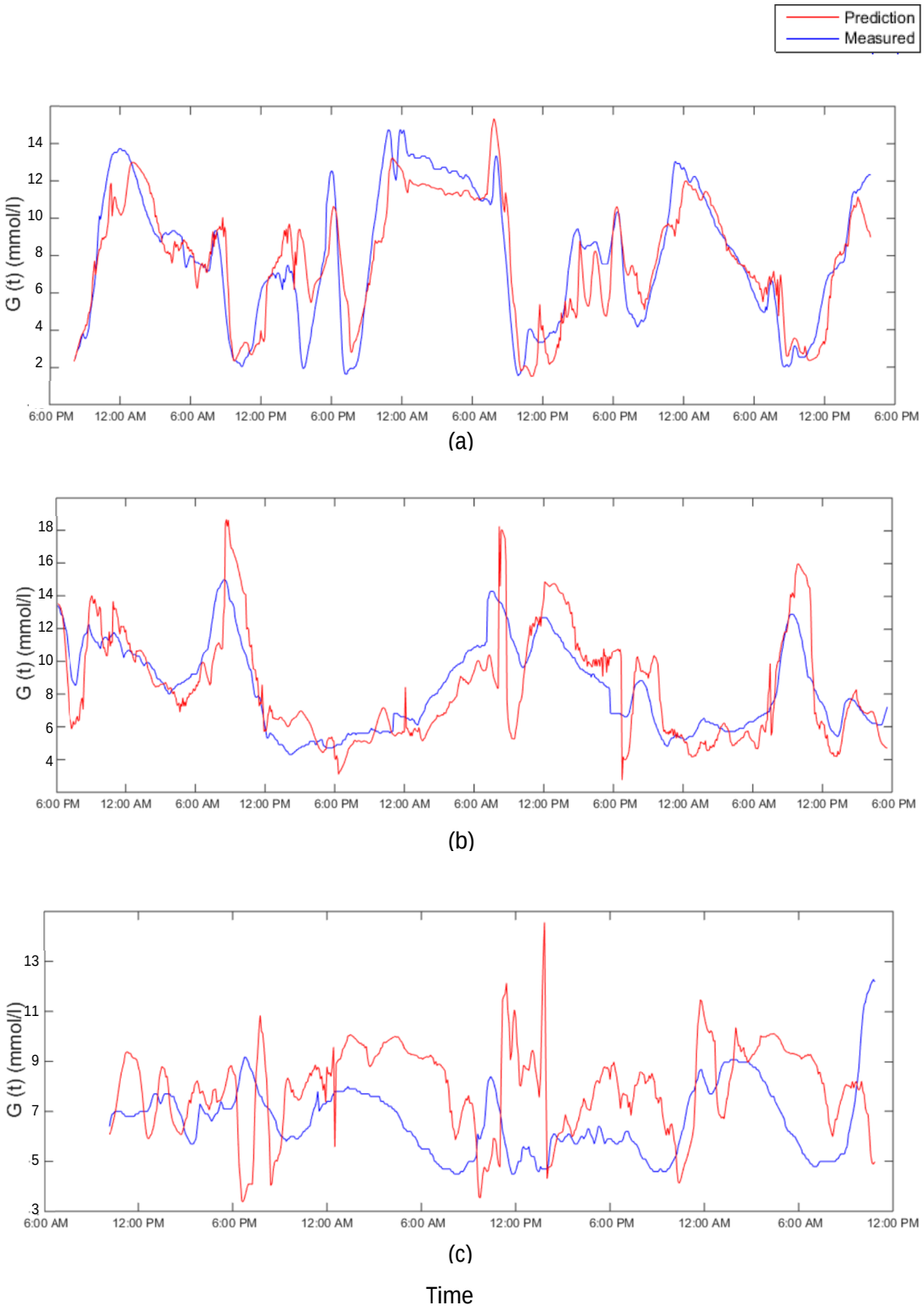

Figure 6.7: One-hour BGC prediction for subject #11(a), #18(b) and #23(c).

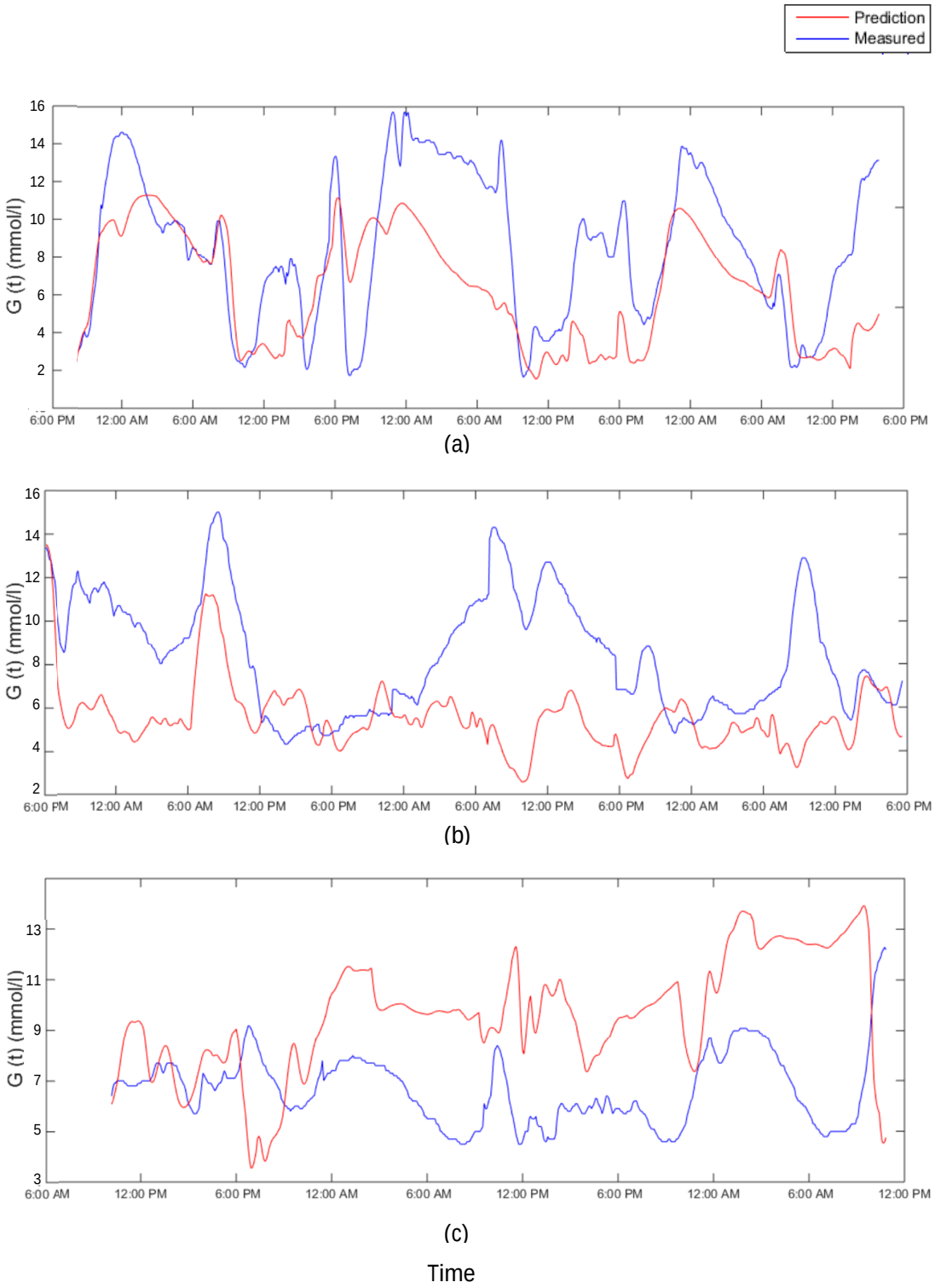

Figure 6.8: Model Predicted Output of BGC prediction for subject #11(a), #18(b) and #23(c).

6.5 Conclusion

For these cohort of volunteers, NSGP modelling was shown to improve BG prediction over prediction with standard GP models. Although the improvement is relatively small, the results presented in this chapter suggest that the use of physical activity inputs can in fact produce increased predictive capability.

Nevertheless, the results concur with the fact that only when a pattern is very similar reflecting a routine daily lifestyle could a high FIT of modelling be attained. A strict compliance of the timing and amount of carbohydrate ingestion, insulin intake and physical activity would reveal routine periodicities and is typically encouraged by clinicians as part of the patient's therapy to maintain safe glucose levels. This would also help in understanding the nature of these parameters to researchers as in this study.

This chapter also reveals the difficulty in modelling data of a free-living nature. This kind of data contains high stochasticity on top of the daily periodicities, in comparison to data collected in a regulated and controlled environment. Physical activity that occurs generally in short and irregular bursts throughout the day while producing a significant impact on BG responses have resulted in difficulties in modelling it, thereby could only be captured better by the identification of local models for the different operating points. This could be due to the shifted equilibrium state of the system from one operating system to another abruptly, triggering various metabolic pathways (Section 6.3). Moreover, because the only truly measurable variables are BG (using CGMS) and physical activity (using armband), while the food intake and insulin dosage were self-reported, the data collection are thus susceptible to various errors such as incomplete data for particular meals/insulin, miscalculation in converting food diaries into equivalent carbohydrates and incorrect recorded timings of food and insulin taken. All these factors, to a certain extent contribute yet more spontaneity to the nature of the free-living data collected.

With NSGP, the presence of the extra flexibility associated with moving the pseudo-inputs can to a certain point model the non-stationarity of the free-living data. As the covariance function hyperparameters are time-varying, the non-stationary GP employed is able to adapt to the nonlinearity in the BG signal better. Standard GPs despite being very flexible, were limited by the form of the covariance function available.

The result showed that both the physical activity inputs (Heat Flux and METs) were needed for better prediction in the NSGP models, producing slightly better result when they are modelled together, and not with each one. This could be attributed to one of the sensors, the armband, where various models of the SenseWear® Armband were reported to tend to overestimate or underestimate energy expenditure during various activities by 15-70 % [108], which is arguably a substantial percentage that could have the effects on modelling. One study showed METs values were overestimated during light to moderate activities [109]. In the case of heat flux sensor, its accuracy could have its readings impaired in the case of different environment temperatures, where exposed limbs could have excessive heat loss in cool condition [110]. A study also reported that a noticeable difference in heat flux measurements observed between left and right arms, suggesting that the vent placement and orientation of the device is an important consideration [108]. The specified errors from each sensor could then be compensated or validated by the other for a more accurate reading of the energy expenditure, as also corroborated by the result from our study.

6.6 Contribution to the Body of Knowledge

In this chapter, a non-parametric modelling was proposed which is an improvement over the standard Gaussian Processes to predict BG using carbohydrate, insulin and physical activity. It was shown that the addition of physical activity into the model actually improves the prediction as opposed to using standard GP, albeit only to a small extent. However, the result suggests that the use of physical activity inputs can further increase the model's predictive capability.

The use of free-living data complicates more of the modelling, especially since the insulin and carbohydrate data used are subject to human errors, where both were self-reported and prone to various errors. Examples of this would be as when translating food diaries into equivalent grams, unreported snacks, sizing of meals and vague description of the meals, and inconsistent timing of report and consumption. Other unaccounted factors known to affect BG includes menstrual cycle [111], psychological stress [112], [113], and the effect from the previous day, for example the initial state of glycogen depots in liver and muscle.

The use of NSGP has helped model the glucose-insulin dynamics with added physical activity parameter over the standard GP as presented. Although the standard GP employed by Valletta is already a flexible model, it is limited to the form of covariance function. Considering the complexity of the physical activity data, more complex covariance functions could be a viable option. The SPGP covariance function although constructed from an underlying covariance function K (which is possibly stationary), is heavily parameterised by the locations of the pseudo-inputs $\bar{\mathbf{X}}$ (non-stationary). Hence, it provides a flexible covariance function much like a non-stationary one, thereby able to model the physical activity parameter as reported better.

Both ARX, a parametric modelling and NSGP, a non-parametric modelling disregard the physiological nature of the blood glucose concentration. The complexity of modelling the physical activity parameters prompts the need for a physiologically-based model to understand primarily more on the role of physical activity in the insulin-glucose dynamics. This could provide more insights on the characteristics of this parameter and hopefully provide better prediction of BG in Type 1 diabetes patients. Chapter 7 will focus more on the development of a physiologically-based model.

Chapter 7: Dynamic Modelling of BGC

The previous chapters have highlighted some of the complications in devising empirical models of BGC. This chapter focuses on the role of physical activity through semi-empirical compartmental models, mainly those originating from years of research based on the minimal model of Bergman *et al.* [12], [114]. It also investigates the effects that physical activity has on the metabolical processes and whether current models have adequately present these causes and effects involving this complex parameter. As frequently highlighted, the main troubling issue in the previous studies is the use of synthetic data affecting the modelling and prediction of BGC, being vastly different to our free-living data. Even one study which tried to rationally reflect the physical activity responses using physiological-based model, the Roy and Parker's (R&P) [51] model, they had the parameter constants estimated from healthy individuals.

This chapter will test the inference of R&P's model and investigate better use of PAEE in such a model using real data as opposed to the synthetic ones normally employed in such studies.

7.1 Introduction

As previously discussed, different to carbohydrate and insulin parameters of which their roles are far better understood - raising and lowering of BG, physical activity induces both of them, complicating the efforts to understand its actual effects, despite it being well recognised. This chapter initially investigates Bergman-type models with just the insulin and glucose inputs against our volunteer datasets. Then, the model will be extended to include parameters from physical activity energy expenditure, this time using physiological-based modelling to try and improve the modelling fidelity as in previous chapters.

7.2 Bergman's Minimal Model

Bergman, a pioneer in the modelling of glucose-insulin dynamics in Type 1 diabetes, proposed a three-compartmental model of BG regulation. Compartment I, X and G represent plasma insulin (µU/ml), remote insulin (µU/ml) and plasma glucose (mg/dl) concentrations as can be seen in Figure 7.1.

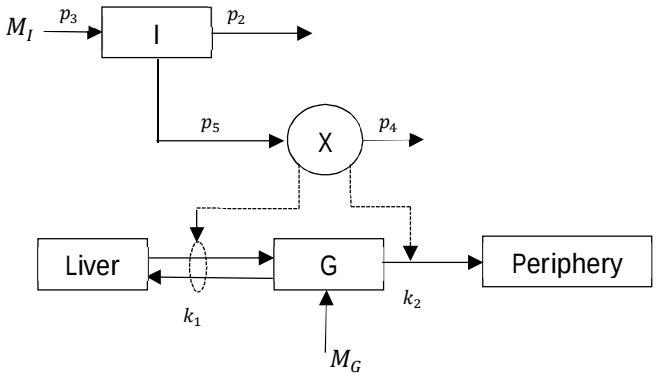

Figure 7.1: Reproduced from Roy and Parker's [133]. Bergman minimal model of insulin and glucose dynamics.

The model assumes that the required insulin is totally infused exogenously (M_I), showing the completely insulin-dependent nature of a T1 diabetes patient. Once the infused insulin reaches the remote compartment (X) from the circulatory system, it actively stimulates the uptake of plasma glucose into the hepatic (liver) and extrahepatic tissues.

Bergman's minimal model describes the relationship between compartments as:

$$\dot{I}(t) = -p_2 I(t) + p_3 M_I(t); \quad I(0) = I_b, \tag{7.1}$$

where M is insulin absorption after injection,

$$\dot{X}(t) = -p_4 X(t) + p_5 (I(t) - I_b); \quad x(0) = 0, \tag{7.2}$$

where I_b is basal insulin, and

$$\dot{G}(t) = -p_1 G(t) - X(t) G(t) + p_1 G_b + \frac{M_G}{Vol_G}; \; G(0) = 0, \tag{7.3}$$

where M_G is the glucose absorption from food and Vol_G is the volume distribution space. The values corresponding to these parameters can be obtained from Table 7.1 [12]. Note that while in Section 5.2 the parameters of the insulin and carbohydrate models were optimised to best fit each individual, this chapter will use the original reference parameters to compute the insulin and glucose quantitative inputs. Parameter p_1 represents the rate at which glucose is removed from the plasma space independent of the influence of insulin. The rate constant p_2 represents clearance of plasma insulin while p_3 indicates rate constant of insulin absorption after injection. p_4 and p_5 govern the rate of appearance of insulin in, and disappearance of insulin from the remote insulin compartment respectively. *Gb* and *Ib* refer to basal glucose and insulin levels while *VG* indicates the glucose distribution space.

Parameter	Value	Units	Initial Values
p_1	0.035	min^{-1}	G(0)=Gb I(0)=Ib X(0)=0
p_2	0.142	min^{-1}	
p_3	0.098	ml^{-1}	
p_4	0.05	min^{-1}	
p_5	0.000028	$ml/\mu U/min^2$	
G_b	4.4	$mmol\,l^{-1}$	
V_G	117	dl	
I_b	[not defined]	μU/ml	

Table 7.1: Parameters of the Bergman Minimal Model

7.3 Modelling Blood Glucose Dynamics without the Exercise Model

The first simulation was done with all the inputs except physical activity from subject #1. The individual's data was selected for this test as it portrays a typical profile for METS, insulin and carbohydrate data as seen in Figure 7.2 below. The BG levels only exceeded the 4.0 – 10.0 $mmol/l$ normoglycaemic band at the end of day 3 data - indicating a good BG control. The most crucial parameter for the selection of this subject is the physical activity data, or specifically METs as depicted in Figure 7.2(a). Despite the fact that this initial test does not consider its effect, it does

however account to some extent the influence of it towards the overall BGC concentration. As mentioned previously, physical activity data have the least understood behaviour. However, because the subject observed, subject #1, bears low spontaneity and more stationarity in his/her METs data and the components, is an advantage whereby the data itself already contain less uncertainty. The insulin and carbohydrate profiles are calculated from Equation 2.1 to 2.5 and Equation 2.6 as seen before using the default physiological parameters.

The minimal model was implemented in Simulink using ODEs evaluated with the Dormand-Prince method using a mixed fourth/fifth order solver which aims for precision and speed (rk45). Simulink was used as a consistent environment to develop this and later models in Chapter 8. The Simulink model of Bergman's equations with the respective inputs and outputs are as shown in Figure 7.3.

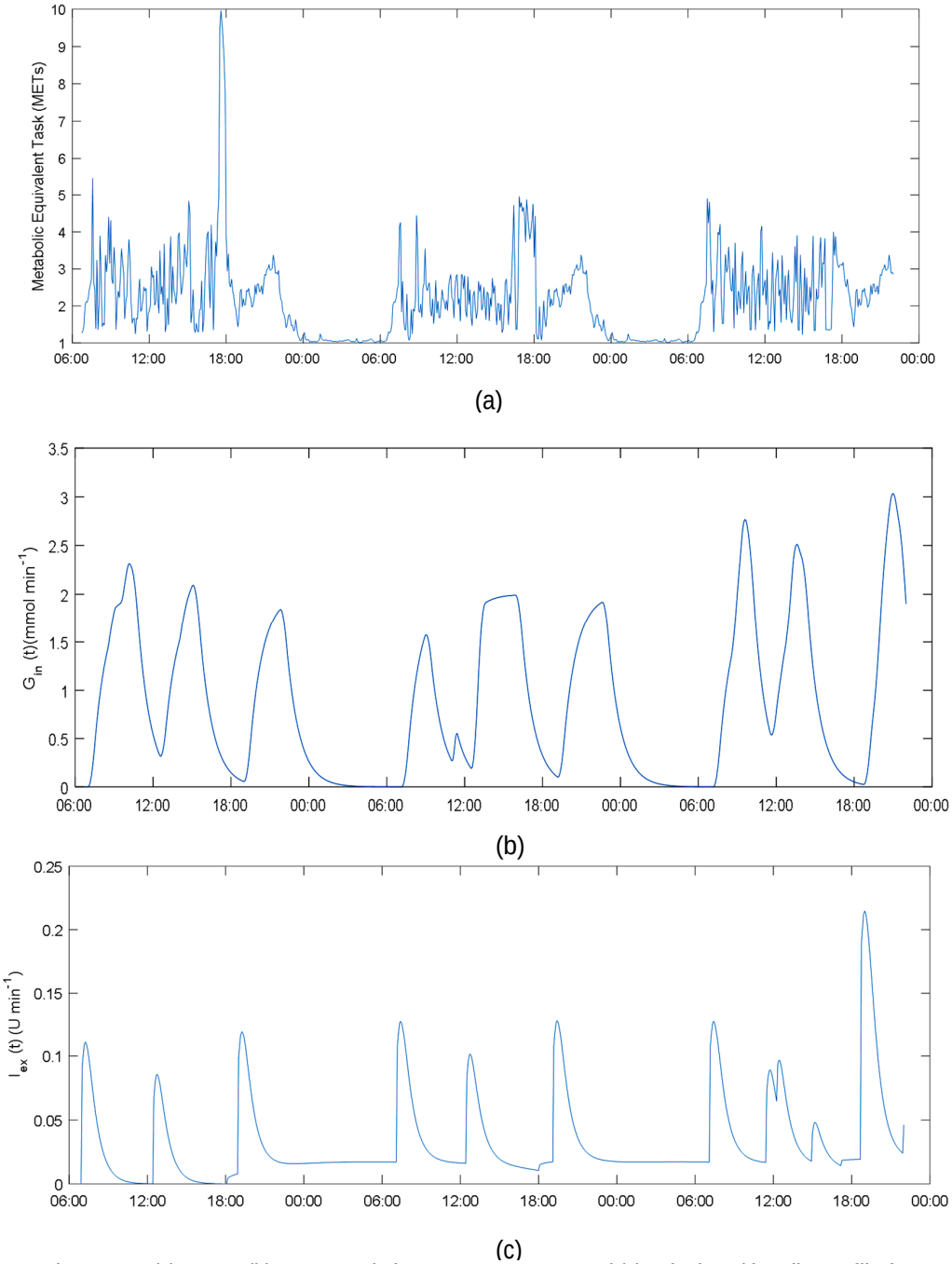

Figure 7.2: (a) METs, (b) computed glucose appearance and (c) calculated insulin profile from subject #1.

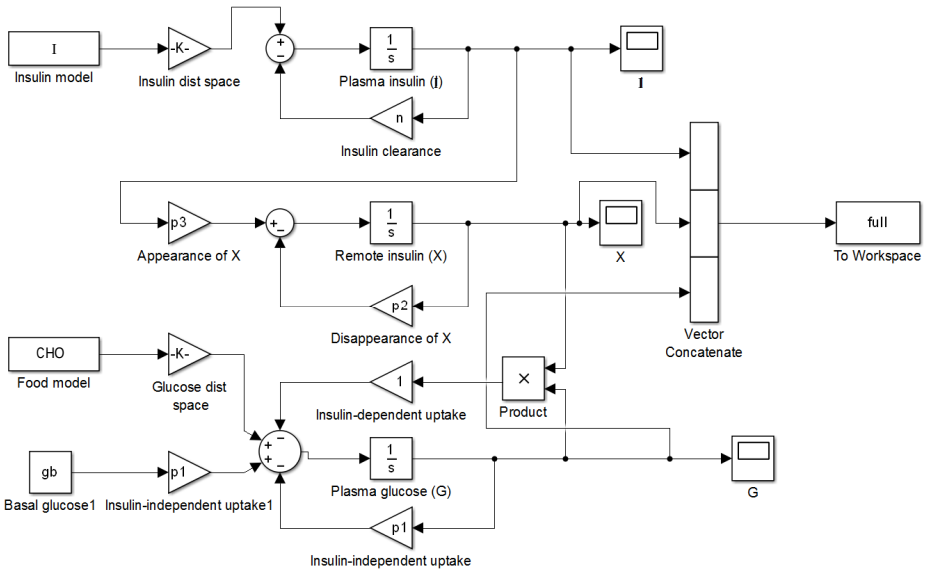

Figure 7.3: Simulink model of the Bergman's minimal model.

7.3.1 Results

Using the insulin and carbohydrates inputs shown in Figure 7.2(b) and Figure 7.2(c) implemented using Simulink model of Figure 7.3 (labelled as I and CHO on figure), the corresponding infinite-step ahead prediction is shown in Figure 7.4. The basal glucose input labelled as *gb* in Figure 7.3 with its initial BG value at $t = 0$ is taken from the first CGMS data point. It can be seen in Figure 7.4 that the main peaks of actual BGC are actually reasonably predicted, albeit much lower in terms of magnitude, by the Bergman model. FIT value for the two plots is 9.6 %, a low value despite having only I and CHO inputs were considered. It was also observed that the BGC is largely influenced by the glucose intake CHO parameter, especially where the major peaks are present and the measured BGC was successfully tracked. The insulin parameter in Figure 7.2(b) also follows closely the CHO pattern, showing persistency and discipline in the volunteer's daily routine, i.e. injecting insulin for each substantial meal intake. This also portrays the effect from the right balance of meal, insulin and physical activity - more predictable BG levels. The right amount of insulin at the right time after meal consumption ensures that BG does not rise uncontrollably as observed in the volunteers' data.

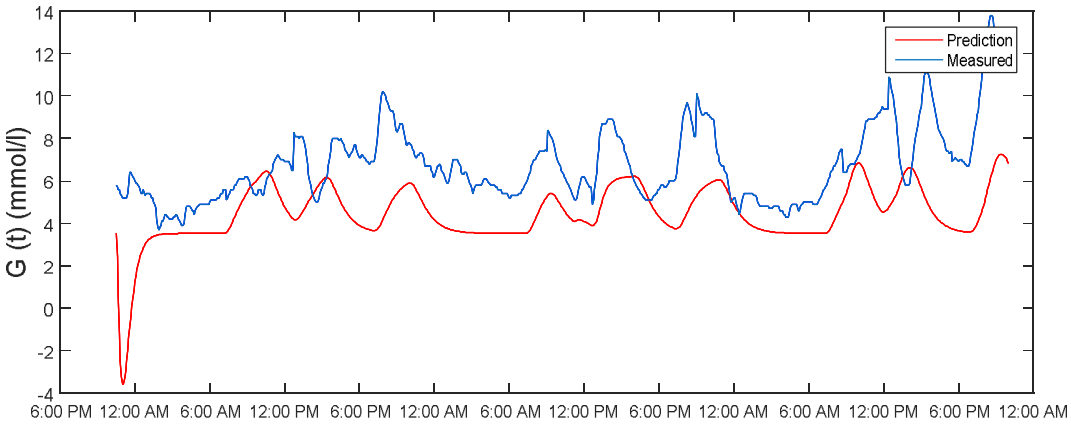

Figure 7.4: Prediction of a BG response using Bergman's Simulink model.

In the case of the other volunteers with more spontaneity components in their data, they appear to show incomparable results. Figure 7.5 shows BGC predictions from subject #11 (dataset 3), #18 (dataset 4) and #23 (dataset 3) which each garnered FITs of 3.2 %, -3.8 % and -8.5 % respectively. Apart from the poor predictions which at times failed to track even the major peaks while ignoring much of the variations, the magnitudes for each prediction were also much lower than those of subject #1's. This applies to the rest of predictions not shown. Note that the high dip in initial BGC prediction exists in all the predictions, which is due to an imperfection within Bergman's model whereas it does not model the phase peak of insulin release, thus the initial values are ignored until after the first few instances [115].

Figure 7.6 shows the corresponding METs (a), computed insulin (b) and calculated glucose appearance (c) in the bloodstream for subject #23, revealing the worst FIT among the three predictions. The figure depicts the exact inputs as the ones in Figure 7.2. There exist significant differences in the way subject #23 managed his/her glucose and insulin intake, as well as physical activity done to the way subject #1 did. There were irregular consumptions of meals and insulin, probably low adherence to the advice of clinicians, and also many spontaneity and bursts of physical activity in the METs data, albeit this parameter was not added to the model. There were also missed or unreported events of insulin injections following ingested meals as outlined in Figure 7.2(c), leading to the poor prediction of BG levels. It is unsurprising that the difference level of control and discipline adhered by subject #1 and subject #23 have resulted in the different performance of FITs obtained.

In summary, Bergman's minimal model can capture some of the dynamics in well-controlled individuals but less able to do so in more poorly controlled individuals (such as subject #23) with more spontaneous PAEE variation. The model was actually introduced in 1979 [12] before it was possible to continuously monitor BG levels such as using the CGMS. Nonetheless, Bergman's minimal model provides a scientific window into how the hormone insulin functions in human beings. Complex interactions were described with ease, in particular the interactions between the insulin sensitivity (muscle and liver), pancreatic b-cell function and the previously under-appreciated insulin independent factors. The minimal model also simultaneously allows clinicians to assess metabolic function and predict which patients are at increased risk. In specific, its major contribution was to provide means of estimating insulin sensitivity thereby avoiding the glucose clamp [26]. The next section will investigate whether the efficacy of the model can be improved by adding parameters of physical activity.

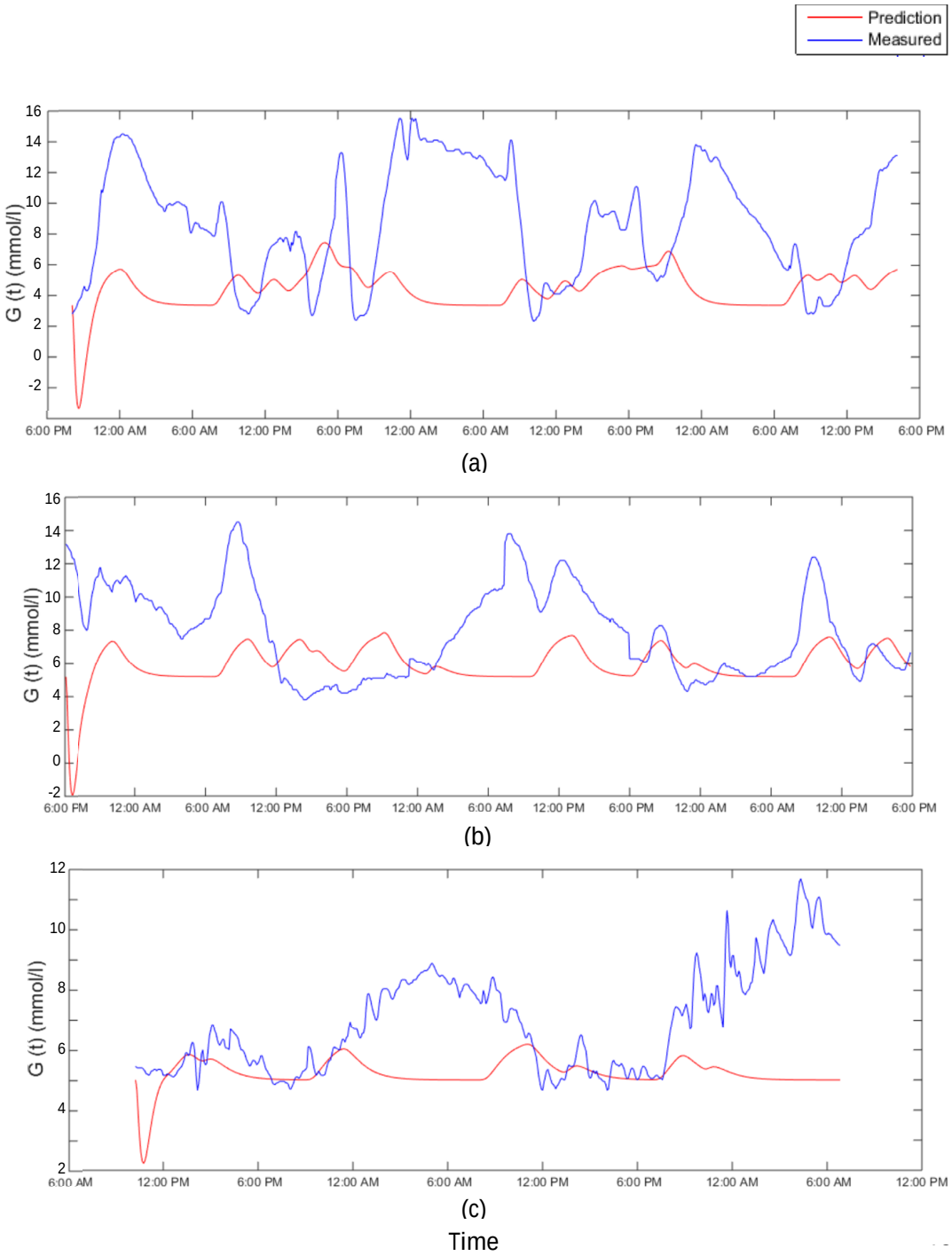

Figure 7.5: Predicted and actual BGC for subject #11(a), #18(b) and #23(c).

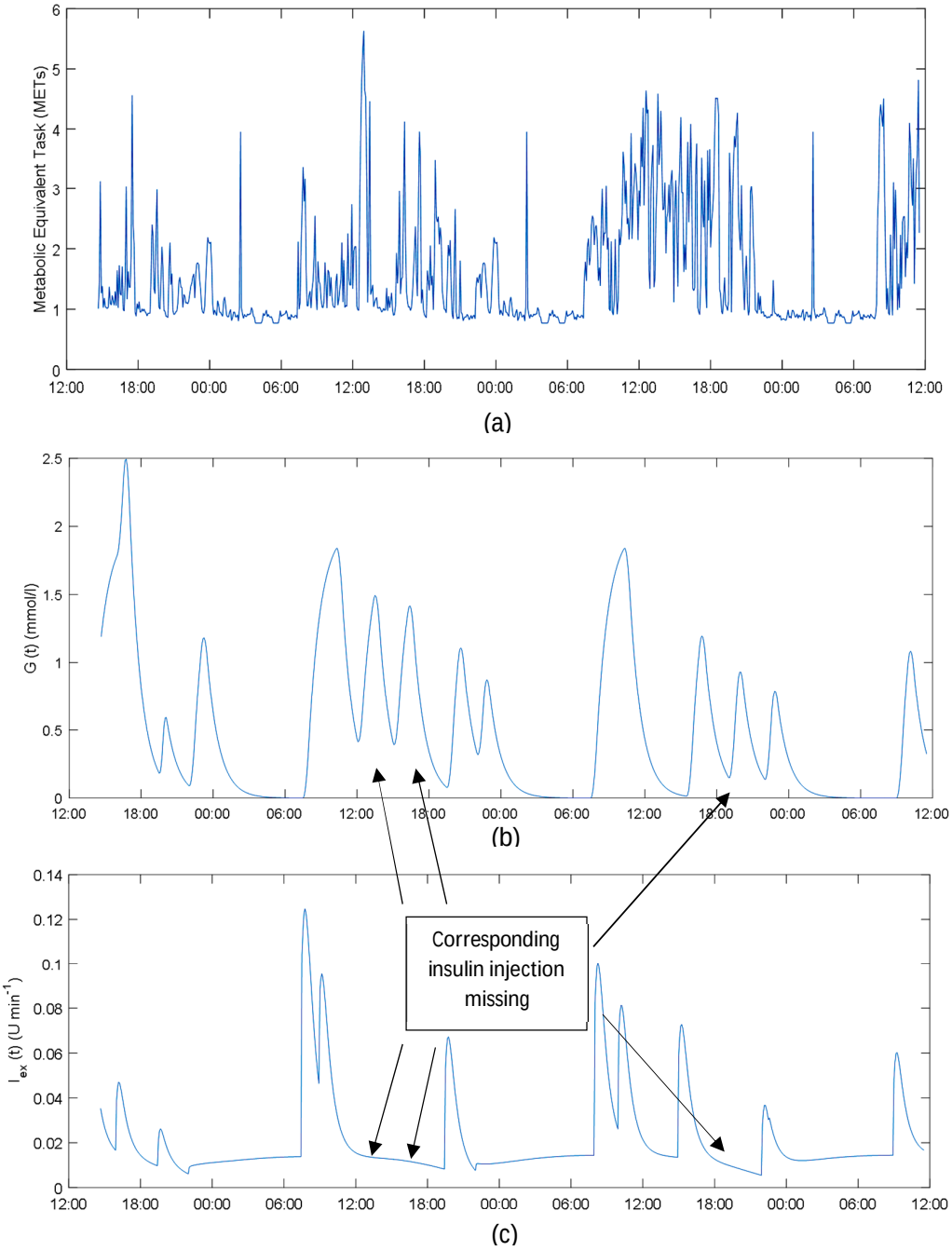

Figure 7.6: (a) METs, (b) computed glucose appearance and (c) calculated insulin profile from subject #23.

7.4 Modelling Blood Glucose Dynamics with Exercise Model

Raw PAEE data utilised for prediction did not yield improvements in the performance of glucoregulatory system models as hoped for, even with non-stationary GP. On the other hand, researchers have also tried to account for quantitative exercise models [27], [51], [116]–[119] rather than raw PAEE data [55], [120]–[122]. They comprise a number of differential equations (DEs); of interest here is the R&P's model [51]. It was extended from the minimal model to account for exercise and contains nine DEs, including six for the effects of exercise. Parameter estimates in the model were derived from data from healthy subjects performing simple exercise protocols over short period of time (<4 hours). It is however unclear how the model would now perform with free-living data collected in the DUK study. This chapter will test the inference of it and investigate real PAEE in such a model.

An important aim of this work is a reliable model built with the free-living data representing real-life conditions of the volunteers rather than the case of simulated data that do not accurately reflect actual daily experience. Such a model especially for the use of an artificial pancreas should possess good performance under realistic conditions. Thus, the proposed approach tries to combine free-living data from CGMS, food intake, insulin, and quantitative physical activity.

7.4.1 Physical Activity Minimal Model

R&P adopted the original Bergman minimal model for use in Type 1 diabetes by including terms for exogenous insulin, meals and physical activity. Six DEs were included to account for the effect of physical activity: One for PVO_2^{max} (specified as E later), one for integrated activity intensity (A), and the others each constituting the activity-induced effects on hepatic glucose production (H; mg/kg/min), insulin clearance (Z; μU/ml/min), glucose uptake (U; mg/kg/min), and decline in rate of glycogenolysis (K; mg/kg/min).

Bergman's minimal model is now extended with the addition of dietary absorption from food ($\frac{M_G}{Vol_G}$):

$$\dot{G}(t) = -p_1[G(t) - G_b] - X(t)G(t) + \frac{W}{Vol_G}[H(t) - K(t) - U(t)] + \frac{M_G}{Vol_G}; G(0) = 0, \quad (7.4)$$

where W is weight (kg) and Vol_G is the glucose distribution space (dl). The blood insulin DE is modified by the influence of Z and insulin absorption after injection (M_I; μU/min):

$$\dot{I}(t) = -nI(t) + p_4 M_I(t) - Z(t), \quad (7.5)$$

where I_b is the basal insulin, insulin action is given by

$$\dot{X}(t) = -p_2 X(t) + p_3(I(t) - I_b). \quad (7.6)$$

Similarly, PVO_2^{max}, a measure of physical activity intensity is modelled by a DE used to describe the delay in reaching the steady state value at the start of activity (intuitively, the delay in increased oxygen uptake and heart rate):

$$\dot{E}(t) = -p_6 E(t) + p_7 M_E(t), \quad 7.7$$

where M_E is the actual intensity of activity above basal level (taken as 8% $VO_2^{max} \approx 1\ MET$). M_E therefore spans 0-92% of input to model (used later as PVO_2^{max}). The coefficients p_6 and p_7 is set both to 0.8 (min^{-1}) in order to reach an approximate settling time of five minutes to be consistent

with physiological studies. Apart from that, DEs representing the processes on hepatic glucose production (*H)*, glucose uptake (*U)* and insulin clearance (*Z)* are given as below:

$$\dot{H}(t) = p_8 E(t) + p_9 H(t), \tag{7.8}$$

$$\dot{U}(t) = p_{10} E(t) + p_{11} U(t),$$

$$\dot{Z}(t) = p_{12} E(t) + Z(t),$$

From the DEs, it can be seen that the rate of each process above increases along with the increasing of activity intensity. The decline of glycogenolysis rate (glycogen in liver breaks down heavily due to conversion to glucose for energy) occurring when hepatic glycogen stores are depleted during prolonged physical activity is modelled by:

$$\dot{K}(t) = \begin{cases} 0, & A(t) < A_{\text{th}} \\ p_{14}, & A(t) \geq A_{\text{th}} \\ -a_8 K(t), & M_E(t) = 0, \end{cases} \tag{7.9}$$

where *A* is the integrated activity intensity given by

$$\dot{A}(t) = \begin{cases} M_E(t), & for\ M_E(t) > 0 \\ -p_{16} A(t), & M_E(t) = 0 \end{cases} \tag{7.10}$$

and A_{th}, a function of exercise intensity and duration is given by

$$A_{\text{th}} = M_E(t)[-1.152 M_E(t) + 87.471]. \tag{7.11}$$

At the start of activity, rate of glucose uptake H increases until energy expenditure A exceeds the A_{th} critical threshold. Reaching this threshold means that exercise is now prolonged and the decline of glycogenolysis rate K starts rising, at the rate given by p_{14}. This is due to the depletion of liver glycogen stores, reducing the net hepatic release. Post activity sees the decline in glycogenolysis returns towards zero as glycogen stores starts to be replenished again, by the gluconeogenesis process. Likewise, integrated activity intensity A also rapidly returns to its initial condition of zero. The corresponding Simulink diagram is shown in Figure 7.7. All the coefficients and parameters presented earlier can be seen in the Simulink diagram with insulin, carbohydrates and physical activity inputs (labelled as I, CHO and PVOREL in figure) on the left end. Note the switches used for value comparison, integrators for differential equations, and the sum and gain block for math operations forming a complete diagram of the equations presented. The parameter estimates and initial values presented in R&P are given in

Table 7.2.

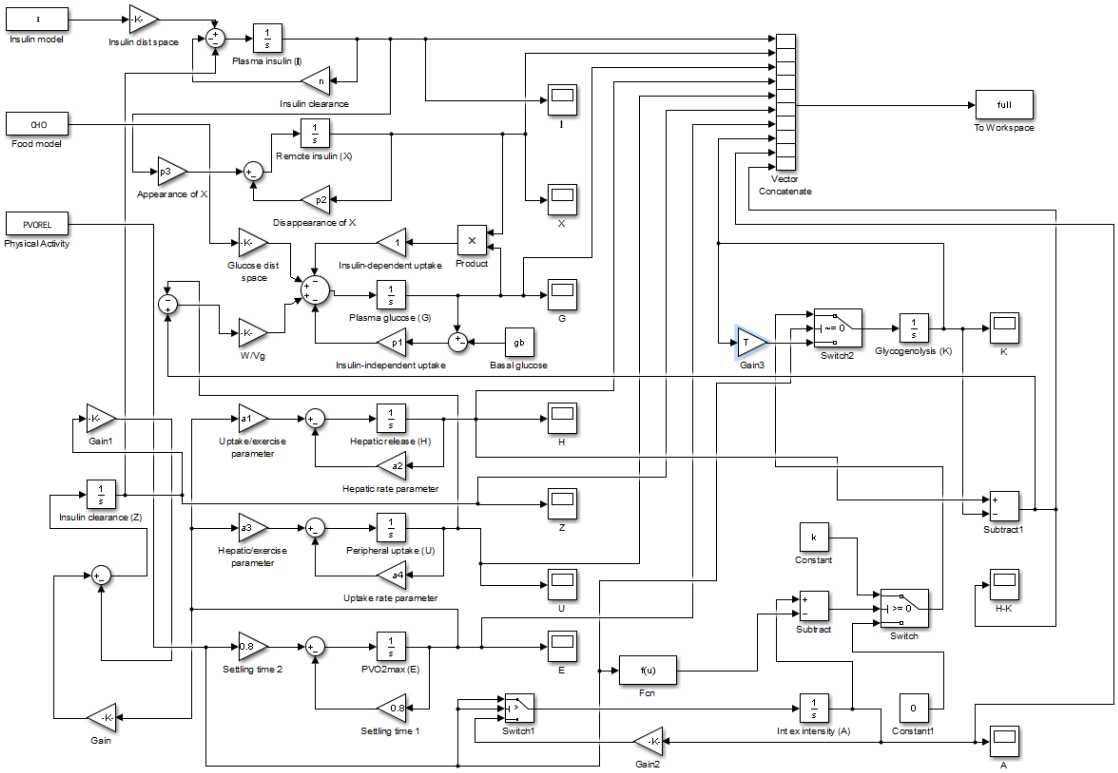

Figure 7.7: Simulink diagram for R&P's physiological model.

Parameter	Value	Units	Initial Values
p_1	0.035	min^{-1}	$G(0)=G_b$
n	0.142	min^{-1}	$I(0)=I_b$
p_4	0.098	min^{-1}	X(0)=0
p_2	0.05	min^{-1}	E(0)=0
p_3	0.000028	$ml/\mu U/min^2$	H(0)=0
p_6	0.8	min^{-1}	U(0)=0
p_7	0.8	min^{-1}	Z(0)=0
a_1	0.00158	$mg/kg/min^2$	K(0)=0
a_2	0.056	min^{-1}	A(0)=0
a_3	0.00195	$mg/kg/min^2$	
a_4	0.0485	min^{-1}	
a_5	0.00125	$\mu U/ml/min$	
a_6	0.075	min^{-1}	
k	0.0108	$mg/kg/min^2$	
p_{15}	0.1667	min	
p_{16}	1000	PVO_2^{max}	
G_b	80	mg/dl	
V_G	117	dl	
I_b	[not defined]	$\mu U/ml$	

Table 7.2: Parameter estimates for R&P's model.

7.4.2 Testing PA Model and Free Living Data

The proposed PA model was evaluated using free living data from the DUK study. Note that the parameter M_E in the form of PVO_2^{max} was estimated from METs data, also collected in the DUK study. There are various ways that researchers have proposed to calculate PVO_2^{max}, with many multiplying METs value to 3.5 ml/min/kg (resting oxygen uptake) [56], [123], [124]. However this has been criticised as being too general and actual measurement actually shows that the value actually varies according to age, body size, fitness quintiles, sex and others as pointed in [125]–[132]. Here, M_E was approximated from METs in terms of its percentage relative to maximum METS, as shown in (7.12) below. Therefore, the measured physical activity being converted is called relative $rPVO_2^{max}$:

$$rPVO_2^{max} = \max\left(0, \frac{\text{METs}}{\text{METs}_{\max}} \times 100 - 8\right), \tag{7.12}$$

where METs is the maximum METs achievable by the individual, and basal activity (~8% VO_2^{max}, equivalently (~1 METs)) is adjusted to 0. The test was initially done to the same individual (subject #1) for assessment of model performance, and further adjustment could then be made accordingly to other subjects.

7.4.3 Results

The DEs were evaluated as earlier, numerically solved using the Dormand-Prince method of fourth/fifth-order solver and implemented in Simulink. Using the probe function available in Simulink, the simulation from time to time can be readily observed. Figure 7.8 shows the corresponding Simulink simulations for parameters *I*, *X*, *H-K*, *K*, *A* and *G* for subject #1. The term and plot of $H(t) - K(t)$ can be thought of representing the overall contribution of liver to BGC. The others represent the insulin plasma (*I*), glucose plasma (*X*), glycogenolysis process (*K*), integrated activity intensity (*A*) and finally glucose concentration (*G*), respectively.

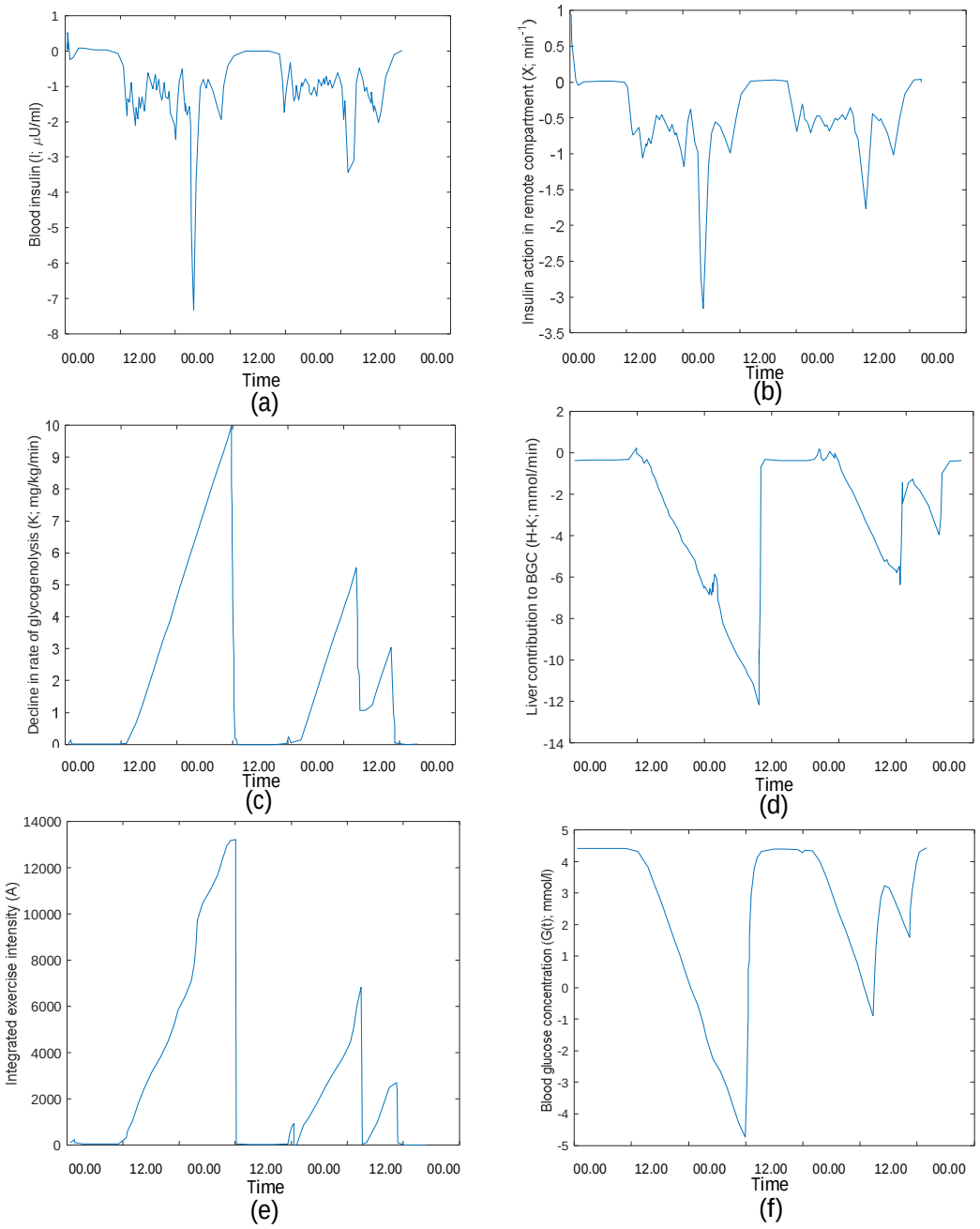

Figure 7.8: Corresponding simulations for parameter *I*(a), *X*(b),*K*(c), *H-K*(d), *A*(e) and *G*(f) for subject #1.

With regards to the overall result, the model was unable to accurately reflect BGC behaviour as being expected for a prediction for Type 1 diabetes patients. There were large differences of prediction performance between models without (Bergman minimal model) and with the physical activity parameters, as evident in Figure 7.4 and Figure 7.9(a). The latter can be seen to have poorly predicted BGC as compared to the former. Discrepancies to actual bodily response were also found where BGC and insulin action were predicted to have negative concentration as in the same Figure 7.9(a) and Figure 7.9(c), which realistically are not possible. The major cause of this is the activity-simulated insulin clearance rate, *Z*. Insulin clearance was seen to overwhelmingly increase above absorbed insulin after the injection, leading to negative insulin concentration afterwards. Apart from this, the model predicts frequent negative contributions from the liver as depicted in Figure

7.9(c), overwhelming the process *K*, when the intended effect of the glycogenolysis sub-model is only to dampen the effect of process *H*. The occurrence of excessive hepatic glucose uptake was opposite to the assumptions made, given that the individual physical activity data did not actually exceed even 50% of VO_2^{max} while also not persistently maintain any activity above basal level longer than the threshold A_{th}.

When free-living activity data were compared to the data used to build the PA model, it was clear that they were markedly different, mainly due to the use of healthy volunteer's data. There was also an assumption of non-fluctuating activity data throughout the data collection period, resulting in an over-simplification of the nature of physical activity. Free-living data, as evident in this study, appear to be more variable than synthetic data used to design such models and also rarely return to basal level (1 MET) for an extended period of time (as was previously seen in Figure 3.5(c)). R&P-type generalisations may work better with data that are non-fluctuating or from healthy individuals, nonetheless they can lead to an excessive decline in rate of glycogenolysis (*K*) when tested with actual data. In summary, this section highlights that a model designed for synthetic data is not able to effectively predict blood glucose when real-world data are used for PAEE, I and CHO. The synthetic data are over-smoothed and follow a non-stochastic distribution due to little or no human spontaneity, hence producing a predictable model. This has resulted in the model's failure when tested with real data such as those collected from the DUK study, especially when the PAEE parameter is added.

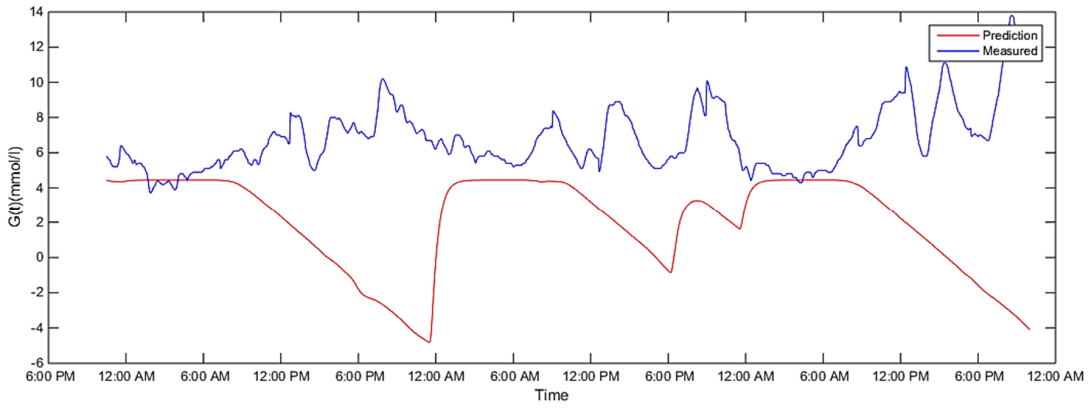

(a)

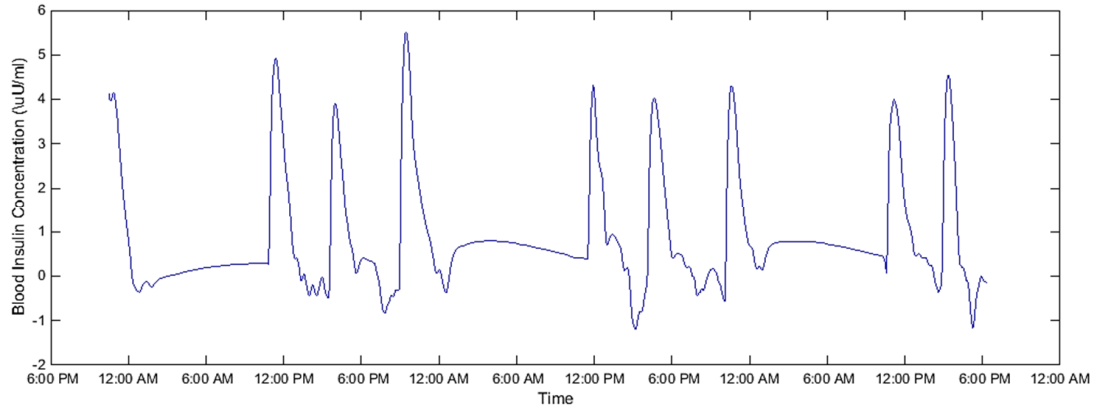

(b)

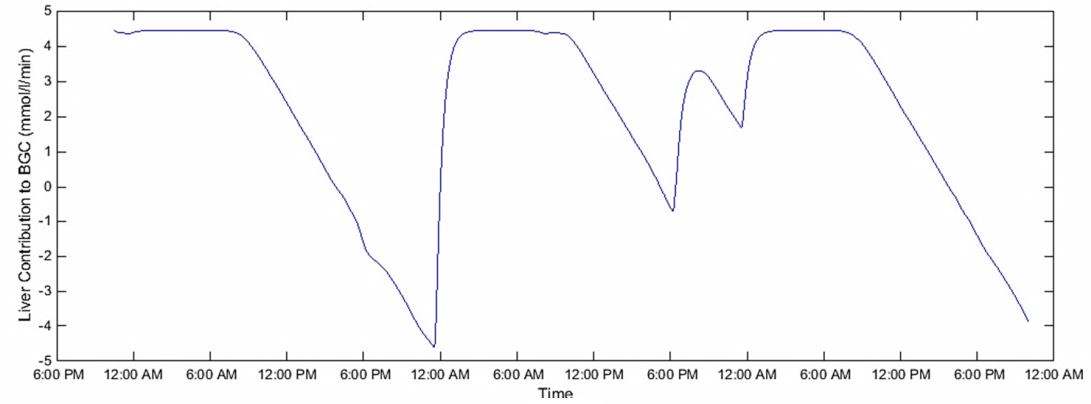

(c)

Figure 7.9: Results for subject #2's modelling using R&P's model.

The parameter estimates used by R&P were also inaccurate, probably as a result of being derived from healthy subjects. The subjects also undertook controlled short-term exercise protocols for parameter estimation that are unlikely to reflect real daily activities. The argument cannot be overstated and has been demonstrated from the results using free-living data derived from people with Type 1 diabetes. Figure 7.10 illustrates that the PA model is actually very sensitive to small changes in the parameter estimates used. The two BGC profiles were predicted to be very different despite their very close basal glucose values (7 % difference). It is apparent that the structure of the model needs revising considering the nature of free-living data we wish it to predict.

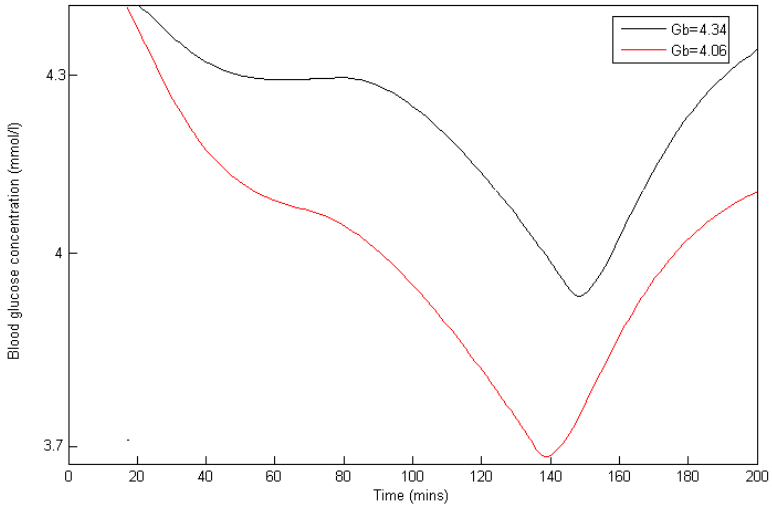

Figure 7.10: BGC profiles for two different basal glucose values, Gb=4.34 $mmol$/l and Gb=4.06 $mmol$/l.

7.5 Contribution to the Body of Knowledge

In this chapter, a modern, physiological-based method for a glucose-insulin compartmental model was presented. A new compartmental model derived from R&P, with the rational of understanding physical activity parameters in Type 1 diabetes patients has been developed. R&P used synthetic data and parameters estimated from healthy individuals and resulting in unrealistic and unrepresentative BGC in people with Type 1 diabetes.

The model's performance was tested using real human data rather than on synthetic and showed that it did not perform equivalently with real data. Therefore, it is imperative that real data and their characteristics are to be used, reflecting the nature of Type 1 diabetes, rather than the synthetic data used previously. METs data were also shown to be more practicable to measure than PVO_2^{max} which is a percentage based on the maximum oxygen consumption - it is not feasible to do this analysis in the free-living environment.

In summary, the R&P-based model has some predictive capability albeit with very significant flaws with the physical activity model. However, the model remains a rational model in comparison to a purely mathematical model with physiological basis for the constituent parts and is potentially suitable for development with improved characteristics.

Chapter 8: Non-Stationary Physiological Based Modelling (NSPM)

Chapter 7 describes an attempt to model the insulin-glucose dynamics based on a method developed by R&P [133] that fails to reflect accurately a real person's BGC profile. Model-estimated BGC was found to drop below zero and blood insulin concentration returned negative-value when using real data rather than the synthetic data the model was designed for. The primary reason for the poor performance in the previous chapter is the impact of the physical activity data on the function of internal organs (i.e. the liver). A general assumption of the exercise model is that it returns to basal level (1 MET) after exercise, but real data from DUK study show that none have returned to basal level for an extended period of the day. As a result, the modelled responses from the glycogenolysis and insulin clearance processes become disproportionately large.

The impact of the PAEE sub-model, and the subsequent activation of other processes, motivate further study of the PAEE sub-model and what parameters of PAEE are best suited to be incorporated in a BG dynamics model. In this chapter, the physical activity sub-model is reviewed and the non-stationary GP model of Chapter 6 is revisited to evaluate whether its predictive capabilities can be enhanced. In Chapter 9, the R&P-based model will also be revisited with the same intention. This chapter will start by reviewing and modifying the processes in the R&P model, the physiological basis of the modelling that are significantly affected by exercise. The exercise model is then further developed and tested on the non-stationary GP model of Chapter 6.

8.1 Process Evaluation

8.1.1 Insulin Clearance

The revision of the model is to steer the physiologically-based model to a much practical response expected in people with Type 1 diabetes. Hence, we should look at the process Z (the effect of physical activity on blood insulin concentration) originally introduced by R&P, derived from two earlier studies [134], [135] of which the parameters of the Equation 7.8 were fitted to and validated against. These two studies were both tested on healthy subjects, where the observed blood insulin concentration decrease may well be due to the decreased insulin secretion, instead of insulin clearance Z. This was confirmed by the study of Zajadacz [136] on diabetes patients, where no change in insulin clearance was observed during activity. Petersen [137] also reported on no decrease in blood insulin at all in diabetic volunteers during medium intensity exercise. This would mean that Z would not exist within Type 1 diabetes patients and this process is thus removed from the model.

8.1.2 Basal Insulin

In the case of basal insulin term I_b, the notion itself does not seem reasonable and present in an individual with diabetes. Basal insulin suggests that whenever blood insulin concentration drops below basal level, the flow of it into the remote compartment would reduce to contain itself within the safe bounds. In the case of diabetics, this is self-contradictory. Physiologically, it is due to the absence of the regulation of exogenous insulin that hinders the proper flow of blood insulin. If bodily response could be regulated by matching blood insulin to basal insulin, then the individual would not be Type 1 diabetic. Type 1 diabetes implies a complete inability to regulate insulin, requiring the need for exogenous insulin delivery. This means that this term does not exist in this

form in Type 1 diabetics and can be removed from the model too. It was because of this basal insulin term that in hypoinsulinaemic conditions, the model insulin action became negative.

8.1.3 Decline of Glycogenolysis Rate

Ewings, in his study [51], omitted the process K. He noted the disproportionate and unrealistic influence of it in R&P's model and determined that only short to medium physical activity at minimal intensity, such that it has negligible effect on the hepatic glucose release, was appropriate for BG prediction. However, the process K will be retained here as it presents a logical explanation of effects due to sustained physical activity exceeding a certain threshold.

8.1.4 Insulin Model

Georga *et al.* [120] proposed a good schematic representation involving free-living data using Support Vector Machines for Regression (SVM). However, it did not make a distinction between Type 1 and Type 2 diabetes (this was rectified later but with a different model - see [138], [139]). Georga *et al.* also based their study on R&P's parameters, but further adding two components, G_{exer} and I_e, to account for the variations in circulating glucose and insulin concentrations during and shortly after exercise. Insulin plasma concentration I_p was added to Tarin's original insulin model as in equation 8.1 below:

$$I_p = \frac{I_{ex}(t)}{V_d} - k_1 I_p(t) + k_2 I_h(t) + k_3 I_i(t), \tag{8.1}$$

However, because Type 1 diabetics is completely insulin deficient and not just impaired, I_p does not apply to our test group and therefore removed from the governing equation. However, the exogenous flow I_{ex} as originally proposed in Tarin's insulin model (Equation 2.6) remains viable and be used instead.

Another reason for the maintaining of the I_{ex} parameter proposed by Tarin [34] is that since Type 1 diabetes patients are completely insulin deficient, circulating insulin concentrations will be entirely dependent on the injected dose and the diffusion from the subcutaneous depot to the capillaries. While many authors attempted to model the time-evolution of insulin after administration, with Nucci and Cobelli critically reviewing the models [33], most only catered the two compartmental models: the subcutaneous depot and blood plasma. The shortcoming of them is, none was able to describe a wide spectrum of insulin preparations. This was overcome by the work of Tarin *et al.* describing various insulin preparations from rapid-acting to long-acting, covering most insulin preparation. Hence, this is seen as a viable selection (as presented in Section 2.4 previously) and will thus be used in the modified PA model.

8.1.5 Basal METs

The reason that the parameter for integrated exercise, A, increases throughout the day (as presented in Section 7.4.1) is due to the overly-estimated decline in the rate of glycogenolysis. This means that to the model, physical activity rarely returns to basal level - 1 MET, ~8% VO_2^{max}. Therefore, an adjustment is made to better reflect the bodily response to physical activity's basal level. Basal level will now be made relative to maximum METs ($METs_{max}$) to ensure A increases and returns to basal level as close to our actual bodily-response as possible.

Relative $rPVO_2^{max}$ is now calculated as 20% of the percentage of $METs_{max}$. The value was determined by testing across the range of values and 20% was found to best fit with free-living

physical activity data and a lucid return to basal level. With this set up, any values that fall below the basal level will be adjusted to 0. The higher the choice of threshold, the greater the number of values requiring adjustment to 0. The selected bound allows the glycogenolysis process to occur, but not excessively, hence mimicking the actual process occurring in the body. Figure 8.1(a), as was previously presented in Figure 7.2 depicting METs data of a volunteer, is converted to the respective $rPVO_2^{max}$ values as shown in Figure 8.1(b). It is evident that with this new basal level, METs values are observed to return more frequently to basal rate level. Unsurprisingly, this is because values within the 20% threshold already cover about 80% of the whole data, and hence represent more fluctuations in the METs data compared to using 1 MET as the threshold. This leads to more variations in physical activity intensity, and not just increasing throughout the day. Because each person will have a unique basal level, having a percentage bound and not a finite value will cover a much wider range of people. This accounts for the existence of different METs basal levels in people [140]–[143], not least the discrepancies that exist in various ways to adjust METs according to individual's attributes (as also presented in Section 7.4.2).

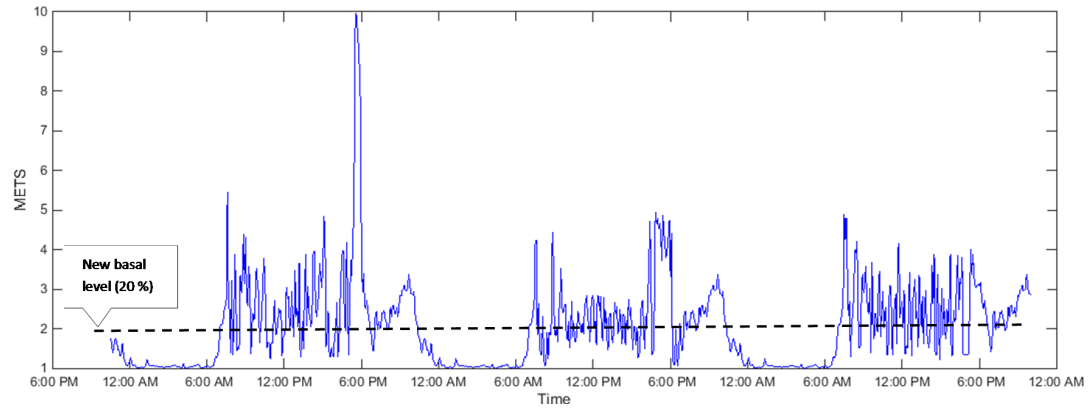

(a)

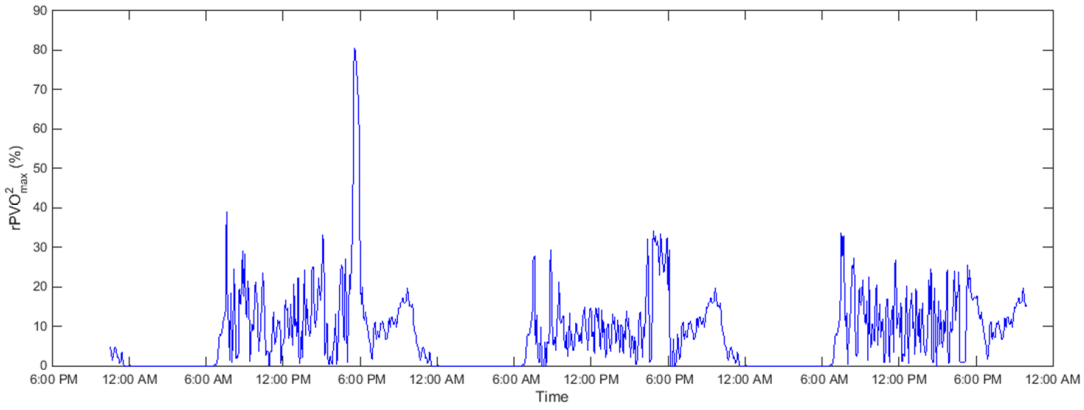

(b)

Figure 8.1: Original METs and $rPVO_2^{max}$, showing more returns to basal level in (b).

8.1.6 Exercise Model (G_{exer})

The above discussion has identified areas of the R&P model that require modification to be able to employ METs in the physiological model. Georga *et al.* [120] added G_{exer} as an additional input variable to the BG model, in addition to insulin and glucose inputs, reflecting glucose appearance as a result of exercise. The term describes the blood glucose variation during exercise and post activity as:

$$G_{exer} = (H - K) - U \tag{8.2}$$

Other parameters remain the same.

8.2 Method and Implementation

The new schematic representation of the method is as shown in Figure 8.2. The standard approach on the left reflects the study discussed in Chapter 6. While on the right, METs input is modified and now evaluated to become a quantitative input, G_{exer}. The Georga *et al.* [120] model was developed from R&P and Ewings [144], and here has been modified to account for more rational processes, such as the removal of I_p, as discussed in Section 8.1.4.

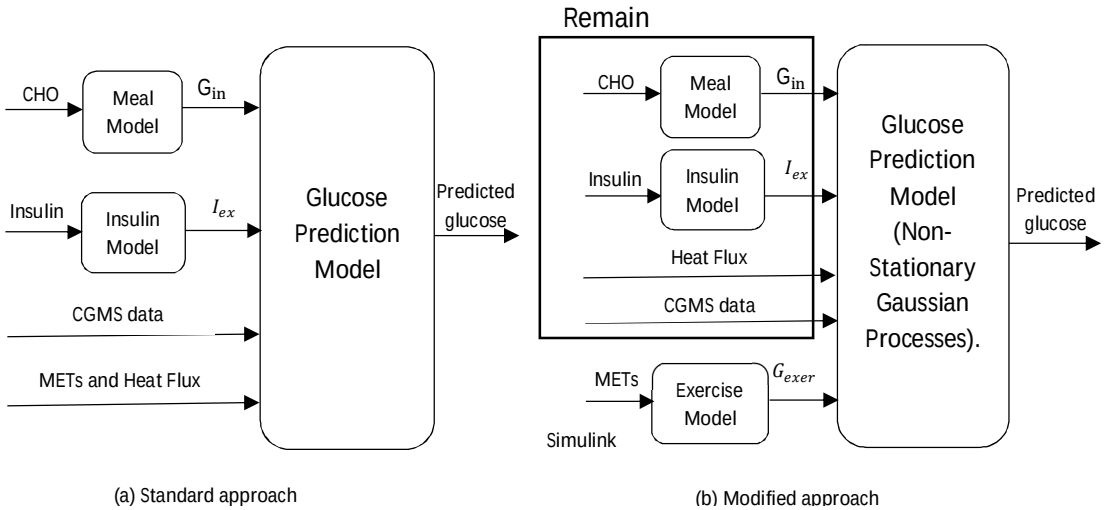

Figure 8.2: Schematic representation of the proposed method. Reproduced and modified from Georga [120].

While these modifications hopefully would enable better prediction, the non-stationarity nature of the free-living data cannot be overlooked. Therefore, this model will be tested using Non-Stationary Gaussian Processes (NSGP) initially utilised in the previous Chapter 6 and the physical activity DEs will be evaluated using Simulink. This is again a dissimilarity to Georga's study that employs only SVM to execute the above. Hence, the model's name being Non-Stationary Physiological-based Modelling (NSPM).

Three tests were done to assess the performance of these physical activity parameters, mainly represented by METs and Heat Flux data. Using the principle that one form of how body dissipates heat into the environment is by convection, the sensor in the SenseWear® armband measures the part of the total thermal energy dissipated to the surroundings [145]. This means that heat lost during physical activity are recorded, with more heat lost being attributed to more work being done by the body [146]. The three tests were:

i. 3 inputs NSPM (CHO, insulin and G_{exer}).
ii. 4 inputs NSPM (CHO, insulin, G_{exer} and Heat Flux).
iii. 5 inputs NSPM (CHO,insulin, METs, G_{exer} and Heat Flux).

NSPM is implemented the same as was done in Chapter 6 using NSGP and the same volunteers, but now with the addition of G_{exer} as an additional input. Primarily, tests were done to assess the performance of the added input G_{exer}. The first test was the addition of G_{exer} as the sole physical activity data without heat flux, the second included the addition of both, while the third included the two together with METs data, even though G_{exer} was actually derived from it, just to determine whether the added METs input will improve the prediction.

Other tests that do not include the G_{exer} parameter were not tested as they amount to the same tests done and presented in Section 6.3. In terms of data type, the same data from all volunteers were used, as well as the same plots from three volunteers (subject #11, #18 and #23) will be figuratively presented for comparison of the models' performance, arranged by those which perform the best, average and poorest.

In reference to Figure 8.2 (b), G_{exer} will first be calculated from METs using DEs, numerically solved using the Dormand-Prince method of fourth/fifth-order solver and implemented in Simulink. CHO and insulin data are modelled as presented in Section 2.3 and 2.4 into quantitative inputs, G_{in} and I_{ex}, respectively.

Inputs consisting data of G_{in}, I_{ex}, CGMS data, heat flux (*Hf*) data, and G_{exer} are then modelled using the Non-Stationary Gaussian Processes formulated as in Section 6.2, with regressors as follows:

$$G(k) = f(G(k-1),\ldots,G(k-n),G_{in}(k-1),\ldots,G_{in}(k-n),I_{ex}(k-1),\ldots,I_{ex}(k-n),Hf(k-1),\ldots,Hf(k-n),\\ G_{exer}(k-1),\ldots,G_{exer}(k-n),Gin(k-1),\ldots,Gin(k-n))+\zeta(k) \quad (8.3)$$

The value for *n* refers to the number of lagged variables reflecting the range of time constants for each variable which were verified by simulations. In our case, since the sample time is five minutes, the n=3 number of lags correspond to lags of 15 minutes, determined to be the most reasonable for the model structure to capture the required system dynamics.

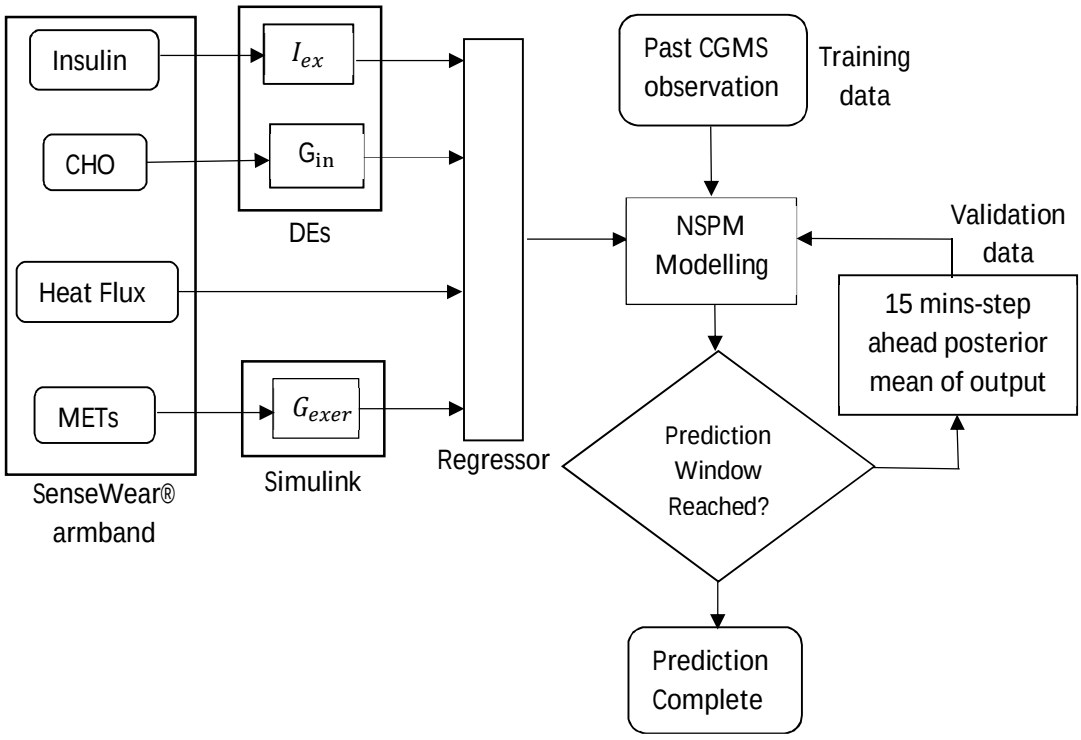

Figure 8.3: Block diagram of the Non Stationary Physiological-based Model (NSPM).

Figure 8.3 shows the process within the NPSM modelling. Initially, data collected using the SenseWear® armband were converted into quantitative data, where insulin and CHO data were modelled by separate DEs, producing the respective I_{ex} and G_{in}. On the other hand, METs data were modelled by Simulink into G_{exer}. All these parameters then become regressors to the NSPM model as presented in Equation (8.3). Using non-stationary Gaussian processes modelling, past observation of glucose levels over a couple of days help it to model the regressors for a desired time span. The model then checks whether the desired prediction period matches the total prediction window set, and until it does, the posterior mean of the output - 15 minutes predictions (3-step ahead) on the validation dataset is fed back into the NSPM model. The process is repeated iteratively until the total prediction window set is met, completing the prediction. The FIT metric as presented in Section 2.8 is again being used to evaluate the prediction performance.

8.3 Results

Table 8.4 summarises the NSPM's performance for the whole volunteer cohort. The discussion starts with individuals' results followed by the model's performance as a whole.

Figure 8.4 shows the plot for the one-hour prediction horizon and in Figure 8.5, the MPO for the three same volunteers stated earlier. It can be seen that for the one-hour prediction horizon, the model was able to moderately track the major variations in BG, despite missing minor ones. Subject #23's prediction shows that the model was unable to track one major peak at 10 A.M., missing by a magnitude of 6 $mmol/l$. As expected, the MPO shows much poorer results, missing even the major curves by a high magnitude. Subject #23's prediction however produced a slightly better fit than that in the previous model presented in Section 6.4.

As in previous discussion, the result can be divided into two: prediction with training and validation data. The latter would be a more noteworthy result to look at as it consists of unseen data which will better test the predictive capability of our model.

The summary for the mean FITs from the whole cohort's result (Table 8.4) can be seen in Table 8.1 below.

Type of predicted data	60 minutes prediction			MPO (infinite-step ahead prediction)		
	Test i	Test ii	Test iii	Test i	Test ii	Test iii
Validation Data (%)	-8.3	-6.1	-41.9	-60.2	-54.9	-69.5
Training Data (%)	65.2	67	-11.2	26.6	34.6	-29.1

Table 8.1 : FITs summary of prediction for NSPM tests.

From the results, Test ii shows the highest FIT over Test i and iii (in the case of negative percentage, lower percentage means higher FIT). Model with added G_{exer} showed better result only when it is modelled together with the other activity inputs, heat flux (Test ii). The addition of METs as in Test iii showed even poorer result than with and without the heat flux input, which is unsurprising given the redundancy of the two parameters - METs and G_{exer}. Another observation that can be seen is that the NSPM predicts better with training data but performs poorly for validation data.

Comparisons of mean FITs to the previous NSGP tests and to Valletta's work [9] using standard GP were also done and presented in Table 8.2, comprising tests considering CHO and I as the default parameters for all the models. The comparison is made on models with added physical activity inputs presented in Section 6.4, where NSGP Test iii (heat flux added) and Test iv (heat flux and METs added) are compared to NSPM Test i (G_{exer} added) and Test iii (G_{exer} and Heat Flux added) and also to standard GP modelling (Heat Flux and METs added) from Valletta's.

Type of data	60 minutes prediction					MPO (infinite-step ahead prediction)				
	GP	NSGP Test		NSPM Test		GP	NSGP Test		NSPM Test	
		(iii)	(iv)	(i)	(ii)		(iii)	(iv)	(i)	(ii)
Validation Data (%)	-5.2	1.9	3.1	-8.3	-6.1	-51	-60.6	-49.2	-60.2	-54.9
Training Data (%)	69	57.8	60.2	65.2	67	29.2	15.1	17.4	26.6	34.6

Table 8.2: FITs summary of prediction for validation and training datasets.

The result from NSPM modelling is also compared to the previous researches, as well as from the work of Georga *et al.*, where they included both insulin and carbohydrate digestion parameters in

the SVM, depicted in Table 8.3. Additionally, the exercise-induced glucose and insulin absorption variations were also considered as inputs in the rest of the studies stated.

Work	Model	FIT (%)	RMSE ($mmol\ l^{-1}$)	No. of Subjects
Gani *et al.* [49]	AR	n/a	0.7	9
Finan *et al.* [88]	ARX	35	2.2	9
Valletta [9]	ARMAX	31	2.0	22
Cescon *et al.*	ARX	n/a	1.9	9
Cescon *et al.*	ARMAX	n/a	1.7	9
Pérez-Gandía *et al.*	Neural Network	n/a	2.5	9
Georga *et al.*	SVM	n/a	1.4	7
ARX with reference parameters (our study)	ARX	32	1.86	18
NSPM (our sudy)	Physiological-Based Model	-6.0	2.8	22

Table 8.3: Comparison of NSGP to previous studies.

From the results, although there is a comprehensive literature backing up the hypothesis, it is evidently shown that NSPM not only failed to improve upon the previous NSGP tests, it was actually worse than the other non-physiological-based models form past researchers discussed. The probable causes for this revelation are further discussed in Section 8.4.

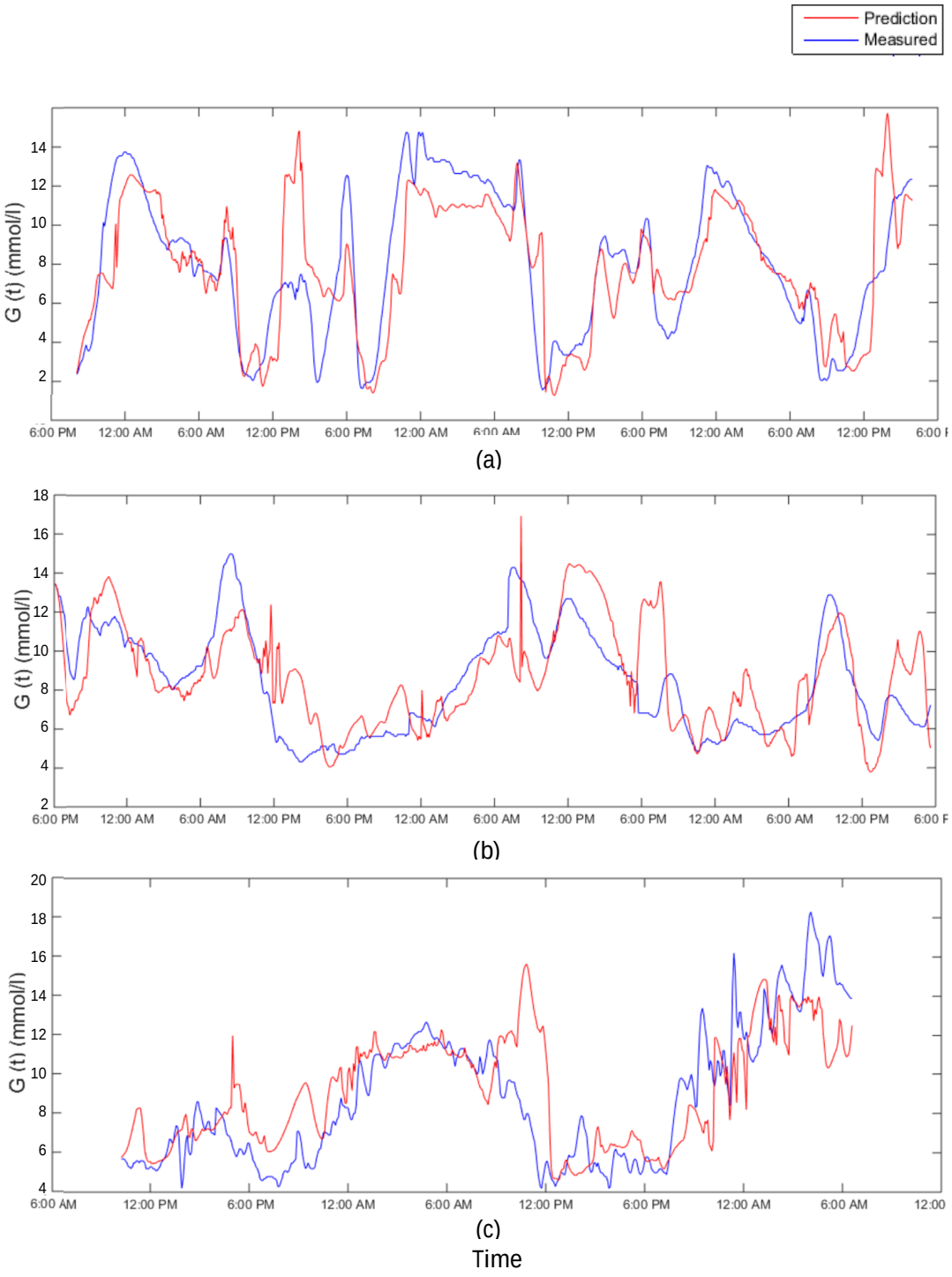

Figure 8.4: One-hour BGC prediction for subject #11(a), #18(b) and #23(c).

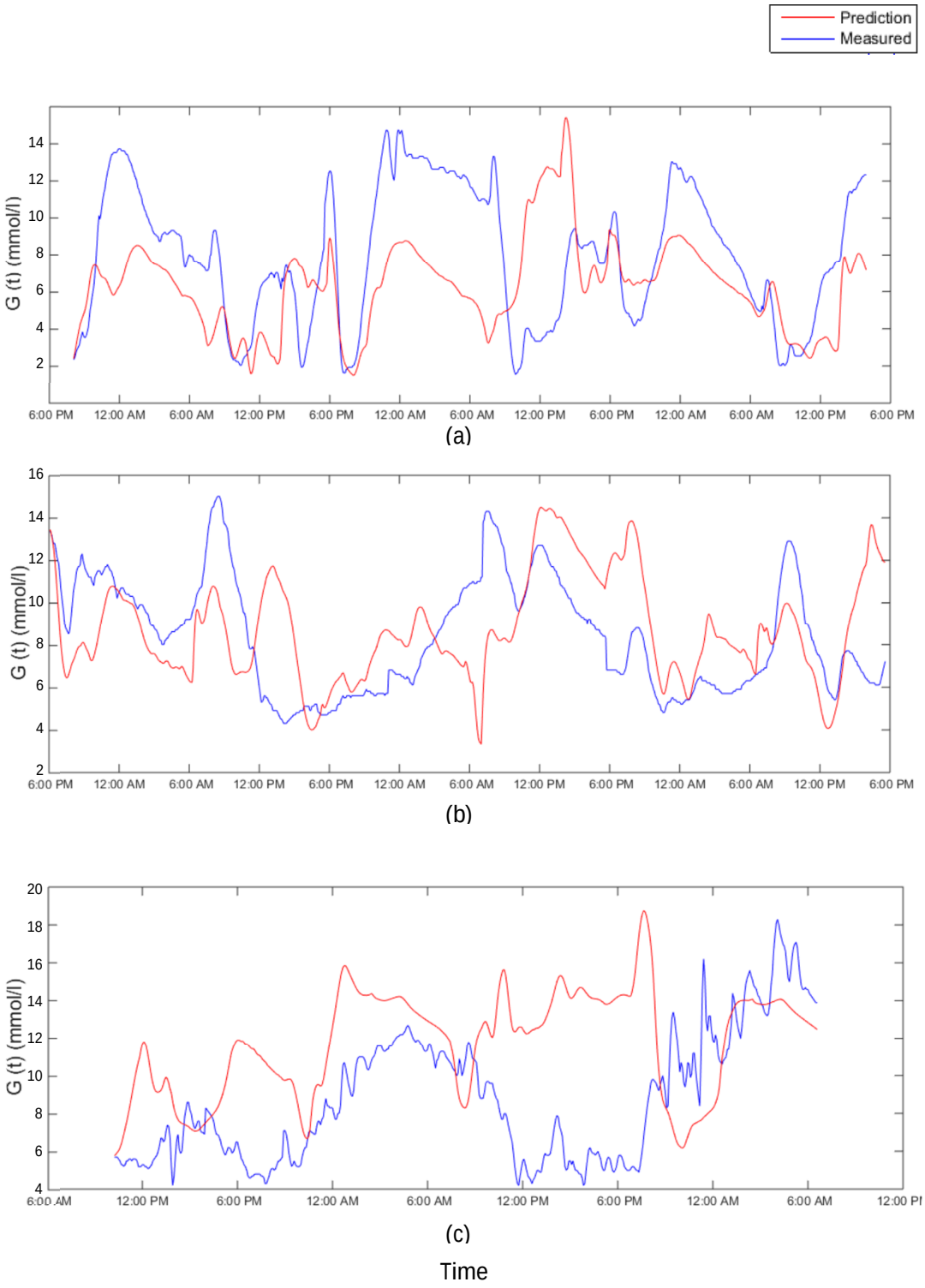

Figure 8.5: Model Predicted Output of BGC prediction for subject #11(a), #18(b) and #23(c).

Subject ID	Dataset	Test i				Test ii				Test iii			
		60 mins		MPO		60 mins		MPO		60 mins		MPO	
		FIT	RMSE	FIT	RMSE	FIT	RMSE	FIT	RMSE	FIT	RMSE	FIT	RMSE
01	1	-15.4	2.4	-24.4	2.6	-16.0	2.4	-21.6	2.5	-5.6	2.2	-12.8	2.4
	2	73.7	0.5	62.2	0.7	70.8	0.5	60.3	0.7	3.7	1.8	1.6	1.8
02	1	10.5	1.5	2.6	1.6	12.1	1.4	-4.3	1.7	-33.7	2.2	-39.0	2.3
	2	-13.8	2.3	-33.2	2.7	-0.5	2.0	-21.9	2.4	-8.4	2.2	-11.4	2.2
	3	69.2	0.5	68.1	0.5	73.1	0.5	34.4	1.1	-18.4	2.0	-23.2	2.1
03	1	-19.0	2.9	-78.7	4.3	-3.1	2.5	-81.1	4.3	-67.3	4.0	-98.0	4.8
	2	64.8	1.1	31.9	2.1	68.8	0.9	39.8	1.8	-48.5	4.5	-113.7	6.5
	3	31.9	2.1	-33.4	4.1	29.8	2.2	-29.2	4.0	-78.1	5.5	-133.1	7.2
05	1	3.8	2.4	-25.2	3.1	4.3	2.3	-10.9	2.7	-52.5	3.7	-94.4	4.8
	2	60.9	1.0	27.1	1.8	67.0	0.8	26.4	1.8	-49.3	3.6	-76.1	4.3
06	1	-97.0	3.2	-270.6	6.1	-95.6	3.2	-282.9	6.3	-145.8	4.1	-157.7	4.2
	2	-7.7	3.1	-87.0	5.3	2.9	2.8	-81.1	5.2	-112.0	6.0	-182.2	8.0
	3	72.3	1.2	26.7	3.2	76.3	1.0	68.5	1.4	-35.9	5.9	-39.2	6.1
07	1	62.4	0.9	0.4	2.4	67.6	0.8	43.8	1.3	15.4	2.0	4.9	2.3
	2	11.5	2.4	4.3	2.6	27.0	2.0	8.2	2.5	10.9	2.4	7.9	2.5
08	1	69.5	1.0	39.2	2.0	67.3	1.1	21.4	2.6	-15.7	3.9	-48.5	5.0
	2	16.5	4.0	-29.3	6.1	21.8	3.7	-16.4	5.5	-1.3	4.8	-31.4	6.2
09	1	63.6	0.8	25.5	1.7	68.6	0.7	41.2	1.3	13.5	2.0	-7.9	2.4
	2	-0.4	2.2	-60.2	3.4	5.4	2.0	-29.6	2.8	0.1	2.1	-6.6	2.3
10	1	67.2	0.7	37.9	1.4	71.0	0.6	47.9	1.1	5.4	2.1	-36.5	3.0
	2	7.4	2.9	-4.9	3.3	16.8	2.6	10.0	2.8	-10.7	3.5	-11.0	3.5
	3	22.1	2.4	14.5	2.7	21.7	2.4	15.8	2.6	-6.8	3.3	-9.7	3.4
	4	-15.6	4.0	-22.5	4.3	-16.3	4.0	-32.4	4.6	-16.0	4.0	-31.2	4.6
11	1	1.7	4.4	-23.9	5.5	-12.2	5.0	-44.9	6.4	-10.5	4.9	-4.4	4.6
	2	69.3	0.9	39.5	1.8	64.6	1.1	16.7	2.5	-38.4	4.2	-52.4	4.7
	3	46.0	2.0	8.2	3.3	36.5	2.3	-10.6	4.0	-34.2	4.9	-40.7	5.1
13	1	69.3	1.2	64.0	1.4	72.6	1.1	62.3	1.5	-9.3	4.3	-13.5	4.5
	2	24.3	2.8	-8.1	4.0	23.8	2.9	11.4	3.3	-36.2	5.1	-44.2	5.4
	3	26.1	3.8	26.9	3.8	14.3	4.4	9.1	4.7	-13.2	5.8	-15.0	5.9
	4	-37.3	3.9	-68.9	4.8	-19.8	3.4	-35.9	3.9	-4.5	3.0	-3.7	3.0
14	1	-26.8	3.5	-147.0	6.9	-23.6	3.4	-88.9	5.3	-21.8	3.4	-36.2	3.8
	2	59.4	1.7	1.3	4.2	58.7	1.7	21.6	3.3	-15.8	4.9	-7.7	4.6
	3	-2.1	3.1	-51.6	4.6	-2.4	3.1	-71.5	5.2	-40.5	4.3	-54.0	4.7
	4	18.5	3.2	-2.8	4.1	24.2	3.0	7.7	3.6	-40.0	5.5	-49.8	5.9
15	1	-13.1	3.4	-133.3	6.9	7.4	2.8	-97.7	5.9	-92.5	5.7	-144.5	7.3
	2	48.3	1.4	26.0	2.0	52.9	1.3	-40.1	3.7	-101.3	5.4	-147.8	6.6
	3	-15.5	2.0	-178.2	4.9	17.6	1.5	-111.2	3.7	-244.0	6.1	-334.1	7.7
16	1	19.9	3.0	-6.5	4.0	11.5	3.4	-18.3	4.5	3.0	3.7	-5.7	4.0
	2	73.5	0.9	62.7	1.3	75.3	0.9	62.6	1.3	16.7	2.9	8.3	3.2
18	1	28.3	2.1	-30.3	3.8	33.5	1.9	-33.1	3.9	-8.7	3.2	-89.5	5.5
	2	65.2	1.2	46.3	1.8	67.5	1.1	53.5	1.5	32.6	2.2	-28.4	4.3
	3	-3.8	2.1	-37.6	2.8	-17.0	2.4	-110.1	4.3	-32.8	2.7	-111.9	4.3
	4	16.8	2.2	-18.9	3.2	21.4	2.1	-13.3	3.0	-9.9	2.9	-87.8	5.0
19	1	-2.0	3.2	-47.3	4.6	-14.3	3.6	-41.1	4.4	8.9	2.8	-25.0	3.9
	2	-23.8	4.0	-59.2	5.1	-20.7	3.9	-46.0	4.7	-2.6	3.3	-19.1	3.9
	3	69.7	1.0	55.2	1.5	70.7	0.9	54.5	1.5	7.8	3.0	-1.1	3.3
20	1	72.2	1.0	57.1	1.6	73.4	1.0	49.8	1.8	2.1	3.6	-20.6	4.4
	2	-91.1	2.9	-182.1	4.3	-127.8	3.5	-262.9	5.5	-187.6	4.4	-274.5	5.7
	3	4.0	2.8	-33.4	3.9	2.7	2.8	-49.0	4.3	-87.7	5.4	-106.2	6.0
	4	-42.6	3.0	-118.4	4.5	-66.4	3.4	-187.7	6.0	-173.4	5.7	-237.9	7.0
21	1	70.4	0.8	49.2	1.3	72.7	0.7	49.5	1.3	7.2	2.5	2.6	2.6
	2	-6.1	2.6	-32.7	3.2	4.1	2.3	-25.9	3.1	-9.8	2.7	-26.3	3.1
22	1	-1.1	4.1	-25.7	5.1	13.1	3.6	-13.0	4.6	7.9	3.8	-1.2	4.1
	2	82.1	0.8	-72.5	7.8	80.5	0.9	47.3	2.4	1.3	4.5	-1.5	4.6
	3	13.1	3.0	-122.1	7.8	20.0	2.8	-38.3	4.8	2.7	3.4	-21.8	4.3
23	1	61.0	1.3	-9.1	3.7	51.2	1.7	30.5	2.4	-15.6	3.9	-26.8	4.3
	2	-105.7	3.2	-156.8	4.0	-96.0	3.1	-145.1	3.8	-108.2	3.3	-179.9	4.4
	3	24.7	2.6	-75.9	6.0	29.3	2.4	-46.7	5.0	-7.0	3.7	-56.7	5.4
	4	-110.6	3.0	-217.1	4.5	-82.9	2.6	-83.5	2.6	-114.6	3.1	-179.1	4.0
24	1	-28.4	3.8	-39.1	4.2	-43.9	4.3	-42.2	4.3	-41.5	4.2	-43.3	4.3
	2	43.0	0.9	-27.9	2.1	47.2	0.9	15.5	1.4	-2.5	1.7	-6.6	1.8
	3	14.7	2.2	-23.5	3.3	9.5	2.4	-17.2	3.1	-5.9	2.8	-13.0	3.0
	4	-12.9	3.7	-31.9	4.3	-15.6	3.8	-29.1	4.3	-12.4	3.7	-15.1	3.8
25	1	-8.7	2.3	-91.5	4.0	0.2	2.1	-63.3	3.4	3.3	2.0	-6.1	2.2
	2	-7.4	3.0	-71.0	4.8	-6.4	3.0	-140.5	6.7	-1.5	2.8	-18.5	3.3
	3	47.3	1.9	-26.1	4.5	57.6	1.5	-45.9	5.2	-1.3	3.6	-6.7	3.8

Table 8.4: Result from physiological based model.

8.4 Discussion

One observation that can be made is that the NSPM predictions performed very well only for trained datasets, something that is not surprising due to the 'seen' nature. In fact, the majority of tests saw higher FITs for prediction with training data using NSPM over other models, but vice-versa with validation data (unseen data). Hence, the model is shown to produce a relatively acceptable prediction with capabilities limited only for predicting seen data and not otherwise. On the other hand, standard GP shows average performance compared to the other two, for both validation and training dataset. Predictions using NSGP modelling remains the best at producing good results even with unseen data.

It can also be observed that with NSPM modelling (unseen data) of which the tests utilised G_{exer}, a quantitative measurement of physical activity, poorer result was obtained than both NSGP with only raw METs used as well as standard GP containing only insulin and CHO inputs. It can be understood that the presence of physical activity data complicates the modelling process, hence poorer prediction could be expected. But the fact that the result was poorer than standard GP without the presence of physical activity input means that the modelling does not properly reflect the underlying physiology, processes and time constants at all well. Despite raw METs being an input to GP that in its form lacks physiological basis, it has yielded better prediction. Therefore, it can be assumed that we are still far from understanding the actual nature of physical activity in Type 1 diabetes.

Additional tests on the NSPM model were with the absence of heat flux parameter (NSPM Test i) and with the addition of raw METs (NSPM Test iii). The former did slightly better in both short and long-term predictions, but both yielded poorer predictions than NSPM Test ii (heat flux with G_{exer}). Raw METs data that initially were resampled at the same time constant as the CGMS data were also tested with longer intervals to see whether the sampling rate had any influence; and it did not. A sampling time of 5 minutes, the same as CGMS, was found to be the most appropriate.

The basal rate bound value that was later set to 20% in the test was found to have a significant impact towards the performance of the predictor. The 20% bound was selected as it was the average value that produced reasonable prediction compared to the higher values. It appears that every volunteer had a different basal rate, resulting in varying prediction performance that varies relative to the bound employed. As was discussed earlier, optimum basal level allows more returns from intensely active activities while also preserving much of the physical activity curve. A change in the value may vastly improve prediction or worsen it further and hence must be chosen wisely. Henceforth, this bound could also be included in the optimisation so as to improve the prediction capability.

In comparison to Georga *et al.* work [120] from which the literature was derived from, she provided compelling results with the use of Support Vector Machines (SVM). Their results have generally shown much better results than from this study. However, the SVM machine acts more like a parametric predictor with less regards to the physiological basis, and the performance capability can be more likely attributed to the machine itself - it describes the data and not the processes varying that data. While in the physiological-based study where Georga *et al.* proposed the G_{exer} parameter, there was no distinction between Type 1 and Type 2 diabetes model. The two were generalised in terms of the response and this alone would have hindered the performance of the model. In the study too, PVO_2^{max} was derived directly from METs by the simple multiplication by 3.5,

when this is an oversimplified approach as explained in Section 7.4.2. Basal rate was also set to be at its lowest MET value (1 MET). This would have caused a devastating effect to the predictor because integrated activity intensity will always rise and never return to its basal rate. This leads to an excessive decline in the rate of glycogenolysis followed by negative concentrations of blood insulin, glucose and predicted BGC. There was also no settling time of 5-7 minutes of the PVO_2^{max} threshold, and the presence of insulin clearance parameter that exists only in Type 2 diabetes patients.

In terms of data training, the good prediction can also be attributed to the long training time, constituting more than half of the data used (66 % of the whole data) [121] and also longer time lags for the exercise-related inputs (varying between 60 minutes to 180 minutes) [120], [121]. If only the discrepancies in the physiological attributes were to be accounted for in the model and not the functionality, the prediction performance would not have been acceptable.

Additionally, the literature involving R&P's exercise model alone would have led to the poor prediction. The model accounts for mild to moderate exercise but the parameter estimates were derived from fitting the model against data of healthy volunteers and tested against synthetic data. The two studies that parameters of the equations were fitted to and validated against were both based on healthy subjects, and could be the reason that blood insulin concentration was observed to decrease; due to the decreased insulin secretion, and not increased clearance. Hence the removal of process Z in the later modified PA model.

Another related factor could also be attributed to the use of clinical data taken from subjects in a controlled environment where they performed rigorous exercises. From the validation data, R&P derived a number of constants to model the physical activity dynamics that largely dictate the overall model. However, they were originally taken from healthy subjects. This is completely different to our data which are of free living and collected only from Type 1 diabetics. Thus, there are two significant points that influence the performance of our model here: the different nature of subject's data and the state of individual's health (diabetics or not). One way to improve these parameter values to account for people with diabetes and free-living data are by incorporating an optimisation technique into the model, which is the subject of the next chapter.

8.5 Contribution to the Body of Knowledge

A modified compartmental model derived from the physical activity minimal model presented by R&P was established. The modifications were done to enhance the physiological basis while ensuring that the model was valid for data collected in free-living conditions. The use of free-living data had helped us understand properly the bodily response and the highly variable nature of the physical activity data. In turn, this has enabled us to significantly improve the prediction capability of the model proposed by R&P albeit not improving the prediction over other models presented in this thesis.

Basal insulin and METs level were modified to account for real diabetes data, resulting in the complete removal of the former and adjustments of the basal level in the latter. A METs with a percentage-based basal rate was shown to be a more accurate description to account for a variety of basal levels in the volunteer data considered here. The addition of the notion G_{exer}, the variations in circulating glucose during and shortly after exercise proposed by Georga *et al.* as an addition to R&P's model was shown to be rational. With G_{exer}, METs data were converted into a data type relative to the physical response during and post activity. Apart from this, because of the variability in free-living data and especially in METs data, a non-stationary Gaussian processes shown in Chapter 6 to improve prediction was employed. Despite this model accounting a detailed physiological basis backing up the literature, the performance was lower than results from tests in Chapter 6. However, the physiological-based modelling remains rational in comparison to the other parametric-oriented predictors.

Chapter 9: Multi-objective Optimisation in Physiology-Based Modelling

In Chapter 5, we discussed the use of optimisation to find the optimum parameters for insulin-glucose dynamics, and have found that significant improvements of the prediction of the linear system identification model (ARX model) could be achieved. This chapter will elaborate on the prospect of using multi-objective optimisation technique to fine-tune the parameters in R&P model derived from healthy individuals, to better match those metabolical processes within Type 1 diabetics. This is to overcome limitations explained in the physiological model encountered in Chapter 8. The attempt and rational to use this technique is also explained in this chapter. An important difference in using optimisation in this Chapter and that utilised in Chapter 5 will also be discussed. Simply put, while Chapter 5 focuses on using optimisation to continually adapt glucoregulatory-sub-models to the bodily response in an individual (intra-patient), this technique aims to fine-tune them towards the whole dataset of Type 1 diabetes cohort (inter-patient) in our study. It is hoped that with this arrangement, the T1 diabetes community is better represented, and finally distinct classifications of diabetes patients is suggested for a more efficient and responsive treatment.

9.1 Introduction

In the simple R&P model, derived parameters were obtained by fitting them against data from healthy individuals within ambulatory environments [133]. There is therefore a discrepancy when one attempts to use this model with data from people with diabetes, especially those with Type 1 diabetes. This is due to the different physiological bodily responses between them. We can see inter-group variations within the study cohort, with more expected of a community that is completely different in their nature e.g., healthy, pre-diabetic, metabolic syndrome, Type 1 and Type 2 diabetics. The poor prediction, as evident in the previous chapter, may be ameliorated by using optimisation for parameter fitting to the study cohort. BG was reasonably well tracked when physical activity data were not included in the modelling. Inclusion of physical activity data, in some form, generally resulted in poorer prediction performance despite there being well known effects in Type 1 diabetes that should be able to be exploited to account for physical activity and improve prediction. Therefore, in this chapter, we will employ optimisation-based parameter-fitting to investigate whether this will allow the effective use of physical activity data to improve BG prediction.

As the problem statement in our case is to find a set of solutions that improves the prediction of BG levels, and in specific raising the closeness-of-fit metric (FIT) of predicted against measured values, GA is one of the many search techniques to this matter.

Especially when the objective involves fine-tuning a set of solution into better values, GA is a predominantly efficient technique to find exact or approximate solutions for this problem. As opposed to neural networks, they are a non-linear statistical data modelling tools, that primarily used for finding patterns in data or modelling complex relationship of input and outputs. But, whenever a problem can actually be quantified of its solution, GA can perform a better directed search of the solution space (e.g in our case, the adjusted R&P parameters). Hence, past studies showing that neural networks solution did not improve over even a standard non-stationary GP models, as depicted in Table 9.6.

9.2 GA-Based Parameter Optimisation

Similar to that presented in Chapter 5, a genetic algorithm will be incorporated in the modelling for the optimisation of the parameters. Table 9.1 shows the parameters associated with physical activity in the R&P model that were derived from healthy subjects. It is reasonable that these parameters are to be optimised to fit Type 1 diabetes volunteers and address the previous limitations. As noted earlier, R&P derived the parameters by fitting and estimating them to the data from [134]. For plasma insulin dynamics, parameters a_5 and a_6 were estimated to quantify the depletion of plasma insulin during exercise and its repletion during the recovery period, by having blood samples taken at regular intervals to measure the plasma insulin level. On the other hand, for the glucose model, blood samples were measured at regular intervals for changes in the hepatic glucose production rate (H; mg/kg/min) and the glucose uptake (U; mg/kg/min), thus producing the estimated parameters a_1 and a_2 for the former and a_3 and a_4 for the latter. Therefore, it is viable that the parameters from a_1 to a_6 are to be optimised in this study, as shown in Table 9.1. Note that the upper and lower limits calculated by R&P satisfy the 95% confidence intervals.

Parameter	R & P Value	Lower limit	Upper limit	Unit
a_1	0.00158	0.0013	0.0019	mg/kg·min2
a_2	0.056	0.0441	0.0679	1/min
a_3	0.00195	0.0015	0.0024	mg/kg·min2
a_4	0.0485	0.0355	0.0617	1/min
a_5	0.00125	0.001	0.0015	μU/ml·min
a_6	0.075	0.0588	0.0912	1/min

Table 9.1: Parameters derived from healthy individuals as in R&P's study, values to be optimised by GA.

People with diabetes are slightly physiologically different to healthy ones in that there is no pancreatic insulin production which also affects the processes of other organs, e.g. kidneys and liver. Although attributes are largely similar across the Type 1 diabetic community, there are small individual variances. Examples of this would be the different renal thresholds for extraction of blood glucose in the urine and mean blood glucose level itself. However, the common parameters are expected to be largely similar and the GA can be used as a tool for optimisation that could be helpful in discovering this.

This optimisation is markedly different to the one presented in Chapter 4 where optimised parameters were already derived from Type 1 diabetes subjects. If we imagine looking at parameters of healthy individuals and diabetes patients on a 2D view, we would see there would be distance between them as there are physiological differences. With optimisation, the idea is to bring the original parameters closer to the (unknown) parameters found in people with diabetes.

Within these unknown parameters there are potentially local optima (LO). One way to speed up the optimisation and avoid these LOs is by seeding the initial population with the referenced parameters in Table 9.1. They are reasonably well tested, validated and accepted by the research community, hence are reasonable to be evaluated first. An initial population was generated with the R&P values appearing in some individuals along with variations from these. Constraints were also placed on the GA, where the farthest values that can be viable would be limited to certain values. As an example, Figure 9.1 shows the generated initial population for the two parameters a_1 and a_2 with its population constrained within [0.0013, 0.0019] and [0.0441, 0.0679], with the range satisfying the upper and lower limit presented in Table 9.1, respectively. The figurative example

shows two individuals (subject #1, subject #2) having parameters very close to reference ones (0.0158, 0.056) while subject #3 and subject #6 have theirs being close to parameter a_1 and one belonging to subject #4 close to a_2. Subject #5's parameters do not appear to be close to neither parameters. Other blue dots depict random points generated by GA on the same plane.

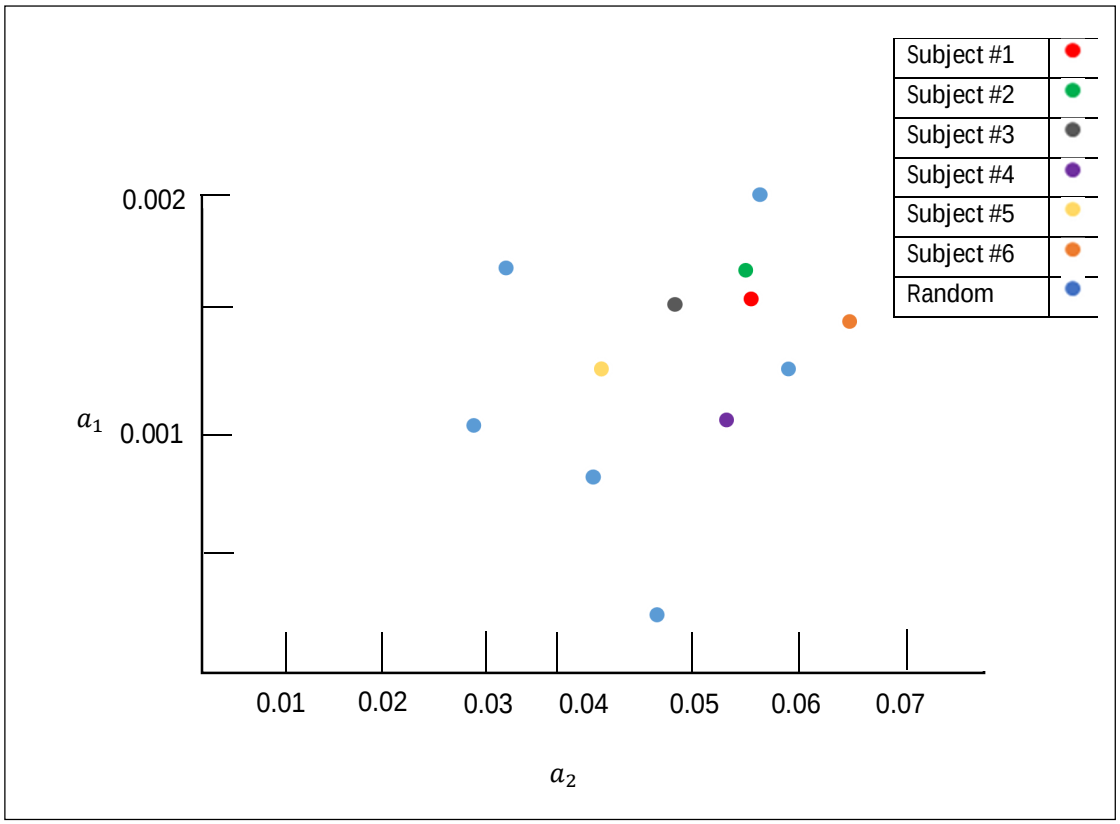

Figure 9.1: Points of a_1 and a_2 for 6 volunteers with randomised populations.

Chapter 5 has as well discussed the rationale of training and validation apart from pure optimisation. Optimisation searches any viable solution that satisfies the constraints placed while achieving the objective function. Predicting better BGC using a number of techniques has been the same objective throughout the study. Specifically, the objective is to minimise the RMSE or maximise the FIT between predicted and measured BGC.

In terms of a patient's diabetes prediction, a desirable solution is not one that could predict well in one dataset while performing poorly in another, but one that predicts acceptably well in both such that a prediction would not be dangerous for an individual to use in their therapeutic regimen. Thus, we might reasonably expect that there will be solution parameter sets that can optimise prediction for an individual and others that will give a good mean performance for the whole cohort studied here – which is what this chapter focuses upon.

9.3 Cohort-Driven Optimisation with Multi-Objective Optimisation

The aim of this investigation is to determine if parameters identified via optimisation from data from Type 1 diabetics can be used instead of those reported in the literature derived from healthy individuals. This is a non-trivial task, as the volunteer cohort is not homogenous with considerable variation in physiological parameters, e.g. age, weight, duration of diabetes, etc. This is different to the optimisation employed in Chapter 5 as there, the objective was intra-patient optimisation, while here, the inter-patient.

Multi-objective optimisation allows for multiple objective functions to be considered simultaneously. In the case here, it should be helpful to accommodate the diverse parameters present in Type 1 diabetes patients. The overall objective is to find a satisfactory compromise solution that works generally for all Type 1 diabetics considered in the study. Without overlooking the importance of intra-patient parameter fitting, it could benefit future researches by determining physiological parameters relevant to the internal dynamics found within people with Type 1 diabetes.

In previous chapters, the main objective was to find the best fit (using the metrics of good fit as presented in Section 2.8: FIT or RMSE) applied on intra-patient optimisation. It is also desirable to minimise the FIT differences between other patients as well. This is so that any fit improvement made will be applicable to all individuals within the study. Therefore, the objective functions would be:

1. Maximising the mean FIT across individuals:

$$\max \frac{\sum \sqrt{\left(1 - \frac{\sqrt{\sum_{k=1}^{N}\left(G(k) - \hat{G}(k)\right)^2}}{\sqrt{\sum_{k=1}^{N}\left(G(k) - \bar{G}\right)^2}}\right)} * 100\%}{n}. \tag{9.1}$$

2. Minimising the standard deviation (SD) of FIT across individuals tested:

$$\min \sigma \frac{\sum \sqrt{\left(1 - \frac{\sqrt{\sum_{k=1}^{N}\left(G(k) - \hat{G}(k)\right)^2}}{\sqrt{\sum_{k=1}^{N}\left(G(k) - \bar{G}\right)^2}}\right)} * 100\%}{n}, \tag{9.2}$$

where n is the number of individuals.

In general, there are two approaches to multi-objective optimisation. The first one, by combining the individual objectives into a single composite function, using various methods such as weighted sum method, utility theory and others, but still, the problem exists in the correct selection of the

weights or utility function characterising the decision-makers preferences (in our case, between maximising the mean FIT and minimising the FIT SD).

Although the multiple objectives do not directly conflict each other, in the instance of a successful iteration in the first objective (mean FIT incremented), the value of SD for all the predictions FIT will much likely also be incremented, hence the second objective being the minimisation of the latter. In simple terms, any change to one of the objectives will result in multiple pareto front or solutions.

As a proof, without any loss of generality we may (using the mean as the origin and the SD as the unit) choose units of measurement in which the n numbers are $x_1, x_2, \dots, x_n$ with $\sum x_i = 0$ and $\sum x_i^2 = n$. Let the variance and SD be both 1, and the new number be x_0.

$$\frac{1}{n+1}(x_0^2 + \sum_{i=1}^{n} x_i^2) - (\frac{1}{n+1}(x_0 + \sum_{i=1}^{n} x_i))^2 - 1 \tag{9.3}$$
$$= \frac{x_0^2}{n+1} + \frac{n}{n+1} - \frac{x_0^2}{(n+1)^2} - 1$$
$$= \frac{n}{n+1}(-1 + \frac{n}{n+1}x_0^2).$$

From Equation 9.3, the change in the variance is found by subtracting 1 from the variance of all n+1 numbers, which will be negative if and only if $nx_0^2 < n + 1$ (the sign is not dependent on the unites of measurement). Thus, the variance will increase when x_0 is higher than $\sqrt{1 + 1/n}$ standard deviations of the mean, but will decrease if x_0 is within it from the mean.

Therefore, it is proven that mathematically, introducing a new value to the set of data (in our case, a new mean FIT following multiple GA iterations) will result in the change of SD value. The statement is especially true when one objective function (Equation 9.1) serves to increase the mean FIT values as its objective, inadvertently increasing the spread of data (SD value) averaged between the previous and current mean FIT. In short, a new higher mean FIT driven by the first objective (maximisation) results in a higher SD and hence, a point farther away from the second objective (minimisation). This is the evident of the conflicting objectives, formed by the first function itself, henceforth the MOGA to be used.

The reason why the second objective (Equation 9.2) functions to minimise the SD FIT values, is to keep the margin between new and previous SD values low, thereby preventing a wider spread between the FITs values. This scenario is figuratively depicted in the result (Section 9.7).

Intuitively speaking, the first objective function can be easily understood as it relates to the model performance over the whole study cohort. The second objective however is intended to ensure that while minimising the mean RMSE across the cohort, the differences between them remain small. For example, the value 10 could be obtained by the addition of 4, 3, 2 and 1 or 6, 3, 1 and 0. However, both of these sums are undesirable because the RMSE values (fit) are unevenly distributed. This may well fail the cohort-driven prediction, which may result in optimised parameters that work well only for a few but poorly in others. By having the second objective, the optimiser should be constrained to prefer individual solutions that also minimise the spread within the multiple FITs, preventing a wide difference between the FITs values throughout the subjects datasets. Therefore, in the case of the stated example, the best solution might be 2,2,3,3, i.e. little difference between each constituent value of objective 2.

In terms of GA operation, in each run the GA searches for probable points in the search plane. While searching for the lowest mean values for every search, only parameters with evenly distributed values will be acceptable and get to reproduce. The result is hopefully parameters binding and reflecting the whole cohort.

While single objective optimisation may have an exclusive optimal solution, multi-objective ones contain sets of compromised solutions, known largely by Pareto-optimal solutions. They are optimal in the sense that no other solutions in the search plane are better to them when all objectives are considered together. Figure 9.2 shows a possible distribution of points in the search plane, with the two objective functions and the curve line depicting Pareto front. Solutions that lie along the Pareto front are non-dominated solutions while those that lie inside the line are dominated because there is always another solution on the line that has at least one objective with better value. In Figure 9.2, orange dots depict initial solutions that are either better only in one objective or the other. Brown dots represent possible solutions after multiple iterations of optimisation, and finally, convergence much likely ends near the green dots called Pareto-optimal solutions. They are deemed optimal in the sense that there is no better solution in both objectives. One cannot say the other is better among them since an improvement in one objective means a degradation in another. The figurative contradictory relationship between the two objectives is presented in the result.

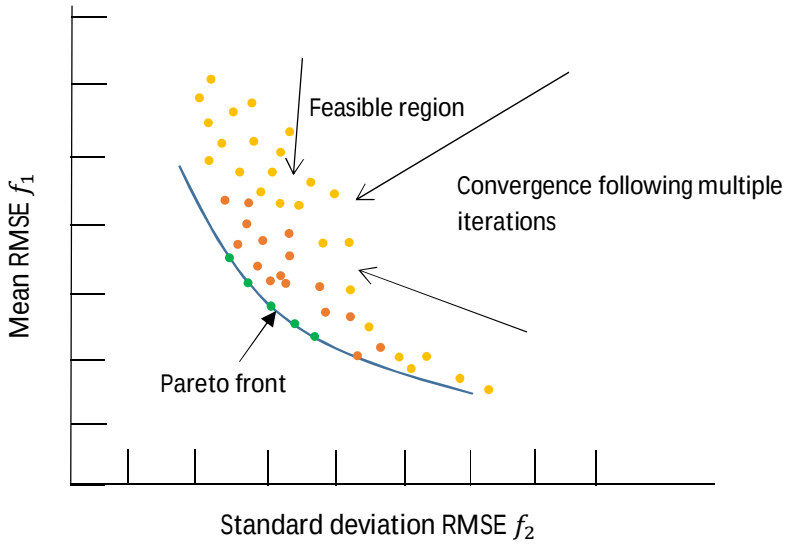

Figure 9.2: Population within the search plane.

9.4 Guarantee of Convergence and Time

In optimisation, a solution is deemed optimal when the search converges to a point where no other better solutions can be found. This optimality can be divided into two: Local Optimum (LO) and Global Optimum (GO). While the former represents the optimal point within the limited candidate solutions or within a neighboring set of candidate solutions, the latter represents the optimal point for the whole candidate solutions and not just those in a particular neighbourhood of values. A depiction of LO and GO is shown in Figure 9.3 below.

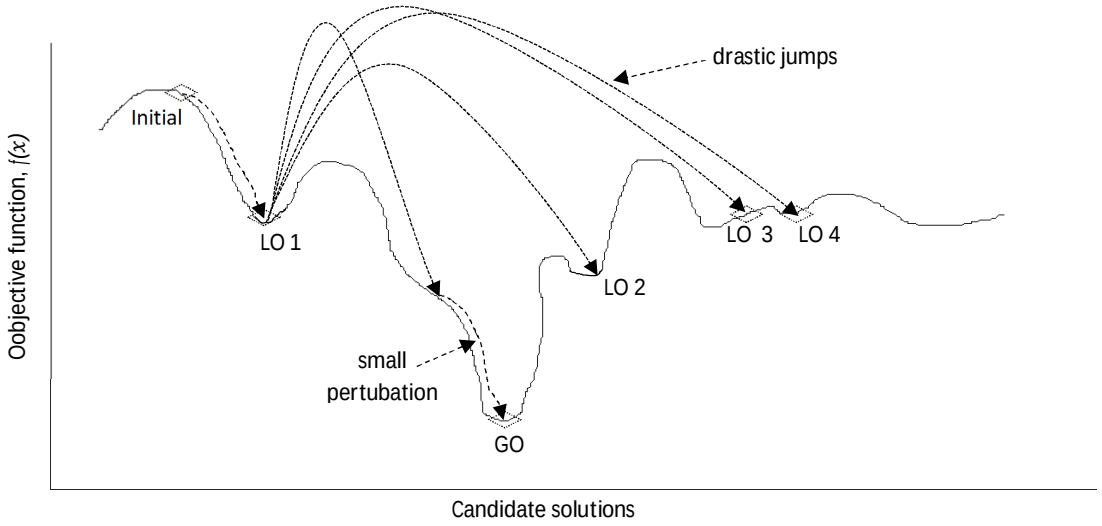

Figure 9.3: Optimality regions within the space, with the candidate solutions.

The optimality plane in Figure 9.3 contains at least three LO and one GO. If the solution gets trapped into the smaller slope, the heuristic will direct the search towards the bottom of LO, usually occurs when the algorithm covers only limited ranges of candidates. This leads to a premature stop at the various LO. As GA works in a stochastic and unpredictable manner, a random sampling of its solution, determined by the crossover and mutation rate, helps to create new candidates solutions and a wider coverage of them in the subsequent generations, shown by the drastic jumps made by the solution from LO1. The altering of the nearby genes within the group also allows some small perturbations which further optimizes the trajectory to the GO as seen in the figure. Another cause for premature halt of the search process is by a no progression after a sustained period of time, called stalling. In other words, poorly formulated problems can often lead to premature convergence and suboptimal solutions [147].

The choice of parameters (population size, crossover rates, etc.) can have a significant impact on the computational complexity and convergence characteristics. In general, the most significant parameters impacting the performance of the solver are: population size, crossover rate and mutation function [148]. A proper balance between the exploration and exploitation ability of GA is desirable but difficult to predict *a priori*. In intuitive explanation, exploration means the searching of the search space as thoroughly as possible while exploitation means the discovery of potentially good solution concentrated in one space. Mutation operators are mostly used to provide exploration while crossover operators are used to promote exploitation. Concurrently, while the crossover works to converge to a specific point in the search space, mutation tries to avoid

convergence and potentially explore all areas of the search space. Vasconcelos *et al.* [148] described multiple GA configurations and highlighted the importance of the balance in mutation, crossover rate and population size. Siamak [149] also investigated the parameters affecting GA performance with population size of 100. In general, as the GA is a stochastic optimisation method, there are no absolute rules for determining these parameters.

However, it is generally accepted that more exploration is appropriate in the beginning of the search process, ensuring the population has the widest coverage while maintaining a certain level of diversity. Furthermore, exploitation is generally better suited to the end of the process to ensure convergence of the population to the global optimum, or GO, as seen in Figure 9.3.

9.4.1 Population Size

Smaller size GA population generally yields faster convergence but the algorithm can be more easily trapped in local optima as there will be less diversity [150]. A large population size however would help the solver as the greater diversity will by necessity cover more of the search space, at the cost of more resource [151].

9.4.2 Mutation Rate

Mutation is a divergence operation intended to occasionally introduce new points into the population away from the current optimal solution, guaranteeing that the probability of searching any given point is always greater than zero, and a drastic jump would increase the likelihood of locating the global solutions and specifically, sifting throughout the candidates for GO, such as those depicted in Figure 9.3.

However, this should not happen too frequently as it can be quite disruptive to convergence, hence a low value (0.005 to 0.01) is typically recommended [152], [153], otherwise convergence may be delayed or not achieved. The Matlab GA Toolbox [154] contains a helpful function in which the Adaptive Feasible Mutation Rate [155] can be utilised. It works by randomly generating directions and step length that are adaptive with respect to the last successful or unsuccessful generation.

9.4.3 Crossover Function

Crossover behaves like a convergence operation intended to pull the population towards the optimal point(s). Since the end goal is to bring population to a convergence, crossover could desirably be higher than the mutation rate. Recommended crossover probability for large search spaces would be typically > 0.5[152]. Here, the initial crossover rate was set to 0.75, experimentally feasible according to the past studies (see, for example, [152], [156]).

9.4.4 Number of Generations

In the general case, the best way to identify the probability would be to do a sensitivity analysis, by running multiple trials in error tests with different probability of mutation and crossover function rates, and to compare the results as will be presented later. Having discussed all of the above, if the problem is already a benchmark problem tested and verified by past researchers, it is reasonable to start from the parameter values suggested in the literature. In our test, the original parameter values from R&P's model will be used as a basis for seeding the population.

Experiments were performed to get the best GA configurations with GA population size varied between 20 – 100, crossover rate varied between 0.1 -1.0 and the mutation rate varied in the range

of 0.005 to 0.01. Each experiment was repeated 10 times and the mean of performance is presented. The test is done to all of the subjects' dataset, using k-fold validation method as presented in Section 3.1.1.

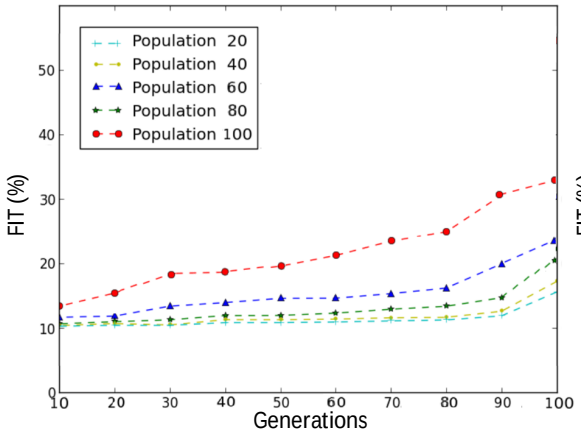

Figure 9.4:Various population size and their FITs after generations.

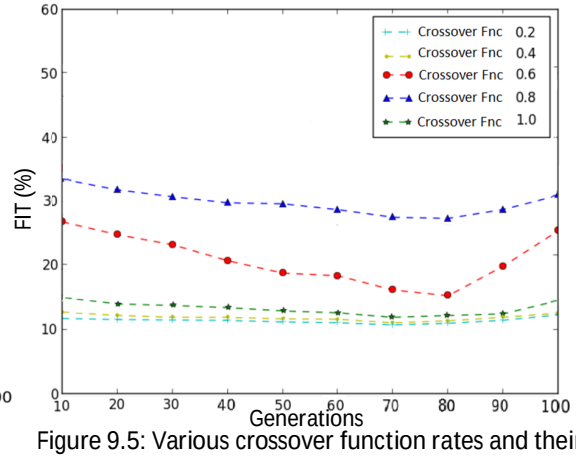

Figure 9.5: Various crossover function rates and their FITs after generations.

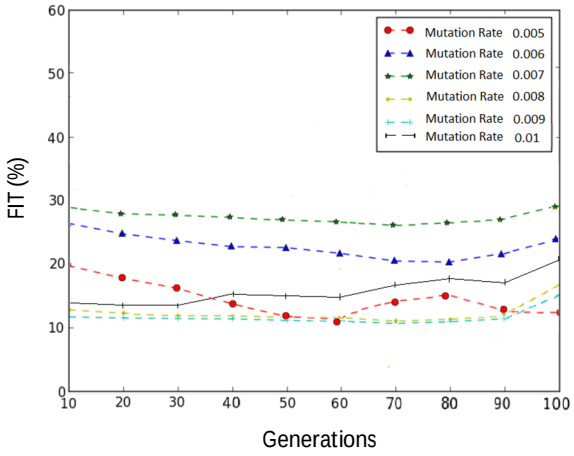

Figure 9.6:Various crossover function rates and their FITs after generations..

Figure 9.4 depicts the various population sizes and the respective FITs. Generally, the use of a large number of population size gets the best performance because the search can be done more widely and the chances of the solution getting stuck at LO reduced. The small population size could also mean a much longer time and more generations are required before a high FIT is attained. Figure 9.4 depicts that a population size of 20 garnered the lowest FIT and improvement even after over 100 generations, while higher population sizes see increased FITs, especially with 100 population.

On the other hand, in a small population size, the crossover and mutation rate are the high determinant for its performance, evident in Figure 9.5 and Figure 9.6. It was shown that a crossover fraction rate of 0.6 and 0.8 were the better values, and others which shown less FITs may show that it may require more time for the search, or the search can end prematurely. In Figure 9.6, the mutation rate of 0.006 and 0.007 were shown to obtain the two highest FITs. The figure also depicts a solution that was probably stuck in a LO, where in the test with mutation rate set at 0.005, the

FIT initially decreased but then increased, only to decrease again, most probably due to insufficient rate of mutation preventing the solution to expand presumably from a LO. However, in this case, it appears that a higher mutation rate does not actually guarantee a faster and more efficient solution, with mutation rate of 0.01 did not perform the best, probably due the search plane being too much widened and the exploration requiring more time.

Based on the result from the varied population size, crossover and mutation rates, we then tested a combination of mutation and crossover rates to observe the corresponding FITs. This time, the population was set to 60 to match the earlier commendable performance shown in Figure 9.4. The result gave out the combination of 0.6 and 0.007 (crossover and mutation rate respectively) producing the best FIT within the lowest time as displayed in Figure 9.7. This also means that the best combination of the rates did not necessarily come from the highest attained FIT in each separate test.

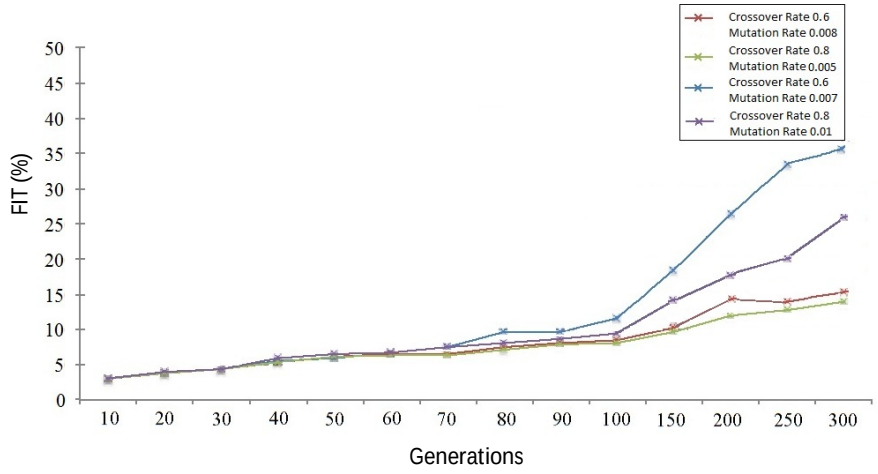

Figure 9.7: Various sets of mutation and crossover rates and the corresponding FITs.

Another assessment was done to evaluate the convergence of solutions, in specific, the performance of FITs alongside the needed iterations limit (Note that the number of iteration and generation may differ). With the test, a time limit can be set accordingly to allow sufficient processing time while reducing CPU wastage.

During the simulation, the iteration limit was gradually increased from 1k to 50k at every hour, incremented in each test, and the FITs value obtained was recorded. Two tests catering two sets of the combination of different mutation and crossover rates, were done for comparison and selection of the most appropriate setting. The result is presented in Figure 9.8.

Figure 9.8 shows the trend between the two investigated sets of mutation and crossover rate. It can be observed that at lower iteration (1K-12K), only a handful of them converged at FITS of 3-10%, indicating the inadequacy of time to complete the search, ending the solution with some premature results. However, as the limit being increased (e.g. 12K-22K) the results show some improvement as better convergence and high FITs are attained, applying to both of the sets (see zone A).

A further increase of the limit (e.g. 20K-32K) shifted the FITs obtained into zone B, showing better FITs than the earlier solutions. In essence, the algorithm was shown to mostly converge at this range. Allowing higher iterations further increased the FIT to 32% and 34.5%, with obtained FITs showing comparable difference between them, where the blue dots solution (mutation rate 0.007, crossover rate 0.8) achieved higher FIT, before they stalled at around 35%. In the case of the red dots solution (mutation rate 0.006, crossover rate 0.6), the solution stalled lower, at 32 % FIT.

At this point, any increase of the iteration only shows limited improvement, depicting unnecessary further increase of the iterations. Essentially, higher iterations limit set will only lead to wastage of CPU usages as the algorithm will continue to run until the limit is reached as observed in zone C, while only keeping the FITs value stagnant. Therefore, the following tests will utilise a maximum iteration of 35k.

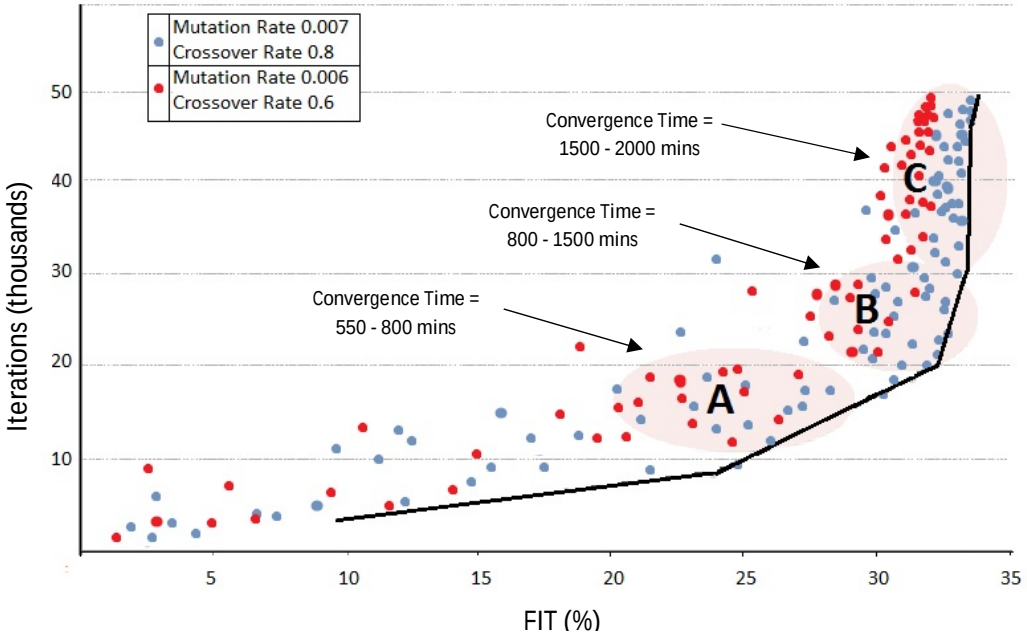

Figure 9.8: Performance of sets of different mutation and crossover rate and their respective iterations.

9.5 Multi Objective Genetic Algorithm-Driven Non-Stationary Physiological-Based Model (MOGA-NSPM)

A diagram that shows the flow process of MOGA-NSPM is illustrated in Figure 9.9. Initially, a number of values are set for the GA parameters such as the population size (set at 60), mutation and crossover rate (0.07 and 0.8 respectively), the number of objective functions (two), the number of parameters to be optimised (6), stopping criterions (time limit, number of generations, number of stall generations) and also the plot function.

Initial solution was then generated with the set population size, including the reference parameters derived from R&P studies, as presented in Section 9.2. In the first iteration, one BG dataset from subject m=1 is selected randomly for training of the model. Following this, other datasets (n^{max}) from subject m are then simulated and for each simulation, the RMSE value was calculated against measured BG to find their FIT. The process was repeated (n +1) until the FITs for all datasets were calculated for subject m. Afterwards, the same process was repeated for subject m+1 until all volunteers within the cohort were evaluated. With all the FITs obtained from the subjects tested, their mean FIT and mean SD were then calculated. Then, these two variables set as maximisation and minimisation problems are evaluated. The operations repeat with the next generated solution until the stopping criterions are satisfied, and one final solution is then produced at the end of operation, denoting the optimised parameters.

In short, a set of parameters is evaluated on every individual's glucoregulatory system, modelled and fitted to their measured BGC data, and afterwards the mean FIT and standard deviation FIT are computed. Then, using GA, a new parameters set is generated and fitted again. Multiple repetitions of this process will refine the set of parameters until finally the process stops upon meeting the stopping criterions. Since the operation was done throughout all volunteers, it is hoped that this will result in optimised parameters which after numerous enhancements eventually become feasible to the whole cohort.

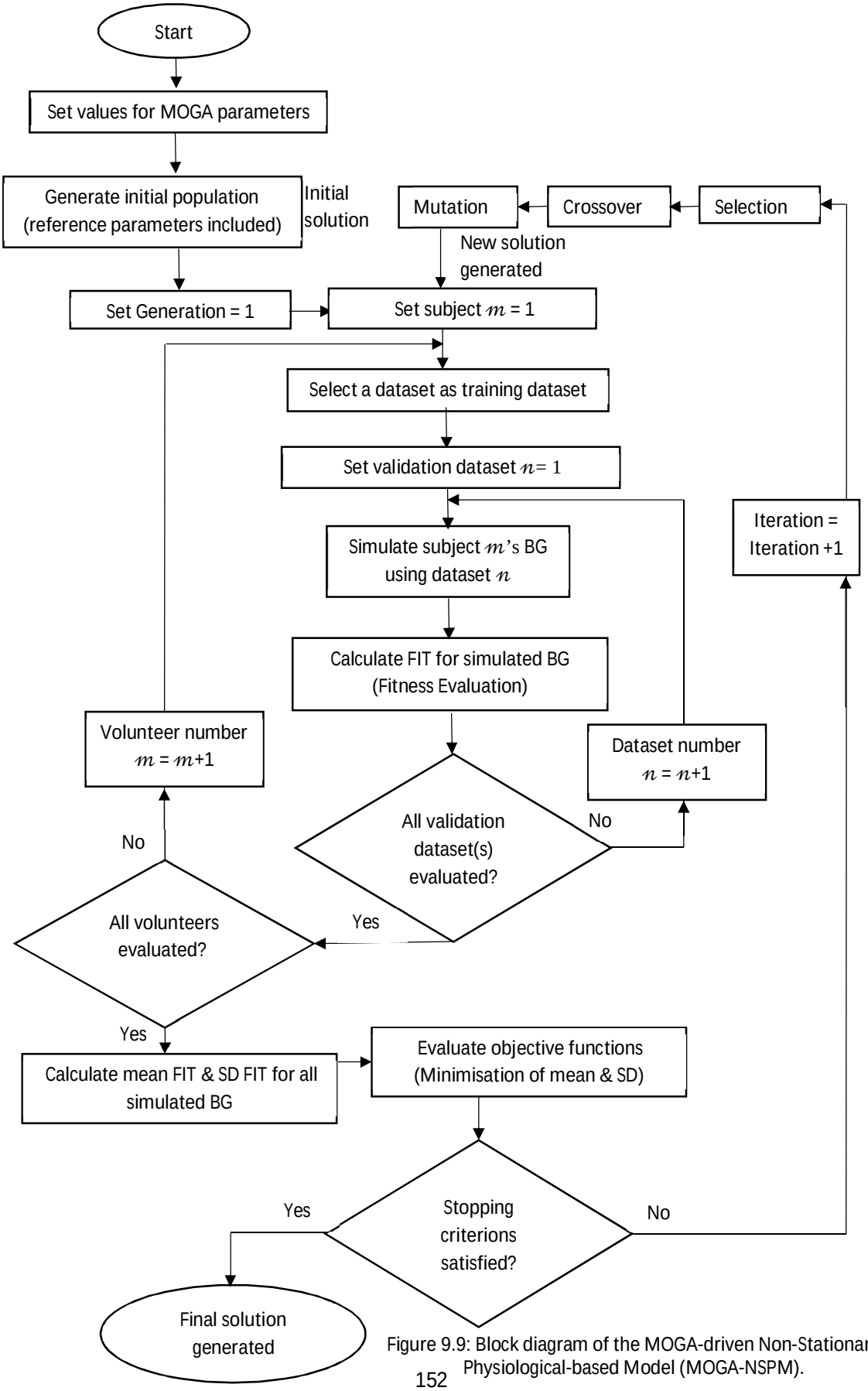

Figure 9.9: Block diagram of the MOGA-driven Non-Stationary Physiological-based Model (MOGA-NSPM).

9.6 Implementation

The test will be done in the Matlab environment using the built-in GA toolbox [43]. Optimisation is a resource-hungry operation, particularly for non-gradient based methods such as this. Our test has 6 variables to be optimised and these are to be evaluated across 22 volunteers. In practical, the test spans all of the volunteers consisting various status and lifestyle for a diverse and unbiased result. A multi-objective optimisation task, with multiple volunteers each having 3-4 datasets of many days, therefore requires high computational resources to find suitable solutions for the parameter sets.

To ameliorate the very large computational burdens, the University of Southampton's powerful supercomputer cluster, Iridis 4 [157], will be utilised. Notable specifications for the supercomputer are login nodes bearing 2.6GHz Intel Sandybridge processors, with each compute node having 16 cores and at least 4GB of RAM per core. These specifications are sufficient to perform the optimisation.

9.6.1 Parallel Approaches to Speed Up Operation

The multi-core functionality will be utilised fully by using the Matlab Parallel Computing Toolbox [158] that lets us solve data-intensive problems capitalizing on the multicore processors in the computer cluster [159].

The nature of this optimisation task is highly repetitive, where GA-generated parameters are tested with the equations inside our model until the conditions are satisfied. A useful Matlab function called the `parfor` loop, designed for parallel-tasking problems where statements within the loop body are iteratively executed not within the same machine, but distributed by the host to the workers (dependent on number of cores) as in Figure 9.10. Each worker has its own unique workspace. Therefore, data needed for calculations are sent from the client to the workers, before being sent back to the client and pieced together. Due to this, Matlab requires knowing which information will go to which worker and what variables will be returning to the client, prompting the need for data transparency and placed constraints when using this function [160]. Examples of such constraints are global variables which cannot be defined within the body of a `parfor`-loop. Sliced variables in loops must also be indexed appropriately so that `parfor` can easily distribute the right part of the variable to the right workers [160]. Figure 9.10 depicts the distribution of jobs from the client to workers in a `parfor` operation. The job is distributed to three workers, typically representing the three processors used in the node. The number of processors usable in one node vary between supercomputers. In our case, the maximum number of processors that can be used are 16 (1 node).

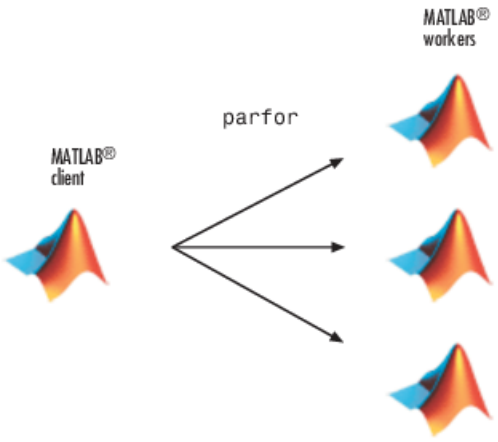

Figure 9.10: Distribution of jobs from the client to workers in Matlab `parfor` operation. Reproduced from [160].

9.6.2 Technical Issues in Implementation

A number of technical issues with parallel implementation of GA on the supercomputer platform under Matlab were encountered. They are briefly described below together with their solution.

1. Cholesky decompositions failed to compute.
   A requirement while implementing Gaussian processes and their approximations require an inversion of a symmetric positive definite matrix [105]. The efficient way to do this is via the Cholesky decomposition. Because the GA generates the random eigenvalues numerous times to test for optimal solutions, there are at times the generated eigenvalues becoming non-positive, resulting in a non-positive matrix, followed by the failure in the Cholesky decomposition computation. Failure in the computation was found to be derived from numerical precision errors, due to very small negative eigenvalues being very close to zero.

   The issue was resolved by evaluating each particular matrix in each computation and when eigenvalues are found to be negative, conversion to the nearest Symmetric Positive Definite Matrix as was proposed by Higham [161] was implemented. Finally, because the matrix is converted to unit diagonals to represent a covariance matrix, it thereby now has values very close to the original solution generated, as well as being positive-definite.

2. Inability to monitor progress in cluster environment.
   Matlab graphical user interface environment by default provides a user-friendly preference to see the progress while a program is executing. Using the plot functions, GA can plot for use the respective Pareto front, current best fitness, score diversity, best individuals and others. There is also a stop button function on the plot for the ease of stopping during execution, a convenient feature where a user can stop the program (which can go up to days) while still keeping the result. This is very helpful, otherwise the time limit must be predefined by the user and then cannot be stopped during operation or the loss of data occurs, unless this function is utilised. Unfortunately, for the computer cluster used, there is no user interface (UI). Because the cluster environment was designed for multiple platforms and various programming languages, it can only cater for a minimal UI, significantly reducing a user's ability to monitor and respond to a running program. Hence, the time limit must be wisely chosen by the user because it can no longer be altered once

it starts operating, until executions finishes. With the Iridis cluster, you can only see the status of submitted jobs and fetch the results once they complete.

3. Time limit option ignored in optimisation run.
   Albeit a time limit has been predefined in the optimisation options, it appears that the programs executed always exceed the pre-set stop time. Numerous times, programs failed to complete after days of waiting due to this problem. Because the cluster environment only allows limited wall-time limit, the running program will automatically be halted whenever it fails to adhere to the requested wall-time, resulting in a total loss of data. Although this can be resolved by increasing the wall-time limit, there is a limit of 120 hours of maximum allowed cluster time in Iridis 4. Apart from this, an ample extra time (up to 20 hours) has been allocated to the GA and yet the program still failed to finish within the allocated time.

   The situation is further made difficult by the lack of monitoring, while a lot of time have been wasted due to the waiting time only to find that it failed to complete within the stipulated wall-time. There is no other way other than via UI to stop Matlab manually while keeping all data. There are a number of possible reasons that could result in the above problem.

4. TimeLimit option available in Matlab GA was ignored due to the way `parfor` function works.
   Because parallel computation works by the distribution of jobs by the host to workers, the host does not incur CPU time at all while waiting for the results. Upon the results being returned back to the host, they were only to be speedily computed for a new population and then sent out to the workers again. As a result, significant amounts of actual time are overlooked leading to job being over-run. One way to solve this is by specifying extra wall-time, adequate enough for the host to complete the whole run using CPU time. Another way to do this is by incorporating a stop function whenever an output function is called, by having the actual time of the cluster PC made as reference rather than the default CPU time. The latter solution was found to work with this problem.

5. Related to the previous problem in (c), one of the reasons for the failure of completion within predefined time limit is the infrequent call of the output functions, whereby it is only called in each iteration, and not every time an objective function is called. Each iteration however could be function evaluations over each individual in the whole population, running to the thousands of iterations. The way to cope with this is to find the balance between mutation rate, crossover rate and population size. All of these variables give particular convergence rate dependent on the trade-off between them, best done using sensitivity analysis and multiple tries of different configurations.

9.7 Results

Using the final solution generated, the value of FITs and RMSEs (as presented in Section 2.8) for all subjects' datasets are calculated for a direct comparison against the result in the previous chapters. The summary of the FITs and RMSEs are recorded in Table 9.2 and Table 9.3.

The respective Pareto Front, depicting the conflicting objectives with their solutions is displayed in Figure 9.11. It can be observed that there are much more points scattered around the first objective plane, and much less on the second, before they converge together at the trade-off curve. The less scatter of solutions depicting low marginal differences between them in the second objective's plane was due to the fact that it is actually dependent on the changes in the first objective's solutions. As discussed earlier, the conflict occurs only when a new better solution was introduced in the first objective (increase of mean FIT), raising its current SD. However, MOGA then sets to find solutions to minimise the second objective, counter-reducing the SD. With the many iterations, as more and more solutions produced values of FIT close to each other, their mean increased but their spread (SD) decreased.

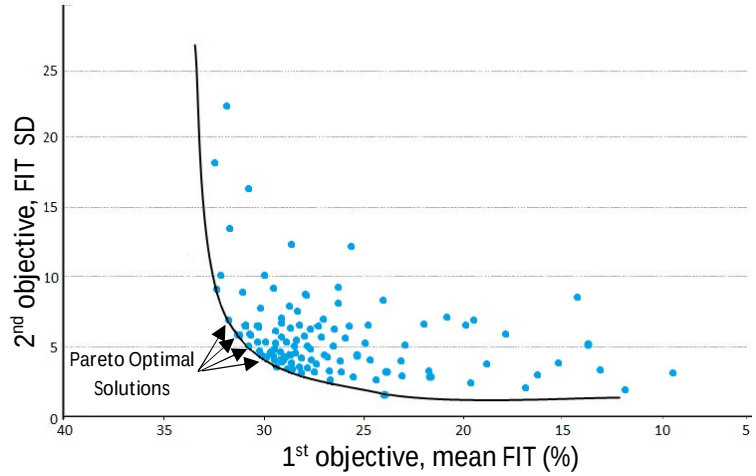

Figure 9.11: Pareto front of the two objectives, mean FIT and SD.

From Table 9.2 and Table 9.3, it is noticeable that MOGA-NSPM performs significantly better than the rest of the models. This includes models tested previously like the standard GA, NSGP and NSPM. In this result, not only the average percentage of FIT is much higher (32.7 %) compared to predictions using standard GP (-5.2 %), but better predictions are seen in terms of the number of predictions made (From all 44 predictions of unseen data, 33 achieved better FITs than standard GP). The better average FIT for MOGA-NSPM is also seen over NSGP and NSPM models, with the former taking 3.1 % and the latter -6.1 % FIT for short term prediction horizon. They remain true also in the long-term prediction horizon (MPO). Note that the comparisons are made to all models which included Heat Flux and METs data as the physical activity inputs (NSGP (Test iv) and NSPM (Test ii). The detailed one-to-one result comparison can be seen in Table 9.6.

Type of predicted data	60 minutes prediction				MPO (infinite-step ahead prediction)			
	Standard GP	NSGP	NSPM	MOGA-NSPM	Standard GP	NSGP	NSPM	MOGA-NSPM
Validation Data (%)	-5.2	3.1	-6.1	32.7	-51.0	-49.2	-54.9	10.7
Training Data (%)	69	60.2	67	10.9	29.2	17.3	34.6	-47.4

Table 9.2: FIT summary of prediction for validation and training datasets.

Type of predicted data	60 minutes prediction				MPO (infinite-step ahead prediction)			
	Standard GP	NSGP	NSPM	MOGA-NSPM	Standard GP	NSGP	NSPM	MOGA-NSPM
Validation Data (%)	2.8	2.6	2.9	1.3	4.0	3.9	4.1	2.1
Training Data (%)	0.5	0.6	0.5	2.4	1.1	1.3	1.0	3.9

Table 9.3: RMSE summary of prediction for validation and training datasets.

Based on the results, this shows that a model which utilises a multi-objective optimisation technique, along with the reference parameters from R&P studies as the initial solution, is indeed a feasible and worthwhile experiment to test upon.

Another relevant observation is that, surprisingly, predictions with seen data did not show better performance than those of unseen data. In terms of average FITs, they also did not show improvements over prediction using standard GP, while the total number of prediction also showed that out of 22 predictions (with seen data), only 5 were better than that of standard GP. This is a contrast to the better predictions with unseen dataset. However, this does not mean that they perform inadequately. Despite the lower average and total number of FITs, all the values were already adequate for general control-predictive purposes and all predictions actually succeeded in tracking BG levels (average FITS for just training data were 10.9 % and -47.4 for short and infinite horizon, respectively). A depiction of this statement is in the prediction plot of 'seen' data in Figure 9.12. It can be observed that despite the downsides mentioned, the model can still track sufficiently measured BG albeit missing some magnitudes. Plots for prediction of 'unseen' data are illustrated in Figure 9.13 and Figure 9.14 for the same volunteers as presented earlier (They show that even with the data from the poorest-predicted BG in subject #23's result, oscillatory behaviour was tracked by MOGA-NSPM with ease, as illustrated in Figure 9.14(c)).

The fact that prediction with seen data does not make better FITs indicates that the optimised values themselves are already good enough for prediction, even without the use of dataset training. Therefore, the enhanced prediction was not due to the performance of the GP model but actually the accuracy of parameters obtained from optimisation themselves.

This is valuable and desirable to clinicians interested to improve prediction ability of BGC in diabetes patients. One of the multiple sets of optimised values from the pareto front, alongside those proposed by R&P are shown in Table 9.4.

Parameter	R&P'S value	MOGA NSPM's value	Lower limit	Upper limit	Unit
a_1	0.00158	0.0106	0.0013	0.0019	mg/kg·min2
a_2	0.056	0.3498	0.0441	0.0679	1/min
a_3	0.00195	0.0016	0.0015	0.0024	mg/kg·min2
a_4	0.0485	0.0601	0.0355	0.0617	1/min
a_5	0.00125	0.0018	0.001	0.0015	μU/ml·min
a_6	0.075	0.0506	0.0588	0.0912	1/min
k	0.0108	0.0108	0.0085	0.0131	mg/kg·min2
T	6.0	6.0	1.86	10.14	min

Table 9.4: Optimised and original values from R&P's model.

It can be seen that although there is little difference between optimised values and original ones, the former still produced vast improvements over conventional GP models in terms of the model's prediction capability. Note that both the upper and lower limits set pre-optimisation were also observed, indicating values lying within the reasonable range. We can confidently say that the values can be used in future research or clinical assessments.

As usual, a comparison from MOGA-NSGP results (RMSE values) to the previous studies is made, depicted in Table 9.5.

Work	Model	FIT (%)	RMSE ($mmol\ l^{-1}$)	No. of Subjects
Gani *et al.* [49]	AR	n/a	0.7	9
Finan *et al.* [88]	ARX	35	2.2	9
Valletta [9]	ARMAX	31	2.0	22
Cescon *et al.*	ARX	n/a	1.9	9
Cescon *et al.*	ARMAX	n/a	1.7	9
Pérez-Gandía *et al.*	Neural Network	n/a	2.5	9
Georga *et al.*	SVM	n/a	1.4	7
MOGA-NSPM	Phycological-Based Model with GA Optimisation	32.7	1.3	22

Table 9.5: Comparison of MOGA-NSPM to previous studies (one-hour prediction).

This time, MOGA-NSGP managed to surpass tests from all works, even with the one that include physical activity incorporated into the model (Georga *et al.*). It also shows that the comprehensive literature finally shows the much-awaited improvements, without disregarding the bodily physiology behind.

Subject ID	Dataset	Standard GP (Hf + METs)				NSGP Test iv				NSPM Test ii				MOGA NSPM			
		60 mins		MPO		60 mins		MPO		60 mins		MPO		60 mins		MPO	
		FIT	RMSE	FIT	RMSE	FIT	RMSE	FIT	RMSE	FIT	RMSE	FIT	RMSE	FIT	RMSE	FIT	RMSE
01	1	-11.7	2.3	-22.9	2.6	3.5	2.0	-14.2	2.4	-16.0	2.4	-21.6	2.5	19.4	1.9	17.6	2.5
	2	76.8	0.4	70.5	0.5	63.1	0.7	56.8	0.8	70.8	0.5	60.3	0.7	60.3	0.7	57.0	0.8
02	1	4.4	1.6	-79.1	2.9	6.3	1.5	-88.3	3.1	12.1	1.4	-4.3	1.7	20.8	1.3	8.7	1.8
	2	-7.5	2.1	-41.9	2.8	-5.7	2.1	-46.8	2.9	-0.5	2.0	-21.9	2.4	12.4	2.2	-25.7	2.5
	3	78.1	0.4	73.1	0.5	72.4	0.5	64.5	0.6	73.1	0.5	34.4	1.1	65.1	0.6	59.9	0.7
03	1	4.6	2.3	-84.0	4.4	14.8	2.0	-96.5	4.7	-3.1	2.5	-81.1	4.3	24.9	1.8	-55.3	3.7
	2	68.9	0.9	13.4	2.6	57.3	1.3	-14.3	3.5	68.8	0.9	39.8	1.8	61.8	1.2	49.7	1.5
	3	13.4	2.4	-150.8	6.9	38.6	1.9	-26.9	3.9	29.8	2.2	-29.2	4.0	38.2	1.9	-13.9	3.5
05	1	-3.2	2.5	-20.2	2.9	0.1	2.5	-6.3	2.6	4.3	2.3	-10.9	2.7	20.1	2.0	-7.9	2.6
	2	68.6	0.8	55.2	1.1	53.5	1.1	-7.9	2.6	67.0	0.8	26.4	1.8	42.0	1.4	1.1	2.4
06	1	-79.2	3.0	-184.3	4.7	-58.0	2.6	-307.0	6.7	-95.6	3.2	-282.9	6.3	36.7	0.3	-116.3	3.6
	2	-3.2	2.9	-86.1	5.3	22.1	2.2	-74.2	5.0	2.9	2.8	-81.1	5.2	34.7	1.9	78.6	0.1
	3	75.2	1.1	41.8	2.5	68.4	1.4	-24.1	5.4	76.3	1.0	68.5	1.4	64.3	1.6	41.9	0.5
07	1	79.6	0.5	33.5	1.6	60.4	0.9	5.9	2.2	67.6	0.8	43.8	1.3	49.5	1.2	-8.1	2.6
	2	5.1	2.6	-11.6	3.0	18.3	2.2	-20.1	3.2	27.0	2.0	8.2	2.5	35.7	1.7	-26.7	0.4
08	1	66.1	1.1	15.3	2.8	66.3	1.1	33.0	2.3	67.3	1.1	21.4	2.6	53.8	1.6	22.1	2.6
	2	22.8	3.7	-6.3	5.0	30.5	3.3	4.1	4.5	21.8	3.7	-16.4	5.5	27.9	0.4	-13.9	5.4
09	1	64.8	0.8	29.8	1.6	63.3	0.8	16.0	1.9	68.6	0.7	41.2	1.3	51.3	1.1	5.4	2.1
	2	26.3	1.6	-42.6	3.1	19.9	1.7	-49.9	3.2	5.4	2.0	-29.6	2.8	14.6	1.8	-26.5	2.7
10	1	68.5	0.7	53.2	1.0	58.5	0.9	25.4	1.6	71.0	0.6	47.9	1.1	54.0	1.0	28.6	1.6
	2	3.6	3.0	-2.6	3.2	9.6	2.8	2.2	3.1	16.8	2.6	10.0	2.8	20.8	0.5	4.5	3.0
	3	16.1	2.6	-2.0	3.2	19.1	2.5	1.5	3.1	21.7	2.4	15.8	2.6	22.9	2.4	0.0	3.1
	4	2.4	3.4	-2.7	3.6	1.1	3.4	-0.7	3.5	-16.3	4.0	-32.4	4.6	94.3	0.6	-6.3	3.7
11	1	11.2	3.9	-16.6	5.2	2.4	4.3	-23.5	5.5	-12.2	5.0	-44.9	6.4	22.8	0.4	-3.0	0.3
	2	65.9	1.0	33.8	2.0	62.3	1.2	15.9	2.6	64.6	1.1	16.7	2.5	55.5	1.4	28.9	2.2
	3	31.7	2.5	2.7	3.5	51.6	1.8	2.5	3.5	36.5	2.3	-10.6	4.0	50.1	0.8	-23.2	0.5
13	1	64.0	1.4	57.9	1.7	63.2	1.5	51.3	1.9	72.6	1.1	62.3	1.5	59.5	1.6	57.1	1.7
	2	20.1	3.0	8.8	3.4	21.7	2.9	8.4	3.4	23.8	2.9	11.4	3.3	17.8	0.1	-27.0	4.8
	3	1.2	2.8	-20.3	3.4	5.1	4.9	-4.3	5.4	14.3	4.4	9.1	4.7	21.8	0.0	8.9	4.7
	4	5.7	3.9	-19.9	4.9	-3.5	2.9	-42.6	4.1	-19.8	3.4	-35.9	3.9	24.4	3.0	110.3	6.0
14	1	-32.5	3.7	-62.4	4.5	-4.9	2.9	-44.9	4.0	-23.6	3.4	-88.9	5.3	16.0	0.3	-16.4	3.2
	2	58.6	1.8	-4.8	4.4	61.9	1.6	15.9	3.6	58.7	1.7	21.6	3.3	50.4	2.1	9.6	3.8
	3	-25.2	3.8	-38.5	4.2	-8.1	3.3	-36.5	4.1	-2.4	3.1	-71.5	5.2	25.2	0.3	-9.0	3.3
	4	8.1	3.6	-2.6	4.0	30.0	2.8	8.0	3.6	24.2	3.0	7.7	3.6	27.1	0.9	11.0	3.5
15	1	2.9	2.9	-7.5	3.2	20.0	2.4	-9.9	3.3	7.4	2.8	-97.7	5.9	24.3	2.3	-44.9	0.3
	2	63.4	1.0	46.1	1.4	51.0	1.3	19.3	2.2	52.9	1.3	-40.1	3.7	44.5	1.5	16.1	2.2
	3	11.2	1.6	-36.3	2.4	25.7	1.3	-33.0	2.4	17.6	1.5	-111.2	3.7	29.4	1.2	-23.5	2.2
16	1	12.4	3.3	-14.2	4.3	25.8	2.8	-20.6	4.6	11.5	3.4	-18.3	4.5	16.1	3.2	51.8	0.0
	2	85.1	0.5	64.7	1.2	71.1	1.0	48.5	1.8	75.3	0.9	62.6	1.3	63.0	1.3	44.8	1.9
18	1	19.5	2.3	-53.2	4.4	29.2	2.1	4.6	2.8	33.5	1.9	-33.1	3.9	55.7	1.3	7.2	2.7
	2	47.6	1.7	-36.2	4.5	48.3	1.7	-43.1	4.8	67.5	1.1	53.5	1.5	43.7	0.1	-50.9	0.0
	3	-3.8	2.1	-90.0	3.9	13.1	1.8	-66.3	3.4	-17.0	2.4	-110.1	4.3	18.7	1.7	64.0	3.3
	4	-1.0	2.7	-82.7	4.9	26.7	2.0	-48.5	4.0	21.4	2.1	-13.3	3.0	46.2	1.4	-5.7	2.8
19	1	-8.3	3.4	-45.5	4.5	3.3	3.0	-38.9	4.3	-14.3	3.6	-41.1	4.4	6.4	0.9	-44.7	0.5
	2	-25.2	4.1	-76.8	5.7	-16.3	3.8	-63.3	5.3	-20.7	3.9	-46.0	4.7	17.3	0.8	-32.1	0.6
	3	71.0	0.9	44.6	1.8	63.2	1.2	17.0	2.7	70.7	0.9	54.5	1.5	54.4	1.5	17.9	2.7
20	1	77.9	0.8	26.6	2.7	67.4	1.2	18.2	3.0	73.4	1.0	49.8	1.8	55.6	1.6	36.7	2.3
	2	-76.4	2.7	-108	3.2	-105.8	3.1	-216.4	4.8	-127.8	3.5	-262.9	5.5	96.4	1.0	205.6	0.5
	3	3.2	2.8	-15.7	3.3	4.0	2.8	-24.0	3.6	2.7	2.8	-49.0	4.3	14.8	0.5	-30.8	0.4
	4	-26.6	2.6	-45.2	3.0	-24.0	2.6	-115.1	4.5	-66.4	3.4	-187.7	6.0	97.3	0.2	-80.8	3.7
21	1	69.9	0.8	15.6	2.2	56.5	1.1	23.4	2.0	72.7	0.7	49.5	1.3	60.1	1.1	26.0	2.0
	2	9.2	2.2	-33.5	3.2	14.2	2.1	-50.7	3.7	4.1	2.3	-25.9	3.1	22.4	2.5	105.8	0.5
22	1	34.1	2.7	2.9	4.0	29.9	2.9	-12.7	4.6	13.1	3.6	-13.0	4.6	67.5	0.2	-25.9	0.2
	2	78.4	1.0	53.7	2.1	76.9	1.0	52.4	2.2	80.5	0.9	47.3	2.4	68.8	1.4	34.9	2.9
	3	1.6	3.4	-7.9	3.8	19.6	2.8	-39.1	4.9	20.0	2.8	-38.3	4.8	42.4	2.4	168.2	0.4
23	1	51.8	1.6	11.5	3.0	49.0	1.7	21.5	2.7	51.2	1.7	30.5	2.4	43.2	1.9	19.9	2.7
	2	-79.5	2.8	-182.3	4.4	-63.6	2.6	-185.6	4.5	-96.0	3.1	-145.1	3.8	93.8	0.0	231.8	0.2
	3	23.2	2.6	-21.0	4.1	31.6	2.3	-39.7	4.8	29.3	2.4	-46.7	5.0	32.7	2.3	-34.6	0.4
	4	-103.8	2.9	-201.7	4.3	-81.4	2.6	-186.8	4.1	-82.9	2.6	-83.5	2.6	27.1	1.8	170.2	3.9
24	1	-26.3	3.8	-15.7	3.5	-38.5	4.1	-45.6	4.4	-43.9	4.3	-42.2	4.3	46.2	0.4	-52.3	0.6
	2	76.3	0.4	44.1	0.9	43.7	0.9	-1.6	1.7	47.2	0.9	15.5	1.4	35.1	1.1	-3.5	1.7
	3	1.0	2.6	-19.9	3.2	7.3	2.4	-13.6	3.0	9.5	2.4	-17.2	3.1	20.0	2.3	-5.2	2.8
	4	-10.5	3.6	-27.0	4.2	-17.0	3.9	-29.5	4.3	-15.6	3.8	-29.1	4.3	10.7	0.6	-29.3	0.3
25	1	3.7	2.0	-152	5.3	10.4	1.9	-42.0	3.0	0.2	2.1	-63.3	3.4	21.0	1.7	-64.1	0.4
	2	-2.5	2.9	-127	6.3	7.1	2.6	-32.9	3.7	-6.4	3.0	-140.5	6.7	4.7	2.7	59.7	0.5
	3	60.2	1.4	-100	7.1	47.2	1.9	-12.6	4.0	57.6	1.5	-45.9	5.2	41.4	2.1	22.5	4.3

Table 9.6: Results in various models with Heat Flux and Mets.

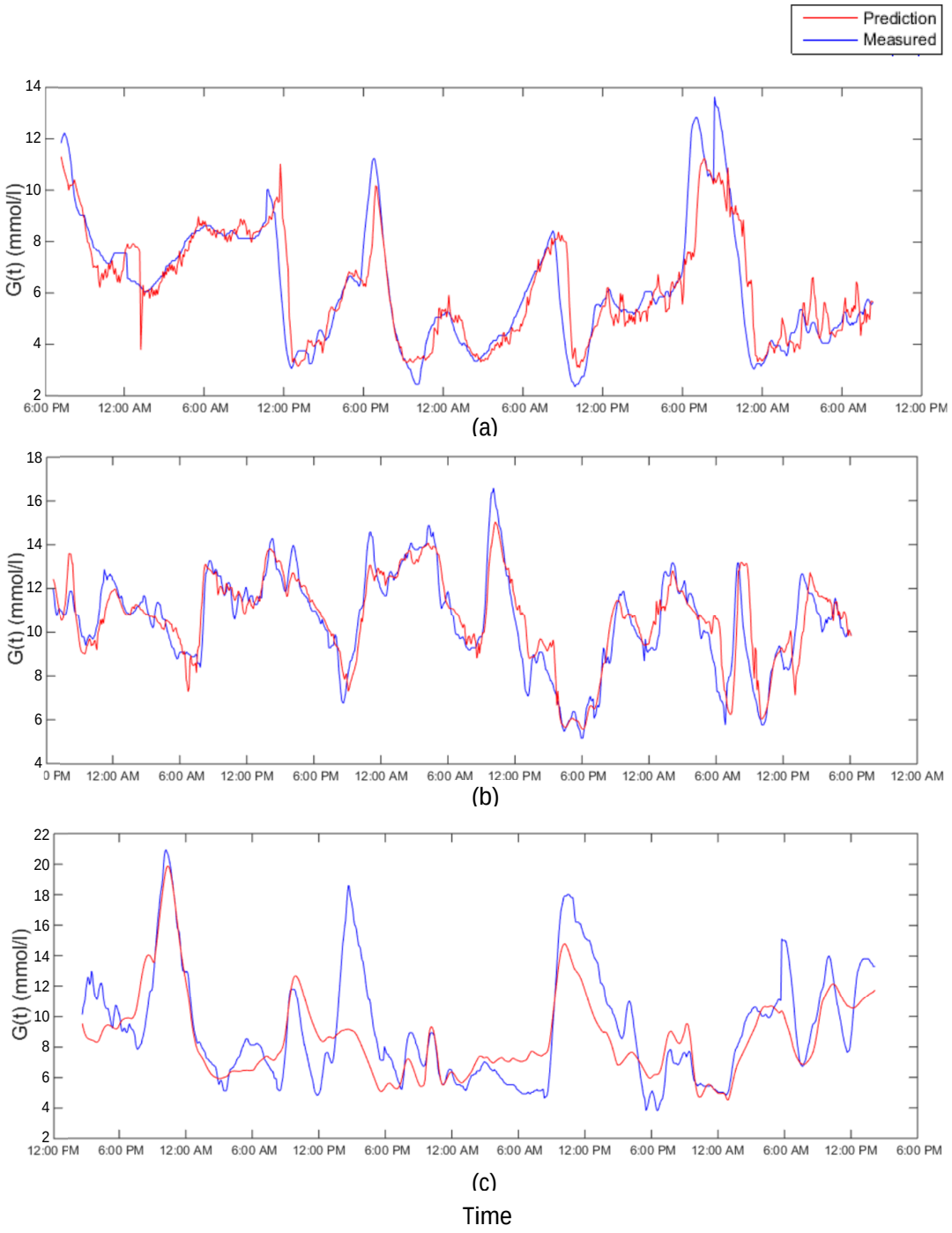

Figure 9.12: One-hour BGC prediction of seen data (training data) for subject #7(a), #10(b) and #20(c). (FITS were 49.5 %, 54 % and 55.5%).

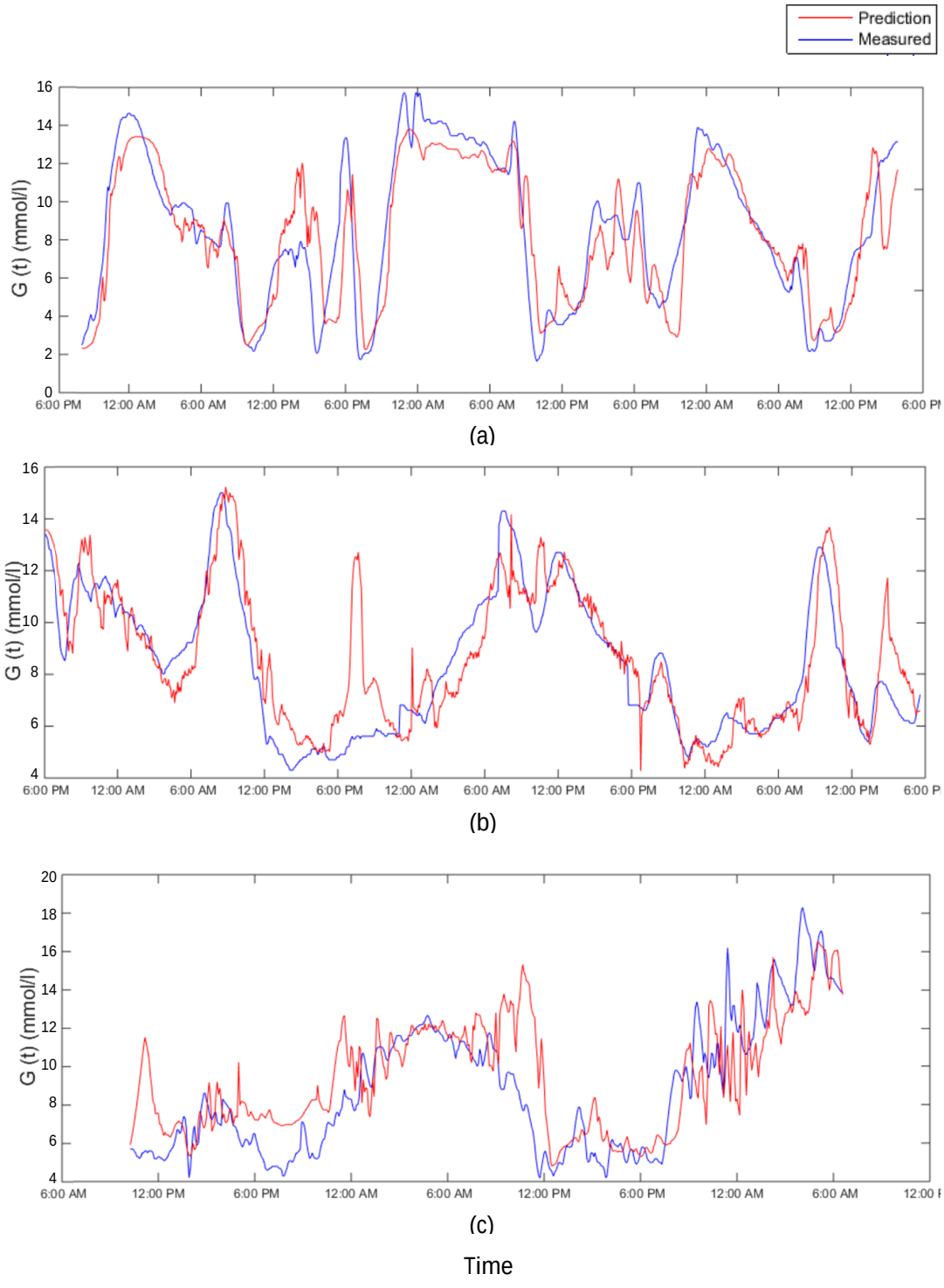

Figure 9.13: One-hour BGC prediction for subject #11(a), #18(b) and #23(c).

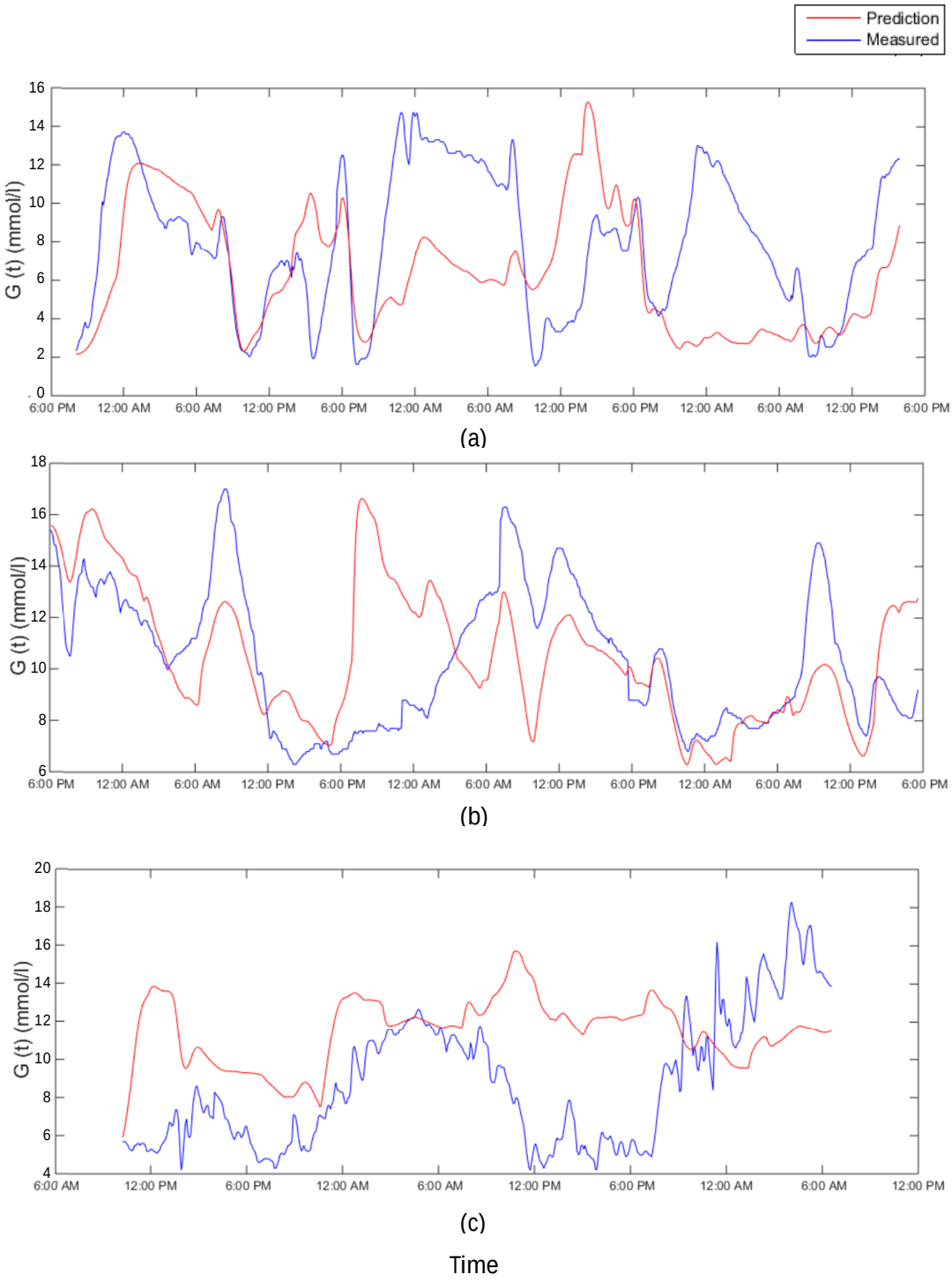

Figure 9.14: Model Predicted Output of BGC for subject #11(a), #18(b) and #23(c).

9.8 Contribution to the Body of Knowledge

In this chapter, an optimisation-based approach to modelling the BG response is proposed that is shown to improve the predictive capabilities of the original model. In a sense, this chapter presented a refined version of the R&P model that has been designed to predict BG values over a range of different volunteer characteristics rather than the one for an idealised human with synthetic data as originally presented. Physiologically, the parameters of the model have been identified from people with Type 1 diabetes rather than healthy volunteers as in the original work. Further, these parameters have been defined from a cohort of heterogeneous volunteers with a wide range in, for example, age, BMI, duration of diabetes and lifestyle parameters. Thus, the revised model should reflect the underlying system physiology more faithfully and has resulted in improved prediction when used with data from people with Type 1 diabetes.

The optimisation technique employed has been shown to improve the prediction ability by focusing on the parameter values within the model. The combination of non-stationary Gaussian processes multi-objectively tuned to the parameters identified by R&P was directed to improving the FIT measure between volunteers rather than for the training data. GA-ARX model in Chapter 5 with single objective optimisation saw successful refinements made onto the diabetes modelling parameters, but only confined to the same dataset. Indeed, the method provides better result but only for the respective person tested on, and cannot be generalised into a bigger group.

The use of a large-scale compute resource allows sufficient iterations to solve this computational intensive problem such that viable solutions that work for all the volunteers can be found. It is realistic to expect that if the NSGP model parameters has been identified with data from narrower subgroups, such as similar ages, BMI, gender, lifestyle, etc. that these predictions could be improved even further.

Chapter 10: Conclusions and Future Work

A variety of modelling approaches were tested using real free-living data from an open, non-randomised and uncontrolled DUK Study of people with Type 1 diabetes. The research continued from the work of Valletta [9] which studied the relationship between daily energy expenditure and glycaemic control using patient-acquired data in a free-living environment. In this study, the patient-acquired data were used to identify mathematical models for the response of blood glucose to carbohydrate ingestion, insulin administration and physical activity. The work presented here focused on developing a better model from those previously available to predict glucose-insulin dynamics alongside the complex parameters of a physical activity model.

10.1 . Conclusion

The first part of this work focused on discovering any hidden and correlated patterns exist within the volunteers' blood glucose data. A number of investigations were made to allow this objective to be achieved, such as allowing the algorithm to search for a predefined pattern in multiple datasets by concatenating them together. The latter was done to allow a motif search to be made throughout all volunteers' datasets to see if there were any recurring patterns that might reflect some correlation in lifestyle, eating behaviour, and physical activities. However, this motif search was inconclusive and found either non-related motifs or poor detection in other areas of the datasets. This might have been due, in part, to inaccurate or unreported impulses arising from meals and/or insulin intake.

An optimisation technique, GA-ARX, was employed to improve BGC prediction of a linear time-invariant ARX model, which saw an improvement in intra-patient modelling. The physiological equilibrium point of the body varies over time due to manifold reasons such as changes in insulin preparations, use of other medications and activity levels. Using the GA to regularly update the ARX model, some of these changes can be accounted for and tested against the individual's datasets. This helps to ensure that the model can follow some of the patients' current bodily metabolism despite any changes in the glucose-insulin-dynamics. However, to ensure the reliability of the model remains high, GA-ARX must update frequently with a short horizon of prediction.

Empirical Non-Stationary Gaussian Process models were able to describe local blood glucose response to carbohydrate ingestion and insulin administration, as well as the effects from physical activity. Physical activity data did improve the quality of the identified dynamic models although only to a small extent.

Due to the complications devising empirical models, the physiology behind glucose-insulin dynamics in Type 1 Diabetes was further investigated. The modelling of blood glucose dynamics without and with the presence of psychical activity was tested. A new compartmental model derived from R&P [133] but using free-living datasets from people with Type 1 diabetes was tested. Previously, such models have only been evaluated with synthetic data and parameters derived from healthy individuals. It was found that that the model did not perform comparably with this real data prompting further research.

The physical activity sub-model in the R&P model was reconsidered and, using relevant physiological basis, the modelling significantly affected by exercise was able to be improved. The final model, NSPM, was achieved by combining this model to the empirical model non-stationary Gaussian processes, which had shown noteworthy results with the physical activity parameter

added earlier. However, despite the well-founded physiological basis, the NSPM model did not manage to improve BG prediction, having poorer result than the previous NSGP.

With the intention of better PAEE sub-modelling, the R&P model was revisited and the parameters initially derived from healthy individuals was reconsidered. It was thought that this needed modification as a model based on parameters derived from healthy individuals might not reflect the dynamics of someone with Type 1 diabetes – the physiological constants are unlikely to reflect those in the individuals studied. Making use of the multi-objective genetic algorithm, two simple statistical measures were exploited for the objective functions to determine better physiological parameters for prediction. The heterogeneous cohort of Type 1 diabetics' data were used to drive the MOGA-NSPM model in search for better-suited parameters for the exercise minimal model. The combination of non-stationary Gaussian processes and multi-objectively tuned parameters for physical activity energy expenditure managed to improve the FIT measure between volunteers, thereby allowing intra-patient parameter values to be determined. This was indeed a different model than the GA-ARX model in Chapter 5 with single objective optimisation which saw successful refinements made onto the parameters, but only confined to the same dataset or volunteer.

10.2 **Further Work**

In general, the methods developed in this work have demonstrated that the result of MOGA-NSPM algorithm shows that the objective of this research was achieved. The combination of several methods that built the model appeared to produce a fruitful result. Some improvements and enhancements are proposed and highlighted as follows:

- Use a more user-friendly supercomputer to refine the models. The multi-objective optimisation method used was computationally expensive and largely time consuming. Some difficulties and limitations were discussed in Section 9.6.2, along with the minimal interface for using the supercomputer. In part, this is due to the university's facility having to cater for many software applications, apart from Matlab, hence the limited support. Various types of supercomputers have also created various different configurations that at times being troublesome when connected to the Matlab Parallel Computing Toolbox [162]. The use of a cloud-based-supercomputer, like the Amazon EC2 which powers Matlab workers on its own clusters [163], could be a better alternative allowing larger and more complex studies.

- The study data used here was heterogeneous by way of covering a wide range of ages, lifestyles and other volunteer demographics. Collecting free-living data from a more homogenous cohort (similar lifestyle, age, body composition, etc.) may help elucidate the factors contributing to differences in glycaemic control. It would be interesting to see how MOGA-NSPM would work within such a cohort and further investigations into the parameters derived for the PAEE-based model could be made.

- Identify the general model structures for blood glucose dynamics that can be personalised by adjusting parameters which characterise the individual, for example age, total fat mass, insulin sensitivity and cardiorespiratory fitness.

- Predict BG levels from further Type 1 diabetic cohorts using the modified physiological-based-model in Chapter 9 to test the viability of the estimated parameters. This opens the prospect of further studies on an artificial pancreas based on these models combined with model-based controllers.

References

[1] Diabetes UK, "Diabetes UK 2014," 2014. [Online]. Available: https://www.diabetes.org.uk/Documents/About Us/Statistics/Diabetes-key-stats-guidelines-April2014.pdf. [Accessed: 30-Mar-2015].

[2] City Population, "United Kingdom: Counties, Unitary Districts and Major Cities in England - Population Statistics in Maps and Charts." [Online]. Available: http://www.citypopulation.de/UK-England.html. [Accessed: 30-Mar-2015].

[3] C. D. Saudek, R. L. Derr, and R. R. Kalyani, "Assessing glycemia in diabetes using self-monitoring blood glucose and hemoglobin A1c.," *JAMA*, vol. 295, no. 14, pp. 1688–97, Apr. 2006.

[4] C. Sammut and G. I. Webb, Eds., *Encyclopedia of Machine Learning*. Boston, MA: Springer US, 2010.

[5] D. E. Goldberg, *Genetic Algorithms in Search, Optimization, and Machine Learning*. Addison-Wesley Longman Publishing Co., Inc., 1986.

[6] G. Williams and J. C. Pickup, *The Handbook of Diabetes*. Wiley-Blackwell, 2004.

[7] C. Cobelli, E. Renard, and B. Kovatchev, "Artificial pancreas: past, present, future.," *Diabetes*, vol. 60, no. 11, pp. 2672–82, Nov. 2011.

[8] A. M. Albisser, B. S. Leibel, T. G. Ewart, Z. Davidovac, C. K. Botz, W. Zingg, H. Schipper, and R. Gander, "Clinical Control of Diabetes by the Artificial Pancreas," *Diabetes*, vol. 23, no. 5, pp. 397–404, May 1974.

[9] J. J. Valletta, "Dynamic Modelling of the Effect of Habitual Physical Activity on Glycaemic Control and the Microvasculature in people with Type 1 Diabetes," University of Southampton, 2011.

[10] S. F. Michaliszyn and M. S. Faulkner, "Physical activity and sedentary behavior in adolescents with type 1 diabetes.," *Res. Nurs. Health*, vol. 33, no. 5, pp. 441–9, Oct. 2010.

[11] M. A. Powers, R. M. Cuddihy, D. Wesley, and B. Morgan, "Continuous glucose monitoring reveals different glycemic responses of moderate- vs high-carbohydrate lunch meals in people with type 2 diabetes.," *J. Am. Diet. Assoc.*, vol. 110, no. 12, pp. 1912–5, Dec. 2010.

[12] R. N. Bergman, Y. Z. Ider, C. R. Bowden, and C. Cobelli, "Quantitative estimation of insulin sensitivity.," *Am. J. Physiol.*, vol. 236, no. 6, pp. E667-77, Jun. 1979.

[13] C. Dalla Man, M. Camilleri, and C. Cobelli, "A system model of oral glucose absorption: validation on gold standard data.," *IEEE Trans. Biomed. Eng.*, vol. 53, no. 12 Pt 1, pp. 2472–8, Dec. 2006.

[14] T. Arleth, S. Andreassen, M. O. Federici, and M. M. Benedetti, "A model of the endogenous glucose balance incorporating the characteristics of glucose transporters," *Comput. Methods Programs Biomed.*, vol. 62, no. 3, pp. 219–234, Jul. 2000.

[15] C. B. Liden, M. Wolowicz, M. Ed, J. S. M. Des, A. Teller, P. D, S. Vishnubhatla, M. S. Ee, R. Pelletier, M. S. Lc, and J. Farringdon, "Accuracy and Reliability of the SenseWear ™ Armband as an Energy Expenditure Assessment Device," *Analyzer*, 2002. [Online]. Available: http://www.integratedfitnesssystems.com/wp-content/uploads/2012/10/Accuracy.pdf.

[16] R. W. Squires, *Essentials of Exercise Physiology*, vol. 70, no. 1. Lippincott Williams & Wilkins, 1995.

[17] D. U. Silverthorn, W. C. Ober, C. W. Garrison, and A. C. Silverthorn, *Human Physiology: an integrated approach*. Pearson, 2001.

[18] C. Freundenrich, "HowStuffWorks 'How Diabetes Works,'" *Howstuffworks.com*, 2001. [Online]. Available: http://science.howstuffworks.com/life/human-biology/diabetes1.htm.

[19] R. Holt and N. Hanley, *Essential endocrinology and diabetes. 5th revised edition*. Wiley-Blackwell, 2006.

[20] R. S. Dinsmoor, "Counterregulatory Hormones (Page 1) :: Diabetes Self-Management," *Diabetes Self Management*, 2006. [Online]. Available: http://www.diabetesselfmanagement.com/Articles/Diabetes-Definitions/counterregulatory_hormones/.

[21] R. M. Blair, E. C. Henley, and A. Tabor, "Soy foods have low glycemic and insulin response indices in normal weight subjects.," *Nutr. J.*, vol. 5, no. 1, p. 35, Jan. 2006.

[22] A. Waugh and A. (Allison W. Grant, *Ross and Wilson anatomy & physiology in health and illness*. Churchill Livingstone, 2014.

[23] R. Hovorka, V. Canonico, L. J. Chassin, U. Haueter, M. Massi-Benedetti, M. Orsini Federici, T. R. Pieber, H. C. Schaller, L. Schaupp, T. Vering, and M. E. Wilinska, "Nonlinear model predictive control of glucose concentration in subjects with type 1 diabetes.," *Physiol. Meas.*, vol. 25, no. 4, pp. 905–20, Aug. 2004.

[24] P. G. Fabietti, V. Canonico, M. O. Federici, M. M. Benedetti, and E. Sarti, "Control oriented model of insulin and glucose dynamics in type 1 diabetics.," *Med. Biol. Eng. Comput.*, vol. 44, no. 1–2, pp. 69–78, Mar. 2006.

[25] E. D. Lehmann and T. Deutsch, "A physiological model of glucose-insulin interaction in type 1 diabetes mellitus.," *J. Biomed. Eng.*, vol. 14, no. 3, pp. 235–42, May 1992.

[26] M. Derouich and A. Boutayeb, "The effect of physical exercise on the dynamics of glucose and insulin.," *J. Biomech.*, vol. 35, no. 7, pp. 911–7, Jul. 2002.

[27] M. Hernández-Ordoñez and D. U. Campos-Delgado, "An extension to the compartmental model of type 1 diabetic patients to reproduce exercise periods with glycogen depletion and replenishment.," *J. Biomech.*, vol. 41, no. 4, pp. 744–52, Jan. 2008.

[28] E. Salzsieder and A. Rutscher, "Identification of the parameters of a glucose/insulin control model based on individually monitored ...," *Proceedings of the 20th Annual International Conference of the IEEE Engineering in Medicine and Biology Society. Vol.20 Biomedical Engineering Towards the Year 2000 and Beyond (Cat. No.98CH36286)*, 1998. [Online]. Available: http://ieeexplore.ieee.org/xpl/abstractReferences.jsp?reload=true&arnumber=746154&contentType=Conference+Publications. [Accessed: 16-Jun-2017].

[29] P. J. Lenart and R. S. Parker, "Modeling exercise effects in type I diabetic patients," in *World Congress*, 2002, vol. 15, no. 1, p. 1348.

[30] E. D. Lehmann, "Preliminary experience with the Internet release of AIDA--an interactive educational diabetes simulator.," *Comput. Methods Programs Biomed.*, vol. 56, no. 2, pp. 109–32, May 1998.

[31] O. K. Hejlesen, S. Andreassen, R. Hovorka, and D. A. Cavan, "DIAS--the diabetes advisory system: an outline of the system and the evaluation results obtained so far.," *Comput. Methods Programs Biomed.*, vol. 54, no. 1–2, pp. 49–58, Sep. 1997.

[32] D. Andre, R. Pelletier, J. Farringdon, S. Safi, W. Talbott, R. Stone, N. Vyas, D. Wolf, S. Vishnubhatla, S. Boehmke, J. Stivoric, and A. Teller, "The Development of the SenseWear armband , a Revolutionary Energy Assessment Device to Assess Physical Activity and Lifestyle," ..., pp. 1–19, 2006.

[33] G. Nucci and C. Cobelli, "Models of subcutaneous insulin kinetics. A critical review.," *Comput. Methods Programs Biomed.*, vol. 62, no. 3, pp. 249–57, Jul. 2000.

[34] C. Tarín, E. Teufel, J. Picó, J. Bondia, and H.-J. Pfleiderer, "Comprehensive pharmacokinetic model of insulin Glargine and other insulin formulations.," *IEEE Trans. Biomed. Eng.*, vol. 52, no. 12, pp. 1994–2005, Dec. 2005.

[35] D. R. Owens and S. Griffiths, "Insulin glargine (Lantus).," *Int. J. Clin. Pract.*, vol. 56, no. 6, pp. 460–6.

[36] C. Hemmingsen and C. A. Johnsen, "Prediction and Control of Blood Glucose in T1DM Patients," 2009.

[37] A.Karim El-Jabali and S. L. Alousi, "Identification of Two Time Series Models of Type 1 Diabetes using Patient`s clinical Database," *J. Appl. Sci.*, vol. 3, no. 4, pp. 274–279, Apr. 2003.

[38] I. Awaludin, R. Ibrahim, and K. S. R. Rao, "A novel modification of ARX to generalize crude oil consumption model," in *TENCON 2009 - 2009 IEEE Region 10 Conference*, 2009, pp. 1–6.

[39] I. Awaludin, R. Ibrahim, and K. S. Rama Rao, "Conventional ARX and Artificial Neural networks ARX models for prediction of oil consumption in Malaysia," in *2009 IEEE Symposium on Industrial Electronics & Applications*, 2009, vol. 1, pp. 23–28.

[40] D. A. Finan, F. J. Doyle, C. C. Palerm, W. C. Bevier, H. C. Zisser, L. Jovanovic, and D. E. Seborg, "Experimental evaluation of a recursive model identification technique for type 1 diabetes.," *J. Diabetes Sci. Technol.*, vol. 3, no. 5, pp. 1192–202, Sep. 2009.

[41] D. A. Finan, *Modeling and Monitoring Strategies for Type 1 Diabetes*. University of California, Santa Barbara, 2008.

[42] D. E. Goldberg, *Genetic Algorithms in Search, Optimization and Machine Learning*. Addison-Wesley Longman Publishing Co., Inc., 1975.

[43] The MathWorks, "How the Genetic Algorithm Works - MATLAB & Simulink - MathWorks United Kingdom." [Online]. Available: http://uk.mathworks.com/help/gads/how-the-genetic-algorithm-works.html#f13721. [Accessed: 03-Feb-2015].

[44] M. Riddell and K. Iscoe, "Physical activity, sport, and pediatric diabetes," *Pediatr. Diabetes*, vol. 7, no. 1, pp. 60–70, Feb. 2006.

[45] J. Kavookjian, B. M. Elswick, and T. Whetsel, "Interventions for Being Active Among Individuals With Diabetes," *Diabetes Educ.*, vol. 33, no. 6, pp. 962–988, Nov. 2007.

[46] G. Sparacino, F. Zanderigo, S. Corazza, A. Maran, A. Facchinetti, and C. Cobelli, "Glucose concentration can be predicted ahead in time from continuous glucose monitoring sensor time-series.," *IEEE Trans. Biomed. Eng.*, vol. 54, no. 5, pp. 931–7, May 2007.

[47] M. Eren-Oruklu, A. Cinar, L. Quinn, and D. Smith, "Estimation of future glucose concentrations with subject-specific recursive linear models.," *Diabetes Technol. Ther.*, vol. 11, no. 4, pp. 243–53, Apr. 2009.

[48] M. Eren-Oruklu, A. Cinar, C. Colmekci, and M. C. Camurdan, "Self-tuning controller for regulation of glucose levels in patients with type 1 diabetes," in *2008 American Control Conference*, 2008, pp. 819–824.

[49] D. A. Finan, F. J. Doyle, C. C. Palerm, W. C. Bevier, H. C. Zisser, L. Jovanovic, and D. E. Seborg, "Experimental evaluation of a recursive model identification technique for type 1 diabetes.," *J. Diabetes Sci. Technol.*, vol. 3, no. 5, pp. 1192–202, Sep. 2009.

[50] S. D. Patek, L. Magni, E. Dassau, C. Karvetski, C. Toffanin, G. De Nicolao, S. Del Favero, M. Breton, C. D. Man, E. Renard, H. Zisser, F. J. Doyle, C. Cobelli, and B. P. Kovatchev, "Modular closed-loop control of diabetes.," *IEEE Trans. Biomed. Eng.*, vol. 59, no. 11, pp. 2986–99, Nov. 2012.

[51] S. M. Ewings, "Dynamic Modelling of Blood Glucose Concentration in People With Type 1 Diabetes," University of Southampton, 2012.

[52] M. L. Pollock, C. Foster, D. Schmidt, C. Hellman, A. C. Linnerud, and A. Ward, "Comparative analysis of physiologic responses to three different maximal graded exercise test protocols in healthy women.," *Am. Heart J.*, vol. 103, no. 3, pp. 363–73, Mar. 1982.

[53] C. Foster, A. S. Jackson, M. L. Pollock, M. M. Taylor, J. Hare, S. M. Sennett, J. L. Rod, M. Sarwar, and D. H. Schmidt, "Generalized equations for predicting functional capacity from treadmill performance," *Am. Heart J.*, vol. 107, no. 6, pp. 1229–1234, Jun. 1984.

[54] Medtronic Inc, "REAL-Time Continuous Glucose Monitoring System," 2015. [Online]. Available: http://www.medtronic.com.au/your-health/diabetes/device/index.htm. [Accessed: 23-May-2013].

[55] D. Andre, R. Pelletier, J. Farringdon, S. Safi, W. Talbott, R. Stone, N. Vyas, D. Wolf, S. Vishnubhatla, S. Boehmke, J. Stivoric, and A. Teller, "The Development of the SenseWear armband , a Revolutionary Energy Assessment Device to Assess Physical Activity and Lifestyle," ..., pp. 1–19, 2006.

[56] B. E. Ainsworth, W. L. Haskell, M. C. Whitt, M. L. Irwin, A. M. Swartz, S. J. Strath, W. L. O'Brien, D. R. Bassett, K. H. Schmitz, P. O. Emplaincourt, D. R. Jacobs, and A. S. Leon, "Compendium of physical activities: an update of activity codes and MET intensities.," *Med. Sci. Sports Exerc.*, vol. 32, no. 9 Suppl, pp. S498-504, Sep. 2000.

[57] M. Sunseri, C. B. C. Liden, J. Farringdon, R. Pelletier, S. Safier, SureshVishnubhatla, J. Stivoric, and A. Teller, "The SenseWear armband as a Sleep Detection Device," *BodyMedia*, 2009. [Online]. Available: http://www.integratedfitnesssystems.com/wp-content/uploads/2012/10/SenseWearAsSleepDetectionDevice.pdf. [Accessed: 24-Aug-2016].

[58] J. Beasley, W. T. Riley, and J. Jean-Mary, "Accuracy of a PDA-based dietary assessment program," *Nutrition*, vol. 21, no. 6, pp. 672–677, Jun. 2005.

[59] C. K. Martin, S. D. Anton, E. York-Crowe, L. K. Heilbronn, C. VanSkiver, L. M. Redman, F. L. Greenway, E. Ravussin, D. A. Williamson, and Pennington CALERIE Team, "Empirical evaluation of the ability to learn a calorie counting system and estimate portion size and food intake," *Br. J. Nutr.*, vol. 98, no. 2, p. 439, Aug. 2007.

[60] R. Kohavi, "A Study of CrossValidation and Bootstrap for Accuracy Estimation and Model

Selection," in *Proceedings of the 14th international joint conference on Artificial intelligence - Volume 2*, 1995, p. 2077.

[61] Dietterich, "Approximate Statistical Tests for Comparing Supervised Classification Learning Algorithms.," *Neural Comput.*, vol. 10, no. 7, pp. 1895–1923, Sep. 1998.

[62] I. Tsamardinos, A. Rakhshani, and V. Lagani, "Performance-Estimation Properties of Cross-Validation-Based Protocols with Simultaneous Hyper-Parameter Optimization," 2014, pp. 1–14.

[63] A. Mueen, E. Keogh, Q. Zhu, S. Cash, and B. Westover, "Exact Discovery of Time Series Motifs," *Proceedings of the 2009 SIAM International Conference on Data Mining*, 2009. [Online]. Available: http://epubs.siam.org/doi/abs/10.1137/1.9781611972795.41.

[64] C. Cassisi, M. Aliotta, A. Cannata, P. Montalto, D. Patanè, A. Pulvirenti, and L. Spampinato, "Motif Discovery on Seismic Amplitude Time Series: The Case Study of Mt Etna 2011 Eruptive Activity," *Pure Appl. Geophys.*, vol. 170, no. 4, pp. 529–545, Aug. 2012.

[65] R. Cabredo, R. Legaspi, and M. Numao, "Finding Motifs in Psychophysiological Responses and Chord Sequences," 2012, pp. 78–89.

[66] by Abdullah Al Mueen, E. Keogh, and C. Vassilis Tsotras Stefano Lonardi, "UNIVERSITY OF CALIFORNIA RIVERSIDE Exact Primitives for Time Series Data Mining," 2012.

[67] Cleveland Clinic, "The Somogyi Effect & The Dawn Phenomenon | Cleveland Clinic," 2014. [Online]. Available: https://my.clevelandclinic.org/health/articles/what-causes-high-blood-sugar-levels-in-the-morning. [Accessed: 03-Jun-2017].

[68] M. Somogyi and M. Kirstein, "Insulin as a cause of extreme hyperglycemia and instability," *Wkly. Bull. St. Louis Med. Soc.*, Feb. 1938.

[69] I. Blumer, "Frequently Asked Questions." [Online]. Available: http://www.ourdiabetes.com/faqs.htm.

[70] Wikipedia, "File:Somogyi rebound.GIF - Wikipedia, the free encyclopedia." [Online]. Available: http://en.wikipedia.org/wiki/File:Somogyi_rebound.GIF.

[71] Y. Mohammad and T. Nishida, "Approximately recurring motif discovery using shift density estimation," *Lecture Notes in Computer Science (including subseries Lecture Notes in Artificial Intelligence and Lecture Notes in Bioinformatics)*, 2013. [Online]. Available: http://download.springer.com/static/pdf/20/chp%253A10.1007%252F978-3-642-38577-3_15.pdf?auth66=1384393555_ef77be5693f637897882d55cd82f2251&ext=.pdf. [Accessed: 16-Jun-2017].

[72] Y. Mohammad and T. Nishida, "Exact multi-length scale and mean invariant motif discovery," *Appl. Intell.*, vol. 44, no. 2, pp. 322–339, Mar. 2016.

[73] Y. Mohammad and T. Nishida, "Scale invariant multi-length motif discovery," in *Lecture Notes in Computer Science (including subseries Lecture Notes in Artificial Intelligence and Lecture Notes in Bioinformatics)*, vol. 8482 LNAI, no. PART 2, Springer International Publishing, 2014, pp. 417–426.

[74] A. Mueen and N. Chavoshi, "Enumeration of time series motifs of all lengths," *Knowledge and Information Systems*, 2014. [Online]. Available: http://www.cs.unm.edu/~mueen/Projects/MOEN/index.html. [Accessed: 31-Aug-2016].

[75] C. D. Truong and D. T. Anh, *Intelligent Information and Database Systems*, vol. 9622. Berlin,

Heidelberg: Springer Berlin Heidelberg, 2016.

[76] M. Ali, T. Bosse, K. V. Hindriks, M. Hoogendoorn, C. M. Jonker, and J. Treur, Eds., *Recent Trends in Applied Artificial Intelligence*, vol. 7906. Berlin, Heidelberg: Springer Berlin Heidelberg, 2013.

[77] J. C. Kuenen, R. Borg, D. J. Kuik, H. Zheng, D. Schoenfeld, M. Diamant, D. M. Nathan, and R. J. Heine, "Does glucose variability influence the relationship between mean plasma glucose and HbA1c levels in type 1 and type 2 diabetic patients?," *Diabetes Care*, vol. 34, no. 8, pp. 1843–7, Aug. 2011.

[78] J.-H. Cho, S.-A. Chang, H.-S. Kwon, Y.-H. Choi, S.-H. Ko, S.-D. Moon, S.-J. Yoo, K.-H. Song, H.-S. Son, H.-S. Kim, W.-C. Lee, B.-Y. Cha, H.-Y. Son, and K.-H. Yoon, "Long-term effect of the Internet-based glucose monitoring system on HbA1c reduction and glucose stability: a 30-month follow-up study for diabetes management with a ubiquitous medical care system.," *Diabetes Care*, vol. 29, no. 12, pp. 2625–31, Dec. 2006.

[79] B. P. Kovatchev, "Diabetes technology: markers, monitoring, assessment, and control of blood glucose fluctuations in diabetes.," *Scientifica (Cairo).*, vol. 2012, p. 283821, Jan. 2012.

[80] N. R. Hill, N. S. Oliver, P. Choudhary, J. C. Levy, P. Hindmarsh, and D. R. Matthews, "Normal reference range for mean tissue glucose and glycemic variability derived from continuous glucose monitoring for subjects without diabetes in different ethnic groups.," *Diabetes Technol. Ther.*, vol. 13, no. 9, pp. 921–8, Sep. 2011.

[81] D. Boiroux, A. K. Duun-Henriksen, S. Schmidt, K. Nørgaard, N. K. K. Poulsen, H. Madsen, J. Bagterp Jørgensen, K. N?rgaard, N. K. K. Poulsen, H. Madsen, and J. B. J?rgensen, "Assessment of Model Predictive and Adaptive Glucose Control Strategies for People with Type 1 Diabetes," *IFAC Proc. Vol.*, vol. 47, no. 3, pp. 231–236, 2014.

[82] F. Ståhl and R. Johansson, "Diabetes mellitus modeling and short-term prediction based on blood glucose measurements.," *Math. Biosci.*, vol. 217, no. 2, pp. 101–17, Feb. 2009.

[83] M. Cescon and R. Johansson, "Linear Modeling and Prediction in Diabetes Physiology," Springer Berlin Heidelberg, 2014, pp. 187–222.

[84] K. R. Kotz, "Multiple disturbance modeling and prediction of blood glucose in Type 1 Diabetes Mellitus," 2011.

[85] R. Hovorka, "Management of diabetes using adaptive control," *Int. J. Adapt. Control Signal Process.*, vol. 19, no. 5, pp. 309–325, Jun. 2005.

[86] W. C. Bevier, H. C. Zisser, L. Jovanovic, D. A. Finan, C. C. Palerm, D. E. Seborg, and F. J. Doyle, "Use of continuous glucose monitoring to estimate insulin requirements in patients with type 1 diabetes mellitus during a short course of prednisone.," *J. Diabetes Sci. Technol.*, vol. 2, no. 4, pp. 578–83, Jul. 2008.

[87] B. W. Bequette, "A critical assessment of algorithms and challenges in the development of a closed-loop artificial pancreas.," *Diabetes Technol. Ther.*, vol. 7, no. 1, pp. 28–47, Feb. 2005.

[88] A. Gani, A. V Gribok, S. Rajaraman, W. K. Ward, and J. Reifman, "Predicting subcutaneous glucose concentration in humans: data-driven glucose modeling.," *IEEE Trans. Biomed. Eng.*, vol. 56, no. 2, pp. 246–54, Feb. 2009.

[89] J. P. H. Wilding, "The role of the kidneys in glucose homeostasis in type 2 diabetes: Clinical

implications and therapeutic significance through sodium glucose co-transporter 2 inhibitors," *Metabolism*, vol. 63, no. 10, pp. 1228–1237, 2014.

[90] V. Tresp, T. Briegel, and J. Moody, "Neural-network models for the blood glucose metabolism of a diabetic.," *IEEE Trans. Neural Netw.*, vol. 10, no. 5, pp. 1204–13, 1999.

[91] T. Briegel and V. Tresp, "A Nonlinear State Space Model for the Blood Glucose Metabolism of a Diabetic," *Autom.* , vol. 50, pp. 228–236, 2002.

[92] G. Baghdadi and A. M. Nasrabadi, "Controlling blood glucose levels in diabetics by neural network predictor.," *Conf. Proc. ... Annu. Int. Conf. IEEE Eng. Med. Biol. Soc. IEEE Eng. Med. Biol. Soc. Annu. Conf.*, vol. 2007, pp. 3216–9, 2007.

[93] A. K. El-Jabali, "Neural network modeling and control of type 1 diabetes mellitus," *Bioprocess Biosyst. Eng.*, vol. 27, no. 2, pp. 75–79, Apr. 2005.

[94] J. A. Florian and R. S. Parker, "A NONLINEAR DATA–DRIVEN APPROACH TO TYPE I DIABETIC PATIENT MODELING," *IFAC Proc. Vol.*, vol. 35, no. 1, pp. 115–120, 2002.

[95] J. A. Florian and R. S. Parker, "Empirical Modeling for Glucose Control in Critical Care and Diabetes," *Eur. J. Control*, vol. 11, no. 6, pp. 601–616, 2005.

[96] G. D. Mitsis, M. G. Markakis, and V. Z. Marmarelis, "Nonlinear modeling of the dynamic effects of infused insulin on glucose: comparison of compartmental with Volterra models.," *IEEE Trans. Biomed. Eng.*, vol. 56, no. 10, pp. 2347–58, Oct. 2009.

[97] R. Bellazzi, L. Ironi, R. Guglielmann, and M. Stefanelli, "Qualitative models and fuzzy systems: an integrated approach for learning from data.," *Artif. Intell. Med.*, vol. 14, no. 1–2, pp. 5–28.

[98] Z. Trajanoski and P. Wach, "Fuzzy filter for state estimation of a glucoregulatory system," *Comput. Methods Programs Biomed.*, vol. 50, no. 3, pp. 265–273, 1996.

[99] D. U. Campos-Delgado, M. Hernández-Ordoñez, R. Femat, and A. Gordillo-Moscoso, "Fuzzy-based controller for glucose regulation in type-1 diabetic patients by subcutaneous route.," *IEEE Trans. Biomed. Eng.*, vol. 53, no. 11, pp. 2201–10, Nov. 2006.

[100] W. A. Sandham, D. J. Hamilton, A. Japp, and K. Patterson, "Neural network and neuro-fuzzy systems for improving diabetes therapy," in *Proceedings of the 20th Annual International Conference of the IEEE Engineering in Medicine and Biology Society. Vol.20 Biomedical Engineering Towards the Year 2000 and Beyond (Cat. No.98CH36286)*, vol. 3, pp. 1438–1441.

[101] L. McCausland and I. M. Y. Mareels, "A probabilistic rule extraction method for an insulin advice algorithm for type 1 diabetes mellitus," in *Proceedings of the 22nd Annual International Conference of the IEEE Engineering in Medicine and Biology Society (Cat. No.00CH37143)*, vol. 1, pp. 623–626.

[102] C. K. I. Williams and C. E. Rasmussen, "Gaussian Processes for Regression," *Adv. Neural Inf. Process. Syst.*, 1996.

[103] J. J. Valletta, A. J. Chipperfield, G. F. Clough, and C. D. Byrne, "Metabolic regulation during constant moderate physical exertion in extreme conditions in Type 1 diabetes," *Diabet. Med.*, vol. 29, no. 6, pp. 822–6, Jun. 2012.

[104] E. Snelson and Z. Ghahramani, "Variable noise and dimensionality reduction for sparse Gaussian processes," in *22nd Conference on Uncertainty in Artificial Intelligence (UAI*

2006), 2006.

[105] E. L. Snelson, "Flexible and efficient Gaussian process models for machine learning," 2007.

[106] C. Pérez-Gandía, A. Facchinetti, G. Sparacino, C. Cobelli, E. J. Gómez, M. Rigla, A. de Leiva, and M. E. Hernando, "Artificial Neural Network Algorithm for Online Glucose Prediction from Continuous Glucose Monitoring," *Diabetes Technol. Ther.*, vol. 12, no. 1, pp. 81–88, Jan. 2010.

[107] D. A. Finan, C. C. Palerm, F. J. Doyle, H. Zisser, L. Jovanovic, W. C. Bevier, and D. E. Seborg, "Identification of empirical dynamic models from type 1 diabetes subject data," in *2008 American Control Conference*, 2008, pp. 2099–2104.

[108] C. B. Liden, M. Wolowicz, M. Ed, J. S. M. Des, A. Teller, P. D, S. Vishnubhatla, M. S. Ee, R. Pelletier, M. S. Lc, and J. Farringdon, "Accuracy and Reliability of the SenseWear ™ Armband as an Energy Expenditure Assessment Device," *Analyzer*, pp. 1–15, 2002.

[109] P. Dudley, D. R. Bassett, D. John, and S. E. Crouter, "Validity of a Multi-Sensor Armband for Estimating Energy Expenditure during Eighteen Different Activities," *J. Obes. Weight Loss Ther.*, vol. 2, no. 7, 2012.

[110] K. Lyden, T. Swibas, V. Catenacci, R. Guo, N. Szuminsky, and E. L. Melanson, "Estimating energy expenditure using heat flux measured at a single body site.," *Med. Sci. Sports Exerc.*, vol. 46, no. 11, pp. 2159–67, Nov. 2014.

[111] K. K. Trout, M. R. Rickels, M. H. Schutta, M. Petrova, E. W. Freeman, N. C. Tkacs, and K. L. Teff, "Menstrual Cycle Effects on Insulin Sensitivity in Women with Type 1 Diabetes: A Pilot Study," *Diabetes Technol. Ther.*, vol. 9, no. 2, pp. 176–182, Apr. 2007.

[112] P. Wiesli, C. Schmid, O. Kerwer, C. Nigg-Koch, R. Klaghofer, B. Seifert, G. A. Spinas, and K. Schwegler, "Acute psychological stress affects glucose concentrations in patients with type 1 diabetes following food intake but not in the fasting state.," *Diabetes Care*, vol. 28, no. 8, pp. 1910–5, Aug. 2005.

[113] A. Riazi, J. Pickup, and C. Bradley, "Daily stress and glycaemic control in Type 1 diabetes: individual differences in magnitude, direction, and timing of stress-reactivity," *Diabetes Res. Clin. Pract.*, vol. 66, no. 3, pp. 237–244, Dec. 2004.

[114] R. N. Bergman, L. S. Phillips, and C. Cobelli, "Physiologic evaluation of factors controlling glucose tolerance in man: measurement of insulin sensitivity and beta-cell glucose sensitivity from the response to intravenous glucose.," *J. Clin. Invest.*, vol. 68, no. 6, pp. 1456–67, Dec. 1981.

[115] N. van Riel, "Minimal Models for Glucose and Insulin Kinetics; a Matlab implementation," *Eindhoven Univ. Technol.*, pp. 1–12, 2004.

[116] D. Svitra, I. Basov, and R. Vilkyt˙, "Modelling of glycaemia dynamics: impact of physical exercises," *Nonlinear Anal. Model. Control*, vol. 15, no. 2, pp. 213–232, 2010.

[117] A. Bock, G. François, T. Prud'homme, and D. Gillet, *A Minimal Excercise Extension for Models of the Glucorregulatory System*, vol. 29. 2011.

[118] C. D. Man, M. D. Breton, and C. Cobelli, "Physical activity into the meal glucose-insulin model of type 1 diabetes: in silico studies.," *J. Diabetes Sci. Technol.*, vol. 3, no. 1, pp. 56–67, Jan. 2009.

[119] J. Kim, G. M. Saidel, and M. E. Cabrera, "Multi-Scale Computational Model of Fuel

Homeostasis During Exercise: Effect of Hormonal Control," *Ann. Biomed. Eng.*, vol. 35, no. 1, pp. 69–90, Dec. 2006.

[120] E. I. Georga, V. C. Protopappas, and D. I. Fotiadis, "Glucose Prediction in Type 1 and Type 2 Diabetic Patients Using Data Driven Techniques," *Knowledge-Oriented Appl. Data Min.*, pp. 277–296, Jan. 2011.

[121] E. I. Georga, V. C. Protopappas, D. Polyzos, and D. I. Fotiadis, "Predictive Modeling of Glucose Metabolism using Free-Living Data of Type 1 Diabetic Patients.," *Conf. Proc. ... Annu. Int. Conf. IEEE Eng. Med. Biol. Soc. IEEE Eng. Med. Biol. Soc. Annu. Conf.*, vol. 2010, pp. 589–92, 2010.

[122] D. K. Rollins, N. Bhandari, and K. R. Kotz, "Critical Modeling Issues for Successful Feedforward Control of Blood Glucose in Insulin Dependent Diabetics," *Control*, pp. 832–837, 2008.

[123] B. E. Ainsworth, W. L. Haskell, A. S. Leon, D. R. Jacobs, H. J. Montoye, J. F. Sallis, and R. S. Paffenbarger, "Compendium of physical activities: classification of energy costs of human physical activities.," *Med. Sci. Sports Exerc.*, vol. 25, no. 1, pp. 71–80, Jan. 1993.

[124] P.-M. Lepretre, J.-P. Koralsztein, and V. L. Billat, "Effect of exercise intensity on relationship between VO2max and cardiac output.," *Med. Sci. Sports Exerc.*, vol. 36, no. 8, pp. 1357–63, Aug. 2004.

[125] M. Kwan, J. Woo, and T. Kwok, "The standard oxygen consumption value equivalent to one metabolic equivalent (3.5 ml/min/kg) is not appropriate for elderly people.," *Int. J. Food Sci. Nutr.*, vol. 55, no. 3, pp. 179–82, May 2004.

[126] D. A. Rubin, R. G. McMurray, J. S. Harrell, A. C. Hackney, D. E. Thorpe, and A. M. Haqq, "The association between insulin resistance and cytokines in adolescents: the role of weight status and exercise.," *Metabolism.*, vol. 57, no. 5, pp. 683–90, May 2008.

[127] S. Kozey, K. Lyden, J. Staudenmayer, and P. Freedson, "Errors in MET estimates of physical activities using 3.5 ml x kg(-1) x min(-1) as the baseline oxygen consumption.," *J. Phys. Act. Health*, vol. 7, no. 4, pp. 508–16, Jul. 2010.

[128] J. S. Harrell, R. G. McMurray, C. D. Baggett, M. L. Pennell, P. F. Pearce, and S. I. Bangdiwala, "Energy costs of physical activities in children and adolescents.," *Med. Sci. Sports Exerc.*, vol. 37, no. 2, pp. 329–36, Feb. 2005.

[129] Arizona State University, "Corrected METs - Compendium of Physical Activities." [Online]. Available: https://sites.google.com/site/compendiumofphysicalactivities/corrected-mets.

[130] N. M. Byrne, A. P. Hills, G. R. Hunter, R. L. Weinsier, and Y. Schutz, "Metabolic equivalent: one size does not fit all.," *J. Appl. Physiol.*, vol. 99, no. 3, pp. 1112–9, Sep. 2005.

[131] J. A. Harris and F. G. Benedict, "A Biometric Study of Human Basal Metabolism.," *Proc. Natl. Acad. Sci. U. S. A.*, vol. 4, no. 12, pp. 370–3, Dec. 1918.

[132] C. De Faria Coelho-Ravagnani, F. Carolina, L. Melo, F. C. P. Ravagnani, F. Homero, P. Burini, and R. C. Burini, "Estimation of the metabolic equivalent (MET) of an exercise protocol based on indirect calorimetry," *Rev Bras Med Esporte*, vol. 19, no. 2, 2013.

[133] A. Roy and R. S. Parker, "Dynamic modeling of exercise effects on plasma glucose and insulin levels.," *J. Diabetes Sci. Technol.*, vol. 1, no. 3, pp. 338–47, May 2007.

[134] R. R. Wolfe, E. R. Nadel, J. H. Shaw, L. A. Stephenson, and M. H. Wolfe, "Role of changes in

insulin and glucagon in glucose homeostasis in exercise.," *J. Clin. Invest.*, vol. 77, no. 3, pp. 900–7, Mar. 1986.

[135] G. Ahlborg, J. Wahren, and P. Felig, "Splanchnic and peripheral glucose and lactate metabolism during and after prolonged arm exercise.," *J. Clin. Invest.*, vol. 77, no. 3, pp. 690–9, Mar. 1986.

[136] B. Zajadacz, A. Skarpańska-Stejnborn, W. Brzenczek-Owczarzak, A. Juszkiewicz, M. Naczk, and Z. Adach, "The influence of physical exercise on alterations in concentrations of neuropeptide Y, leptin and other selected hormonal and metabolic parameters in sportspeople," *Biol. Sport*, vol. 26, no. 4, pp. 309–324, Dec. 2009.

[137] K. F. Petersen, T. B. Price, and R. Bergeron, "Regulation of net hepatic glycogenolysis and gluconeogenesis during exercise: impact of type 1 diabetes.," *J. Clin. Endocrinol. Metab.*, vol. 89, no. 9, pp. 4656–64, Sep. 2004.

[138] E. I. Georga, V. C. Protopappas, D. Ardigò, D. Polyzos, and D. I. Fotiadis, "A Glucose Model Based on Support Vector Regression for the Prediction of Hypoglycemic Events Under Free-Living Conditions," *http://dx.doi.org/10.1089/dia.2012.0285*, 2013.

[139] E. I. Georga, V. C. Protopappas, and D. I. Fotiadis, "Predictive Metabolic Modeling for Type 1 Diabetes Using Free-Living Data on Mobile Devices," in *Wireless Mobile Communication and Healthcare*, vol. 55, 2011, pp. 187–193.

[140] C. J. K. Henry, "Basal metabolic rate studies in humans: measurement and development of new equations.," *Public Health Nutr.*, vol. 8, no. 7A, pp. 1133–52, Oct. 2005.

[141] W. N. Schofield, "Predicting basal metabolic rate, new standards and review of previous work.," *Hum. Nutr. Clin. Nutr.*, vol. 39 Suppl 1, pp. 5–41, 1985.

[142] M. Singh, D. K. Dureha, S. Yaduvanshi, and P. Mishra, "Effect of aerobic and anaerobic exercise on basal metabolic-rate," *Br. J. Sports Med.*, vol. 44, no. Suppl_1, pp. i26–i26, Sep. 2010.

[143] A. J. Hulbert and P. L. Else, "Basal Metabolic Rate: History, Composition, Regulation, and Usefulness," *Physiol. Biochem. Zool.*, vol. 77, no. 6, pp. 869–876, 2004.

[144] S. M. Ewings, S. K. Sahu, J. J. Valletta, C. D. Byrne, and A. J. Chipperfield, "A Bayesian network for modelling blood glucose concentration and exercise in type 1 diabetes," *Stat. Methods Med. Res.*, vol. 24, no. 3, pp. 342–372, Jun. 2015.

[145] C. Liden, M. Wolowicz, and J. Stivoric, "Characterization and implications of the sensors incorporated into the SenseWear armband for energy expenditure and activity detection," *Bodymedia Inc.*, pp. 1–7, 2002.

[146] B. M. Forseth, "Accuracy of SenseWear Armband Mini-Fly for Estimating Energy Expenditure in Normal Weight, Overweight, and Obese Individuals," 2014.

[147] Jie Chen, Bin Xin, Zhihong Peng, Lihua Dou, and Juan Zhang, "Optimal Contraction Theorem for Exploration–Exploitation Tradeoff in Search and Optimization," *IEEE Trans. Syst. Man, Cybern. - Part A Syst. Humans*, vol. 39, no. 3, pp. 680–691, May 2009.

[148] J. A. Vasconcelos, J. A. Ramírez, R. H. C. Takahashi, and R. R. Saldanha, "Improvements in Genetic Algorithms," *IEEE Trans. Magn.*, vol. 37, no. 5, 2001.

[149] G. Ahlborg and P. Felig, "Lactate and glucose exchange across the forearm, legs, and splanchnic bed during and after prolonged leg exercise.," *J. Clin. Invest.*, vol. 69, no. 1, pp.

45–54, Jan. 1982.

[150] J. Grefenstette, "Optimization of Control Parameters for Genetic Algorithms," *IEEE Trans. Syst. Man. Cybern.*, vol. 16, no. 1, pp. 122–128, Jan. 1986.

[151] V. Kapoor and S. Dey, "An Empirical Study of the Role of Control Parameters of Genetic Algorithms in Function Optimization Problems," vol. 31, no. 6, pp. 20–26, 2011.

[152] J. Grefenstette, "Optimization of Control Parameters for Genetic Algorithms," *IEEE Trans. Syst. Man. Cybern.*, vol. 16, no. 1, pp. 122–128, Jan. 1986.

[153] K. A. De Jong and W. M. Spears, "An analysis of the interacting roles of population size and crossover in genetic algorithms," Springer, Berlin, Heidelberg, 1991, pp. 38–47.

[154] The MathWorks, "Global Optimization Toolbox," 2016. [Online]. Available: https://www.mathworks.com/help/gads/. [Accessed: 13-May-2017].

[155] The MathWorks, "Genetic Algorithm Options - Adaptive Feasible Mutation Rate." [Online]. Available: https://www.mathworks.com/help/gads/genetic-algorithm-options.html. [Accessed: 13-May-2017].

[156] K. A. De Jong and W. M. Spears, "An analysis of the interacting roles of population size and crossover in genetic algorithms," Springer, Berlin, Heidelberg, 1991, pp. 38–47.

[157] University of Southampton, "The Iridis Computer Cluster." [Online]. Available: http://www.southampton.ac.uk/isolutions/staff/iridis.page. [Accessed: 13-May-2017].

[158] Mathworks, "MATLAB Parallel Computing Toolbox 2016a User Guide," 2009.

[159] University of Southampton, "The Iridis Computer Cluster." .

[160] L. Shure, "Using parfor Loops : Getting Up and Running," 2014. [Online]. Available: http://blogs.mathworks.com/loren/2009/10/02/using-parfor-loops-getting-up-and-running/.

[161] N. J. Higham, "Computing a nearest symmetric positive semidefinite matrix," *Linear Algebra Appl.*, vol. 103, pp. 103–118, May 1988.

[162] Mathworks, "MATLAB Parallel Computing Toolbox 2016a User Guide," 2009.

[163] The MathWorks, "Parallel Computing on the Cloud with MATLAB - MATLAB." [Online]. Available: https://www.mathworks.com/products/parallel-computing/parallel-computing-on-the-cloud.html. [Accessed: 29-May-2017].

[164] Association of the British Pharmaceutical Industry, "Controlling blood glucose levels." [Online]. Available: http://www.abpischools.org.uk/page/modules/diabetes/diabetes4.cfm.

Appendix A

Additional information on the Clinical Tests done in the Diabetes UK Study

Microvascular measurements (leg blood flow)

- This will be measured using a non-invasive and painless technique, that have no known effects on skin or muscle:
  Whilst lying flat, an elastic gauge will be placed around your calf and a cuff will be placed around your thigh. In addition two low-intensity laser probes (skin and muscle probe) will be attached to the skin of your calf. Small increases in pressure will then be applied via the cuff and maintained. Each step will last approximately 4 minutes. The cuff will then be rapidly inflated for 3 minutes. The whole process will take no longer than 1 hour.

Measurement of peripheral circulation

- *Ankle / Brachial Pressure Index (ABI)* - is a simple measurement for assessing peripheral macrovascular function (blood flow in legs). Low ABI (<0.9) is an independent predictor of increased cardiovascular disease risk. We want to assess relationships between ABI and other measures such as physical activity levels and fitness. With you rested and lying flat on your back, blood pressure cuffs will be placed bilaterally on your upper arm (brachial pressure) and ankle and then inflated. An ultrasound probe will be placed over your arm and leg arteries in turn. This is a painless and very safe procedure.

Measurement of muscle strength

- *Handgrip strength* – We also wish to examine the relationship between how active you are and how strong your muscles are. We can do this simply by asking you to squeeze a small measuring device that you hold in your hand (a Jamar dynamometer). We will use for the analysis the best score out of the total three measurements from each hand. The Jamar dynamometer is simple to use, accurate, reproducible in its measurements and the most widely used and reported upon devices assessing muscle strength.

Measurement of fitness

- *VO_2 max* – By breathing into a mask while exercising on a treadmill, we can measure the amount of oxygen you breathe in and how much carbon dioxide you breathe out. We will gradually increase the difficulty of the exercise until the maximal oxygen consumption is recorded (VO_2max). People with type 1 diabetes are usually young and physically active; this will give us an indication of the fitness level of each and every volunteer which we can then relate to their glycaemic control.

Measurement of metabolic rate

- *Indirect calorimetry* – By breathing into a mask while you are lying on a bed we are able to measure how much oxygen you breathe in and how much carbon dioxide you breathe out. From these measurements, we can calculate the respiratory quotient (the ratio of the volume of carbon dioxide produced to the volume of oxygen consumed) and the resting energy expenditure (calories you 'burn' up at rest).

Blood test

- The usual blood test which is used to assess various conditions, specifically kidney, liver and thyroid functions, glycated haemoglobin (HbA_1C - gives an indication of the glycaemic control during the last three months) and cholesterol levels (lipid profile).

Measurement of protein excretion

- *Microalbuminiria* – This test measures the levels of albumin (the most abundant protein in the blood plasma) in the urine. Microalbuminiria is a marker of increased risk of cardiovascular and kidney diseases.

Measurement of body composition

- *Bioimpedance* – A small current of fixed frequency is passed through the body. The recorded impedance (opposition to flow of current) can be used to estimate the amount of body fat.
- *DEXA Scan* – Uses two X-ray beams of different energy levels which scan the whole body. Depending on the X-ray's absorption, an estimate of the amount of body fat can be obtained.
- *Bod Pod* – Calculates the body volume by measuring the volume of air displaced while the person is sitting inside a comfortable chamber. Using the volume and the mass of the person (measured by an electronic scale), the density can be calculated. This is then used to calculate the proportion of fat and lean mass by using scientifically derived equations.

Appendix B

Guardian® Real-Time Continuous Glucose Monitoring System

The Guardian® Real-Time System continuously measures glucose levels, even while apatient sleeps and displays an updated version every 5 minutes. This information can be downloaded to a computer which can then be used to analyse the daily trends in glucoselevels. This system is indicated for use in diabetes patients 18 years and older.

System Components

The Guardian® Real-Time System uses three components, a glucose sensor, a transmitterand a monitor.

Glucose Sensor

- The glucose sensor is a tiny electrode which is worn by the patient for up to 3 days.
- The sensor is easily inserted by patients, caregivers or healthcare professionals under the skin using the Sen-serter®, an automatic insertion device.
- As many as 288 glucose readings are recorded by the sensor each day.

Transmitter

- The transmitter connects to the glucose sensor and attaches to the skin by an adhesive patch (1.5" x 0.8").

- Using radio frequency, the transmitter sends glucose values from the sensor to themonitor every five minutes.
- The transmitter is small (1.4" x 1.1" x 0.3"), lightweight (less than ¼ of an ounce), ergonomically shaped (won't pinch with movement) and designed to minimise skinirritation.
- The transmitter is waterproof; hence patients can shower, bathe or swim while wearing both the transmitter and the sensor.

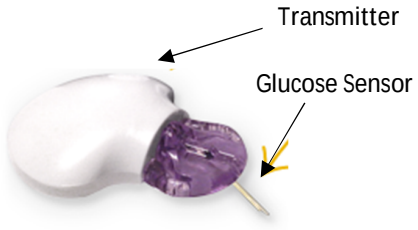

Monitor

- The monitor receives continuous sensor readings from the transmitter and displaysglucose values every 5 minutes.
- To calibrate the system, a minimum of two meter measurements are entered into themonitor each day (every 12-hours). A fingerstick measurement is required to confirmhigh or low sensor values prior to making a self-management decision.
- The monitor should not be exposed to water: however, patients can easily shower or bathe without interrupting their glucose data since the monitor will receive a signal as long as it is within 2 metres of the transmitter.

Monitor

Complete System